1. Udgave.

J. Birch Hansen.

Denne afhandling er af Danmarks tekniske Højskole antaget til forsvar for den tekniske doktorgrad.

Danmarks tekniske Højskole, den 30. juni 1953
ANKER ENGELUND
Rektor

Forsvaret finder sted fredag den 25. september 1953 kl.14 paa Danmarks tekniske Højskole, Festsalen, Sølvgade 83.

DK 624.131.4
DK 624.131.5
DK 624.136.6
DK 624.137.4
DK 624.137.5

EARTH PRESSURE CALCULATION

by

JØRGEN BRINCH HANSEN

Chief Engineer

Christiani & Nielsen

Application of a new Theory of Rupture
to the Calculation and Design of
Retaining Walls, Anchor Slabs, Free Sheet Walls,
Anchored Sheet Walls, Fixed Sheet Walls, Braced Walls,
Double Sheet Walls and Cellular Cofferdams

With Summaries in English and Danish

THE DANISH TECHNICAL PRESS
THE INSTITUTION OF DANISH CIVIL ENGINEERS
COPENHAGEN 1953

Printed in Denmark by
S.L. MØLLERS BOGTRYKKERI

CONTENTS

PREFACE

"There are two approaches to a natural problem. They are the approach of the pure scientist and that of the engineer. The pure scientist is interested only in truth. For him there is only one answer - the right one - no matter how long it takes to get it. For the engineer, on the other hand, there are many possible answers, all of which are compromises between truth and time, for the engineer must have an answer now; his answer must be sufficient for a given purpose, even if not true. For this reason an engineer must make assumptions - assumptions which in some cases he knows to be not strictly correct - but which will enable him to arrive at an answer which is sufficiently true for the immediate purpose."

These remarks by H.Q. Golder (1948) describe better than anything else the author's own approach to the subject of earth pressure calculation. His principal aim has not been to find the mathematically exact solutions, however complicated, but, on the contrary, to indicate the simplest solutions which are sufficiently correct for practical purposes.

The above citation is actually Golder's opening to an article about C.A. Coulomb who, in 1776, founded the classical earth pressure theory. Although, since then, innumerable papers and books have been written on the subject of earth pressure, little actual progress has been made. Of course, many valuable tests have been carried out, and considerable practical experience has been gained, but general theories capable of accounting for the observed facts have been very scarce.

That this is so can be seen from the fact that up to the present day the most commonly used earth pressure theory is still Coulomb's. Actually, Coulomb himself developed his theory for a certain type of structure, viz. retaining walls, for which it proved to be an excellent approximation. Later, however, his theory has - for want of better methods - been applied to several other structures with more or less misleading results; mainly because the possible movements of these structures are not compatible with the possible deformations of the earth, corresponding to the simple figures of rupture considered in Coulomb's theory.

The purpose of the present work is to introduce a new general method for the calculation of earth pressures. It embraces a far wider field of possible rupture-figures than those previously known, and this enables the choice of rupture-figures compatible with the movements of the considered structures in the state of failure. The corresponding calculations have been made possible, partly by means of the well-known Kötter's Equation, and partly by means of a connection, established by the author, between two known but hitherto unrelated methods of calculation.

Earth pressure calculation has, admittedly, not been made simpler by the introduction of the author's method, but this is the price one has to pay for greater accuracy. Still, most of the calculation methods developed in the present work are relatively simple as compared with many of the methods in common use for the calculation of other structures as, for example, bridges.

With regard to economy, it is evident that smaller factors of safety can be allowed when more exact calculation methods are available. Therefore, the author's method, when employed in combination with suitable safety factors, should be able to effect considerable savings as compared with conventional design methods.

ACKNOWLEDGEMENTS

In my capacity as chief engineer of the Central Designing Office of the contracting firm of CHRISTIANI & NIELSEN, Copenhagen, I have had the opportunity to deal with the design of a large number of marine structures and foundations. In so doing, I have often experienced the shortcomings of the conventional earth pressure theories and the need for more appropriate methods.

In my endeavours to develop such new methods and to prepare the present book, I have received every possible support, help and encouragement from the owners of the firm, Dr.-Ing. RUD. CHRISTIANI and Mr. ALEX. CHRISTIANI, M.Sc. For this I am exceedingly grateful. Further, I wish to thank all my colleagues in the firm for their valuable co-operation on various occasions.

I have also been fortunate enough to have had close contact with the TECHNICAL UNIVERSITY OF DENMARK, especially with its President, Professor, Dr. A. ENGELUND, as well as with Professor A. E. BRETTING and Professor, Dr. H. LUNDGREN, to all of whom I am greatly indebted for their kind interest and encouragement. In this connection I should also like to mention, that I was kindly permitted to carry out my small-scale model tests in Professor Bretting's laboratory.

I wish to extend special thanks to Mr. KNUD MORTENSEN, C.E., who, with keen interest and considerable skill, has gone through the whole manuscript, checking all formulae and most of the numerical calculations. In the course of this work, Mr. Mortensen suggested a number of important additions and amendments, and the ensuing discussions with him have been very inspiring to me.

I am also grateful for the very neat work done by Miss E. BARUËL, who prepared the final figures and graphs, and to Miss E. RIISBØL-JENSEN, who made some of the preliminary ones. For expert typing and valuable assistance as regards the English translation, I sincerely thank Miss HILDA BOJESEN, who prepared the final edition for printing, and Mrs. CATHERINE HENKE, who made the preliminary typewritten edition.

The final edition has been typed on a Vari-Typer, kindly placed at my disposal by Messrs. FREDERIK LARSEN, Copenhagen. The actual reproduction and printing have been carried out by Messrs. S. L. MØLLERS BOGTRYKKERI, Copenhagen, whom I thank for their excellent work.

Finally, I should like to express my gratitude to the LAURITS ANDERSENS FOND and to the OTTO MØNSTEDS FOND for the financial support granted me.

As the main part of my work on earth pressure theories has been done at home in my spare time during the past six years, I feel deeply indebted to my wife, Mrs. ELSEBETH BRINCH HANSEN, and to my children, PER and EVA, for their great patience and understanding.

Copenhagen, 11th June, 1953.

J. BRINCH HANSEN

READER'S GUIDE

The present book is divided into 9 main sections and an Appendix. Each main section is indicated by a single numeral (e.g. Section 7), primary subsections by two numerals (e.g. Section 74) and secondary subsections by three numerals (e.g. Section 742).

Formulae are indicated by four numerals, the first two of which refer to the primary subsection, in which the formula occurs (e.g.: Formula 7405 is the fifth formula in Section 74). Figures are usually indicated by two numerals and a capital letter; the numerals refer to the primary subsection, in which the figure occurs (e.g.: Fig. 74C is the third figure in Section 74). Examples are, finally, indicated by two numerals and a small letter; the numerals refer to the primary subsection, in which the example occurs (e.g.: Example 74b is the second example in Section 74).

All the main symbols or notations are listed in the Appendix. For such symbols, which may attain positive or negative values, the sign rules are indicated, and these must always be observed carefully. Some of the basic concepts are indicated in Section 12; others may be found by means of the Index in the Appendix. References are also listed in the Appendix, and in the text they are indicated by the name of the author and the year of publication.

In order to get an initial idea of the new calculation method it should suffice to read the English or the Danish summary in the Appendix. A more thorough general orientation may be obtained by reading Sections 1, 31, 341, 35-37, 41, 47, 59, 61-63, 65 and 91-92.

In order to solve a practical problem, e.g. concerning the design or calculation of a certain earth retaining structure, it is usually sufficient - after having obtained the general orientation mentioned above - to study the pertaining subsections in Sections 7 or 8.

If the problem presents unusual features, or is of a more theoretical nature, it may prove necessary to study selected parts of Sections 3-6 in order to work out a solution.

As an aid to practical calculations, the Appendix contains a set of tables, by means of which the internal forces in a rupture-circle can be calculated for friction angles of 0° and 30°. It also contains a set of graphs, by means of which the earth pressure on a vertical wall (horizontal ground surface) can be calculated for any location of the rotation centre on the wall, and for any friction angle.

For the preparation of tables, such as those in the Appendix and in Section 5, a calculating machine is necessary. Otherwise, all calculations can be effected by means of a slide rule, as has been done in the numerical examples. In all these examples, the units m (metres) and t (metric tons) have been used, but any other system of units (e.g. ft and lbs) may equally well be used. The quantities indicated in the tables and graphs in the Appendix are all dimensionless.

1. INTRODUCTION

11. Earth Pressure Problems

Earth pressure problems, taken in their widest sense, are concerned with the determination of the stresses acting inside earth masses or between these masses and structures in contact with them.

However, such problems are usually subdivided into at least 3 different groups, viz.:

1) Lateral earth pressure problems.
2) Foundation problems.
3) Stability problems.

The main object of the present work is to deal with the lateral earth pressure problems. However, the method developed for this purpose is in principle also applicable to foundation and stability problems.

Lateral earth pressure problems are sometimes further sub-divided into the following 3 groups:

1a) Earth pressure against rigid walls.
1b) Earth pressure against flexible walls.
1c) Earth pressure against underground structures.

The third of these groups will not be considered in the present work. With regard to the first two groups, no distinction will be made between rigid and flexible walls, and for the following reason:

The author's theory is a theory of rupture, i.e., the calculation is based on the state of failure. In such a state the elastic deformations of most structures can be disregarded in comparison with the plastic deformations and movements. Consequently, all walls can be considered either completely rigid, or made up of a finite number of rigid parts connected by yield hinges.

The present work will be concerned exclusively with problems of plane strain, or with such problems which may with sufficient accuracy be treated as plane.

The following structures shall be dealt with: retaining walls, anchor slabs, free sheet walls, anchored sheet walls, fixed sheet walls, braced walls, double sheet walls and cellular cofferdams.

12. Some Basic Concepts.

Earth pressure is the force acting between the earth and a structure such as, for example, a wall. If the wall does not move at all, we have the so-called earth pressure at rest. If the wall is forced against the earth, we have passive pressure, and, if it retreats from the earth, we have active pressure.

The pressure centre of a wall (or part of a wall) is the point, in which the corresponding earth pressure resultant intersects the wall. The rotation centre of a wall (or part of a wall) is the point, about which the wall rotates in the state of failure.

A rotation is described as positive, when it involves an increase of the angle (through the earth) between the wall and the original ground surface; in a negative rotation this angle is decreased. Further, a rotation is termed "normal", when all points at the wall move in the direction of the corresponding normals to the wall.

The condition of failure for the earth is: $\tau = c + \sigma \tan \varphi$, where c (the cohesion) and φ (the friction angle) are constants. If $c = 0$, the earth is said to be cohesionless, and if $\varphi = 0$, frictionless. The earth has an effective unit weight γ (uplift deducted), and its surface may be loaded with a vertical unit surcharge p. In the theoretical case of $\gamma = 0$, the earth is termed weightless, and in the case of $p = 0$, it is said to be unloaded.

When a sliding movement takes place between wall and earth we have: $f = a + e \tan \delta$, where e and f are the unit normal and tangential earth pressures respectively, whereas a (the adhesion) and δ (the wall friction angle) are constants. If $a = 0$ and $\delta = 0$, the wall is said to be perfectly smooth, and, in the case of $a = c$ and $\delta = \varphi$, perfectly rough.

A line of rupture (or rupture-line) is a curve, for which the normal and shear stresses in any small element satisfy the condition of failure. This condition is also satisfied by the stresses in a line forming angles $90^\circ \pm \varphi$ with the rupture-line. This second line, which, according to the definition, is also a rupture-line, is sometimes called a pseudo-rupture-line.

The whole pattern of rupture-lines in the earth (or a finite part of the earth) is termed a figure of rupture (or rupture-figure).

When the condition of failure is fulfilled for any point within a certain finite area, this area is called a rupture-zone (or plastic zone), and the corresponding rupture-figure is termed a zone-rupture.

When the failure condition is fulfilled for all points on a certain curve only, this curve is a rupture-line, and the corresponding rupture-figure is termed a line-rupture. In a line-rupture, the pseudo-rupture-lines are all infinitely short. Finite areas, in which the condition of failure is not fulfilled for any point in the interior, are called elastic zones.

More complicated rupture-figures, containing more than one plastic or elastic zone, are termed composite ruptures.

13. Short Historical Review

The classical earth pressure theory was founded in 1776 by Coulomb, who introduced most of the basic concepts and assumptions still generally used in earth pressure calculations. Thus he stated the so-called Coulomb's law of shearing resistance: $\tau = c + \mu\sigma$, and he introduced the principle of determining the active earth pressure as a maximum value. Further, by assuming that the lines of rupture were straight he derived the well-known Coulomb formula for active earth pressure on a retaining wall.

Rankine, in 1857, approached the problem in an entirely different way. He started by investigating the conditions of equilibrium and failure for an infinitely small earth element in a semi-infinite earth mass. By further assuming the lines of rupture to be straight, and with the aid of the boundary conditions at the ground surface, he developed the well-known Rankine formulae for active and passive states of failure in the ground.

Whereas Coulomb and Rankine were able to deal with straight rupture-lines only, Kötter succeeded in 1903 in deriving the differential equation governing the stresses in a curved rupture-line. Very little use has been made of Kötter's equation since then, probably because it is not quite simple. In the present work, however, extensive use shall be made of it.

At approximately the same time began the development of the different theories of plasticity, chiefly by Saint Venant (1871), von Mises (1913), Prandtl (1920, 1927), Hencky (1928), Nadai (1928), Jürgenson (1934) and Odqvist (1934). Although most of these theories were developed for metals they could also be applied to earth. Based on Coulomb's failure condition Prandtl determined in 1920 the rupture-figures corresponding to the pressure of weightless or frictionless earth on a perfectly rough wall. In 1926 v. Karman solved the corresponding problem for heavy earth with internal friction.

Stability investigations and earth pressure calculations based on the maximum principle but assuming circular rupture-lines, were made by Fellenius in 1927. The circular rupture-line enables a simple analysis to be made for frictionless earth, because the unknown normal stresses do not enter into the moment equation about the centre of the circle. Later investigations (Skempton 1948 , Cadling and Odenstad 1950) have shown that this so-called "$\varphi = 0$"-method usually gives very reliable results, at least when used in stability analyses.

A corresponding calculation can be made for earth with internal friction, when suitable logarithmic spirals are used as rupture-lines. This is due to the fact that for such a spiral the angle between radius-vector and normal is constant, and when this angle is equal to φ , the unknown stresses in the spiral are directed towards its pole. Consequently, they do not enter into the moment equation about the pole. The first to make extensive use of this method was Rendulic (1935 and 1940), who succeeded in determining the general relation between the

magnitude of the earth pressure on a smooth vertical wall and the location of its pressure centre. Rendulic was also the first to calculate a composite rupture.

Until 1936, little or no attention was paid to the deformations accompanying the stresses in the earth. This may be due to the fact that in the plane case of plastic equilibrium the stresses can be determined without any investigation of the deformations. However, in 1936, Terzaghi drew attention to the fact that the deformations in the earth must be compatible with the movements of the wall. Consequently, the earth pressure must be a function of these movements. This is a very important fact, which the author has made one of the basic principles of his new method.

Ohde was well aware of the above-mentioned fact when, in 1938, he investigated in great detail the two special cases of a vertical wall rotating about its lower and upper edge respectively. In the latter case he assumed a circular rupture-line and made use of Kötter's equation. This, in combination with the 3 equilibrium conditions for the earth mass above the rupture-line, enabled him to determine the magnitude of the earth pressure and the location of its pressure centre. Moreover, Ohde was probably the first to point out the essential difference between a zone-rupture and a line-rupture. In a new series of articles (1948-53) Ohde has further developed his earth pressure theories.

In recent years the theories of plasticity have been developed considerably, mainly by Sokolovski (1942), Freudenthal (1950), Nadai (1950), Drucker, Hodge and Prager (1950-51). The author has also made a small contribution (Brinch Hansen 1952). It should be specially mentioned that Sokolovski has dealt with a great number of earth pressure and foundation problems. He considers zone-ruptures exclusively, however.

The above-mentioned works are mainly theoretical. As regards tests and practical experience, a considerable number of authors have concerned themselves with active earth pressure, whereas only a few have studied passive earth pressure (e.g. Franzius 1924). The most remarkable earth pressure tests have been made recently by Tschebotarioff (1948-51) and Rowe (1952), who have both proposed empirical calculation methods for anchored sheet walls.

The few names mentioned above indicate, in the author's opinion, the most important steps towards a clearer understanding of earth pressure problems and development of suitable calculation methods.

Many other authors have made more or less valuable contributions to earth pressure literature, which is now so plentiful that it would be quite out of the question to give a comprehensive review of it. Short historical summaries have been given by Feld (1928 and 1940), Brown (1948), Ohde (1948) and others. Further, Golder (1948) has written about Coulomb, and Cook (1951) about Rankine.

The list of references given in the Appendix is also far from being complete. It contains only the contributions which, in the author's opinion, are the most valuable.

14. Methods of Calculation

Practically every known method of earth pressure calculation belongs to one or another of the following four groups:

1) Extreme-methods (e.g. Coulomb, Fellenius, Rendulic)
2) Theories of plasticity (e.g. Rankine, Prandtl, Kötter, Frontard, Ohde)
3) Theories of elasticity (e.g. Boussinesq, Rifaat, Bretting)
4) Empirical methods (e.g. Christiani, Danish Rules, Tschebotarioff, Rowe)

An extreme-method is characterized by the fact that it makes use of one equilibrium-condition only, but supplements it by the necessary number of extreme-conditions, stating that the earth pressure should be a maximum (active pressure) or a minimum (passive pressure). It is essential that the unknown stresses in the rupture-line do not enter into the equations. This is obtained by choosing a logarithmic spiral as a rupture-line and taking the moments about its pole (Rendulic). From this moment equation the earth pressure can be found, provided that the location of the pressure centre is known. In the special case of frictionless earth the spirals become circles (Fellenius), and in the case of an infinitely distant pole they become straight lines (Coulomb).

The theories of plasticity determine, in principle, the 3 unknown stresses at any point by means of the 2 equilibrium conditions for a small earth element in combination with the failure condition. In practice, however, the exact integrations can only be carried out in a few simple cases, for example, with straight rupture-lines (Rankine) or with spiral and straight rupture-lines (Prandtl). Numerical integrations have been carried out by v. Karman and others.

From the 3 above-mentioned equations it is possible to derive a single equation expressing the variation of the stress in any given rupture-line (Kötter). In order to utilize this equation, however, it is necessary to know the stress in the rupture-line at the ground surface (or at another boundary). Unfortunately, this knowledge can only be obtained when the rupture-line intersects the surface at a certain angle, or when the earth is cohesionless and unloaded.

One way to utilize Kötter's equation is to consider only the boundary conditions at both ends of a rupture-line without investigating the equilibrium of the earth above the rupture-line. Such methods shall be termed boundary-methods. They presume that the rupture-line meets the surface and the wall at the statically correct angles, so that the boundary stresses can be determined. As Kötter's equation furnishes a relation between these stresses, the unit earth pressure can be calculated at the point where the rupture-line meets the wall. In special cases this can be done without investigating the actual shape of the rupture-line (Frontard), but in the general case this shape must be determined or assumed to be known (Jáky).

Kötter's equation, however, may also be used in an entirely different way, viz. for investigating the equilibrium of the earth mass above a rupture-line. Methods based on this principle, using all 3 conditions of equilibrium, but no extreme-condition, shall be termed equilibrium-methods. They presume that the

general shape of the rupture-line is known, and that the boundary stresses in the rupture-line at ground surface can be determined. In this case the equations of equilibrium enable the calculation of the earth pressure as well as the location of its pressure centre, provided that the location of the rotation centre is given (Ohde).

A special theory of plasticity is the so-called limit analysis (Drucker, Hodge and Prager). In this method it is shown that the actual value of the earth pressure lies within an interval, the limits of which can be determined by means of so-called statically admissible stress fields and kinematically admissible velocity fields respectively. For the latter it is found that the rupture-line must be a logarithmic spiral, and the calculation is then carried out as in Rendulic's method, using the extreme-principle.

Theories of elasticity are either exact or approximate. In the former case the 3 stresses and the 2 displacements at any point are, in principle, determined by Hooke's law and the equilibrium conditions for a small earth element. However, such exact calculations are only possible in very simple cases, for example that of a concentrated force on the surface of a semi-infinite elastic medium (Boussinesq).

Therefore, in applying theories of elasticity to earth pressure problems, some very simplifying assumptions are usually made. It may be assumed, for example, that passive earth pressure increases in direct proportion to the deflection of the wall, the ratio between pressure and deflection being proportional to the depth (Rifaat). For frictionless earth a more refined approximate theory of elasticity has been developed (Bretting).

Many of the approximate theories of elasticity must actually be considered as semi-empirical and are, as such, borderline cases of the fourth group, the empirical methods. These are based either on model tests (Tschebotarioff, Rowe), full-scale tests or general practical experience (Christiani, Danish Rules).

The empirical methods and the theories of elasticity both aim at an investigation of the stresses and deformations occuring under actual working conditions. This implies the advantage that the actual deformations of the structures can be calculated, and that the risk of cracking of reinforced concrete sections can be investigated. The safety against the first local failure can also be determined, but not the safety against the ultimate total failure.

Conversely, the extreme-methods and the theories of plasticity aim at an investigation of the stresses occurring in the state of failure. This implies the advantage that the safety against ultimate failure can be determined, and that the calculations become simpler and are independent of the previous "history" of the structure. The most notable shortcomings of these methods are that neither the actual deformations under normal working conditions nor the safety against local failure or cracking can be determined.

In practical engineering there seems to be an increasing tendency to employ design methods which are based on the state of failure. Coulomb's method was probably one of the first instances of this, and the conventional design of reinforced concrete sections is another. As further examples can be mentioned K.W.

Johansen's "rupture-line-theory" for slabs (1943), H. Lundgren's "stringer theory" for cylindrical shells (1949) and the "limit analysis" of Drucker, Hodge and Prager for general designing purposes (1951). The author's new earth pressure theory is based on the same principle.

15. Limitations of Known Methods

In order to be fully satisfactory a general earth pressure theory should enable a reasonably correct calculation of the earth pressure corresponding to any assumed movement of the retaining structure. We shall examine the known methods from this point of view.

Empirical methods may be very useful, but their proper application is usually limited to such constructions and conditions as they were originally developed for. Being thus neither general nor having any theoretical basis, they do not satisfy the requirements.

The theories of elasticity are far too complicated for practical use in engineering problems, unless very simplifying assumptions are made, and if such assumptions are made the methods usually give too inaccurate results. Moreover, all theories of elasticity possess the inherent defect of not giving any information about the safety against ultimate failure.

Of the extreme-methods we shall first consider Coulomb's. Actually, it is a method for calculating zone-ruptures, and as such its severest limitation is that it uses straight rupture-lines only. For active pressures this involves insignificant deviations only, but for passive pressures it often leads to considerable errors. For the calculation of line-ruptures Coulomb's method cannot be used at all, as it allows neither the determination of the pressure centre nor that of the rotation centre.

Although Fellenius' method may be used for zone-ruptures, its most important application is for the calculation of line-ruptures. As the rupture-line is a circle and the earth above the circle rotates as a rigid body, the rotation centre of the wall must be the normal projection of the centre of the circle on the wall. However, a unique solution is only possible for frictionless earth. If a circular rupture-line is used for earth with internal friction then additional and more or less arbitrary assumptions are necessary in order to solve the problem.

No such assumptions are necessary in Rendulic's method, because logarithmic spirals are used here as rupture-lines. Like Fellenius' method, Rendulic's can be used for zone-ruptures as well as for line-ruptures. It has the drawback, however, of not providing any definite relation between the spiral rupture-line and the corresponding rotation centre for the wall (at least when the earth is assumed incompressible). Actually, the spiral must be considered as an approximation of an unknown circular rupture-line.

In the theory of limit analysis (Drucker, Hodge and Prager) this drawback does not occur, as the rotation centre of the wall is found to be the normal projection of the pole of the spiral on the wall. However, this theory is based upon

an assumption regarding the dilatation, which does not seem to conform to experimental facts.

Exact solutions by means of the theories of plasticity such as Rankine's and Prandtl's may be very valuable, but they are only correct when the boundary conditions are properly satisfied. Otherwise, they are merely approximations. Moreover, Prandtl's solution is limited to the special cases of frictionless or weightless earth. Both solutions concern zone-ruptures only and are inapplicable to line-ruptures.

The boundary-methods must be subdivided into two groups. Those in which the shape of the rupture-line need not be known (Frontard) may lead to the correct results when the proper boundary conditions are used. Such methods, however, are limited to the special cases of frictionless or weightless earth. Those methods which require the knowledge of the shape of the rupture-line (Jáky) suffer from the defect that the equilibrium conditions for the earth mass above the rupture-line are usually not satisfied. This may imply very serious errors. Both groups of boundary-methods can only be applied to zone-ruptures, because they can only determine the earth pressure at a point where a rupture-line meets the wall.

We now have only the equilibrium-method left. Ohde used this method for the calculation of a line-rupture, but in the present work it shall be shown that it can also be applied to zone-ruptures and composite ruptures. Theoretically, a rupture-line should always make certain definite angles with the ground surface and the wall, but this requirement cannot be fulfilled by simple rupture-lines such as circles. However, for other angles the boundary conditions become indefinite, in which case it seems impossible to use the equilibrium-method at all. Ohde succeeded in doing so only because he considered the special case of cohesionless earth with an unloaded surface, in which case the boundary stress is zero, independent of the angle between rupture-line and surface.

It will thus be seen that none of the known methods satisfy the requirements for a general earth pressure theory, at least not in their present form.

16. Proposed New Method

In most cases, particularly for line-ruptures, it is impossible to satisfy at the same time the theoretical boundary conditions at both ends of a simple rupture-line and the equilibrium conditions for the earth mass above the rupture-line. The question then arises: Is it most important to do the former or the latter?

An answer to this question is provided by the fact that at least one of the extreme-methods, viz. the "$\varphi = 0$"-analysis by means of circular rupture-lines, is known to yield very reliable results (Skempton 1948, Cadling and Odenstad 1950) in spite of the fact that the critical rupture-circle usually meets the ground surfaces at angles differing considerably from the statically correct ones.

Consequently, it seems justifiable to draw the conclusion that the exact fulfilment of the boundary conditions (as regards the angles between rupture-lines and boundaries) is of minor importance and can, in fact, be completely disregarded without giving rise to important errors.

The only remaining obstacle to a general application of the equilibrium-method is the fact that, when a rupture-line does not meet a boundary at the statically correct angle, the corresponding boundary stress in the rupture-line is indefinite.

The author has overcome this difficulty in the following way: Let us consider a problem which can be solved by means of the extreme-method, employing, for example , spiral rupture-lines. The same problem might be solved by means of the equilibrium-method, if the boundary stress at one end of the spiral were known. A comparison will show that if a certain boundary stress is assumed the two methods will lead to identical results. Further investigation will show that this boundary stress corresponds to a special boundary condition, which does not require a certain angle between rupture-line and boundary, but merely indicates the boundary stress as a function of the actual angle.

By the thus established connection between the extreme-method and the equilibrium-method two things have been obtained. First, a special boundary condition has been found which enables the use of the equilibrium-method, irrespective of the value of the angle between rupture-line and boundary. Second, the results of such a calculation will be identical with those of a corresponding extreme-calculation and, therefore, just as reliable.

So far, we have considered the same rupture-line in both methods, viz. a logarithmic spiral, because in the general case of $\varphi \neq 0$ an extreme-calculation can only be made with such spirals. However, in the equilibrium-method the calculations will be simpler with circular rupture-lines, and in many cases, especially for line-ruptures, the actual rupture-lines must be circles (when incompressibility is assumed and the elastic deformations are disregarded). In fact, it is necessary to use circles in order to determine the location of the rotation centre for the wall.

Therefore, the next step is to consider an equilibrium-calculation in which the rupture-line is composed of one or more circles (or straight lines). When the same boundary condition is used as for the spiral, this must lead to very nearly the same results as those obtained with a single spiral rupture-line, simply because the two rupture-lines usually deviate only very slightly from each other.

That the calculated earth pressure is not influenced very much by reasonably small deviations from the actual rupture-line can be seen, for example, from this fact: The active earth pressure on a rough vertical wall, as calculated by means of Coulomb's method with a straight rupture-line, differs only by a few percent from the actual value, although the actual rupture-line is composed of a straight and a curved part.

In Kötter's equation and the author's boundary condition we have now the means of carrying out an equilibrium-calculation for a rupture-line of any shape. However, as already mentioned, it is preferable to use rupture-lines composed of circles (and straight lines), as this gives the simplest calculations, is sufficiently correct and often necessary for kinematical reasons.

17. Short Review of Contents

After the general introduction, given in the present Section 1, the known methods of calculation are described in greater detail in Section 2. First, in Section 21, the extreme-methods of Coulomb, Fellenius and Rendulic are considered. Next, in Section 22, the theories of plasticity are dealt with, embracing the theoretical solutions of Rankine and Prandtl, the boundary-methods of Frontard and Jáky as well as Ohde's equilibrium-method and the Limit Analysis of Drucker, Hodge and Prager. In Section 23, some theories of elasticity are mentioned, viz. the methods of Rifaat and Bretting. Finally, in Section 24, some empirical methods are considered, viz. those of Christiani, the Danish Rules, Tschebotarioff and Rowe.

In Section 3, the theoretical basis of the author's new method is developed. Section 31 states the basic assumptions and main principles. In Section 32 some geometrical formulae together with formulae for surcharges and earth weights are given. Next, in Section 33, formulae are developed for the internal stresses and their resultants in circular and straight rupture-lines. The boundary conditions are developed in Section 34 for ground surfaces, walls and internal boundaries. Further, in Section 35, a number of rupture-figures are analysed, including line-ruptures, zone-ruptures and some composite ruptures. In Section 36, the possible states of failure are discussed, both those occurring in earth pressure investigations of single and composite structures, and those envisaged in stability investigations. Finally, in Section 37, it is indicated how the soil constants should be determined, and a proposal for the introduction of suitable safety factors is given.

Section 4 deals with the general methods for calculating the earth pressures corresponding to different figures of rupture. The general principles are described in Section 41. In Section 42, line-ruptures are investigated, and in Section 43, zone-ruptures. Different types of composite ruptures are dealt with in Sections 44, 45 and 46. Finally, in Section 47, a tentative proposal is made for determining the approximate distribution of the calculated earth pressures.

Section 5 considers the problem of determining the earth pressure on a rigid vertical wall, rotating about any given point. The ground surface is assumed horizontal. Three simple special cases are investigated, viz. frictionless earth, weightless earth and cohesionless, unloaded earth. After an introduction in Section 51 zone-ruptures are investigated in Section 52, line-ruptures in Section 53 and different composite ruptures in Sections 54, 55, 56, 57 and 58. At first only two friction angles are considered, viz. 0° and 30°, but in Section 59, it is shown how the results can be applied, approximately, to other friction angles. In Section 5 a number of photographs are reproduced, indicating the results of model tests made by the author.

In Section 6, some more complicated cases are considered. Section 61 shows how the general case of heavy earth with surcharge, cohesion and internal friction can be treated approximately by superposition of the individual cases. Section 62 deals with the effect of water pressures, both hydrostatic and hydrody-

namic. Section 63 treats different cases of layered or stratified earth, for which simplified approximate calculation methods are proposed. Further, Section 64 deals with cohesive earth, in which part of the earth front can stand unsupported while the wall moves away from it. Finally, in Section 65, sloping surfaces and inclined walls are investigated.

In Section 7, the new method is applied to a number of practical earth pressure problems. Different design methods are developed and several numerical examples are given. Section 71 deals with retaining walls, Section 72 with anchor slabs, Section 73 with free sheet walls, Section 74 with anchored sheet walls, Section 75 with fixed sheet walls and, finally, Section 76 with braced walls in cuts, and with unyielding walls.

Section 8 deals with some stability and foundation problems. In Section 81, the new method is applied to the stability of cellular cofferdams on rock, and, in Section 82, to cellular cofferdams in earth, or double sheet walls. Finally, Section 83 indicates some other possible applications, viz. regarding the determination of anchor lengths, the stability of slopes, and strip foundations.

In Section 9, the new method and its applications are reviewed. The necessity of comparing its results with experiments and practical experience is stressed, and a few general comparisons are made. Lastly, the author's original contributions to the subject of earth pressure calculation are listed, and the most important of the still unsolved problems are mentioned.

Finally, the present book contains an Appendix, including a list of notations and sign rules, an English and a Danish Summary, a list of references and an Index. Moreover, the Appendix contains 5 tables, by means of which a comparatively easy application of Kötter's equation is made possible, and 20 graphs, by the aid of which it is possible to calculate the earth pressure on a vertical wall for any given location of the rotation centre.

2. THE KNOWN METHODS

21. EXTREME-METHODS

211. General

A method, in which earth pressure problems are solved by means of a single condition of equilibrium in connection with a maximum or minimum condition, shall here be termed an extreme-method.

If the problem shall be solved without making additional assumptions, it is necessary to choose such rupture-lines that an equation of equilibrium can be developed in which the unknown stresses in the rupture-line do not enter. This condition is, in the general case of $\varphi \neq 0$, satisfied by the moment equation about the pole of a logarithmic spiral, the radius-vectors of which make an angle φ with the normals (Rendulic). In the special case of frictionless earth the spirals become circles (Fellenius), and in the case of an infinitely distant pole straight lines are obtained (Coulomb).

The principle of the extreme-method is now to choose, of all the possible rupture-lines, the one for which the earth pressure resultant (determined by means of the above-mentioned equilibrium equation) attains an extreme value, i.e., a minimum for passive earth pressure and a maximum for active. If this is done analytically, the extreme-condition gives as many equations as the number of independent geometrical parameters for the rupture-line. These equations, in combination with the above-mentioned equilibrium condition, suffice to determine the parameters of the rupture-line and the magnitude of the earth pressure, provided that the direction of the earth pressure resultant as well as the location of its pressure centre are known. In the special case of a straight rupture-line (Coulomb) it is not necessary to know the location of the pressure centre.

212. Coulomb's Method

The principle of this method is the following: We consider an earth wedge bounded by the surface, the wall and a straight rupture-line through the foot of the wall. All forces acting upon this wedge are projected on a line making an angle φ with the rupture-line. This gives an equation, from which we can find the normal earth pressure component E as a function of the angle β between rupture-line and horizon. Differentiating E with respect to β, and putting the differen-

tial quotient equal to zero (according to the extreme-condition) a second equation is obtained which, together with the original equation, suffices to determine β and E.

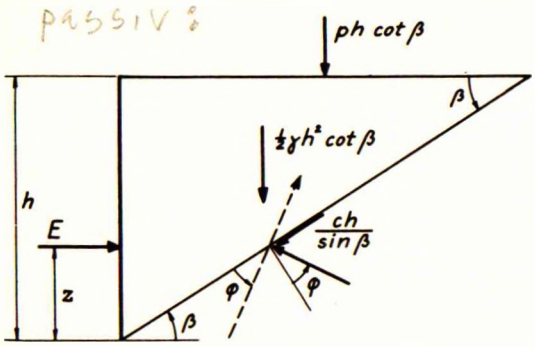

Fig. 21A: Coulomb's method for a smooth vertical wall

Fig. 21A shows the case of a smooth vertical wall and a horizontal ground surface. The surface is loaded with a surcharge p per unit area, and the height of the wall is h. The earth has a unit weight γ, a friction angle φ and a cohesion c, corresponding to Coulomb's law regarding the greatest possible value of the shearing stress τ in a plane with the normal stress σ:

$$\tau \leq c + \sigma \tan \varphi \qquad 2101$$

By projection of the acting forces on the dotted line, we get an equation which can be written in the following form:

$$E = (\tfrac{1}{2}\gamma h^2 + ph) \cot \beta \tan(\beta+\varphi) + ch \frac{\cos \varphi}{\sin \beta \cos(\beta+\varphi)} \qquad 2102$$

Putting the differential quotient of E with respect to β equal to zero, an equation is obtained which can only be satisfied when:

$$\cos(2\beta+\varphi) = 0 \qquad \text{or} \qquad \beta = 45^\circ - \tfrac{1}{2}\varphi \qquad 2103$$

Inserting 2103 in 2102 the extreme value of the earth pressure is found:

$$E = (\tfrac{1}{2}\gamma h^2 + ph) \tan^2(45^\circ + \tfrac{1}{2}\varphi) + 2ch \tan(45^\circ + \tfrac{1}{2}\varphi) \qquad 2104$$

With positive values of φ and c we get the passive earth pressure, whereas negative values give the active pressure.

Fig. 21B shows a case which in several ways is more general, because it concerns a sloping ground surface and an inclined wall with a roughness corresponding to a wall friction angle δ. In one way it is more special, however, because we consider cohesionless earth only. Using in principle the same procedure as above we can find:

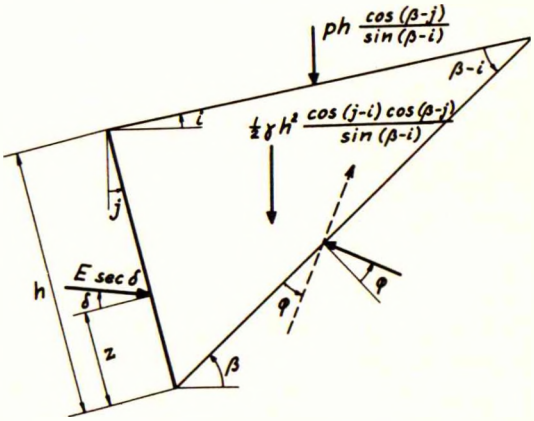

Fig. 21B: Coulomb's method for inclined wall and cohesionless earth

$$\cot(\beta-i) = \tan(\varphi+\delta+i-j) + \sec(\varphi+\delta+i-j)\sqrt{\frac{\sin(\varphi+\delta)\cos(\delta-j)}{\sin(\varphi+i)\cos(j-i)}} \qquad 2105$$

$$E = \left[\tfrac{1}{2}\gamma h^2 + ph\sec(j-i)\right]\frac{\cos\delta\sec(\delta-j)\cos^2(\varphi+j)}{\left[1 \mp \sqrt{\frac{\sin(\varphi+\delta)\sin(\varphi+i)}{\cos(\delta-j)\cos(j-i)}}\right]^2} \qquad 2106$$

φ and δ should be assumed positive for passive pressure, negative for active pressure. i and j should also be inserted with correct signs; in Fig. 21B, they are shown positive. Of the double signs in 2106 the upper one should be used for passive pressure and the lower for active.

It should be noted that h is measured along the wall, that p is the vertical surcharge per unit area of the sloping surface, and that E is the earth pressure component normal to the wall.

As long as we consider only a rupture-line through the foot of the wall, Coulomb's theory does not provide us with any means of determining the earth pressure distribution, not even the location of the pressure centre.

This difficulty is usually overcome by assuming that a rupture-line departs from any point of the wall. In that case the developed formulae are valid for any depth h smaller than the total height of the wall. This shows that the pressure distribution must be "hydrostatical", i.e., the p-term in E must correspond to a uniform distribution and the γ-term to a triangular distribution.

However, it must also be assumed that the stresses in the straight rupture-line are hydrostatically distributed, and this is actually the fact. It will then be found that the remaining two conditions of equilibrium for the earth wedge cannot be satisfied, except in special cases such as, for example, that of a horizontal surface and a smooth vertical wall.

This means that either the earth pressure distribution is not hydrostatical, or the rupture-line is not straight, or both. Actually, Coulomb's method must be considered as an approximate means of calculating a zone-rupture; in this case the actual earth pressure distribution is hydrostatical, but the actual rupture-line is usually not straight.

In spite of this theoretical inconsistency, it has been found that active earth pressures calculated by means of Coulomb's method are only a few percent smaller than the correct values. On the other hand, passive earth pressures as found by Coulomb's method may exceed the correct values by 50% or more.

Consequently, Coulomb's method is most suitable in the case of active zone-ruptures. Such ruptures occur, for example, in the backfill of retaining walls, and for these structures the method is, therefore, a very reliable means of design and calculation.

For line-ruptures Coulomb's method cannot be used at all, because the location of the pressure centre (z) does not enter into the calculation of E.

213. Fellenius' Method

When applied to frictionless earth, the principle of this method is the following: We consider an earth wedge bounded by the surface, the wall and a circular rupture-line through the foot of the wall (Fig. 21C). The moments of all forces acting upon this wedge are taken about the centre of the circle. Provided that the location of the pressure centre is known, this gives an equation, from which we can find the earth pressure E as a function of the geometrical parameters α and β of the circle. Putting the differential quotients of E, with regard to α and β respectively, equal to zero, two additional equations are obtained which, together with the original equation, suffice to determine α, β and E.

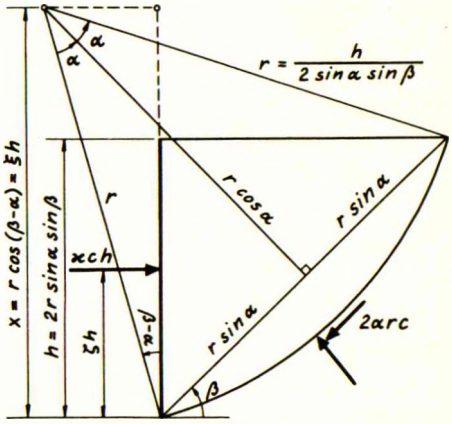

Fig.21C: Fellenius' method for frictionless earth

Fig. 21C illustrates the case of a smooth vertical wall and a horizontal ground surface. It is easy to show that, when $\varphi = 0$, the earth pressure is the sum of a "hydrostatical" component and a component which is proportional to ch, so that we can write:

$$E = \tfrac{1}{2}\gamma h^2 + ph + ch\kappa \qquad 2107$$

In order to determine κ we consider the case $\gamma = 0$, $p = 0$. By taking the moments of the acting forces about the centre of the circle the unknown normal stresses in the circle are eliminated, and we find:

$$\kappa = \frac{\alpha\,(1 + \cot^2\alpha)(1 + \cot^2\beta)}{\cot\alpha \cot\beta + 1 - 2\zeta} \qquad 2108$$

Differentiating 2108 partially with regard to α and β respectively, and putting the differential quotients equal to zero, we get the following equations:

$$\alpha \cot\beta\,(1 + \cot^2\alpha) = (2\alpha \cot\alpha - 1)(\cot\alpha \cot\beta + 1 - 2\zeta) \qquad 2109$$

$$\cot\alpha\,(1 + \cot^2\beta) = 2 \cot\beta\,(\cot\alpha \cot\beta + 1 - 2\zeta) \qquad 2110$$

When ζ is known, 2109-10 can be solved by trial, for example by estimating a value of α, finding the corresponding β from 2109 and investigating whether 2110 is satisfied. If not, α must be changed until satisfactory agreement is obtained. When α and β have been determined, 2108 gives κ, and 2107 yields then E. c should be assumed positive for passive pressure, negative for active pressure.

Fellenius himself did not give his method quite as general a form as described above. He put, arbitrarily, $\zeta = \frac{1}{3}$ and found then $\alpha = 15°$, $\beta = 47.5°$ and $\kappa = 1.916$. This he considered a better approximation than the value $\kappa = 2$, which is found by means of a straight rupture-line (using 2104 with $\varphi = 0$).

However, if Fellenius' method is considered as an approximate means of calculating a zone-rupture, then the last term in 2107 corresponds evidently to a uniform distribution, and one must put $\zeta = \frac{1}{2}$. This would give $\alpha = 0°$, $\beta = 45°$ and $\kappa = 2$ in agreement with 2104.

On the other hand, Fellenius' method may be considered as an excellent means of calculating a line-rupture. In that case his calculation is correct but concerns only the special case of $\zeta = \frac{1}{3}$, or (from a kinematical point of view), $\xi = 2.21$, as the location of the rotation centre of the wall is determined by the following equation (see Fig. 21C):

$$\xi = \frac{x}{h} = \tfrac{1}{2}\,(1 + \cot\alpha \cot\beta) \qquad 2111$$

This gives the method a much wider application than realized by Fellenius himself, as it enables the determination of the earth pressure and the location of the pressure centre, corresponding to any given location of the rotation centre of the wall. That this is so can be seen from the fact that, with a given ξ, the four equations 2108-11 allow the determination of the four unknown quantities α, β, κ and ζ.

Apart from the determination of the pressure centre the earth pressure distribution cannot be determined by means of the described method.

Fellenius used circular rupture-lines also in the case of $\varphi \neq 0$, but as it is necessary in this case to make additional, more or less arbitrary assumptions, the method is not a pure extreme-method any longer.

214. Rendulic's Method

This method may be considered as an extension of Fellenius' to the case of $\varphi \neq 0$. As rupture-lines, logarithmic spirals are used, with an angle φ between the radius-vectors and the normals. This implies that, apart from a possible cohesion c, the resulting stress on each element of the rupture-line is directed towards the pole of the spiral, so that only the cohesion gives any moment about the pole.

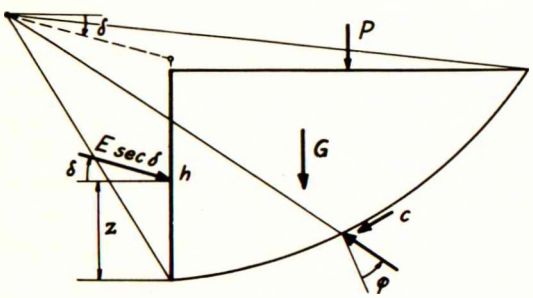

Fig. 21D: Rendulic's method for earth with internal friction

The theoretical principle of the method is now the following: We consider an earth wedge bounded by the surface, the wall and a spiral rupture-line through the foot of the wall (Fig. 21D). The moments of all forces acting upon this wedge are taken about the pole of the spiral.

Provided that the location of the pressure centre is known this gives an equation, from which we can find the earth pressure E as a function of two geometrical parameters of the spiral. Putting the partial differential quotients of E, with respect to these parameters, equal to zero, two additional equations are obtained which, together with the original equation, suffice to determine the two parameters and E.

However, an analytical calculation as described would become rather complicated. Therefore, only the original moment equation is used in its analytical form to determine the value of E corresponding to any estimated position of the spiral, and with a fixed location of the pressure centre. The critical spiral, i.e., the one making E a maximum (active pressure) or a minimum (passive pressure), is then found by trial.

Rendulic himself carried out his calculations in a slightly different way, but the principles were essentially the same and the results exactly the same. He considered in great detail the special case of a smooth vertical wall, cohesionless earth with $\varphi = 30°$ and a horizontal, unloaded surface. Apart from rupture-lines consisting of a single spiral he also investigated composite rupture-lines consisting of a logarithmic spiral and a straight line meeting at some point of the wall.

In this way Rendulic succeeded, as the first, in determining the complete relationship between the magnitude of the earth pressure (E) and the location of its pressure centre (z). He found a curve resembling closely the one marked "smooth" on Graph 13 in the Appendix.

Further, he tried to determine the rotation centre of the wall, corresponding to any given critical spiral. In order to do this he had to make certain assumptions, and as a result of these he deduced the following rule: The rotation centre is the point where the wall is intersected by a straight line through the pole parallel to the direction of the earth pressure resultant (Fig. 21D).

However, if we assume incompressibility of the earth, the above result cannot be correct. In this case the actual rupture-line must be a circle which, in Rendulic's method, is approximated by a logarithmic spiral. The actual rotation centre must be the normal projection of the centre of the circle on the wall, and this point will only in special cases coincide with the point determined by Rendulic's rule. Consequently, the location of the rotation centre can actually not be determined by means of Rendulic's method.

Finally, Rendulic also tried to determine the distribution of the earth pressure. To this end he assumed that a spiral rupture-line must depart from any point of the wall and that, therefore, his relation between E and z should be valid for any depth smaller than the total height of the wall. This enabled him to determine pressure diagrams which bear a marked resemblance to the tentative pressure diagrams proposed by the author (Section 473).

However, Rendulic was apparently not aware that also his pressure diagrams are merely tentative approximations, since in a line-rupture only one rupture-line meets the wall. Consequently, the pressure distribution is in principle indeterminable.

22. THEORIES OF PLASTICITY

221. General

Theories of plasticity are based on the assumption that a state of failure exists at any point within a certain area (zone-ruptures) or on a certain curve (line-ruptures). By means of this assumption, in connection with the equations of equilibrium, it is in principle possible to solve earth pressure problems.

In the case of plane strain Coulomb's law is usually accepted as the condition of failure:

$$\tau = c + \sigma \tan \varphi \qquad 2201$$

A rupture-line is defined as a line in which τ and σ satisfy the relation 2201. In all other lines τ is smaller than the function of σ indicated by the right side of 2201.

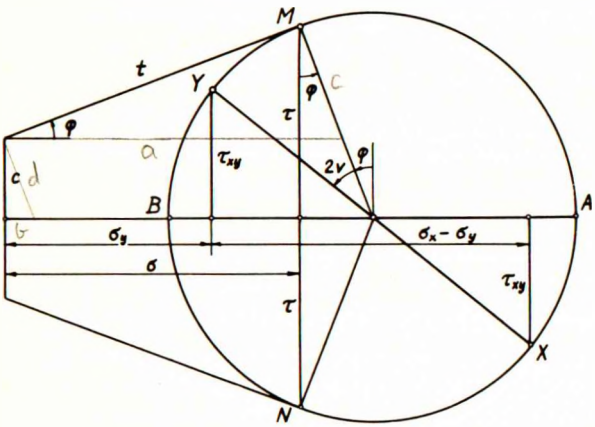

Fig.22A: Mohr's circle for stresses

The variation of the stresses in different lines through a point may be illustrated by means of Mohr's circle (Fig.22A). From this it can be seen that two different rupture-lines (corresponding to points M and N on the circle) pass through each point, making angles of $90^\circ \pm \varphi$ with each other. The lines of principal stresses (corresponding to points A and B) bisect the angles between the rupture-lines.

Fig. 22A also shows that, if σ_x, σ_y and τ_{xy} are the stresses in any pair of orthogonal lines (corresponding to points X and Y), the failure condition 2201 can be expressed as follows:

$$(\sigma_x - \sigma_y)^2 + 4\tau_{xy}^2 = \left[(\sigma_x + \sigma_y) \sin \varphi + 2c \cos \varphi\right]^2 \qquad 2202$$

Using an orthogonal coordinate system with a horizontal X-axis and a vertical Y-axis (positive downwards), the equations of equilibrium for an infinitely small earth element are:

$$\frac{\partial \sigma_x}{\partial x} + \frac{\partial \tau_{xy}}{\partial y} = 0 \qquad \frac{\partial \sigma_y}{\partial y} + \frac{\partial \tau_{xy}}{\partial x} = \gamma \qquad 2203\text{-}04$$

In principle, the 3 equations 2202-04, together with the necessary statical boundary conditions, suffice to determine the 3 stresses σ_x, σ_y and τ_{xy} at any point where failure occurs. This determination of the stresses is thus possible without any investigation of the deformations. However, this does not mean that arbitrary deformations can be associated with the calculated stresses.

Instead of the 3 unknown stresses we can introduce 2 other variables, viz., the resulting stress $t = \sigma \sec \varphi$ in the rupture-line (exclusive of the cohesion c), and the angle v between rupture-line and horizon. By means of Fig. 22A we find:

$$\begin{matrix}\sigma_x \\ \sigma_y\end{matrix} = (t \sec \varphi + c \tan \varphi) \mp (t \tan \varphi + c \sec \varphi) \sin(2v+\varphi) \qquad 2205$$

$$\tau_{xy} = (t \tan \varphi + c \sec \varphi) \cos(2v+\varphi) \qquad 2206$$

As 2205-06 satisfy 2202, we have the 2 equations 2203-04 for the determination of t and v. By different transformations the following equation can be derived:

$$\frac{\partial t}{\partial s} + 2 (t \tan \varphi + c \sec \varphi) \frac{\partial v}{\partial s} + \gamma \sin(v+\varphi) = 0 \qquad 2207$$

and a similar one for the other rupture-line. s is the arch length of the rupture-line in question.

In the special case of cohesionless earth ($c = 0$), equation 2207 is reduced to the following, which is known as Kötter's equation:

$$\frac{\partial t}{\partial s} + 2t \tan \varphi \frac{\partial v}{\partial s} + \gamma \sin(v+\varphi) = 0 \qquad 2208$$

In the other special case of frictionless earth ($\varphi = 0$) equation 2207 yields:

$$\frac{\partial \sigma}{\partial s} + 2c \frac{\partial v}{\partial s} + \gamma \sin v = 0 \qquad 2209$$

In the present work any of the 3 equations 2207-09 will be referred to as Kötter's equation.

In two special cases it is possible to indicate simple, exact solutions of the equations 2202-04, viz., by assuming straight rupture-lines (Rankine) or by considering frictionless or weightless earth (Prandtl).

Kötter's equation can be utilized in two different ways. In the special cases of weightless or frictionless earth it is possible to integrate 2207 without knowing the actual shape of the rupture-line. This enables the solution of some earth pressure problems by means of Kötter's equation and the boundary conditions alone, without any investigation of the equilibrium of the earth mass above the rupture-line. Such methods shall be termed boundary-methods (Frontard, Jáky).

If the general shape of the rupture-line is known, as is the case for line-ruptures, Kötter's equation, in combination with a boundary condition at one end, enables the determination of the stresses in the rupture-line. An earth pressure calculation can then be carried out by means of the 3 equilibrium conditions for the earth mass above the rupture-line. Such methods shall be termed equilibrium-methods (Ohde and the author).

222. Rankine's Solution

Rankine (1857) considered the case of a semi-infinite cohesionless earth mass with a sloping surface making an angle i with the horizon. He assumed the whole earth mass to be in a state of failure and could then show that the rupture-figure consists of two systems of straight parallel lines, intersecting each other at angles of $90° \pm \varphi$.

That straight rupture-lines are a possible solution can be seen from 2207, which is satisfied when v = constant and: $\frac{\partial v}{\partial s} = 0$

$$t = \gamma(s'-s)\sin(v+\varphi) + t' \qquad 2210$$

v can be determined by the condition that the resulting stress on a vertical line must be parallel to the surface. Conversely, the resulting stress on a line parallel to the surface must be vertical.

Analytically, Rankine's solution for the case p = 0, c = 0 can be expressed by means of the following equations, where d is the vertical depth below the surface:

$$\sigma_x = \gamma d K^2 \qquad \sigma_y = \gamma d(1+K^2\tan^2 i) \qquad \tau_{xy} = \gamma d K^2 \tan i \qquad 2211\text{-}13$$

The constant K is determined by:

$$\frac{1}{K} = \sec\varphi \mp \sqrt{\sec^2\varphi - \sec^2 i} \qquad 2214$$

The upper sign is valid for the passive state, the lower for the active. As $dd = dy = -dx \cdot \tan i$, it is easy to ascertain that the equations 2211-14 satisfy the equilibrium conditions 2203-04 as well as the failure condition 2202.

In employing the Rankine theory it is usually assumed that the presence of a wall does not alter the stresses in the earth. This implies, however, that only in special cases will the resulting stress on the wall have the exact direction consistent with the actual roughness of the wall. This is the most serious shortcoming in the Rankine theory.

In the special case of a horizontal surface and a smooth vertical wall the same (correct) result is obtained as by means of Coulomb's theory. The corresponding figures of rupture are shown in Fig. 22B (the active state left, the passive right).

Actually, Rankine-zones occur in practically all cases of zone-ruptures, viz. near the ground surface. Another Rankine-zone will occur near the wall except when it is perfectly rough ($\delta = \varphi$), but between these two zones the Rankine state is generally not possible.

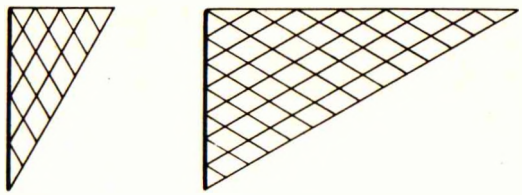

Fig.22B: Active and passive Rankine-zones

223. Prandtl's Solution

Prandtl (1920 and 1927) considered the case of a sector-shaped zone of weightless earth ($\gamma = 0$). He found that in this case the rupture-figure consists of a system of straight lines through the apex and a system of logarithmic spirals with the apex as their pole.

For $\gamma = 0$, equation 2207 requires t = constant when v = constant, which shows that in weightless earth the stress is constant along any of the straight rupture-lines. The variation of t along a spiral rupture-line is found by integration of 2207:

$$t = (t' + \frac{c}{\sin \varphi}) \, e^{2(v'-v)\tan \varphi} - \frac{c}{\sin \varphi} \qquad 2215$$

In this case a polar coordinate system is the most suitable. The equations of equilibrium for a small earth element will then be:

$$r \frac{\partial \sigma_r}{\partial r} + \frac{\partial \tau_{rv}}{\partial v} + \sigma_r - \sigma_v - \gamma r \cos v = 0 \qquad 2216$$

$$r \frac{\partial \tau_{rv}}{\partial r} + \frac{\partial \sigma_v}{\partial v} + 2\tau_{rv} + \gamma r \sin v = 0 \qquad 2217$$

The failure condition is expressed by an equation such as 2202, when σ_x, σ_y and τ_{xy} are substituted by σ_r, σ_v and τ_{rv}.

In the case of $\gamma = 0$, $c = 0$, Prandtl's solution can be expressed by means of the following equations, where $\mu = \tan \varphi$:

$$\sigma_r = K(1+2\mu^2)e^{-2\mu v} \qquad \sigma_v = Ke^{-2\mu v} \qquad \tau_{rv} = K\mu e^{-2\mu v} \qquad 2218\text{-}20$$

The constant K must be determined by the boundary conditions. The passive state is obtained with a positive μ, the active with a negative μ. It is easy to ascertain that the equations 2218-20 satisfy the equilibrium conditions 2216-17 as well as the failure condition (corresponding to 2202).

In the special case of frictionless earth ($\varphi = 0$), the problem can also be solved when $\gamma \neq 0$, $c \neq 0$. The rupture-lines are then concentric circles and straight lines through the centre, and the stresses are:

$$t = \sigma_r = \sigma_v = K_o - 2vc + \gamma r \cos v \qquad \tau_{rv} = c \qquad 2221\text{-}22$$

Prandtl-zones seldom occur alone, but often in combination with Rankine-zones. The apex is usually located at some singular point such as, for example, the point where the ground surface meets the wall. When the wall is perfectly rough, the Prandtl-zone may touch the wall in its entire length. As an example, the figures of rupture for the special case of a horizontal surface and a rough vertical wall are shown in Fig. 22C (the active state left, the passive right).

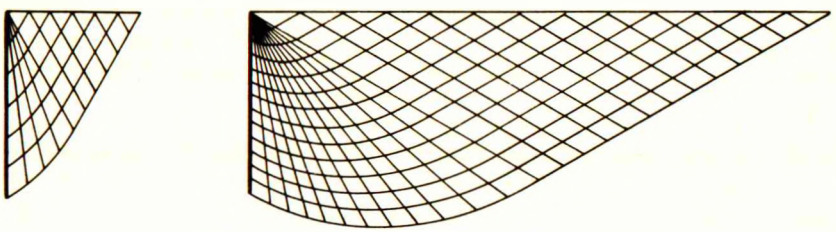

Fig. 22C: Active and passive Prandtl-zones in weightless earth

In the general case of $\gamma \neq 0$, $\varphi \neq 0$, no exact mathematical solution can be indicated, but approximate solutions can be obtained in different ways (v. Kármán 1926 and Ohde 1938).

224. Boundary-Methods

The characteristic feature of a boundary-method is the use of Kötter's equation in connection with the boundary conditions at both ends of the rupture-line, whereas the equilibrium of the earth mass above the rupture-line is not investigated.

The statically correct boundary conditions for the general case shall not be given here, but are developed in Sections 342-43. It can be mentioned, however, that a rupture-line should intersect a perfectly smooth boundary at an angle of $45^\circ \pm \frac{1}{2}\varphi$ and a perfectly rough boundary at an angle of $90^\circ \pm \varphi$, the sign depending on the direction of the shear stress in the rupture-line. The corresponding relations between the stress t in the rupture-line and the external normal stress p_s (smooth boundary) or p_r (rough boundary) are:

$$t' = p_s \tan(45^\circ \pm \tfrac{1}{2}\varphi) \pm c \qquad 2223$$

$$p_s = (t'' \mp c) \cot(45^\circ \pm \tfrac{1}{2}\varphi) \qquad p_r = t'' \cos \varphi \qquad 2224\text{-}25$$

Fig. 22D illustrates an earth pressure calculation by means of the boundary-method, concerning the case of passive earth pressure against a rough, inclined

wall. The earth is frictionless and has a horizontal surface loaded with a vertical surcharge p.

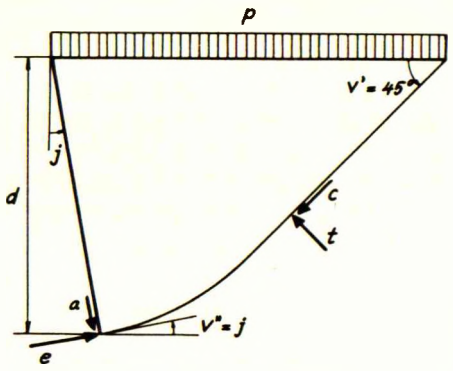

Fig.22D: Boundary-calculation for pressure of frictionless earth

According to the above-mentioned boundary conditions, we must have, for $\varphi = 0$:

$$v' = 45^\circ = \tfrac{1}{4}\pi \qquad 2226\surd$$

$$t' = p + c \qquad 2227\surd$$

$$v'' = j \qquad e = t'' \qquad 2228\text{-}29\surd$$

If we now insert these two sets of values separately in 2221, substituting r cos v by the vertical depth d, we get two equations, from which K_o can be eliminated. This gives the following expression for the unit earth pressure normal to the wall:

$$e = \gamma d + p + c\,(1 + \tfrac{1}{2}\pi - 2j) \qquad 2230\surd$$

In this case the boundary method yields the correct result in spite of the fact that the equilibrium of the earth mass above the rupture-line has not been investigated. Serious errors may be introduced, however, when the boundary conditions are not quite clear, or when the method is used in the general case of $\gamma \neq 0$, $\varphi \neq 0$.

Frontard (1922 and 1948) investigated a slope, making an angle i with the horizon, in a frictionless material (Fig.22E). He assumed that the rupture-line must make angles of 45° with the upper surface and the inclined slope respectively. This gives, using 2223-24 with $\varphi = 0$:

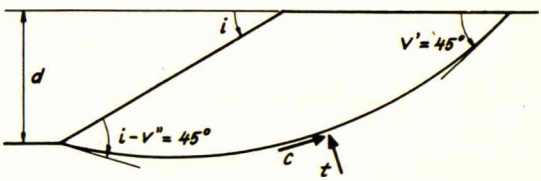

Fig.22E: Boundary-calculation for slopes in frictionless earth

$$v' = 45^\circ = \tfrac{1}{4}\pi \qquad t' = -c \qquad v'' = i - 45^\circ = i - \tfrac{1}{4}\pi \qquad t'' = c \qquad 2231\text{-}34\surd$$

When these two sets of values are inserted separately in 2221, substituting r cos v by d and changing the sign of c, two equations are obtained, from which K_o can be eliminated. This leads to the following formula for the critical height of the slope:

$$d = \frac{c}{\gamma}\,(2 + \pi - 2i) \qquad 2235\surd$$

Whereas this formula is correct for $i \to 0$, it gives for $i = \frac{1}{2}\pi$ (vertical bank) only about half the height obtained by a "$\varphi = 0$"-analysis (Fellenius).

This must be due to the arbitrary choice of v". Actually, at a singular point, such as the foot of the slope, no definite value can be assigned to v".

Jáky (1936) made a similar mistake when he investigated slopes in a material with internal friction. In this case it is necessary to know the shape and position of the rupture-line in order to use Kötter's equation. Jáky assumed a circular rupture-line, intersecting the upper surface and the inclined slope at the statically correct angles. By means of Kötter's equation and the boundary conditions alone he then developed a formula for the critical height of the slope. However, its value is very problematical, as an investigation of the earth mass above the rupture-circle (which Jáky did not carry out) will show that the conditions of equilibrium are usually far from being fulfilled.

225. Equilibrium-Methods

The characteristic feature of an equilibrium-method is that the unknown quantities are determined by means of the 3 conditions of equilibrium for the earth mass above the rupture-line, without the aid of any extreme-conditions. The general shape of the rupture-line must be known (or approximated), and the necessary determination of the stresses in the rupture-line is effected by means of Kötter's equation and a boundary condition.

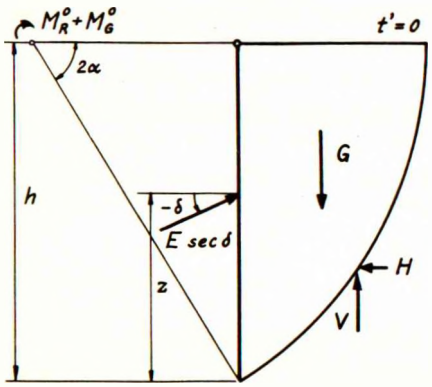

Fig. 22F: Equilibrium-calculation for cohesionless unloaded earth

As a typical example we shall consider Ohde's calculation (1938) of the active earth pressure on a vertical wall rotating about its upper edge. The earth is assumed cohesionless and the surface horizontal and unloaded (Fig. 22F).

Ohde first showed that the assumed movement of the wall excludes the existence of a zone-rupture behind the wall. Consequently, only a single rupture-line can occur, and this must be a circle, when the elastic deformations are disregarded and incompressibility is assumed. Moreover, the centre of this circle must be located at a normal to the wall through the rotation centre in order to enable the earth wedge to follow the movement of the rigid wall.

For a circular rupture-line it is easy to integrate Kötter's equation, putting $ds = r\,dv$ and assuming r = constant. By means of further integrations the resultant of the stresses in the whole rupture-circle can be determined or, rather, its vertical component V, horizontal component H and moment M_R^o about the centre of the circle. Such formulae are developed in Section 33.

However, all these formulae contain an unknown stress t' (e.g. at the ground surface), which must be determined by a boundary condition. In the case

considered by Ohde this condition is simple and obvious: when $p = 0$ and $c = 0$, we must have $t' = 0$ at the surface.

The only unknown quantities in the problem are the following 3 : the central angle (2α) of the circle, the normal component (E) of the earth pressure, and the height (z) of the pressure centre above the foot of the wall. For their determination we have the following 3 equations of equilibrium for the earth mass above the rupture-line:

$$(V - G) \cos \delta - H \sin \delta = 0 \qquad E = H \qquad 2236\text{-}37$$

$$E (h - z) = M_G^o + M_R^o + E \tan \delta \cdot h \cot 2\alpha \qquad 2238$$

From 2236 the angle α can be found, then E from 2237 and, finally, z from 2238. It is, however, impossible to determine the actual distribution of the earth pressure by means of this method.

After having carried out the calculation as described, Ohde tried to determine the earth pressure distribution empirically as a simple curve. He assumed, however, that the pressure curve could have no point of contraflexure, and on this (wrong) assumption he found it impossible to make the stresses at the lowest points of the wall and the rupture-line agree. As a result he rejected Kötter's equation as a basis for his calculation and substituted it by an empirical pressure distribution involving certain constants which had to be determined by extreme-conditions. The calculation thereby became considerably more complicated, and actually less accurate than his original calculation by means of Kötter's equation.

In the general case of $p \neq 0$, $c \neq 0$ an equilibrium-calculation is confronted by the difficulty that a unique boundary condition can only be indicated when the rupture-line meets the boundary at the statically correct angle (see Section 224). In most line-ruptures this will not be the case, and consequently the equilibrium-method in its existing form cannot be used.

In the present work, the author has solved this problem by establishing a connection between the equilibrium-method and the extreme-method, by means of which a general application of the equilibrium-method has been made possible. The new method, of which a detailed account is given in Section 3, is essentially an equilibrium-method, although in some cases it employs the principles of the boundary-method, too.

226. Limit Analysis

A special theory of plasticity has recently been developed by Drucker and Prager (1951) under the name of "Limit Analysis", and they have also attempted to apply it to earth pressure problems.

They define first a statically admissible stress field by the conditions that it should satisfy the equilibrium equations and the yield inequality at any point, as well as the statical boundary conditions.

Further, they define a kinematically admissible velocity field by the conditions that it should satisfy the kinematical boundary conditions and, at any point, the equation:

$$\varepsilon_1 + \varepsilon_2 = \varepsilon_{nn} \sin \varphi \qquad 2239$$

where $\varepsilon_1 + \varepsilon_2$ represents the rate of dilatation and ε_{nn} the rate of maximum shear strain.

In order to calculate earth pressures by means of this method it is necessary to assume a fixed distribution of the earth pressure. If any statically admissible stress field can be indicated, the corresponding value of the earth pressure is an approximation which is somewhat on the safe side. On the other hand, if any kinematically admissible velocity field can be indicated, the corresponding value of the earth pressure is an approximation which is somewhat on the unsafe side.

In this way it is theoretically possible to find the limits of an interval, within which the actual value of the earth pressure must lie. However, statically admissible stress fields can only be indicated in very special cases, so that one usually has to be content with kinematically admissible velocity fields. Of such fields one must, of course, try to find one which is as little as possible on the unsafe side.

One consequence of 2239 is that, if a thin plastic layer between two parallel lines is subjected to shear, the lower line remaining in a fixed position, then the velocity vectors of points at the upper line must make angles of φ with the corresponding tangents of the line.

Now, Drucker and Prager consider the rupture-line in a line-rupture as a narrow plastic zone. Then, the only way in which the rotating rigid earth wedge can satisfy the above requirement, is by being bounded by a logarithmic spiral and rotating about its pole. In this way Drucker and Prager arrive at a velocity field which, according to 2239, is kinematically admissible.

The calculation of the corresponding earth pressure must now take place in the same way as in Rendulic's method, making use of the moment equation about the pole and the extreme-principle (in order to find the value which is as little as possible on the unsafe side).

It will be seen that, according to Drucker and Prager, the rotation centre of the wall coincides with the normal projection of the pole of the spiral on the wall.

With regard to 2239, it must first be remarked that, according to tests, it is, at the most, fulfilled for a certain porosity of the earth. Even if the earth happens to possess this porosity, so that 2239 is correct in the initial state of failure, it cannot be so when failure progresses, because the earth obviously cannot go on dilating indefinitely. When the shear strain has reached a certain value, the rate of dilatation must be zero.

In a line-rupture, the plastic zone is actually exceedingly narrow, which means that even small movements of the earth wedge will produce very great shear

strains in the narrow plastic zone. Moreover, the failure is actually progressive, starting from the foot of the wall. By the time it has reached the surface, the shear strains in practically the whole rupture-line will have become so great that 2239 cannot possibly be valid any longer. Instead of this, incompressibility must be assumed in the narrow plastic zone, which means that the rupture-line must be a circle instead of a spiral.

23. THEORIES OF ELASTICITY

231. General

Theories of elasticity are based on Hooke's law, assuming proportionality between deformations and stresses. By means of this assumption, in connection with the equations of equilibrium for a small earth element, it is in principle possible to solve earth pressure problems by considering the earth as a perfectly elastic medium.

However, as general solutions of the equations cannot be indicated, and as the boundary conditions are usually extremely complicated, exact calculations of this type have not, generally speaking, been carried out.

The only exception is Boussinesq's solution (1885) of the problem concerning the effects of a concentrated force acting on the surface of a semi-infinite elastic solid. This method has, later, been applied by Weiskopf (1945) to the problem of determining the earth pressure, due to a concentrated surcharge, on an unyielding wall. JOGE, ASCE, Vol 109, No 2, PP. 271

By making various simplifying assumptions it is possible to develop approximate theories of elasticity. As regards foundation pressures, the most common method of this kind is the method of subgrade reaction, which assumes proportionality between the unit normal pressure at any given point of a structure and the normal deflection of this point. A great number of applications, mainly concerning foundation problems, have been indicated by Hayashi (1921), whereas Rifaat (1935) and Blum (1951) have used the method on lateral earth pressure problems.

An interesting example of another type of approximate elasticity theories is the method developed by Bretting for the calculation of flexible sheet walls in clay. This method has never been published in full, but a short account of it has been given by the author (Brinch Hansen 1948).

The most serious shortcoming of the theories of elasticity is, that although they may approximately determine the actual stresses in the soil, they cannot give any indication of the safety against ultimate failure.

232. Methods of Subgrade Reaction

As an example of such methods we shall discuss the work of Rifaat (1935). He considers a vertical, free sheet wall, driven into cohesionless earth with a horizontal surface, and subjected to an exterior horizontal force.

The active earth pressures are disregarded, and the passive pressures are defined by the equation: $e = By$, where y is the horizontal deflection, and B is a function of the depth x. If the wall is elastic with a moment of inertia J and a modulus of elasticity E, we get then the following differential equation:

$$-EJ \frac{d^4y}{dx^4} = e = By \qquad 2301$$

which can be solved when B is given as a function of x. Rifaat investigated different possibilities and found, by comparison with model tests, that the best agreement was obtained by assuming B proportional to the depth x. The arbitrary constants in the solution of 2301 are, of course, determined by the boundary conditions.

Unfortunately, this method cannot be applied to active earth pressures, because in this case a very small deflection usually suffices to develop the minimum value of the pressure, so that proportionality between deflections and pressures no longer exists, not even approximately.

233. Bretting's Method

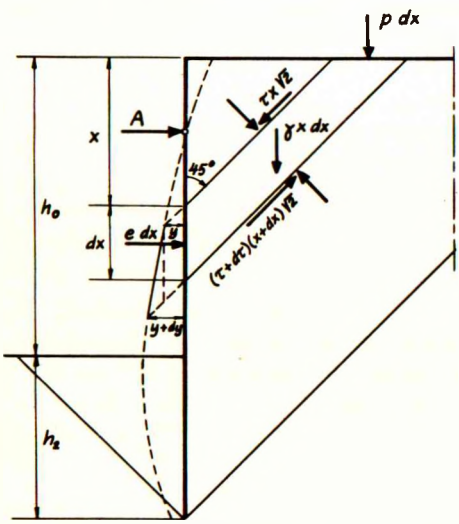

Fig.23A: Bretting's method for anchored sheet walls in clay.

As shown in Fig. 23A, Bretting considers a vertical, anchored sheet wall in clay with a horizontal surface. He assumes the lines of maximum shear stress to be inclined at 45° at both sides of the wall, which is assumed perfectly smooth. Moreover, he assumes that the movements of all soil particles are parallel to these lines.

We consider now an earth element between two consecutive shear lines. From Fig. 23A it will be seen that the movement in the lower line is $dy \cdot \sqrt{2}$ greater than that in the upper line. As the distance between the lines is $dx : \sqrt{2}$, the increase of a former right angle will be:

$$\frac{dy \cdot \sqrt{2}}{dx : \sqrt{2}} = 2 \frac{dy}{dx} = -\frac{\tau}{G} \qquad 2302$$

where G is the modulus of elasticity for shear, and τ is positive when directed as in Fig. 23A . Equation 2302 presumes, of course, that no shear stresses existed in the clay prior to the deflection of the wall.

Next, we project all forces acting upon the considered earth element on the direction of the shear lines. In this way the following expression for the unit earth pressure is obtained:

$$e = \gamma x + p - 2\tau - 2x \frac{d\tau}{dx} \qquad 2303$$

(with changed sign of e)

Combining this with the usual relation 2301 and eliminating τ by means of 2302, we get the following differential equation in y:

$$EJ \frac{d^4y}{dx^4} - 4Gx \frac{d^2y}{dx^2} - 4G \frac{dy}{dx} - \gamma x - p = 0 \qquad 2304$$

This equation is valid above dredge-line level. Below this level a similar procedure can be used, giving the equation:

$$EJ \frac{d^4y}{dx^4} - 4G\,(2x-h_o) \frac{d^2y}{dx^2} - 8G \frac{dy}{dx} - \gamma h_o - p = 0 \qquad 2305$$

The equations 2304-05 can only be solved approximately and either graphically or analytically, e.g., by expressing y as a polynomium in x. A full solution of the problem can, of course, only be obtained with the aid of the boundary conditions, of which altogether 8 are necessary. A further discussion of these would, however, lead too far here.

The theory described has, in a slightly different form, been used by Bretting for the design of a big quay wall in Bangkok, built by Christiani & Nielsen in 1940-41. Very reasonable results were obtained in this case, although various objections can be raised against the theory (Tschebotarioff 1949 and 1951).

24. EMPIRICAL METHODS

241. General

The empirical methods for calculating earth pressures are based either on model tests (Tschebotarioff, Rowe), on full-scale tests (Spilker, Peck), or on general practical experience (Christiani, Danish Rules). Such methods must be characterized as semi-empirical, which are based on assumptions involving empirical constants, which can only be determined by comparing the results with practical experience. Examples of the latter are Terzaghi's "General Wedge Theory" (1941) as well as his calculation method for cellular cofferdams (1944).

A common feature of the empirical methods is, that such a method is usually applicable only to constructions and conditions similar to those on which the

method has been based. This limitation is a serious drawback, because there are always a considerable number of variables in any earth pressure problem.

Empirical calculation methods have been proposed for many different structures. As examples can be mentioned Spilker's method (1937) for determining the pressure of sand on braced walls, Peck's method (1943) for the corresponding problem in clay, Terzaghi's method (1944) for investigating the stability of cellular cofferdams and Rimstad's method (1940) for designing double sheet walls.

Of special interest are the empirical methods for the design of anchored sheet walls. Several such methods exist and four of them shall be described here, viz., Christiani's method, the so-called "Danish Rules", Tschebotarioff's method and Rowe's method.

242. Christiani's Method

Up to about 50 years ago, sheet walls were made almost exclusively of timber, and were designed by means of certain empirical rules, which had proved satisfactory in practice.

In the beginning of the present century, increasing water depths were demanded, and, at the same time, new materials were made available, viz., reinforced concrete and steel sheet piles. The question then arose of how these new types of anchored sheet walls were to be designed.

In most countries where such design methods were attempted, the sheet walls were considered as vertical beams, subjected to active and passive earth pressures calculated by means of Coulomb's or Rankine's methods. However, when ordinary allowable stresses for the materials in question were used, very heavy sheet walls were found to be necessary, so that the new materials could not compete economically with empirically designed timber sheet walls.

The first to find a practical solution to this problem was the Danish engineer, Rud. Christiani. He started by making check computations of a number of existing timber sheet walls, according to the above-mentioned method. He thereby found nominal stresses in the timber, which were 3-4 times as great as the allowable stresses normally used. He concluded then that some redistribution of the earth pressures must take place, making the actual moments considerably smaller than the calculated ones, and he assumed, finally, that the same would apply to sheet walls of steel or reinforced concrete. Therefore, he decided to design such sheet walls for the calculated moments, but with "allowable" stresses 3-4 times as great as those ordinarily used.

The first structure, which was designed and constructed by Christiani & Nielsen in accordance with this principle, was a pier at Aalborg, Denmark, built in 1906. It consists of two sheet walls of reinforced concrete, anchored together and with sand fill in between. The structure proved to be cheaper than a corresponding timber structure and, although the sheet walls are underdesigned according to recent investigations (Tschebotarioff 1951), the pier still stands after 47 years of satisfactory service.

The success of this "daring experiment" (Tschebotarioff) enabled Christiani & Nielsen to carry out a considerable number of quay walls with sheet walls of reinforced concrete. Such structures were first made in Denmark and northern Europe, and later, all over the world. Gradually the firm developed a light and very economical type of wharf structure known as the "C&N-wharf". A description of this development has been given by the author (Brinch Hansen 1946).

After Christiani's introduction of the empirical calculation principle described above, other Danish engineers tried to solve the same problem in a different way, viz., by changing the earth pressure distribution assumed in Coulomb's theory. This resulted in the empirical method known as the "Danish Rules".

243. Danish Rules

The Danish Rules for the design of anchored sheet walls in sand were first published by the Danish Society of Civil Engineers in 1923. Slightly revised editions appeared in 1937 and 1952. They have been cited by Rimstad (1940), Agatz (1943) and Tschebotarioff (1951).

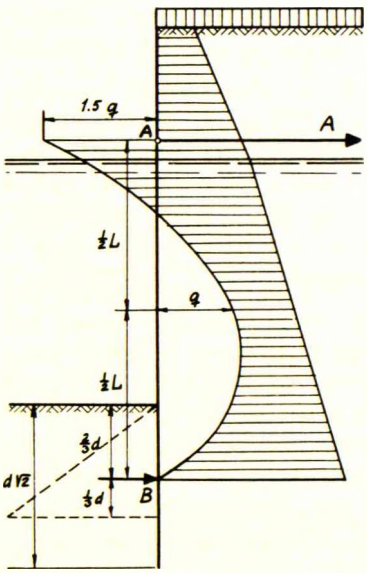

Fig. 24A: The Danish Rules for anchored sheet walls in sand.

Fig. 24A shows a sheet wall anchored at point A. It is assumed simply supported here and at another point B, located at the pressure centre of the passive pressure necessary for equilibrium.

The diagram of the active earth pressure is first calculated according to Coulomb's theory (with $\delta_a = 0$), but is then modified by means of a parabola, decreasing the pressure in the middle of AB by an amount q and increasing the pressure at A by 1.5 q. The pressure q is given by the formula:

$$q = k \frac{10\,H + 2\,L}{10\,H + 3\,L} p_m \qquad 2401$$

where L is the length AB, p_m is an average value of the unit active Coulomb pressure, whereas H represents the load above anchor level (measured as the corresponding height of earth with submerged unit weight). Finally, k is given by a complicated empirical formula but is approximately equal to 0.8.

Assuming simple supports at A and B the corresponding reactions and maximum moments are calculated. The wall and the anchors are then designed with allowable stresses which are 25% higher than usual. The theoretically necessary driving depth d is determined by the condition that the passive earth pressure, calculated according to Coulomb's theory (with $\delta_p = \frac{1}{2}\varphi$), should equal the reaction B. The actual driving depth should then be $d \cdot \sqrt{2}$, corresponding to a nominal safety factor of 2.

This method was based on the study of a considerable number of existing sheet walls. Although of a purely empirical nature and open to considerable doubt as regards the assumed pressure distribution (Tschebotarioff 1949), this method has proved very satisfactory in practice, having enabled the construction of a great number of sufficiently safe and very economic structures (Brinch Hansen 1946).

244. Tschebotarioff's Method

Some of the most careful and comprehensive model tests ever made with anchored, flexible sheet walls were carried out by Tschebotarioff (1948, 1949, 1951) at Princeton University. In most of these tests the backfill was deposited successively and no dredging took place in front of the wall. As a result of his tests Tschebotarioff proposed the following design method for sand:

A driving depth D = 0.43 H is selected (Fig. 24B), and under this condition a hinge (zero moment) is assumed at dredge-line level. Consequently, the wall is calculated as a beam, simply supported at this level and at anchor level. The active earth pressure is determined by the formula:

$$e_h = \tfrac{1}{3}\gamma h f''' \left(1 - \frac{a}{Hf'}\right) + \tfrac{1}{4}p_s \qquad 2402$$

where γ is the unit weight of the fill and p_s the unit surcharge, while the significance of H, h and a, will be apparent from Fig. 24B. The coefficient f''' expresses the effect of wall friction and can be put equal to 0.9, whereas f' is intended to account for capillarity and the effect of passive earth pressures above anchor level. Tschebotarioff recommends putting f' = 3.5.

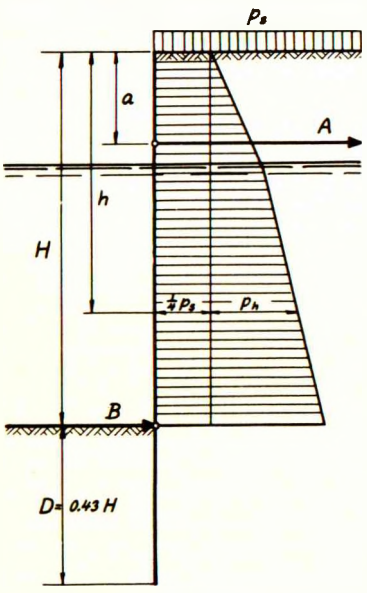

Fig. 24B: Tschebotarioff's method for anchored sheet walls in sand.

The wall is designed for the calculated maximum moment with allowable stresses 33% higher than usual. For the anchors no such increase is allowed and they should, moreover, not be designed for the reaction A found by the calculation but for a greater force A' determined by:

$$\frac{A}{A'} = f''\left(1 - \frac{a}{Hf'}\right) \qquad 2403$$

where f'' is a coefficient which must not exceed 1.0.

For the case of a backfill of soft clay, deposited in a semi-fluid state, Tschebotarioff has indicated a similar design method. He uses, in the main, a factor 0.5 for the active pressure, whereas for the passive pressure he employs the method indicated by Skempton (1946).

245. Rowe's Method

Another remarkable series of tests with flexible, anchored sheet walls has recently been carried out by P.W. Rowe (1952), who has studied the influence of surcharge, anchor level, anchor yield, dredge level, pile flexibility and soil density (only cohesionless soils were used).

For yielding anchors Rowe, as did Tschebotarioff, finds in the main the Coulomb distribution of the active pressure, but with increasing flexibility the moments (and, to a smaller degree, the anchor pull) are reduced considerably, which Rowe attributes mainly to a rise of the resultant of the passive pressure.

Rowe finds the relative moment reduction to be a function of the "flexibility number" $h^4 : EJ$ and the density of the soil. On this he bases his proposed design method, of which the main features are the following.

The calculation is started according to the method of "free earth support" (Blum 1931) with the ordinary Coulomb pressure diagrams. For the active pressure $\delta_a = \frac{2}{3}\varphi$ is assumed, and for the passive pressure $\delta_p = 0$ in combination with a safety factor 1.5. At the foot of the wall a horizontal shear force is assumed to act, corresponding to the vertical load on the wall times tan δ_a.

The calculated maximum moment is now used to draw a moment-flexibility curve. For the considered type of wall a "structural" curve is also drawn, indicating the relation between the flexibility and the allowable moments (for steel a stress of 1250 kg/cm^2 is used). The design is then based on the point of intersection between these two curves.

The calculated anchor pull is first reduced on account of the flexibility of the wall, but is then increased again to allow for differential yield. These two corrections usually cancel each other approximately.

In the case of a non-yielding anchorage Rowe proposes, according to Stroyer (1935), to multiply the calculated maximum moment by a reduction factor:

$$\frac{M_r}{M_o} = \frac{2\lambda_a}{1 + \lambda_a^2} \qquad 2404$$

before making the further reduction for flexibility.

For yielding anchors, Rowe's method is probably the best empirical method proposed so far, but for unyielding anchors its combination with Stroyer's reduction factor does not seem quite satisfactory.

3. BASIS OF THE NEW METHOD

31. ASSUMPTIONS AND PRINCIPLES

311. Basic Assumptions

The earth may consist of gravel, sand, silt, clay or any other material encountered in the foundation technique (except solid rock). Also such materials as, for example, grain, cement, coal and ore may be included in the general term "earth". The essential requirement is that the material obeys Coulomb's law, at least approximately. This law states that a shearing stress τ, to which corresponds a normal stress σ, is limited by the condition:

$$\tau \leq c + \mu\sigma = c + \sigma \tan \varphi \qquad 3101$$

where c (the cohesion) and φ (the angle of internal friction) are assumed to be constants for the material in question.

Equation 3101 is principally valid for dry earth. For moist or submerged earth the total normal stress σ_t will consist of a so-called neutral pressure u_w in the pore water and an effective stress σ_e between the soil particles. As the shearing resistance is only affected by the effective stress, we must actually have:

$$\tau \leq c_e + \sigma_e \tan \varphi_e = c_e + (\sigma_t - u_w) \tan \varphi_e \qquad 3102$$

The constants c_e and φ_e are called the true cohesion and the true friction angle respectively.

We shall now consider two extreme cases. The first concerns fully saturated clays. On account of their extremely low permeability, their water content will practically be constant during the construction period. This means that they can be considered incompressible, and that any change of the total normal stress σ_t will be taken up exclusively as a change in the neutral pressure u_w, leaving the effective pressure σ_e, and consequently also the shear strength, unaltered.

The same result can evidently be obtained by using 3101 with $\varphi = 0$ and c equal to the shear strength (actually half the undrained compression strength). When 3101 is used in this way, the constants c and φ are called the apparent cohesion and the apparent friction angle respectively. Thus, fully saturated clays can be considered as frictionless materials, when we use 3101.

Actually, this is an approximation only, because, although 3101 and 3102 may indicate the same shear strength, the angles between the rupture-lines and the directions of the principal stresses should actually be $45^\circ \pm \frac{1}{2}\varphi_e$ (according to 3102), whereas 3101 gives 45° for $\varphi = 0$. However, in the case of straight rupture-lines Skempton (1948) has shown that 3101 will lead to correct values of the earth pressures but to wrong positions of the rupture-lines, and the author (Brinch Hansen 1952) has shown the same in a case of foundation pressures involving curved rupture-lines.

The other extreme case concerns sand and gravel. These materials are usually so highly permeable that the neutral pressures u_w at any time can be assumed to correspond to the depths below the water table (hydrostatical water pressures) or to the hydraulic heads found by a flow net construction (hydrodynamic pressures).

Consequently, when the water pressures and the earth pressures are considered separately, the latter can be calculated on the basis of 3101 with σ equal to the grain pressure. This implies, however, that for the earth we must reckon with the submerged unit weight, i.e., the unit weight of the saturated soil minus the hydrostatic uplift. In the case of hydrodynamic water pressures an additional correction must be made on account of the hydraulic gradients (see Section 622).

In most cases, c will be negligible for sand and gravel, so that these may be termed cohesionless materials. However, a small content of clay may make sand somewhat cohesive without reducing the permeability too much. Using 3101 with σ equal to the grain pressure we have thus for clayey sand a case of $c \neq 0$, $\varphi \neq 0$.

Although equation 3102 might be used as the basis of a plasticity theory, as has actually been done by the author (Brinch Hansen 1952), this leads to almost insurmountable complications. In order to arrive at comparatively simple results it is necessary to use the simpler equation 3101, and, as has been shown above, this is actually possible at least in the extreme cases of very low and very high permeabilities, corresponding to the important practical cases of fully saturated clays, and sand and gravel respectively.

In cases of intermediate permeabilities, such as may exist in mixtures of sand and clay, and in silts, it is hardly possible to make any reliable earth pressure calculation without investigating, by calculation and experiment, the neutral pressures at different times. This may sometimes also be necessary for fully saturated clays, viz., when they are consolidating (e.g. in earth dams) or swelling (e.g. after excavation of overlying layers). Such cases are usually extremely complicated and shall not be dealt with in the present work. The same applies to partially saturated clays. A few indications have been given by Skempton and Bishop (1950).

The earth may be stratified, but within each separate layer it is assumed to be homogeneous and isotropic. Actually, these conditions are seldom fulfilled in nature, and, particularly for clay, the anisotropic consolidation is probably of some importance (Brinch Hansen and Gibson 1949). However, in order to arrive at comparatively simple calculations the above assumptions shall be made in the present work.

The shearing stress acting between a structure (here generally called a wall) and the earth is, in analogy with Coulomb's law, assumed to be limited by the condition:

$$f \leq a + e \tan \delta \qquad 3103$$

where e and f are the normal and tangential components respectively of the unit earth pressure. a (the adhesion) cannot exceed c, and δ (the angle of wall friction) cannot exceed φ. The maximum values of a and δ, which will occur in case of a relative tangential movement between wall and earth, are assumed to be constants for the wall and earth in question. If no such movement takes place lower values of a and δ can occur.

In the special case $a = 0$, $\delta = 0$ the wall is called perfectly smooth, and in the other special case $a = c$, $\delta = \varphi$ it is called perfectly rough. Actual walls will generally approximate rather closely the latter case, but, nevertheless, it is often preferred to assume the walls to be smooth, this being simpler and usually on the safe side.

With regard to the movements of the wall, it is assumed that these are great enough to produce a state of rupture in the earth, but that they, on the other hand, are small in comparison with the height of the wall. The wall itself may, or may not, be in a state of failure. In the latter case a limited number of yield hinges are supposed to develop.

In many cases the movement of the wall in its own plane can be assumed negligible in comparison with its movements perpendicular to this plane. This is usually the case when the wall is founded on firm bottom, or on piles, or is driven into firm ground. In such cases the wall is said to make "normal" movements only (e.g. a normal rotation). In certain other cases (e.g. anchor slabs and cellular cofferdams) the tangential movements are not negligible, as the wall may be lifted in the state of failure. For perfectly smooth walls this problem is, of course, of no importance.

Elastic deformations of earth or wall are assumed to be small of a higher order than the plastic deformations, and these are, as already mentioned, supposed to be small ~~of a higher order than~~ in relation to the height of the wall.

One consequence of this is that an elastic earth zone, the interior of which is not in the state of failure, can be assumed to move as a rigid body. Another consequence is that the wall, in which either no cross section at all, or a finite number of sections, are in a plastic state, will move either as one rigid body or as a finite number of rigid parts connected by links (yield hinges). Each such part rotates in the state of failure about a certain rotation centre.

We shall assume that the earth is incompressible, i.e. that even in a plastic zone the volume of the earth does not change through the deformation. This assumption is made in most plasticity theories and is very accurate for saturated clay, whereas for sand it is only correct after the shear strain has reached a certain minimum value. In cases of progressive failure it is a very good approximation, even for sand (see Section 226).

Actually, we shall generally not consider problems, the solution of which requires the exact calculation of the deformations in plastic zones, but mainly problems which can be solved either without considering the deformations at all, or by qualitative consideration only of the deformations.

In the present work only plane problems shall be considered or, more strictly speaking, states of plane strain. In addition, such problems may be considered, which, with sufficient accuracy, can be treated as plane (e.g. cellular cofferdams).

312. Main Principles

The main principles of the proposed new method for dealing with earth pressure problems are, briefly described, the following:

An earth pressure problem involves, generally, a number of given forces and dimensions as well as some unknown ones, which should be determined by the calculation. Incidentally, unknown dimensions can seldom be determined directly, and it is therefore usually necessary to start the calculation with estimated values of the unknown dimensions and correct them later if necessary.

In the calculation we shall consider the state of failure. On the other hand the structure should , of course, be designed in such a way that there is a certain safety against failure. This is achieved by carrying out the calculation, not with the actual loads and shear strengths, but with the actual loads multiplied by certain safety factors, and with the actual shear strengths divided by other safety factors.

The first step of the calculation consists in determining or choosing the type of movement to be performed by the structure in the state of failure. In some cases the movement can be chosen so as to obtain the maximum efficiency (example: an anchor slab will resist the greatest possible anchor pull by a translation). In other cases the movement is practically given (example: a retaining wall must tilt forward, rotating about a point below its foot).

For more complicated structures more than one state of failure may be possible (example: an anchored sheet wall may fail, either because the anchorage yields, or because the soil in front of its foot yields, or because a yield hinge develops in the wall proper). In such cases any one of the possible states of failure can be chosen as the basis of the design, it being mainly a matter of economy and convenience as to which is preferred.

When the type of movement of the structure in the state of failure has been determined, the possible figures of rupture in the adjacent earth masses must be investigated. If at all possible, only such figures of rupture should be considered, which imply movements of the earth masses compatible with those of the structure.

The next step is to calculate the earth pressures acting between the structure and the adjacent earth masses. These pressures will depend on the assumed rupture-figures in the earth, and they can be calculated if we know the internal stresses in the lines of rupture.

This knowledge is obtained by two different means. First, we use Kötter's equation, which determines the stresses at any point of a curved rupture-line, provided that they are known at one point of the line. Second, we use a special boundary condition, which is developed in such a way that the most reliable results are obtained (see Section 16).

When the internal stresses in the rupture-lines are known we can calculate the earth pressures by means of the statical conditions of equilibrium for the different earth zones bounded by rupture-lines, ground surfaces, walls or other boundaries. For each separate zone we have, of course, 3 conditions of equilibrium.

Often more than one figure of rupture may satisfy the kinematical conditions. The final calculation must then be based on the most critical rupture-figure, i.e., the one for which the work done by the earth pressure (acting upon the earth) is a minimum.

When the earth pressures on the structure have been determined, we must finally consider the equilibrium of the structure proper. This gives another 3 statical conditions, but in some cases only 2 of these are necessary to solve the main problem.

As already mentioned, the original problem will usually present one or more unknown quantities. The assumed movement of the structure may involve additional unknown quantities (example: the location of the rotation centre for a free sheet wall). Finally, the assumed rupture-figures in the earth will add a new set of unknown quantities, viz., their geometrical parameters.

If the problem is to be soluble the total number of unknown quantities must equal the total number of conditions (statical, kinematical and geometrical). However, this can actually be obtained in most practical earth pressure problems.

Example 31a

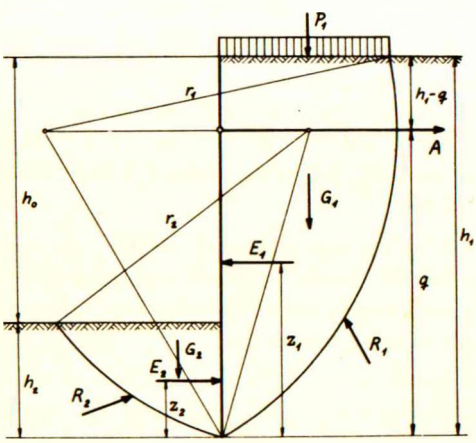

Fig.31A: Forces acting upon anchored sheet wall and adjacent earth wedges.

In order to demonstrate the application of the above-mentioned principles to a practical earth pressure problem, we shall consider an anchored sheet wall (Fig.31A). The wall is assumed to be perfectly smooth.

The depth h_1-q of the anchor point is given as well as the free height h_0. The driving depth h_2 and the anchor force A are unknown quantities.

In the state of failure the wall is supposed to rotate about the anchor point. This involves no additional unknown quantities.

At each side of the wall a single circular rupture-line is assumed to develop in the earth. The movements of the rigid wall and the two earth wedges (which rotate as rigid bodies about the centres of the respective circles) can only be compatible, when the centres of both circles are situated at a normal to the wall through

the anchor point (which is the rotation centre for the wall). This means that each circle involves only one unknown parameter, for example its radius r.

As additional unknown quantities we must consider the two earth pressure resultants E_1 and E_2 as well as the heights z_1 and z_2 of the corresponding pressure centres. This means that we have altogether 8 unknown quantities (A, h_2, r_1, r_2, E_1, E_2, z_1 and z_2). However, we have also 8 equations, viz., 3 statical equilibrium conditions for each earth wedge and 2 for the wall (horizontal projection and moment equation). The third equilibrium condition for the wall (vertical projection) has, of course, no importance, when the wall is perfectly smooth.

In practice, we must start the calculation with an estimated value of h_2. For each earth wedge the 3 equilibrium conditions determine the respective values of r, E and z. We investigate then whether the earth pressures on the wall satisfy the moment equation about the anchor point. If not, h_2 must be changed until this condition is fulfilled. Then, A can be found by horizontal projection of the forces acting upon the wall.

32. GEOMETRY AND LOADS

321. Sloping Surface and Inclined Wall

Fig. 32A shows a wall with a height h (measured along the wall), making an angle j with the vertical (pos. in Fig. 32A). The ground surface makes an angle i with the horizon (pos. in Fig. 32A) and is loaded with a vertical surcharge p per unit area of the sloping surface. The unit weight of the earth is γ.

Further, Fig. 32A shows a circular rupture-line through the foot of the wall. It has a chord length k and cuts off a width w of the ground surface (measured along this surface). The central angle of the circle is 2α, its radius is r and its chord makes an angle β with the horizon (pos. in Fig. 32A).

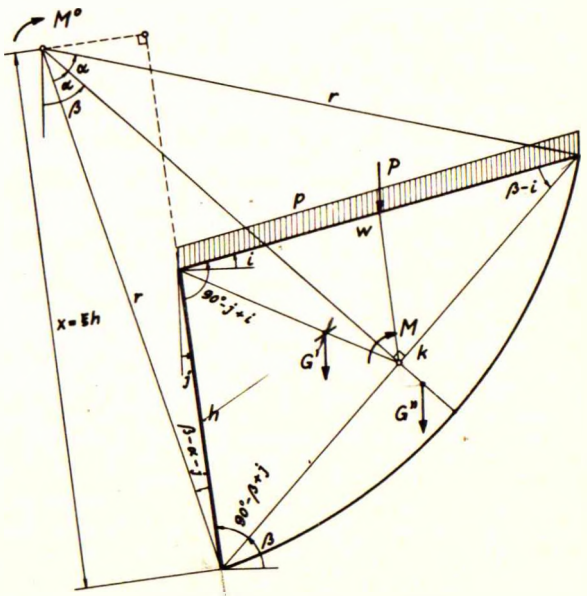

Fig. 32A: Surface load and earth weight for single rupture-circle.

From Fig. 32A the following geometrical relations may be derived:

$$r = \frac{k}{2 \sin \alpha} = \frac{h \cos(j-i)}{2 \sin \alpha \sin(\beta-i)} \qquad 3201$$

$$k = 2r \sin \alpha = \frac{h \cos(j-i)}{\sin(\beta-i)} \qquad 3202$$

$$h = \frac{k \sin(\beta-i)}{\cos(j-i)} = \frac{2r \sin\alpha \sin(\beta-i)}{\cos(j-i)} \qquad (3201)\ (3202) \qquad 3203$$

$$w = \frac{h \cos(\beta-j)}{\sin(\beta-i)} = \frac{k \cos(\beta-j)}{\cos(j-i)} = \frac{2r \sin\alpha \cos(\beta-j)}{\cos(j-i)} \qquad (3202) \qquad 3204$$

The distance of the rotation centre from the foot of the wall is:

$$x = r \cos(\beta-\alpha-j) = \frac{k \cos(\beta-\alpha-j)}{2 \sin\alpha} = \frac{h \cos(j-i) \cos(\beta-\alpha-j)}{2 \sin\alpha \sin(\beta-i)} \qquad (3202)\ (3201) \qquad 3205$$

The total surface load on the earth wedge is:

$$P = pw = pk \cos(\beta-j) \sec(j-i) \qquad (3204) \qquad 3206$$

and its moment about the middle point of the chord:

$$M_P = -\tfrac{1}{2} pk^2 \sin(\beta-i) \cos(\beta-j) \sec^2(j-i) \sin j \qquad 3207$$

The total earth weight of the wedge bounded by the surface, the wall and the rupture-line is:

$$G = \gamma k^2 \left[G^{\gamma z} + \tfrac{1}{2} \sin(\beta-i) \cos(\beta-j) \sec(j-i) \right] \qquad 3208$$

where:

$$G^{\gamma z} = \tfrac{1}{4} (\alpha + \alpha \cot^2\alpha - \cot\alpha) \qquad 3209$$

The corresponding moment about the middle point of the chord is:

$$M_G = \gamma k^3 \left[M_G^{\gamma x} \sin\beta + \tfrac{1}{12} \sin\beta - \frac{\sin(\beta-i)\cos(\beta-j)}{12 \cos(j-i)} \left[\cos\beta + \frac{2 \sin(\beta-i) \sin j}{\cos(j-i)} \right] \right] \qquad 3210$$

where:

$$M_G^{\gamma x} = -\tfrac{1}{8} (\alpha + \alpha \cot^2\alpha - \cot\alpha) \cot\alpha \qquad 3211$$

When the moving earth mass is located on the concave side of the circle (as in Fig.32A), the circle is called concave, and when it is located on the convex side, the circle is called convex. All the above formulae are valid for a concave circle when positive values of α and r are used. They are valid for a convex circle when negative values of α and r are used.

For a straight rupture-line the above formulae are valid with $\alpha = 0$. With this value 3209 yields $G^{\gamma z} = 0$ and 3211 gives $M_G^{\gamma x} = -\frac{1}{12}$.

In order to facilitate the practical use of the above formulae the quantities $G^{\gamma z}$ and $M_G^{\gamma x}$, which are functions of α only, have been evaluated in Table 1 in the Appendix.

When the rupture-line consists of more than one circle (Fig.32B), the preceding formulae are valid for P_1, P_2 etc. and G_1, G_2, etc. For the remaining loads and their moments about the middle points of the respective chords the following general formulae may be developed:

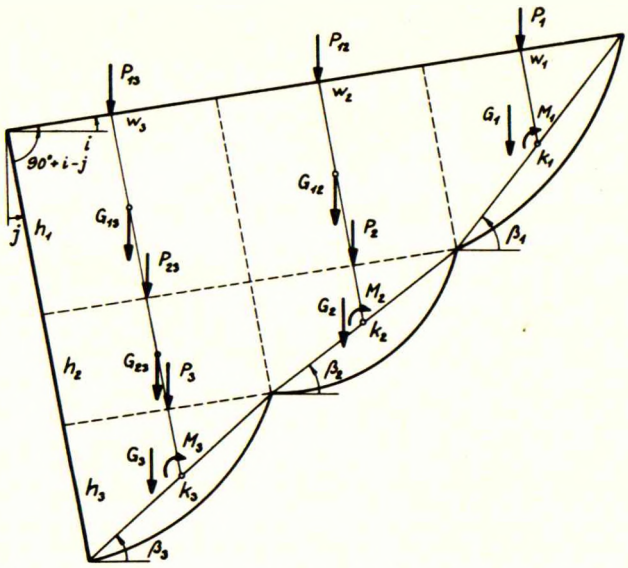

Fig.32B: Surface loads and earth weights for composite rupture-line.

$$P_{mn} = p_m w_n \qquad M_{Pmn} = -P_{mn}\left[\sum_{m}^{n-1} h_x + \tfrac{1}{2}h_n\right]\sin j \qquad 3212\text{-}13$$

$$G_{mn} = \gamma_m h_m w_n \cos(j-i) \qquad M_{Gmn} = -G_{mn}\left[\sum_{m+1}^{n-1} h_x + \tfrac{1}{2}h_n + \tfrac{1}{2}h_m\right]\sin j \qquad 3214\text{-}15$$

322. Horizontal Surface and Vertical Wall

We shall here consider a very important special case, viz., a horizontal surface (i = 0) and a vertical wall (j = 0). Inserting these values in the preceding formulae we get first the following geometrical relations:

$$r = \frac{k}{2\sin\alpha} = \frac{h}{2\sin\alpha\sin\beta} \qquad k = 2r\sin\alpha = \frac{h}{\sin\beta} \qquad 3216\text{-}17$$

$$h = k\sin\beta = 2r\sin\alpha\sin\beta \qquad 3218$$

$$w = h\cot\beta = k\cos\beta = 2r\sin\alpha\cos\beta \qquad 3219$$

$$x = r\cos(\beta-\alpha) = \frac{k\cos(\beta-\alpha)}{2\sin\alpha} = \tfrac{1}{2}h\,(1+\cot\alpha\cot\beta) \qquad 3220$$

For the surface load and the earth weight respectively we find:

$$P = pk\cos\beta \qquad M_P = 0 \qquad 3221\text{-}22$$

$$G = \gamma k^2(G^{\gamma Z} + \tfrac{1}{4}\sin 2\beta) \qquad M_G = \gamma k^3(M_G^{\gamma X}\sin\beta + \tfrac{1}{12}\sin^3\beta) \qquad 3223\text{-}24$$

G^{YZ} and M_G^{YX} are still given by 3209 and 3211.

For a rupture-line consisting of more than one circle we find in the case of i = 0, j = 0:

$$P_{mn} = p_m w_n \qquad M_{Pmn} = 0 \qquad G_{mn} = \gamma_m h_m w_n \qquad M_{Gmn} = 0 \qquad 3225\text{-}28\ \surd$$

33. STRESSES IN RUPTURE-CIRCLE

331. General Case

We consider an infinitely small earth element (Fig.33A) and use the polar coordinates r and v, the latter being measured from the vertical. By projection of all forces (the indicated stresses multiplied by the corresponding side-lengths) on the radius and the tangent respectively the following equations are obtained:

$$r\frac{\partial\sigma_r}{\partial r} + \frac{\partial\tau_{rv}}{\partial v} + \sigma_r - \sigma_v - \gamma r\cos v = 0 \qquad 3301\ \surd$$

$$r\frac{\partial\tau_{rv}}{\partial r} + \frac{\partial\sigma_v}{\partial v} + 2\tau_{rv} + \gamma r\sin v = 0 \qquad 3302\ \surd$$

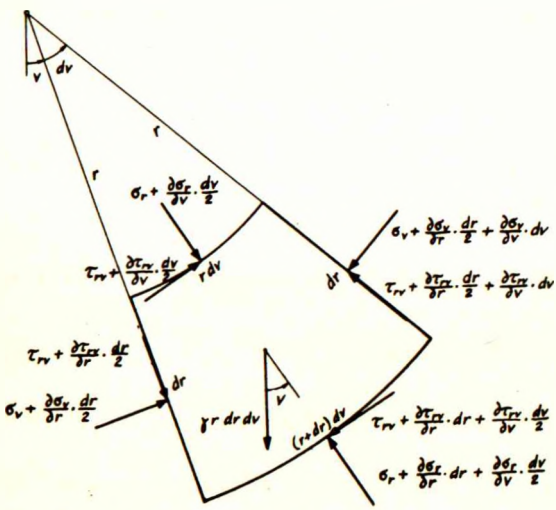

Fig.33A: Small earth element in rupture-circle

We shall now investigate the stresses in a rupture-circle with its centre in the pole of the coordinate system. Inserting the stresses σ_r and τ_{rv} in Coulomb's law (3101) we find:

$$\tau_{rv} - \mu\sigma_r \leq c \qquad 3303\ \surd$$

The function indicated on the left side of 3303 must have a constant value in the rupture-line proper and, as regards the variation in the radial direction, it must either be constant (zone-rupture) or attain a maximum value at the rupture-line (line-rupture). In both cases we have:

$$\frac{\partial(\tau_{rv} - \mu\sigma_r)}{\partial r} = 0 \qquad \frac{\partial(\tau_{rv} - \mu\sigma_r)}{\partial v} = 0 \qquad 3304\text{-}05\ \surd$$

Multiplying 3301 with $\mu = \tan\varphi$, subtracting it from 3302 and using 3304, we get:

$$\frac{\partial(\sigma_v - \mu\tau_{rv})}{\partial v} + \mu(\sigma_v - \sigma_r) + 2\tau_{rv} + \gamma r \sec\varphi \sin(v+\varphi) = 0 \qquad 3306$$

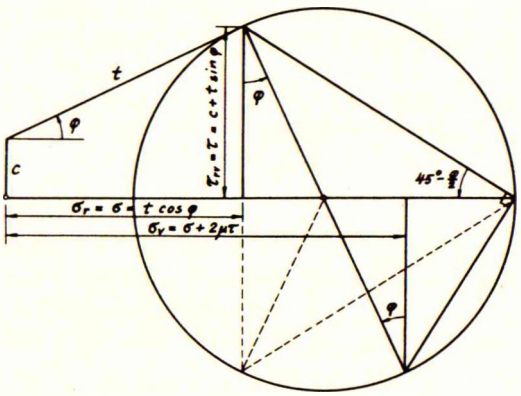

Fig.33B: Mohr's circle for stresses

For the sake of simplicity we shall in the following omit the subscripts on the stresses σ and τ in the rupture-line proper. For the other normal stress we get by means of Mohr's circle (Fig.33B):

$$\sigma_v = \sigma + 2\mu\tau \qquad 3307$$

Using 3305 and 3307 to eliminate the normal stresses from 3306, we find the following differential equation in τ alone, valid for the rupture-line proper:

$$\frac{d\tau}{dv} + 2\mu\tau + \gamma r \sin\varphi \sin(v+\varphi) = 0 \qquad 3308$$

This is Kötter's equation for the variation of the shear stress in a rupture-line. Kötter (1903) derived it for cohesionless earth, and Jáky (1936) showed that it is also valid for earth with cohesion.

The solution of 3308 is, for r = constant (circle):

$$\tau = Ke^{-2\mu v} + \gamma r \sin\varphi \cos\psi \cos(v+\varphi+\psi) \qquad 3309$$

where K is a constant stress and ψ a constant angle defined by:

$$\psi = \arctan 2\mu \qquad \text{or} \qquad \tan\psi = 2\tan\varphi \qquad 3310$$

If v' and τ' are corresponding values, then 3309 gives:

$$K = e^{2\mu v'}\left[\tau' - \gamma r \sin\varphi \cos\psi \cos(v'+\varphi+\psi)\right] \qquad 3311$$

Instead of the stresses σ and τ in the rupture-line we shall now introduce the cohesion c and the remaining stress t which makes an angle φ with the normal. From Mohr's circle (Fig.33B) it will be seen that:

$$\sigma = t\cos\varphi \qquad \tau = c + t\sin\varphi \qquad 3312\text{-}13$$

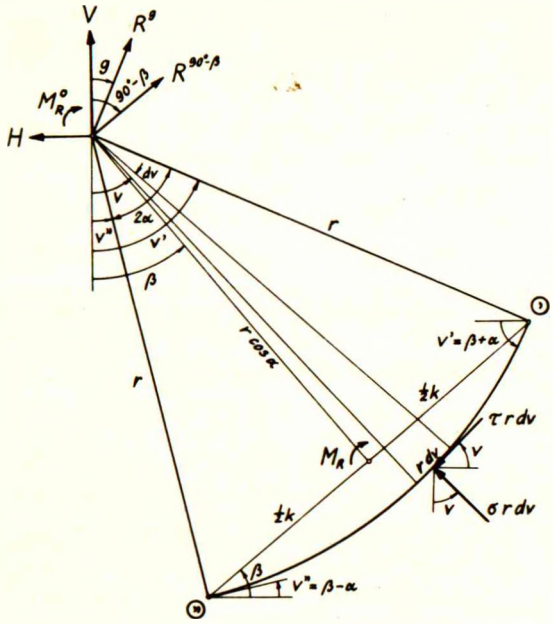

Fig.33C: Resultants of stresses in rupture-circle

We consider now a rupture-circle with a radius r, a chord-length k, a central angle 2α and an angle β between chord and horizon (Fig.33C). The point at which the boundary stresses are known is called the starting point (') and the other end the finishing point (''). β should be assumed positive when the starting point is located above the finishing point, i.e. when the chord falls towards the wall. We have then:

$$v' = \beta + \alpha \qquad 3314$$

$$v'' = \beta - \alpha \qquad 3315$$

Using 3309 for the finishing point, inserting K from 3311, eliminating τ' and τ'' by means of 3313 and, finally, using 3314-15, we get for the stress t'':

$$t'' = \gamma r \cos\psi \left[\cos(\beta-\alpha+\varphi+\psi) - \nu \cos(\beta+\alpha+\varphi+\psi)\right] + \nu t' + \frac{c(\nu-1)}{\sin\varphi} \qquad 3316$$

where:

$$\nu = e^{4\mu\alpha} \qquad 3317$$

Introducing k instead of r by means of 3201 we find:

$$t'' = \gamma k \,(t^{\gamma x} \sin\beta + t^{\gamma y} \cos\beta) + (t' + \frac{c}{\sin\varphi})\, t^t - \frac{c}{\sin\varphi} \qquad 3318$$

where:

$$t^t = e^{4\mu\alpha} = \nu \qquad 3319$$

$$t^{\gamma x} = \frac{\cos\psi}{2\sin\alpha}\left[\nu \sin(\psi+\varphi+\alpha) - \sin(\psi+\varphi-\alpha)\right] \qquad 3320$$

$$-t^{\gamma y} = \frac{\cos\psi}{2\sin\alpha}\left[\nu \cos(\psi+\varphi+\alpha) - \cos(\psi+\varphi-\alpha)\right] \qquad 3321$$

Next, we shall determine the resultants of the stresses acting in the rupture-circle on the moving earth mass outside this circle (Fig.33C). On each element rdv of the circle acts a shear stress τ, given by 3309, and a normal stress σ, which can be found by means of Mohr's circle (Fig.33B):

$$\sigma = (\tau - c)\cot\varphi \qquad 3322$$

The resulting force in a direction making an angle g with the vertical is:

$$R^g = \int_{v''}^{v'} \left[\sigma \cos(v+g) - \tau \sin(v+g)\right] r \, dv \qquad 3323$$

Eliminating σ by means of 3322, inserting τ from 3309, carrying out the integration, inserting K from 3311, eliminating τ' by means of 3313 and, finally, using 3314-15, we can find:

$$\begin{aligned} R^g = {} & \tfrac{1}{2}\gamma r^2 \cos^2\psi \left[\sin(2\psi-g) + 2\alpha \sec\psi \cos(\psi-g) - \nu \sin(2\alpha+2\psi-g)\right. \\ & \left. + \sin(2\beta+2\varphi+g)\left[\nu - \sec\psi \cos(2\alpha-\psi)\right]\right] \\ & + \left(t' + \frac{c}{\sin\varphi}\right) r \cos\psi \left[\sin(\beta+\alpha+\varphi-\psi+g) - \nu \sin(\beta-\alpha+\varphi-\psi+g)\right] \\ & - 2cr \cot\varphi \sin\alpha \cos(\beta+g) \end{aligned} \qquad 3324$$

The <u>vertical</u> component V is obtained with $g = 0$, and the <u>horizontal</u> component H with $g = -90^\circ$. If, at the same time, r is substituted by k by means of 3201, we get:

$$\begin{aligned} V = {} & \gamma k^2 \left[V^{\gamma z} + V^{\gamma x} \sin(2\beta+2\varphi)\right] - ck \cot\varphi \cos\beta \\ & + \left(t' + \frac{c}{\sin\varphi}\right) k \left[V^{tx} \sin\beta + V^{ty} \cos\beta\right] \end{aligned} \qquad 3325$$

$$\begin{aligned} H = {} & \gamma k^2 \left[H^{\gamma z} + H^{\gamma y} \cos(2\beta+2\varphi)\right] - ck \cot\varphi \sin\beta \\ & + \left(t' + \frac{c}{\sin\varphi}\right) k \left[H^{tx} \sin\beta + H^{ty} \cos\beta\right] \end{aligned} \qquad 3326$$

containing the following functions of α and φ:

$$-V^{tx} = H^{ty} = \frac{\cos\psi}{2\sin\alpha}\left[\nu \cos(\psi-\varphi+\alpha) - \cos(\psi-\varphi-\alpha)\right] \qquad 3327$$

$$V^{ty} = H^{tx} = \frac{\cos\psi}{2\sin\alpha}\left[\nu \sin(\psi-\varphi+\alpha) - \sin(\psi-\varphi-\alpha)\right] \qquad 3328$$

$$-H^{\gamma y} = V^{\gamma x} = \frac{\cos^2\psi}{8\sin^2\alpha}\left[\nu - \sec\psi \cos(\psi-2\alpha)\right] \qquad 3329$$

$$V^{\gamma z} = \frac{\cos^2\psi}{8\sin^2\alpha}\left[\sin 2\psi - \nu \sin(2\psi+2\alpha) + 2\alpha\right] \qquad 3330$$

$$H^{\gamma z} = \frac{\cos^2\psi}{8\sin^2\alpha}\left[\cos 2\psi - \nu \cos(2\psi+2\alpha) - 2\alpha \tan\psi\right] \qquad 3331$$

The moment about the <u>centre of the circle</u> is:

$$M_R^o = \int_{v''}^{v'} \tau \, r^2 \, dv \qquad 3332$$

Inserting τ from 3309, carrying out the integration, inserting K from 3311, eliminating τ' by means of 3313 and, finally, using 3314-15, we can find:

$$M_R^o = \gamma r^3 \cos\psi \left[2 \sin\varphi \sin\alpha \cos(\beta+\varphi+\psi) - \tfrac{1}{2}(\nu-1) \cos\varphi \cos(\beta+\alpha+\varphi+\psi) \right] + (t' + \frac{c}{\sin\varphi}) \tfrac{1}{2} r^2 (\nu-1) \cos\varphi \qquad 3333$$

The moment about the middle of the chord is (Fig. 33C):

$$M_R = M_R^o + R^{90^\circ-\beta} r \cos\alpha \qquad 3334$$

Inserting 3333 and 3324 (with $g = 90^\circ-\beta$) in 3334, and, at the same time, introducing k instead of r by means of 3201, we get:

$$M_R = \gamma k^3 (M_R^{\gamma x} \sin\beta + M_R^{\gamma y} \cos\beta) + (t' + \frac{c}{\sin\varphi}) k^2 M_R^t \qquad 3335$$

containing the following functions of α and φ:

$$M_R^t = \frac{\cos\psi \cot\alpha}{4 \sin\alpha} \left[\cos(\psi-\varphi-\alpha) - \nu \cos(\psi-\varphi+\alpha) + \tfrac{1}{2}(\nu-1) \cos\varphi \sec\psi \sec\alpha \right] \qquad 3336$$

$$M_R^{\gamma x} = \frac{\cos\psi \cot\alpha}{16 \sin^2\alpha} \Big[2\alpha \cos\psi - 4 \sin\varphi \sin(\psi+\varphi) \tan\alpha + \sin 2\varphi \cos(\psi-2\alpha) + \cos\psi \sin 2\psi - \sin(\psi+\varphi+\alpha) \left[2\nu \cos\psi \cos(\psi-\varphi+\alpha) - (\nu-1) \cos\varphi \sec\alpha \right] \Big] \qquad 3337$$

$$M_R^{\gamma y} = \frac{\cos\psi \cot\alpha}{16 \sin^2\alpha} \Big[2\alpha \sin\psi + 4 \sin\varphi \cos(\psi+\varphi) \tan\alpha - \cos 2\varphi \cos(\psi-2\alpha) - \cos\psi \cos 2\psi + \cos(\psi+\varphi+\alpha) \left[2\nu \cos\psi \cos(\psi-\varphi+\alpha) - (\nu-1) \cos\varphi \sec\alpha \right] \Big] \qquad 3338$$

From Figs. 33A and 33C it will be seen that τ is assumed positive when, acting upon the moving earth mass outside the rupture-line, it is directed from the starting point (') towards the finishing point (''), i.e., towards the foot of the wall. The corresponding pressure in the rupture-line is called passive, whereas the pressure corresponding to a negative τ is called active.

Noting also the previously indicated sign rules for α and β it will be found that the preceding formulae are valid in all cases if:

c, φ, ψ and μ are assumed positive for passive pressure,
c, φ, ψ and μ are assumed negative for active pressure,
α and r are assumed positive for a concave circle,
α and r are assumed negative for a convex circle,
β is assumed positive, when the chord falls towards the wall,
β is assumed negative, when the chord rises towards the wall.

In order to facilitate the practical use of the above formulae, the quantities t^t, $t^{\gamma x}$, $t^{\gamma y}$, V^{tx}, V^{ty}, H^{tx}, H^{ty}, $V^{\gamma x}$, $V^{\gamma z}$, $H^{\gamma y}$, $H^{\gamma z}$, M_R^t, $M_R^{\gamma x}$ and $M_R^{\gamma y}$,

which are functions of φ and α only, have been evaluated for $\varphi = \pm 30^\circ$ and $-90^\circ \leq \alpha \leq +90^\circ$ in the Tables 2a-b and 3a-b in the Appendix.

It should be noted that the superscripts x, y and z respectively denote that the multiplier is a sine-function, a cosine-function, and a constant (=1) respectively. Further, the argument of the function is usually β itself, only for V^{yx} and H^{yy} is the argument $2\beta+2\varphi$.

For a straight rupture-line ($\alpha \to 0$) the following formulae can be derived:

$$t'' = \gamma k \sin(\beta+\varphi) + t' \qquad 3339$$

$$R^g = \tfrac{1}{2}\gamma k^2 \sin(\beta+\varphi)\cos(\beta+\varphi+g) + kt'\cos(\beta+\varphi+g) - ck\sin(\beta+g) \qquad 3340$$

$$V = \tfrac{1}{4}\gamma k^2 \sin(2\beta+2\varphi) + kt'\cos(\beta+\varphi) - ck\sin\beta \qquad 3341$$

$$H = \tfrac{1}{2}\gamma k^2 \sin^2(\beta+\varphi) + kt'\sin(\beta+\varphi) + ck\cos\beta \qquad 3342$$

$$M_R = \tfrac{1}{12}\gamma k^3 \cos\varphi \sin(\beta+\varphi) \qquad 3343$$

As usual, φ and c should be assumed positive for passive pressure and negative for active pressure.

332. Frictionless Earth

In the special case of frictionless earth ($\varphi = 0$), we have:

$$\tau_{rv} = \tau = c \qquad \sigma_r = \sigma_v = \sigma = t \qquad 3344\text{-}45$$

With these values 3306 yields:

$$\frac{d\sigma}{dv} + 2c + \gamma r \sin v = 0 \qquad 3346$$

For r = constant (circle) the solution is:

$$\sigma = K_o - 2cv + \gamma r \cos v \qquad 3347$$

If v' and σ' are corresponding values we get:

$$K_o = \sigma' + 2cv' - \gamma r \cos v' \qquad 3348$$

Using 3347 for the finishing point of the rupture-circle (Fig. 33C), inserting K_o from 3348 and, finally, using 3314-15, we get for the stress σ'':

$$\sigma'' = 2\gamma r \sin\alpha \sin\beta + 4\alpha c + \sigma' \qquad 3349$$

Introducing k instead of r by means of 3201 we find:

$$\sigma'' = \gamma k \sin\beta + ct^c + \sigma' \qquad \text{where:} \qquad t^c = 4\alpha \qquad 3350\text{-}51$$

Next, we shall determine the resultants of the stresses acting in the rupture-circle (Fig.33C) on the earth above this circle. On each element rdv of the circle acts a shear stress $\tau = c$ and a normal stress σ, given by 3347.

The resulting force in a direction making an angle g with the vertical can be found by means of 3323. Inserting $\tau = c$ and σ from 3347, carrying out the integration, inserting K_o from 3348 and, finally, using 3314-15, we can find:

$$R^g = \tfrac{1}{2}\gamma r^2 \left[4 \sin^2\alpha \sin\beta \cos(\beta+g) + (2\alpha - \sin 2\alpha)\cos g\right] + 2rc\left[\sin\alpha \sin(\beta+g) - 2\alpha \sin(\beta-\alpha+g)\right] + 2r\sigma' \sin\alpha \cos(\beta+g) \qquad 3352$$

The vertical component V is obtained with $g = 0$, and the horizontal component H with $g = -90^\circ$. If, at the same time, r is substituted by k by means of 3201, we get:

$$V = \gamma k^2 (V^{\gamma z} + \tfrac{1}{4}\sin 2\beta) + ck\,(V^{cx}\sin\beta + V^{cy}\cos\beta) + k\sigma'\cos\beta \qquad 3353$$

$$H = \tfrac{1}{2}\gamma k^2 \sin^2\beta + ck\,(H^{cx}\sin\beta + H^{cy}\cos\beta) + k\sigma'\sin\beta \qquad 3354$$

where:

$$V^{\gamma z} = \tfrac{1}{4}(\alpha + \alpha\cot^2\alpha - \cot\alpha) = G^{\gamma z} \qquad 3355$$

$$-V^{cx} = H^{cy} = 2\alpha\cot\alpha - 1 \qquad V^{cy} = H^{cx} = 2\alpha \qquad 3356\text{-}57$$

The moment about the centre of the circle is given by 3332 which, with $\tau = c$, and using 3314-15, yields:

$$M_R^o = 2\alpha c r^2 \qquad 3358$$

The moment about the middle of the chord can be found by means of 3334. Inserting 3358 and 3352 (with $g = 90^\circ - \beta$) and, at the same time, introducing k instead of r by means of 3201, we get:

$$M_R = \gamma k^3 M_R^{\gamma x} \sin\beta + ck^2 M_R^c \qquad 3359$$

where:

$$M_R^c = \tfrac{1}{2}(\alpha - \alpha\cot^2\alpha + \cot\alpha) \qquad 3360$$

$$M_R^{\gamma x} = \tfrac{1}{8}(\alpha + \alpha\cot^2\alpha - \cot\alpha)\cot\alpha = -M_G^{\gamma x} \qquad 3361$$

The preceding formulae are valid in all cases, if only:

c is assumed positive for passive pressure,
c is assumed negative for active pressure,
α and r are assumed positive for a concave circle,
α and r are assumed negative for a convex circle,
β is assumed positive, when the chord falls towards the wall,
β is assumed negative, when the chord rises towards the wall.

In order to facilitate the practical use of the above formulae the quantities t^c, V^{YZ}, V^{cx}, V^{cy}, H^{cx}, H^{cy}, M_R^c and M_R^{YX}, which are functions of α only, have been evaluated for $-90^\circ \leq \alpha \leq +90^\circ$ in Table 1 in the Appendix.

For a straight rupture-line the formulae 3339-43 can be used with $\varphi = 0$ and $t = \sigma$.

34. BOUNDARY CONDITIONS

341. General Principle

A boundary is a line separating two mediums with different physical properties. As examples may be mentioned the surface of a structure, a free or loaded earth surface, and an internal boundary between two layers of different earth.

Whenever a rupture-line intersects a boundary it will be found that the statical equilibrium conditions at the point of intersection cannot be fully satisfied, unless the angle between rupture-line and boundary has a certain definite value, or unless all stresses vanish at this point.

It is possible, and even probable, that the figures of rupture actually developing in nature will have such a composition that they satisfy fully the boundary conditions. However, in order to do this they must, in most cases, be rather complicated and, therefore, unsuitable for practical calculation.

From a practical point of view it will generally be necessary to consider the simplest type of rupture-figure compatible with the movement of the structure. But, as this figure will usually not satisfy all the statical boundary conditions, the following question arises: Which relation should be assumed to exist between the stresses at both sides of a boundary in order to obtain the closest agreement between calculation and experience?

In order to answer this question we shall make use of the well-known fact that extreme-calculations of slopes by means of simple rupture-lines (circles for $\varphi = 0$ and logarithmic spirals for $\varphi \neq 0$) actually yield very reliable results, in spite of the fact that the critical rupture-lines do not intersect the boundaries at the statically correct angles.

Correspondingly, we shall assume that the most reliable results are obtained when we base our equilibrium calculation on such a boundary condition, that it leads to the same results as an ordinary extreme-calculation in cases where the extreme-calculation can be carried out at all.

Fig. 34A is supposed to show the result of an equilibrium-calculation, carried out by means of Kötter's equation and a certain (but so far unknown) relation between the stresses at both sides of a boundary. The earth surface may have any shape, and the loading may consist of forces of any kind and acting in any direction.

In the general case we would have to use logarithmic spirals as rupture-lines in an extreme-calculation. We assume, therefore, that we have also used

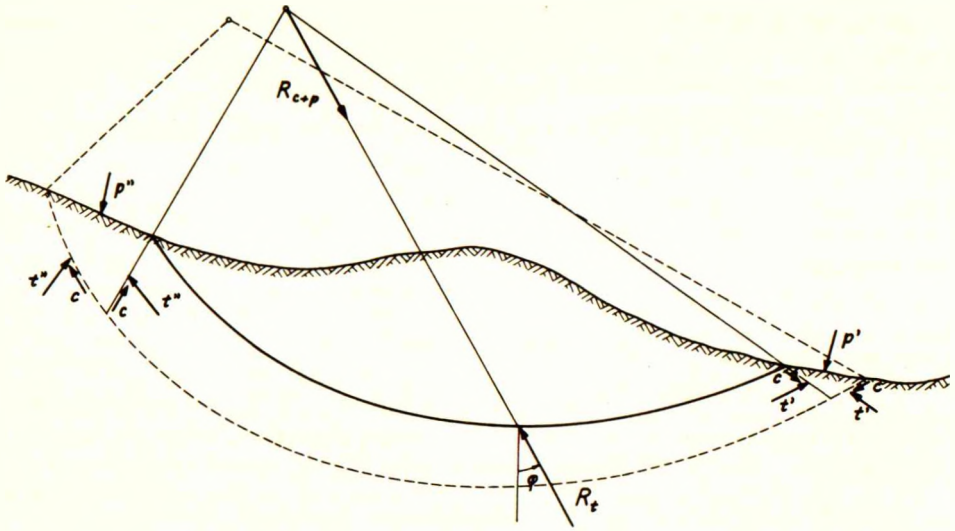

Fig.34A: Critical spiral in equilibrium-calculation

them in our equilibrium-calculation, and that, as a result of the latter calculation, we have found the full-drawn spiral in Fig. 34A. In that case the resultant R_t of the oblique stresses t in the rupture-line is in equilibrium with the resultant R_{c+p} of the cohesive stresses c in the rupture-line and all other forces acting upon the earth above the rupture-line. As R_t must go through the pole, the same applies to R_{c+p}.

It should be noted that in an equilibrium-calculation we consider the state of failure, which means that we operate with a nominal safety factor of 1. The actual safety is introduced by multiplying the loads and dividing the soil constants with suitable factors before the proper calculation is made.

We shall now investigate under what conditions the full-drawn spiral may also be the critical spiral found by an extreme-calculation. As is known, the critical spiral is the one for which the ratio between the overturning and the stabilizing moments about the pole has a maximum value. Moreover, as the nominal safety factor is 1, this maximum value should be equal to 1.

This means that, for the critical spiral, the overturning and the stabilizing moments are numerically equal, so that the total moment, about the pole of the spiral, of all forces acting upon the earth mass above the spiral, is zero. Further, the extreme-condition is satisfied if the same applies to any other spiral infinitely near the critical one.

Such a spiral is the dotted one in Fig. 34A. The earth mass above this spiral can be divided into four parts, which we shall consider separately.

Firstly, the earth mass above the full-drawn spiral is known to be in equilibrium, so that the forces acting on it give zero moment about any point and hence also about the pole of the dotted spiral.

Next, we consider the narrow earth band between the two spirals and the outermost radius-vectors of the full-drawn spiral. A small element of this band is shown in Fig. 34B. If we denote the angle between rupture-line and horizon by v, and the radius of the osculating circle by r, the radius-vector of the full-drawn spiral will have a length r cos φ and will make an angle v+φ with the vertical. The corresponding quantities for the dotted spiral are (r+Δr) cos φ and (v+Δv) + φ.

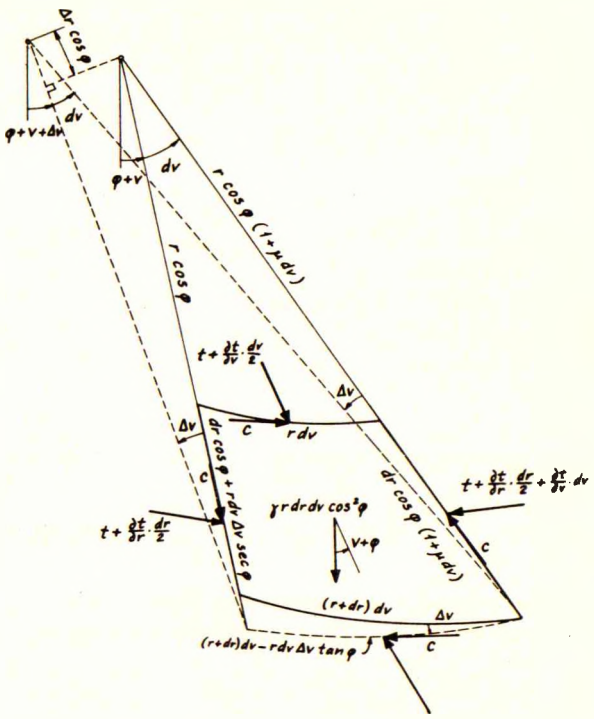

Fig. 34B: Small earth element between spirals

The three sides of the element in Fig. 34B are rupture-lines and we know, therefore, the directions and magnitudes of the stresses acting in them. The fourth side (the dotted one) is, however, not a rupture-line proper, as it makes a small angle Δv with the direction of the rupture-line. Therefore, we do not know the magnitude of the oblique stress acting in it, but from Mohr's circle (Fig. 33B) it will be seen that the angle between the direction of this stress and the normal to the section will remain unchanged (= φ) by an infinitely small rotation of the section. Consequently, the oblique stress in the dotted spiral gives no moment about the pole of this spiral.

The forces acting on the element in Fig. 34B are obtained by multiplying the indicated stresses by the corresponding side-lengths. Expressing the fact that the total moment of all these forces (including the gravity forces) about the pole of the dotted spiral should be zero, we get the following condition:

$$\frac{\partial t}{\partial v} + 2\mu t + 2c \sec \varphi + \gamma r \sin(v+\varphi) = 0 \qquad 3401$$

Eliminating t by means of 3313 we find:

$$\frac{\partial \tau}{\partial v} + 2\mu \tau + \gamma r \sin \varphi \sin(v+\varphi) = 0 \qquad 3402$$

Equation 3402 is, in fact, identical with Kötter's equation 3308, and as we actually use this equation as a basis for our equilibrium-calculation, we have proved that the moment, about the pole of the dotted spiral, of all forces acting upon the considered earth band, is zero.

All we have left now are the two small triangular elements at the extreme ends of the narrow earth band (Fig. 34A). If we can also ascertain that the moment, about the pole of the dotted spiral, of the forces acting on each of these elements is zero, then the extreme-condition is completely satisfied, and we shall find the same spiral whether we make an equilibrium- or an extreme-calculation.

The forces acting on one of the small triangular elements are the surface load p and the stresses c and t in the rupture-lines. The weight of the element can be disregarded, as it is small of a higher order than the above-mentioned forces. Further, the moment will be zero when the resultant perpendicular to the radius-vector is zero. Finally, as the radius-vector is a pseudo-rupture-line, we can give the following general rule for obtaining the required boundary condition:

We consider a small triangular element between the boundary, the rupture-line and a pseudo-rupture-line. Then the proper boundary condition is obtained by expressing that the resultant perpendicular to the pseudo-rupture-line of the surface forces acting on the element should be zero.

We have now proved that if we make an equilibrium-calculation by means of Kötter's equation and boundary conditions obtained as described above, we shall find the same spiral as would be found by an extreme-calculation.

The main unknown quantity in the problem (a force, a safety-factor or a dimension) is found in the extreme-method by means of the moment equation about the pole of the critical spiral. As this equation must also be satisfied in the equilibrium-method, it is evident that the same value of the unknown quantity will be found in both methods.

342. Stress at Ground Surface

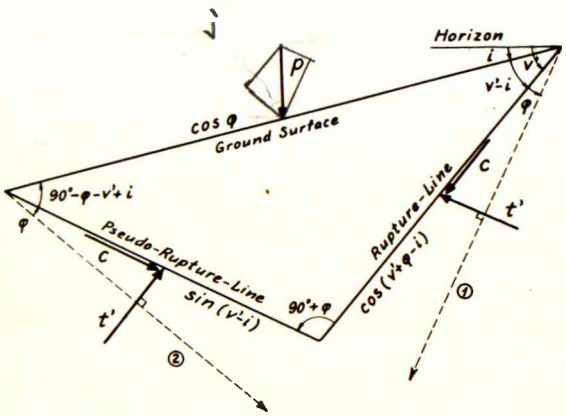

Fig. 34C: Small earth element at ground surface

We consider first the case of a sloping ground surface, making an angle i with the horizon (Fig. 34C). i is assumed positive when the surface of the moving earth mass falls from the starting point of the rupture-line towards the wall. The rupture-line makes an angle v' with the horizon (positive when the rupture-line falls from the starting point). The stresses c and t' act in the rupture-line directly below the surface. The ground surface is loaded by a vertical surcharge p per unit area of the sloping surface.

Fig. 34C shows an infinitely small earth element between the surface, the rupture-line and a pseudo-rupture-line. The side-lengths of the element are proportional to the sines of the opposite angles. By projection on the two dotted lines 1 and 2 respectively, the following equations are obtained:

$$p \sin(v'+\varphi) + c \cos(v'+\varphi-i) - t' \sin(v'-i) = 0 \qquad 3403$$

$$p \cos v' + c \sin(v'-i) - t' \cos(v'+\varphi-i) = 0 \qquad 3404$$

These two equations can be satisfied simultaneously only for special values of v', which may be determined by elimination of t':

$$c \cos\varphi \sin i \sin(2v'+\varphi-i) + (p \sin\varphi + c \cos\varphi \cos i) \cos(2v'+\varphi-i) + p \sin i = 0 \qquad 3405$$

Such an equation of the type:

$$X \sin 2u + Y \cos 2u + Z = 0 \qquad \text{yields:} \qquad \tan u = \frac{X \pm \sqrt{X^2+Y^2-Z^2}}{Y - Z} \qquad 3406\text{-}07$$

In the special case of cohesionless earth ($c = 0$) equation 3405 gives:

$$\cos(2v'+\varphi-i) = -\frac{\sin i}{\sin\varphi} \qquad 3408$$

and, in the case of frictionless earth ($\varphi = 0$):

$$\cos(2v'-2i) = -\frac{p}{c} \sin i \qquad 3409$$

and, finally, in the case of a horizontal surface ($i = 0$):

$$v' = 45^\circ - \tfrac{1}{2}\varphi \qquad 3410$$

When v' has been determined in this way, t' may be found from 3403 or 3404. In such cases where 3405 cannot be fulfilled, we must, as explained in Section 341, use 3403 for the determination of t'. Using also 3314 we find:

$$t' = p \frac{\sin(\beta+\alpha+\varphi)}{\sin(\beta+\alpha-i)} + c \frac{\cos(\beta+\alpha+\varphi-i)}{\sin(\beta+\alpha-i)} \qquad 3411$$

In the case of frictionless earth ($\varphi = 0$), we get:

$$\sigma' = p \frac{\sin(\beta+\alpha)}{\sin(\beta+\alpha-i)} + c \cot(\beta+\alpha-i) \qquad 3412$$

In the special case of a horizontal surface ($i = 0$), equations 3411-12 are reduced to:

$$t' = p \frac{\sin(\beta+\alpha+\varphi)}{\sin(\beta+\alpha)} + c \frac{\cos(\beta+\alpha+\varphi)}{\sin(\beta+\alpha)} \qquad 3413$$

$$\sigma' = p + c \cot(\beta+\alpha) \qquad 3414$$

As regards sign rules for c, φ, α and β, see Section 331 (p. 58).

343. Earth Pressure on Wall

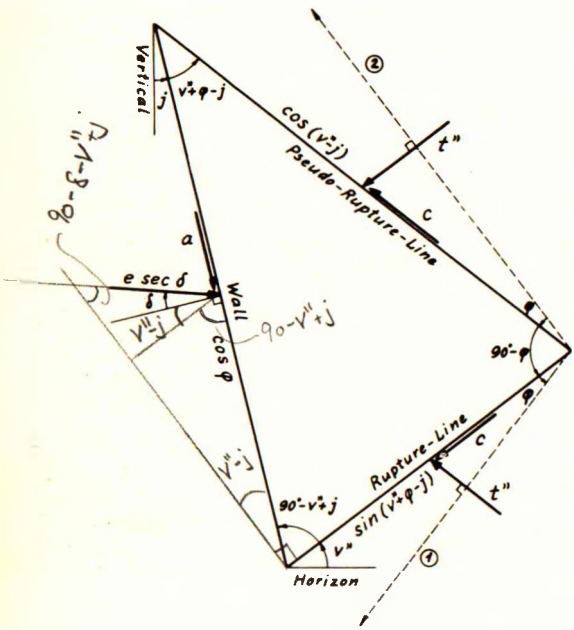

Fig. 34D: Small earth element at wall

Next, we shall consider the case of an inclined wall, making an angle j with the vertical (Fig. 34D). j is assumed positive when the moving earth mass is overhanging with regard to the wall. The rupture-line makes an angle v" with the horizon (positive when the rupture-line falls towards the finishing point). The stresses c and t" act in the rupture-line at the wall. The stresses between wall and earth consist of an adhesion a and an oblique stress, which has a normal component e and makes an angle δ with the normal to the wall. a and δ are assumed positive when the tangential earth pressure acts downwards on the earth and upwards on the wall.

Fig. 34D shows an infinitely small earth element between the wall, the rupture-line and a pseudo-rupture-line. By projection on the two dotted lines 1 and 2 respectively, the following equations are obtained:

$$t'' \cos(v''-j) + (c+a) \sin(v''+\varphi-j) - e \sec\delta \cos(v''+\varphi+\delta-j) = 0 \qquad 3415\,\surd$$

$$t'' \sin(v''+\varphi-j) + (c-a) \cos(v''-j) - e \sec\delta \sin(v''+\delta-j) = 0 \qquad 3416\,\surd$$

These two equations can be satisfied simultaneously only for special values of v", which may be determined by elimination of e:

$$\cos(2v''+\varphi+\delta-2j) = \frac{t'' \sin\delta + c \sin\varphi \sin\delta + a \cos\varphi \cos\delta}{t'' \sin\varphi + c} \qquad 3417$$

If we make the plausible assumption that:

$$\frac{a}{c} = \frac{\tan\delta}{\tan\varphi} \qquad 3418\,\surd$$

which, at least, is correct both for a perfectly smooth wall ($a = 0$, $\delta = 0$) and for a perfectly rough wall ($a = c$, $\delta = \varphi$), then 3417 is reduced to:

$$\cos(2v''+\varphi+\delta-2j) = \frac{\sin\delta}{\sin\varphi} \qquad 3419$$

In the special case of cohesionless earth ($c = a = 0$), equation 3417 is reduced to 3419, independently of the assumption 3418. In the case of frictionless earth ($\varphi = \delta = 0$) equation 3417 gives:

$$\cos(2v''-2j) = \frac{a}{c} \qquad 3420$$

Further, in the case of a perfectly smooth wall ($a = 0$, $\delta = 0$), we find:

$$v''_S = 45^\circ - \tfrac{1}{2}\varphi + j \qquad 3421$$

and, finally, in the case of a perfectly rough wall ($a = c$, $\delta = \varphi$), provided that a tangential movement takes place between wall and earth:

$$v''_r = -\varphi + j \qquad 3422$$

When v" has been determined in this way, e may be found from 3415 or 3416. In such cases where 3417 cannot be fulfilled, we must, as explained in Section 341, use 3415 for the determination of e. Using also 3315 we find:

$$e = t''\frac{\cos\delta\cos(\beta-\alpha-j)}{\cos(\beta-\alpha+\varphi+\delta-j)} + (c+a)\frac{\cos\delta\sin(\beta-\alpha+\varphi-j)}{\cos(\beta-\alpha+\varphi+\delta-j)} \qquad 3423$$

In the case of frictionless earth ($\varphi = \delta = 0$) we get:

$$e = \sigma'' + (c+a)\tan(\beta-\alpha-j) \qquad 3424$$

In the special case of a vertical wall ($j = 0$), equations 3423-24 are reduced to:

$$e = t''\frac{\cos\delta\cos(\beta-\alpha)}{\cos(\beta-\alpha+\varphi+\delta)} + (c+a)\frac{\cos\delta\sin(\beta-\alpha+\varphi)}{\cos(\beta-\alpha+\varphi+\delta)} \qquad 3425$$

$$e = \sigma'' + (c+a)\tan(\beta-\alpha) \qquad 3426$$

When the unit normal earth pressure e has been determined, the unit tangential earth pressure f can be found by means of equation 3103. f is positive, when a and δ are positive, i.e., when the tangential earth pressure acts downwards on the earth and upwards on the wall.

As regards sign rules for c, φ, α and β, see Section 331 (p.58).

344. Rupture-Lines Meeting at Wall

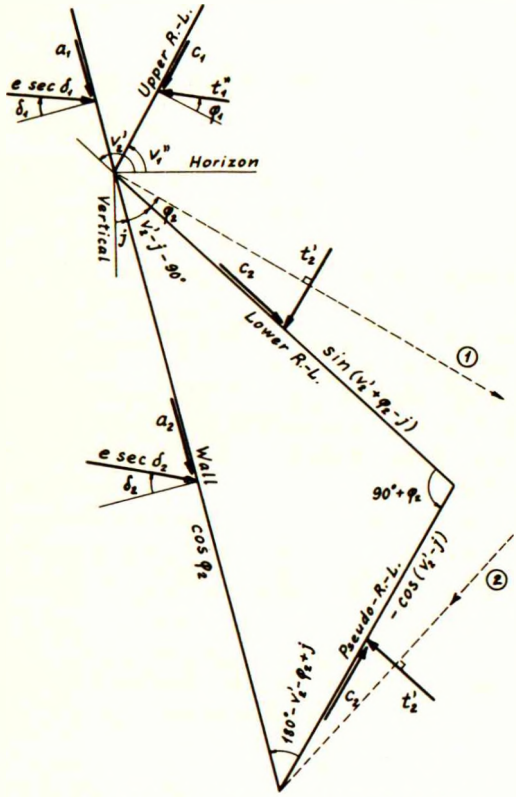

Fig. 34E shows two rupture-lines, which meet at a wall. All quantities in connection with the upper rupture-line are denoted by the subscript 1, whereas those connected with the lower one are given the subscript 2. At the meeting point a stress t_1'' acts in the upper rupture-line and a stress t_2' in the lower rupture-line (in addition to the cohesions c_1 and c_2). At the meeting point the two rupture-lines make angles of v_1'' and v_2' respectively with the horizon (both pos. in Fig. 34E).

Further, Fig. 34E shows an infinitely small earth element between the wall, the lower rupture-line and a pseudo-rupture-line. By projection on the two dotted lines 1 and 2 respectively, we obtain two equations similar to 3415-16 (but with subscripts 2 and with ' instead of "). As usual, we must use 3415 which, by means of 3314 with subscripts 2, gives:

$$t_2' = e\,\frac{\cos(\beta_2+\alpha_2+\varphi_2+\delta_2-j)}{\cos\,\delta_2\,\cos(\beta_2+\alpha_2-j)} - (c_2+a_2)\,\frac{\sin(\beta_2+\alpha_2+\varphi_2-j)}{\cos(\beta_2+\alpha_2-j)} \qquad 3427$$

A comparison with extreme-calculations of composite rupture-figures has shown that the correct result, at least for frictionless earth, is obtained by assuming e to be the same at both sides of the meeting point. Consequently, we can insert 3423 (with subscripts 1) in 3427. The resulting equation can be simplified by putting $\varphi_1 = -\varphi_2$ and $c_1 = -c_2$. Further, we have usually also $\delta_1 = -\delta_2$ and $a_1 = -a_2$, viz., when a tangential movement takes place between wall and earth at both sides of the meeting point, and in opposite directions. Under these circumstances we find:

$$t_2' = t_1''\,\frac{\cos(\beta_1-\alpha_1-j)\,\cos(\beta_2+\alpha_2+\varphi_2+\delta_2-j)}{\cos(\beta_2+\alpha_2-j)\,\cos(\beta_1-\alpha_1-\varphi_2-\delta_2-j)}$$

$$- (c_2+a_2)\,\frac{\cos\,\delta_2\,\sin(\beta_1-\alpha_1+\beta_2+\alpha_2-2j)}{\cos(\beta_2+\alpha_2-j)\,\cos(\beta_1-\alpha_1-\varphi_2-\delta_2-j)} \qquad 3428$$

In the case of frictionless earth ($\varphi = \delta = 0$) we get:

$$\sigma_2' = e - (c_2+a_2)\tan(\beta_2+\alpha_2-j) \qquad 3429$$

$$\sigma_2' = \sigma_1'' - (c_2+a_2)\left[\tan(\beta_1-\alpha_1-j) + \tan(\beta_2+\alpha_2-j)\right] \qquad 3430$$

The formulae for a vertical wall are, of course, obtained with $j = 0$. For a perfectly smooth wall we must put $a_2 = 0$ and $\delta_2 = 0$, and for a perfectly rough wall $a_2 = c_2$ and $\delta_2 = \varphi_2$.

It is possible that the above formulae for rupture-lines meeting at a wall are actually valid only for $\delta_1 = \delta_2$ (e.g., frictionless earth or a perfectly smooth wall), because it can be shown that only in this case is it possible to carry out an extreme-calculation of the problem.

345. Rupture-Lines Meeting in Earth

When two rupture-lines meet inside a homogeneous, isotropic earth mass, they must make either an angle 0° with each other (passive or active pressure in both lines) or angles $90^\circ \pm \varphi$ with each other (passive pressure in one line and active in the other). The stress t is the same in both rupture-lines at their point of intersection ($t_2' = t_1''$).

This is a consequence of the statical equilibrium conditions for a small earth element at the point of intersection, and is also shown by Mohr's circle (Fig.33B). In choosing here to satisfy fully the boundary conditions instead of letting the rupture-lines meet at an arbitrary angle and using our special boundary condition, we have been guided by the following considerations:

Firstly, an investigation of possible rupture-figures shows, that this fixing of the angle between the rupture-lines does not make the rupture-figures unduly complicated. In fact, if we did not fix this angle in advance, the rupture-figures would involve too many variables.

Secondly, it has been found that an extreme-calculation for a certain composite rupture-figure (in frictionless earth), in which the said angle is taken as one of the variables, leads to the result that this angle must be 90°, which is the statically correct value.

Consequently, we shall usually follow the rule that rupture-lines must meet each other at the statically correct angles 0° or $90^\circ \pm \varphi$. This does not apply, however, to rupture-lines meeting each other at the wall (Section 344).

There is one other possible exception, as pointed out by Prager and Hodge (1951). From a purely statical point of view, two rupture-lines may make any angle with each other, provided that they meet at a so-called "line of discontinuity". At both sides of this line there must be the same shear stress in the line and the same normal stress perpendicular to the line, whereas the normal stresses parallel to the line may be different from each other.

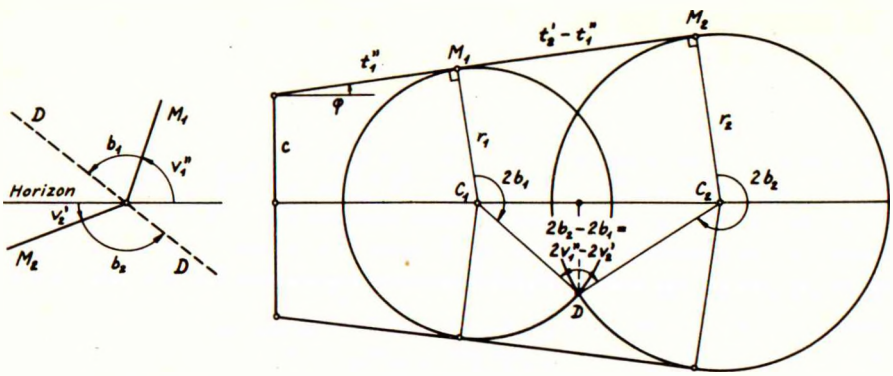

Fig.34F: Line of discontinuity and corresponding Mohr circles

This is illustrated by Fig. 34F, where the common point D of the two Mohr circles corresponds to the line of discontinuity D. The radii to this point make an angle with each other, which is twice the angle between the rupture-lines M_1 and M_2. By means of the triangle DC_1C_2 we can find:

$$(t_2'-t_1'')^2\sec^2\varphi = (t_1''\tan\varphi + c\sec\varphi)^2 + (t_2'\tan\varphi + c\sec\varphi)^2$$
$$- 2\,(t_1''\tan\varphi + c\sec\varphi)(t_2'\tan\varphi + c\sec\varphi)\cos 2(\beta_1-\alpha_1-\beta_2-\alpha_2) \qquad 3431$$

Solving this equation with respect to t_2' we get:

$$t_2' = t_1'' + (t_1'' + \frac{c}{\sin\varphi})\,2K\,(K + \sqrt{1+K^2}) \qquad 3432$$

where:
$$K = \mu\sin(\beta_1-\alpha_1-\beta_2-\alpha_2) \qquad 3433$$

For <u>frictionless</u> earth ($\varphi = 0$) we can find:

$$\sigma_2' = \sigma_1'' + 2c\sin(\beta_1-\alpha_1-\beta_2-\alpha_2) \qquad 3434$$

From a kinematical point of view several objections can be raised against a rupture-figure involving one or more lines of stress discontinuity. In spite of this, such a figure may be used as a convenient means of approximate calculation, and, as it is "statically admissible", according to the theory of limit analysis, it gives a result which is on the safe side.

346. Internal Boundary

Internal boundaries are lines separating layers of earth with different values of one or more of the constants γ, φ, c.

Fig. 34G shows an infinitely small earth element, in which the internal boundary is a diagonal. The sides of the element are rupture-lines and pseudo-rupture-lines. In the case of the boundary being the upper limit of a capillary zone, a capillary pressure p_c may act perpendicularly to the boundary.

By projection on the two dotted lines 1 and 2 two different equations are obtained. These can only be satisfied simultaneously, when a certain relation exists between the angles v_2' and v_1'' or (in the case of $v_2' = v_1'' = v$) when v has a certain value.

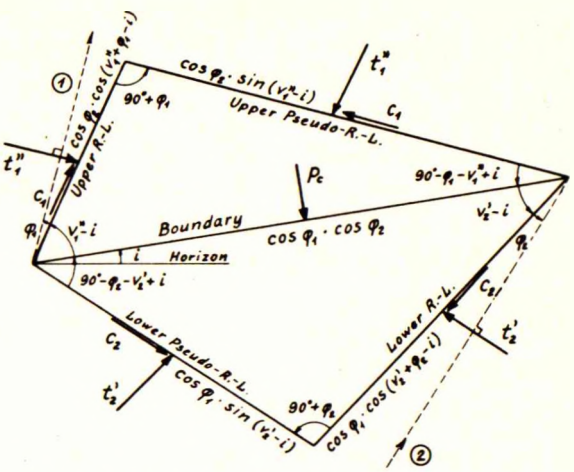

Fig.34G: Small earth elements at internal boundary

If we try to use our special boundary condition we are confronted by the difficulty that the two pseudo-rupture-lines in Fig. 34G are generally not parallel. Therefore, neither of the above-mentioned two equations can provide the proper boundary condition. This difficulty corresponds to the fact that it is impossible to carry out an extreme-calculation of the problem, unless the two rupture-lines are logarithmic spirals with the same pole.

Consequently, we can only indicate a proper boundary condition in the special case of the two pseudo-rupture-lines being parallel, i.e.:

$$\varphi_1 + \beta_1 - \alpha_1 = \varphi_2 + \beta_2 + \alpha_2 \qquad 3435$$

In this case we find by projection on the dotted lines 1 and 2, which are now parallel:

$$t_2' = t_1'' \frac{\sin(\beta_1-\alpha_1-i)}{\sin(\beta_2+\alpha_2-i)} + (c_2-c_1) \frac{\cos(\beta_2+\alpha_2+\varphi_2-i)}{\sin(\beta_2+\alpha_2-i)} + p_c \frac{\sin(\beta_2+\alpha_2+\varphi_2-i)}{\sin(\beta_2+\alpha_2-i)} \qquad 3436$$

According to the calculation method of Drucker and Prager (see Section 226), the rupture-line in a line-rupture must always be composed of logarithmic spirals with a common pole. In that case, 3435 is automatically satisfied, which means that the problem of stratified earth is always soluble according to this method.

However, when incompressibility of the earth in the rupture-line is assumed we must, for kinematical reasons, have $v_2' = v_1'' = v$. In the case of a zone-rupture the two equations obtained by projection on the lines 1 and 2 enable the determination of the statically correct angle v and the stress t_2', when t_1'' is known. In the case of a line-rupture v is given, and 3435 shows then that we can only indicate a proper boundary condition when $\varphi_1 = \varphi_2 = \varphi$, i.e., in the case of a constant friction angle. In this special case 3436 is reduced to:

$$t_2' = t_1'' + (c_2-c_1) \frac{\cos(\beta_2+\alpha_2+\varphi-i)}{\sin(\beta_2+\alpha_2-i)} + p_c \frac{\sin(\beta_2+\alpha_2+\varphi-i)}{\sin(\beta_2+\alpha_2-i)} \qquad 3437\surd$$

If we have frictionless earth ($\varphi = 0$) at both sides of the internal boundary, we get:

$$\sigma_2' = \sigma_1'' + (c_2 - c_1) \cot(\beta_2 + \alpha_2 - i) + p_c \qquad 3438$$

Finally, it will be seen that, if only γ changes at the boundary, whereas φ and c are constant, we have the same stress at both sides ($t_2' = t_1''$), unless a capillary pressure p_c is present.

35. FIGURES OF RUPTURE

351. Introduction

A rupture-figure consists generally of a combination of rupture-lines and rupture-zones. A rupture-line is a curve, in which the shear and normal stresses satisfy the failure condition at any point. A rupture-zone (or a plastic zone) is a finite area, in which the failure condition is satisfied at any point. Through each point of a rupture-zone pass two rupture-lines, making angles of $90° \pm \varphi$ with each other. Finally, an elastic zone is an area in which the failure condition is not satisfied at any point in the interior, whereas it may be satisfied at some of the boundaries.

For the sake of simplicity all figures illustrating the present Section 35 are drawn for the simple case of a vertical wall ($j = 0$), a horizontal ground surface ($i = 0$) and frictionless earth ($\varphi = 0$).

352. Line-Ruptures

The simplest type of rupture is a line-rupture (L-rupture), in which only the points at a certain curve are in the state of failure. Such a rupture-line may also be considered as an infinitely narrow plastic zone, and when we assume constant volume of the earth in the plastic state, the velocity vectors at the rupture-line must be tangential to this line.

Outside the rupture-line proper only elastic deformations occur, and as these can be disregarded in comparison with the plastic deformations in the rupture-line, the elastic zone above the rupture-line must move as a rigid body. Taken in combination with the required tangential velocity vectors at the rupture-line, this leads to the conclusion that the rupture-line must be a circle or (in special cases) a straight line. The elastic zone above the rupture-line rotates about the centre of the circle (or translates in the direction of the straight line).

We shall distinguish between the following three types of line-ruptures:

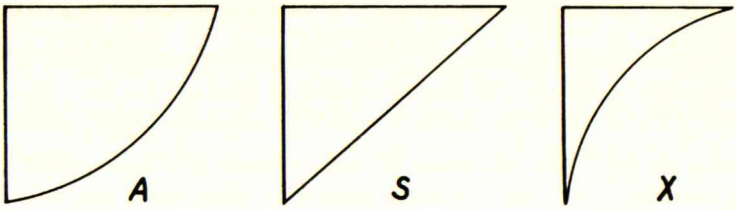

Fig.35A: Line-ruptures

1) The concave rupture (rupture A), in which the moving earth mass is located at the concave side of the circle (Fig. 35A, left).

2) The convex rupture (rupture X), in which the moving earth mass is located at the convex side of the circle (Fig. 35A, right).

3) The straight rupture (rupture S), in which the rupture-line is straight. It is a special case of both the previous ones and shall, therefore, generally not be considered separately (Fig. 35A, centre).

The elastic zone above a single rupture-line will be termed an A-zone, an X-zone or an S-zone respectively.

353. Zone-Ruptures

A rupture-figure, in which the whole area above the lowest rupture-line is in the state of failure, is called a zone-rupture (Z-rupture). We shall here distinguish between two different types of zone-ruptures, which we shall associate with the names of Rankine and Prandtl respectively, although these rupture-types by their definitions have a considerably wider scope than the special cases treated by Rankine and Prandtl:

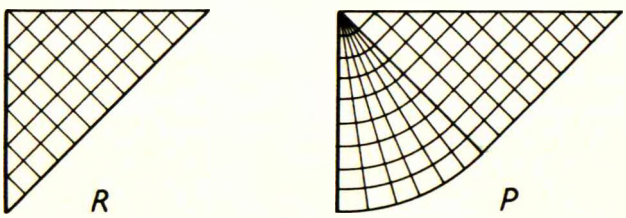

Fig.35B: Zone-ruptures

1) The Rankine-rupture (rupture R) is characterized by the fact that the rupture-lines at any point have finite curvatures. The rupture-lines may be straight, as shown in Fig. 35B (left), but can also be curved.

2) The Prandtl-rupture (rupture P) is characterized by the fact that it contains at least one singular point, in the vicinity of which the curvature of one set of the rupture-lines approaches infinity. The other set of rupture-lines may be straight, as shown in Fig. 35B (right), but can also be curved. The rupture-figure shown might be considered as a

combination of a P-zone and an R-zone, but for the sake of brevity the whole figure is termed a P-rupture. The singular point in the rupture-figure must coincide with a singular point on the wall, usually the point of intersection between the wall and the ground surface.

The lower boundary of a rupture-zone is, usually, a rupture-line and will be termed an R-line or a P-line respectively. In most cases the R-lines are straight, whereas the P-lines in special cases may be circles (in frictionless earth) or logarithmic spirals (in weightless earth). Otherwise these lines are curves of unknown shape, but in the present work they will be approximated by a suitable combination of circles and straight lines.

354. Composite Ruptures

When a rupture-figure comprises more than one elastic or plastic zone it is termed a composite rupture. Of such figures almost an infinity exists and we shall, therefore, only consider the simplest types here.

With regard to the boundaries between different zones, it is evident that the boundary between two elastic zones must be a rupture-line, if a relative movement takes place at all. The boundary between a wall and an elastic earth zone is, however, not a proper rupture-line; at least, Kötter's equation cannot be applied to it, as 3304 is not valid here.

The boundary between two plastic zones will usually be a rupture-line or an envelope of rupture-lines. However, it can also be a line of constant strain, provided that the strain in this line is the same in both zones. Kötter's equation is probably not applicable to an envelope of rupture-lines.

The boundary between an elastic and a plastic zone is, in most cases, a rupture-line or an envelope of rupture-lines. It can, however, also be a line of zero strain in the plastic zone. When we assume a constant volume in the plastic state, the lines of zero strain will make angles of $\frac{1}{2}\varphi$ with the rupture-lines and 90° with each other. In frictionless earth ($\varphi = 0$) the rupture-lines proper are also lines of zero strain.

When we have two separate zones, each with a rupture-line as a lower boundary, the following four combinations are possible:

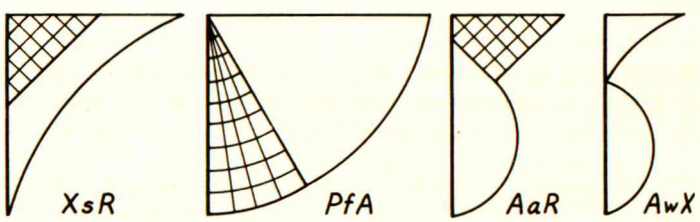

Fig.35C: Types of composite ruptures

1) The two rupture-lines are completely separated (indicated by an s between their symbols). There may be passive or active pressure in the two lines, independently of each other (Fig. 35C, extreme left).

2) The two rupture-lines meet in the earth and are flush with each other (indicated by an f between their symbols). There must be either passive pressure in both lines, or active pressure in both (Fig. 35C, centre left).

3) The two rupture-lines meet in the earth and make an angle $90^{\circ} \pm \varphi$ with each other (indicated by an a between their symbols). There must be passive pressure in one line and active pressure in the other (Fig. 35C, centre right).

4) The two rupture-lines meet at the wall (indicated by a w between their symbols). There must be passive pressure in one line and active pressure in the other (Fig. 35C, extreme right).

As in Fig. 35C, the symbol for any composite rupture shall be written in such a way that the capital letters indicating the different zones are given, starting from the foot of the wall and proceeding upwards towards the surface. Between each pair of capital letters a small letter will be placed, indicating the type of connection between the corresponding rupture-lines.

From one point of view we shall distinguish between s-ruptures, f-ruptures, a-ruptures and w-ruptures. From another point of view we shall distinguish between ZZ-ruptures, ZL-ruptures, LZ-ruptures and LL-ruptures, where the first letter indicates the type of the lower zone and the second letter the type of the upper one. By combination we can get $4 \times 4 = 16$ different types (LsZ etc.) of composite ruptures with two zones.

Further, as L may mean either A or X, and as Z may mean either R or P, we have actually $2 \times 2 \times 16 = 64$ imaginable rupture-figures with two zones. However, it can be shown that most of these must be rejected as being geometrically, kinematically or statically impossible.

A figure of rupture is called geometrically possible, if a drawing can be made of it. It is called kinematically possible, if the deformations and movements implied by it are compatible with each other and with the movements of a rigid wall (in which yield hinges may develop). Finally, it is called statically possible, if the equations of equilibrium for each of the different finite zones can be satisfied.

Of the above-mentioned 64 figures we can at once disregard the $2 \times 4 \times 2 = 16$ ZZ-ruptures (PsR etc.), as these are either geometrically impossible or identical with the simple Z-ruptures R or P. Further, in a w-rupture the lower line must always be of type A; the remaining $3 \times 1 \times 4 = 12$ cases are geometrically impossible, but 4 of them have already been rejected as ZZ-ruptures. This leaves $64 - 16 - 12 + 4 = 40$ geometrically possible figures with two zones. These are all shown in Figs. 35D-E, and we shall now investigate them from a kinematical point of view.

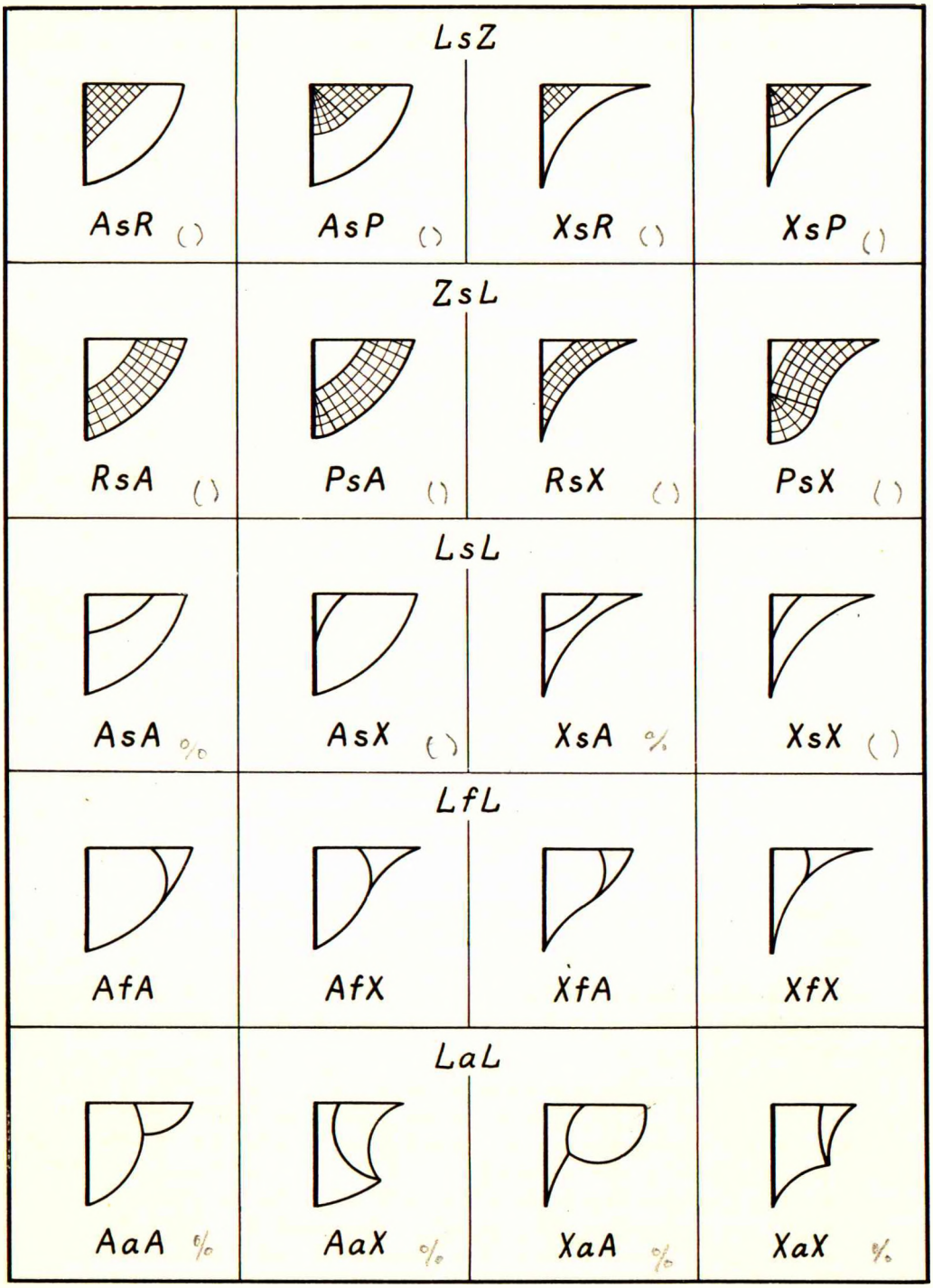

Fig.35D: Composite ruptures with 2 zones

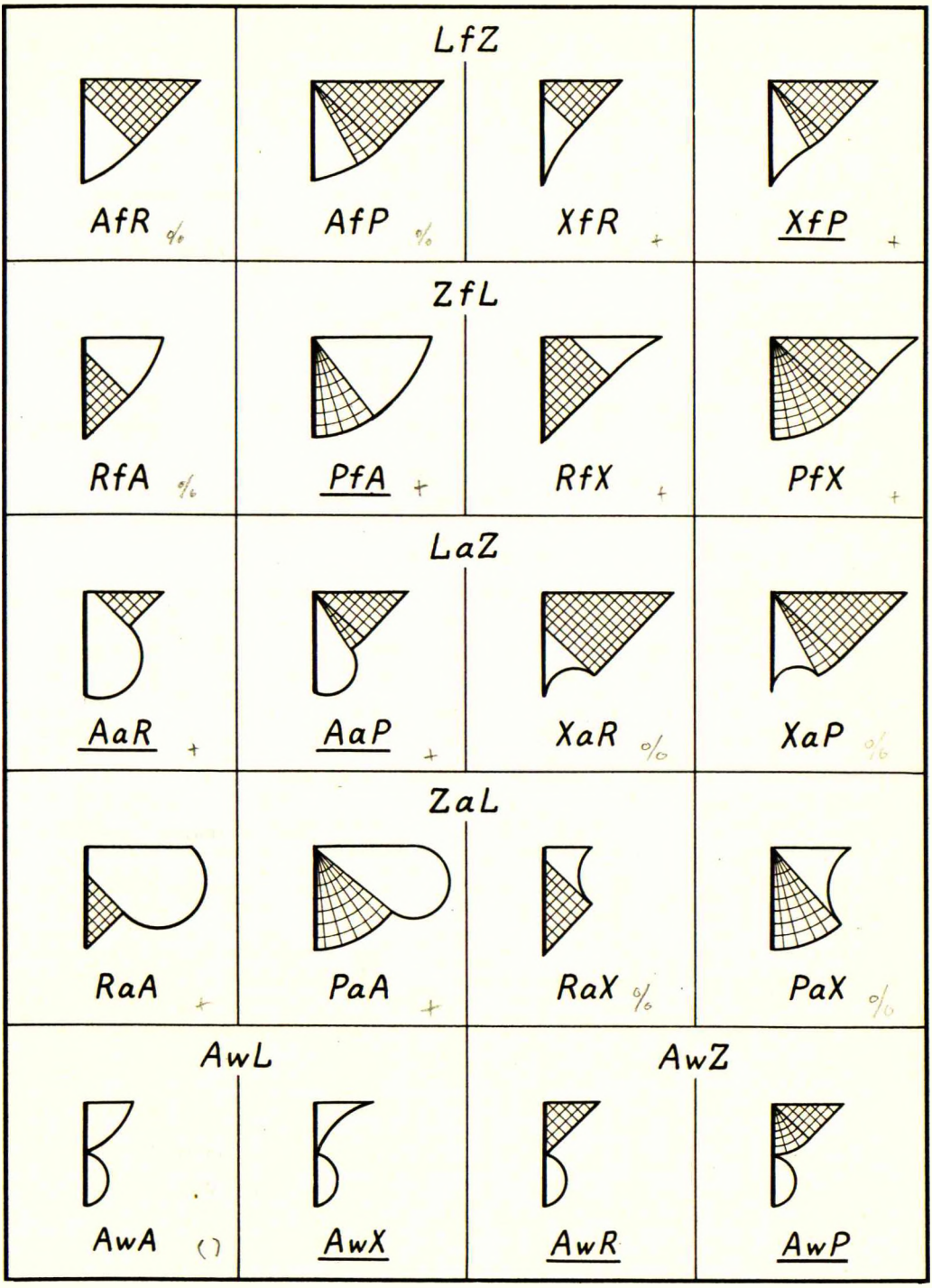

Fig.35E: Composite ruptures with 2 zones

In the LsZ- and ZsL-ruptures (AsR etc., RsA etc.) a jump or an angle must develop in the earth front. Therefore, these 8 figures are only possible, either when the earth has cohesion (allowing it to stand to a certain height without lateral support), or when the wall consists of two hinged parts (as in the case of a sheet wall with a yield hinge).

In the LsL-ruptures (AsA etc.) a jump must develop in the earth front, unless the upper circle has the wall as a tangent. As jumps are incompatible with the movements of a wall, the figures AsA and XsA are kinematically impossible. For the figures AsX and XsX the same remarks apply as made in connection with the ZsL-ruptures.

In the LfL- and LaL-ruptures (AfA etc., AaA etc.) the kinematical compatibility requires the occurrence of a third rupture-line and, further, that the centres of all 3 circles be located at one straight line. Only in that case is it possible to make the common circular boundary cover itself by infinitely small rotations of the two elastic (rigid) zones about their respective centres.

When two rupture-lines meet at an angle $90^{\circ} \pm \varphi$, the shear stresses must both be directed either towards or away from the meeting point, and the same applies to the movements of the two zones. From this fact it follows that the LaL-ruptures (AaA etc.) are kinematically impossible.

In the f-ruptures AfR, AfP and RfA the two zones must move in the same direction, but this implies that their common boundary-line should rotate in different directions. They are, therefore, kinematically impossible. The same applies to PfA, when $r_A < r_P$, whereas this rupture is kinematically possible for $r_A > r_P$. The f-ruptures XfR, XfP, RfX and PfX are all kinematically possible, as the common boundary-line can rotate in the same direction, when the two zones are moving in the same direction.

In the a-ruptures XaR, XaP, RaX and PaX the two zones must either move in different directions, or their common boundary-line must rotate in different directions. They are, therefore, kinematically impossible. The a-ruptures AaR, AaP, RaA and PaA are all kinematically possible, as the common boundary-line can rotate in the same direction.

For the w-ruptures AwA, AwX, AwR and AwP the same remarks apply as made in connection with the ZsL-ruptures. However, with the exception of AwA these ruptures can also occur in cohesionless earth or for a rigid wall without any hinge; but in the latter case the centres of the two circles in AwX must be located at the same normal to the wall.

Of the 40 geometrically possible figures we have now rejected 13 as being kinematically impossible (AsA, XsA, AaA, AaX, XaA, XaX, AfR, AfP, RfA, XaR, XaP, RaX and PaX). The same applies to 11 more (AsR, AsP, XsR, XsP, RsA, PsA, RsX, PsX, AsX, XsX and AwA) except in the special cases of earth with cohesion or a wall with a yield hinge.

Regarding the remaining 40 - 13 - 11 = 16 kinematically possible figures with two zones, a statical investigation, which cannot be given here due to lack of space, has shown that at least 5 are statically impossible (XfR, RfX, PfX,

RaA and PaA). The same seems to apply to 4 others (AfA, AfX, XfA and XfX), although the author has not succeeded in proving this definitely.

In the general case we are then left with the following 16 - 5 - 4 = 7 statically and kinematically possible rupture-figures with two zones: XfP, PfA, AaR, AaP, AwX, AwR and AwP (underlined in Fig. 35E). In addition to these we have, of course, the 4 simple figures with one zone: A, X, R and P, as well as more complicated rupture-figures.

Some of the rupture-figures actually occurring in nature are found to be comparatively simple ruptures with one or two zones as those described above. Others, however, prove to be more complicated, involving three or more zones. Some important examples are shown in Fig. 35F, and most of them will be mentioned later in different connections.

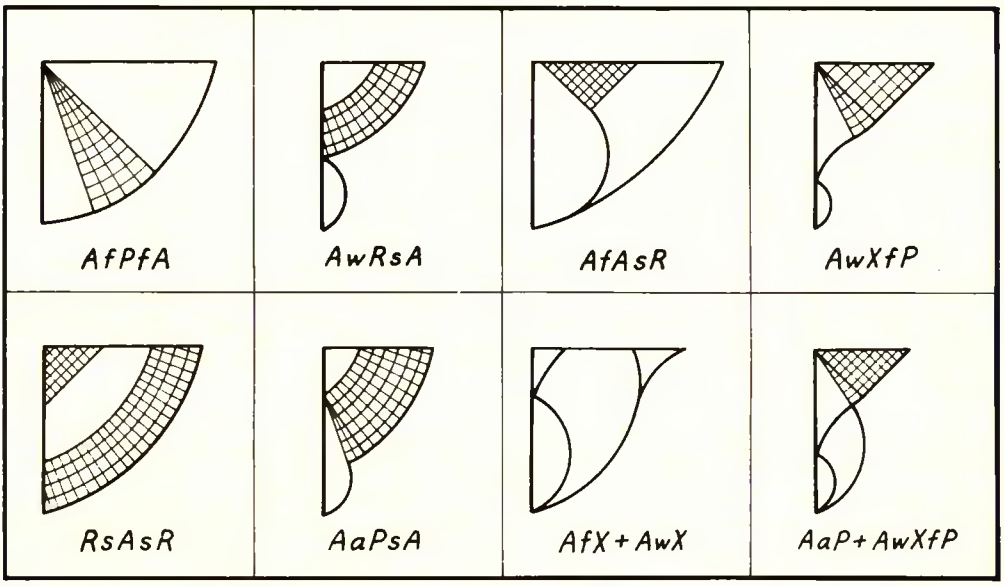

Fig.35F: Composite ruptures with more than 2 zones

The last two ruptures in Fig. 35F are of a special kind. Each of them consists of two different rupture-figures superposed upon each other. By the rotation of the wall the movements and deformations associated with the two rupture-figures will take place simultaneously. This is indicated by a + between their respective symbols.

355. Special w-Ruptures

In earth with cohesion a rupture-line need not start from the foot of the wall, nor need it reach the ground surface. In fact, it may start from any point of the wall (which we shall indicate by a w before its symbol) and may

end at any higher point of the wall (which we shall indicate by a w after its symbol).

This gives us theoretically 3 × 4 = 12 new rupture-figures with a single zone. In 8 of these, where the rupture-line ends at the wall, the zone must, however, be an A-zone, so that the remaining 6 figures of this type are geometrically impossible.

The 6 geometrically possible w-ruptures with a single zone (wA, wX, wR, wP, Aw and wAw) are shown in Fig. 35G. With the exception of wAw they are also kinematically and statically possible.

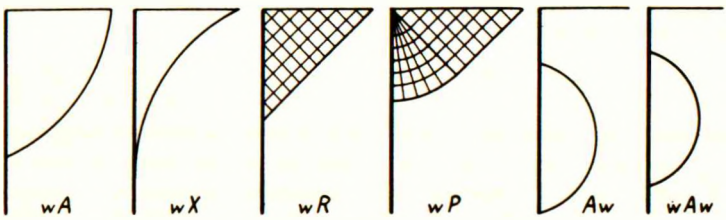

Fig. 35G: Special w-ruptures

Also the ordinary composite ruptures with two or more zones can be modified in a similar way, but it would lead too far to investigate such ruptures in detail here.

w-ruptures can also occur in cohesionless earth, viz., when a yield hinge develops in the wall and the lower part of the wall does not move. The lowest rupture-line starts then from the yield hinge.

356. Calculation of Rupture-Figures

A rupture-figure will always involve a number of geometrical parameters, which should be determined by the calculation. When these parameters are known, we can calculate the unit earth pressure at any point where a rupture-line meets the wall. We need only start from the surface and use the boundary conditions from Section 34, as well as the stress formulae from Section 33.

In a zone-rupture a rupture-line meets the wall at any point, and the earth pressure is, therefore, in principle a known function of the geometrical parameters of the rupture-lines. Consequently, these parameters are the only unknown quantities in the problem. Moreover, only the parameters of the lowest rupture-line are usually considered, a simple assumption being made concerning the distribution of the earth pressure on the wall.

For the determination of the unknown quantities, we have the 3 statical equilibrium conditions for the whole earth mass above the lowest rupture-line. Therefore, a rupture-line must be chosen which involves not more than 3 independent geometrical parameters. It can be shown, however, that very good approximate results can be obtained by employing a rupture-line with only 1 or 2 inde-

pendent parameters and, correspondingly, using only 1 or 2 of the equilibrium conditions, provided that these conditions are properly selected.

Generally, an infinite number of possible rotation centres for the wall correspond to a certain zone-rupture. These centres are located within a certain area, the limits of which can be found, theoretically, by an investigation of the possible deformations and movements within the plastic zone.

In a line-rupture only one rupture-line meets the wall, and the earth pressure distribution is, therefore, in principle, indeterminable. Consequently, we must consider the magnitude of the earth pressure, and the location of the pressure centre, as 2 unknown quantities, in addition to the geometrical parameters of the rupture-line.

On the other hand, in addition to the 3 statical equilibrium conditions, we have here one other condition specifying, for example, that the rotation centre (or the pressure centre) should have a given location. As we have thus altogether 4 conditions, and 2 unknown statical quantities, this leaves 2 unknown geometrical parameters for the rupture-line. Fortunately, a single circle through the foot of the wall involves exactly 2 such parameters.

In the case of a composite rupture, we can in principle consider first one zone and then the other. For f- and a-ruptures the plastic zone (if any) is calculated first, or, is assumed to be of the same shape as the corresponding complete zone-rupture. Next, the elastic zone is calculated in a similar way as in an ordinary line-rupture. For s- and w-ruptures, the upper zone must always be calculated first and the lower one afterwards.

A detailed account of the calculation for different rupture-figures shall be given in Section 4.

357. Choice Between Rupture-Figures

In order to avoid the most serious errors of previous earth pressure theories, the general principle must be to consider, if at all possible, only rupture-figures which are geometrically, kinematically and statically possible. If, for example, the rotation centre of a wall is given, then only rupture-figures compatible with the corresponding type of movement should be considered. Or, if the pressure centre of a wall is given, then only rupture-figures satisfying this statical condition should be taken into consideration.

However, it will often be found that, corresponding to a given rotation centre (or pressure centre), more than one rupture-figure may fulfil the kinematical and statical conditions. The problem then arises of which one of these figures should be chosen as the basis for the calculation of the earth pressure.

In earth pressure calculations by means of the extreme-method, the principle is to select the critical rupture-line, i.e., the one for which the earth pressure resultant is a minimum (passive pressure) or a maximum (active pressure). This is evidently correct, if the location of the pressure centre is given, because, for a greater passive (or a smaller active) pressure the average shear

stress in the critical rupture-line would exceed the value indicated by Coulomb's law (3101).

However, in the case of a given rotation centre, the corresponding criterion must be that the moment of the earth pressure about the rotation centre should be a minimum (passive pressure) or a maximum (active pressure).

The above-mentioned principles can be summarized in the following general rule: By a given, kinematically possible displacement of the structure the total work done by the earth pressure (acting upon the earth) should be a minimum.

The rupture-figure, for which this minimum occurs, is called the critical one. However, as in any practical case only a few rupture-figures can be investigated, we can never be sure of having found the real critical one as defined above. Therefore, we can actually only distinguish between more or less critical rupture-figures, and of these we must naturally choose the most critical one.

The general form, which we have given the above rule, has the advantage that the rule can also be applied to composite ruptures, in which the total earth pressure on the wall is neither passive nor active. The rule is also applicable to more complicated cases such as, for example, that of a wall in which yield hinges have developed.

36. STATES OF FAILURE

361. General

In the design of an earth retaining structure by means of a theory of rupture, it is necessary to base the calculation on certain assumptions concerning the movements of the structure in the state of failure.

Only such states of failure should be considered, which are kinematically and statically possible. A state of failure is described as kinematically possible, when the deformations and movements of the structure are compatible with each other and with the possible restraints imposed on it by other structural elements. Further, a state of failure is described as statically possible, when the equations of equilibrium for the structure (or any finite part of it) can be satisfied by a suitable choice of the unknown quantities (forces, dimensions or safety-factors).

When discussing different states of failure it will be practical to distinguish between single structures (without or with yield hinges) and composite structures (e.g. a sheet wall connected by anchor bars to anchor slabs). Further, we must distinguish between earth pressure investigations (which may include investigations of foundation pressures) and stability investigations.

The determination of the earth pressure (or foundation pressure) on a wall is only possible when a rupture-line starts at the ground surface (or a free earth front) and ends at a point of the wall (usually its foot). This applies to both sides of a wall and - in the case of a composite structure - to all the in-

dividual walls. If rupture-lines are used, which do not fulfil this condition completely, one or more of the earth pressures cannot be determined, and we are then only able to investigate the stability of the structure.

In earth pressure investigations by means of the plasticity theory, the earth pressures are found to be functions, not of the actual movements (or rates of movements) of the different rigid parts of the structure, but of the types of these movements or, more strictly speaking, of the coordinates of the different rotation centres.

Apart from the earth pressures, the structure may have one or more exterior forces acting upon it. Some of these forces may correspond to restraints imposed upon the structure by other structural elements. A tie-bar connection involves one such force, a hinged connection two, and a rigid connection two forces and a moment. The latter also applies to a yield hinge developing at a point where the wall is fixed to a more massive structure. A yield hinge developing at a point, where the moment attains an extreme value (constant section modulus), involves, however, only a moment and an axial force, because the transversal force must be zero here.

A special exterior force is the point resistance S acting upwards on the base of a comparatively thin wall. Strictly speaking, this force should include a transversal as well as an axial component, but we shall disregard the former, this being on the safe side and also making the calculations considerably simpler. If the wall rises in the state of failure, we must have $S = 0$, and if it sinks S must be equal to the ultimate point resistance (calculated in a similar way as for piles and with a suitable safety factor). Finally, if the wall does not move axially, S can have any value between the mentioned extremes and must, therefore, be considered as an unknown quantity. In that case, the rotation centre is located at the wall proper (or its extension).

Lodret Væg

For the determination of the unknown quantities, we have first 3 statical equilibrium conditions for each separate rigid part of the structure. Further, we may have a number of kinematical conditions.

Two parts, which are rigidly connected, must have the same rotation centre. If they have a hinged connection, their rotation centres must be situated at a straight line through the hinge, and if one of the parts is unyielding the other must rotate about the hinge. Finally, if two parts have a tie-bar connection, their rotation centres are independent of each other, unless one of the parts is unyielding, in which case the other must rotate about a point of the tie-bar (or its extension).

In some cases additional statical or kinematical conditions are imposed arbitrarily upon the structure, usually for the sake of economy. It is, for example, often specified that the greatest positive and negative moments in a wall should be numerically equal. Another example concerns an anchor slab, the movement of which is usually chosen to be a translation, thus enabling the anchor slab to resist the greatest possible anchor pull.

The total number of statical and kinematical conditions indicates the number of unknown quantities which can be determined by the calculation. The re-

maining ones must be fixed in advance. The unknown quantities may be dimensions, angles, forces, moments, safety-factors and coordinates of rotation centres. A number of examples shall be given in the following.

362. Single Structures

The simplest cases concern a wall which, in the state of failure, rotates as one rigid body about a certain rotation centre. By means of the 3 equilibrium conditions for the wall we can always determine 3 unknown quantities.

When the location of the rotation centre is given, the corresponding restraining forces will usually be unknown quantities. In the case of a wall rotating about a yield hinge, which has developed at the point where the wall is fixed to a more massive structure, the three restraining forces are unknown quantities.

Example 36a: A fixed sheet wall (Fig.36A). Provided that the wall is designed in such a way that a yield hinge develops at the top only, it will rotate about this point. The unknown quantities are: the yield hinge moment (M_1) as well as the axial force (N_1) and the transversal force (A) in the yield hinge. In principle, the design can be made with any chosen driving depth (h_2) within certain limits, but for economical reasons the driving depth is usually determined by the condition that the greatest positive and negative moments in the wall should be numerically equal.

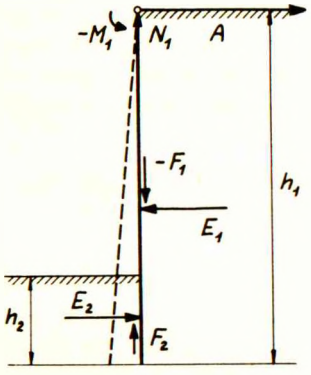

Fig.36A: Fixed sheet wall

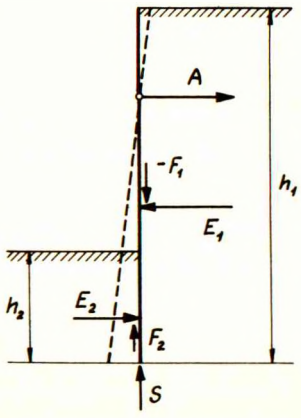

Fig.36B: Anchored sheet wall

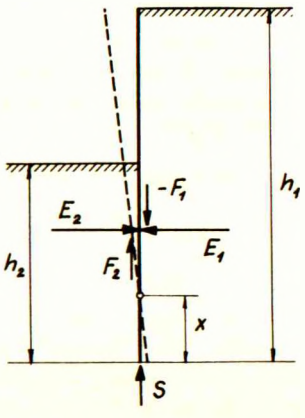

Fig.36C: Free sheet wall

When the wall can rotate freely about a given rotation centre, there will be two restraining forces only. They may be the two force components in a hinge, but can also be independent of each other (e.g. an anchor pull and a point resistance). As the third unknown quantity a force, a dimension or a safety factor may be chosen.

Example 36b: An anchored sheet wall (Fig.36B). When the anchorage is unyielding, the rotation centre must be located at the anchor, and if the ultimate point resistance is not exceeded, it must be located at the wall. Consequently, the wall must rotate about the anchor

point. Provided that the wall is made so strong that no yield hinge will develop, the unknown quantities may be: the anchor pull (A), the point resistance (S) and the driving depth (h_2).

In some cases, only one coordinate of the rotation centre is given; the other is then one of the unknown quantities. Correspondingly, there will be one restraining force only (e.g. an anchor pull or a point resistance). As the third unknown quantity a force, a dimension or a safety factor may be chosen.

Example 36c: A free sheet wall (Fig.36C). If the ultimate point resistance is not exceeded, the rotation centre must be located at the wall proper. Provided that the wall is made so strong that no yield hinge will develop in it, the unknown quantities may be: the height of the rotation centre (x), the point resistance (S) and the driving depth (h_2).

Other cases, in which only one coordinate of the rotation centre is known, may occur for walls without point resistance (e.g. when they rise in the state of failure). The "known" coordinate may not be given a priori but may be chosen arbitrarily, whereas the other coordinate is unknown. The second unknown quantity may be the location of an exterior force with a given inclination, and the third the magnitude of this force, a dimension or a safety factor.

Example 36d: An anchor slab, the movement of which is chosen so as to be a translation (Fig.36D). The unknown quantities are: the direction of the translation (β), the anchor pull (A) and the location of the anchor point (q). When the anchor slab is designed according to such a calculation no movement other than the assumed translation is possible, as only this movement can give a resultant in the line of the anchor pull.

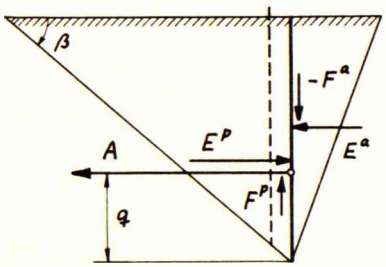

Fig.36D: Translating anchor slab

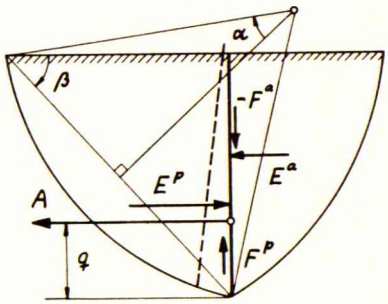

Fig.36E: Rotating anchor slab

When the rotation centre is unknown, we must consider both of its coordinates as unknown quantities. The third may be a force, a dimension or a safety factor. This case occurs when a structure is not restrained in any way, apart from an exterior force of given inclination and location acting upon it.

Example 36e: An anchor slab with a given anchor point and a given inclination of the anchor pull (Fig.36E). The unknown quantities are : the two parameters of the rotation centre (α, β) and the anchor pull (A).

In the case of a zone-rupture, the earth pressure can be found without knowing the actual position of the rotation centre, provided that it is known to be located within a certain area. However, the full design of a structure will usually require the determination of the exact location of the rotation centre.

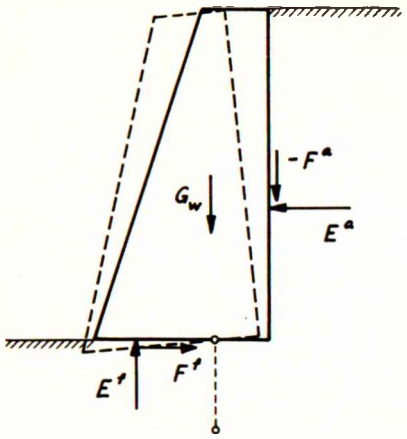

Fig.36F: Retaining wall

Example 36f: A retaining wall founded direct on the ground (Fig.36F). In order to mobilize the necessary friction, its base must move away from the fill, and, in order to resist the overturning moment, the toe must settle more than the heel. Consequently, the rotation centre must be located somewhere below the base. This knowledge is sufficient to determine the earth pressure on the back of the wall, because a zone-rupture will occur here. However, the foundation pressure on the base is a function of the actual coordinates of the rotation centre. In a rational design the 3 equations of equilibrium for the wall should be used to determine the following 3 unknown quantities: the coordinates of the rotation centre and a dimension (e.g., the base width) or a safety factor.

So far, we have only considered cases, in which the wall rotates as one rigid body. We shall now deal with the more complicated case, in which the wall, in the state of failure, moves as two or more rigid parts connected by yield hinges. Each of these parts rotates then about its individual rotation centre (certain parts may be stationary, however). Yield hinges may develop, either at points where the moment attains an extreme value (in which case the transversal force is zero), or at points where the section modulus changes suddenly (e.g., at the point where a wall is fixed to a more massive structure).

The earth pressures on the different parts of the wall are, generally, functions of the coordinates of all rotation centres and all yield hinges. These coordinates are not independent, however, because for kinematical reasons a yield hinge and the rotation centres for the two adjoining parts must lie on a single straight line. A number of the mentioned coordinates are unknown quantities in the problem. Other unknown quantities are, usually, the moments and axial forces in the yield hinges. Finally, certain dimensions, exterior forces or safety factors may also be unknown quantities.

For each separate part of the wall we have 3 statical equilibrium conditions, i.e., 3N equations if the wall moves as N rigid parts connected by yield hinges. Consequently, we can always determine 3N unknown quantities. We may in certain cases impose additional conditions on the structure, requiring, for example, the numerical equality of different yield hinge moments.

In the simple case of a wall with one moving and one stationary part, we may investigate the moving part separately. It rotates, naturally, about the yield hinge, and the unknown quantities are: the moment and axial force in the yield hinge, and the height of the moving part. A more complicated investigation is required to determine the driving depth which is necessary to ensure that the lower part actually remains stationary.

Example 36g: A free sheet wall with a yield hinge (Fig.36G). When the driving depth is sufficiently great, the lower part will remain stationary while the upper part rotates about the yield hinge. The unknown quantities are as mentioned above (M_1, N_1, h_3), and are determined by means of the 3 equilibrium conditions for the upper part.

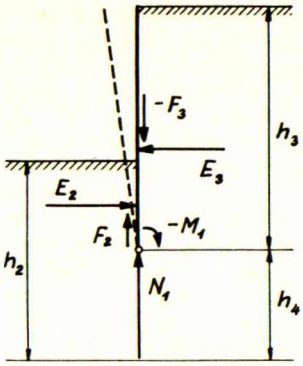

Fig.36G: Free sheet wall

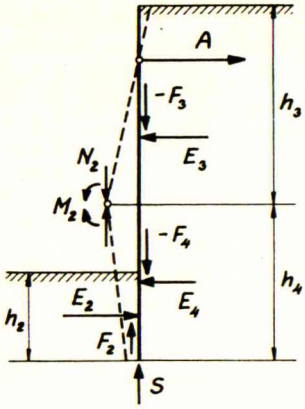

Fig.36H: Anchored sheet wall

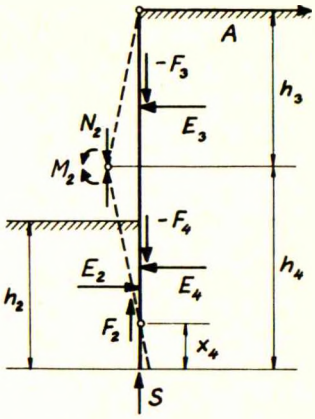

Fig.36I: Anchored sheet wall

We have already seen that, in the case of a zone-rupture, the earth pressure on a rigid wall is independent of the actual location of the rotation centre. In the case of a wall with yield hinges, this is not absolutely correct, but may be assumed as an approximation. Therefore, it is not necessary to determine the actual rotation centre for a part of the wall which is in contact with plastic earth zones only.

Example 36h: An anchored sheet wall with an unyielding anchorage and a yield hinge in the wall (Fig.36H). The upper part rotates about the anchor point, and the lower part can be assumed to rotate about a point below its foot, provided that the design is made accordingly (compare Example 36d). The actual position of the lower rotation centre is unimportant, as zone-ruptures will occur at both sides of the lower part. The unknown quantities are then the following 6: the heights of the two parts (h_3, h_4), the anchor pull (A), the moment (M_2) and the axial force (N_2) in the yield hinge, and the point resistance (S). They can be determined by means of the $2 \times 3 = 6$ equilibrium conditions for the two parts of the wall.

In the above-mentioned case the exact location of the lower rotation centre cannot be determined, because its coordinates do not enter into the equilibrium equations. In the general case, however, the height of the lower rotation centre can be determined by the calculation, if so desired, but then one of the unknown quantities in the former problem must be considered as a given quantity.

Example 36i: An anchored sheet wall as in Example 36h, but with a greater driving depth (Fig.36I). The upper part rotates about the anchor point, and the lower part about a point between dredge level and the foot of the wall. The driving depth can be chosen arbitrarily (within certain limits), and the problem involves then the following 6 unknown quantities: the height of the upper part (h_3), the anchor pull (A), the moment (M_2) and axial force (N_2) in the yield hinge, the point resistance (S), and the location of the lower rotation centre (x_4). If the wall had been fixed at the top, a second yield hinge would have developed here; the fixing moment could be determined by assuming it to be numerically equal to the other yield hinge moment.

363. Composite Structures

A composite structure consists of two or more walls. They may be interconnected rather firmly (e.g. cellular cofferdams) or rather loosely (e.g. double sheet walls, and sheet walls anchored to anchor slabs). As unknown quantities,

we must always consider the forces acting in the connections between the individual walls. Such a connection may involve one force only (e.g. the axial force in an anchor bar), or two forces (e.g. the axial and transversal forces in a hinge), or three forces (e.g. the axial and transversal forces and the moment in a rigid connection).

Further, if the walls fail simultaneously, it is necessary that their movements be compatible with each other. This implies that for two rigid walls with a rigid connection the rotation centres must coincide, whereas in the case of a hinged connection the two rotation centres must be located at a straight line through the hinge. For a tie-bar connection, the rotation centres are independent of each other.

The earth pressures on an individual wall will be functions of the coordinates of the corresponding rotation centre alone, provided that the rupture-figures for this wall are completely separated from the rupture-figures for the other walls. Otherwise, the earth pressures may be functions, also of the coordinates of other rotation centres, and in that case it may prove impossible to determine such earth pressures at all.

For each individual wall we have, as usual, 3 statical equilibrium conditions, i.e., in the case of N walls, we have 3N equations. Consequently, we can always determine 3N unknown quantities. In a check computation of a structure with given dimensions, the unknown quantities will mainly be coordinates of rotation centres, forces in the connections and safety factors; whereas in a design the safety factors and some of the coordinates will be given (or can be chosen) and are substituted by unknown dimensions.

If the walls are assumed to fail simultaneously, then the same safety factors should be used for all the individual walls. However, it is also possible to base the design on the assumption that the walls do not fail simultaneously, in which case we should design the individual walls with different safety factors. This means, that, in the design of one wall, another wall with a greater safety factor is considered stationary, whereas in the design of the latter wall itself it is supposed to move. As, theoretically, even a slight difference in the respective safety factors is sufficient to justify such a procedure, it can also be used when the safety factors are the same. Expressed in another way, this is a consequence of the fact that the stresses in a plastic state are independent of the absolute magnitude of the deformations and movements.

Example 36j: A sheet wall and an anchor slab, connected by anchor bars (Fig.36J). The anchor slab is designed to translate, and the sheet wall to rotate about a point below its foot (Fig.36J, left). As zone-ruptures will occur at both sides of the sheet wall, the actual position of the rotation centre is unimportant. The unknown quantities are then the following 6: the anchor pull (A), the driving depth (h_2) and the point resistance (S) of the sheet wall and, for the anchor slab, the depth (h), the location of the anchor point (q), and the direction of the translation (β).

Instead of choosing, for the sheet wall, a rotation centre below its foot, we can also choose a rotation centre above the anchor (Fig.36J, right). The unknown quantities are the same as before, but the earth pressures on the sheet wall are, naturally, not the same, as they must now correspond to the new rotation centre. Consequently, a different design will be obtained.

As we are free in the choice of the rotation centre of the sheet wall, provided that it does not make the anchor point move towards the anchor slab, we may in the limiting case choose

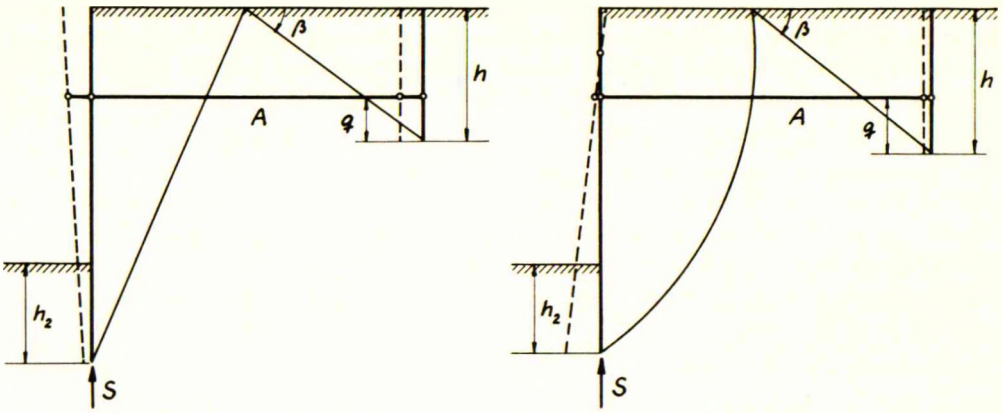

Fig.36J: Sheet wall and anchor slab, connected by anchor bars

the anchor point proper as rotation centre. This means that the sheet wall and the anchor slab can actually be designed independently of each other.

It should be noted that with regard to the anchor length we can only determine a lower limit, viz., by the condition that the rupture-figures for the sheet wall and the anchor slab respectively should be completely separated from each other. The corresponding anchor length may not be sufficient, however, for reasons which shall be explained in Example 36 1.

364. Stability Investigations

In the preceding Sections 362-63, we have dealt exclusively with earth pressure investigations, for which it is necessary, on each side of each wall, to have a rupture-line running from the ground surface to the wall, without touching or enclosing any other wall.

However, other types of failure are possible, which do not satisfy this condition (Figs. 36K-L). In such cases one or more of the individual earth pressures cannot be determined, but the safety of the whole structure (or a part of it) against sliding can be calculated. Therefore, calculations for failures such as those shown in Figs. 36K-L are referred to as stability investigations.

Whereas earth pressure investigations are generally most easily carried out by means of the equilibrium-method, stability investigations are usually simplest when the extreme-method is employed, using as rupture-lines logarithmic spirals ($\varphi \neq 0$) or circles ($\varphi = 0$). This method has been described by many authors, e.g. Fellenius (1927), Rendulic (1935), Skempton (1948) and Brinch Hansen (1952).

However, for systematical reasons, the stability investigations shall here be discussed under the assumption that the equilibrium-method is used. As we have proved in Section 341, the results will be practically the same as found by means of the extreme-method.

We shall first consider the case of a rupture-line leading from one ground surface to another, clear below the structure (Fig. 36K). We have here a rupture A with a circular rupture-line, and the earth mass above this circle must rotate about its centre. In all, 4 conditions must be satisfied, viz. 3 equilibrium

conditions for the moving earth mass (including the structure) and 1 condition expressing that the stresses at the two ground surfaces (as determined by 3411) should satisfy the stress equation 3318. Consequently, we can determine 4 unknown quantities.

The simplest case concerns a structure with no direct connection to any structure outside the moving earth mass (Fig. 36K, left). Three of the unknown quantities are the geometrical parameters of the circle and the fourth may be the safety factor. It should be noted that it is impossible to determine the earth pressures on individual parts of the structure.

More complicated cases may occur when a wall is connected to a structure outside the moving earth mass, e.g., by a tie-bar connection. If the wall and the restraining structure can fail simultaneously (Fig. 36K, centre), no restriction is imposed on the movements of the wall. In this case we can find the 3 parameters of the circle, and either the safety factor or the necessary restraining force.

If the restraining structure is unyielding (possessing a greater factor of safety than the wall), it restrains the movements of the wall in a given way (Fig. 36K, right). Circles compatible with this possess less than 3 independent parameters, and we can therefore, in addition, determine the restraining forces as well as the safety factor for the wall.

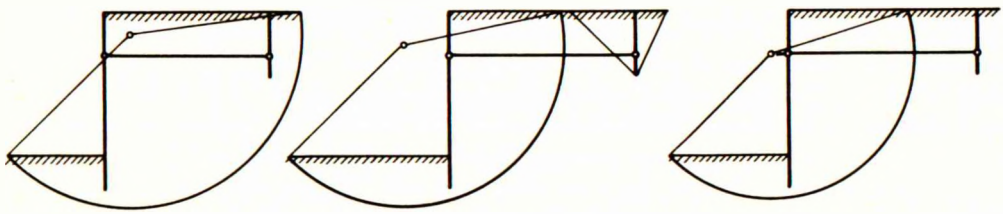

Fig. 36K: Unrestrained and restrained A-failures

Example 36k: A sheet wall and an anchor slab, connected by anchor bars (Fig. 36K). In an unrestrained A-failure (Fig. 36K, left) the critical circle does not intersect any structural elements. The unknown quantities are: the safety-factor and the 3 parameters of the critical circle. They can be determined by means of 3 equilibrium conditions and 1 stress condition as explained above.

In a restrained A-failure, the critical circle intersects the anchor bars. If we wish to find the anchor pull (A_1) which will provide the sheet wall with a given safety (n_1) against failure, the unknown quantities are: the anchor pull and the 3 parameters of the critical circle (Fig. 36K, centre). As a yielding anchorage is presumed, the anchor slab should be designed for the calculated pull (A_1) with the same safety factor (n_1) as specified for the wall.

If desired, we can also calculate the anchor pull (A_2) which is necessary to ensure that the anchor point of the sheet wall does not move horizontally (Fig. 36K, right). In this case the unknown quantities are: the anchor pull, the safety factor (n_2) for the sheet wall and 2 parameters of the critical circle, which must have its centre on the anchor. As an unyielding anchorage is presumed, the anchor slab must be designed for the calculated anchor pull (A_2) with at least the same safety factor (n_2) as found for the wall.

In the above-mentioned stability failures, the rupture-line consists of one circle, running from one ground surface to another without touching any of the walls (Fig. 36K). We shall now consider another group of stability failures, in which the rupture-line is composite and touches one or more of the walls (Fig. 36L).

The main rupture-line may run from a ground surface clear below one wall to the foot of another wall, where it meets a secondary rupture-line (Fig.36L, left and centre). For kinematical reasons the centres of the two rupture-circles must be located at the same normal to the wall at which they meet, provided that this normal is not located below the wall proper. In actual stability investigations by means of the extreme-method the two centres are usually assumed to coincide, i.e., a single circle (or spiral) is used.

In the equilibrium-method, the unknown quantities may be the safety factor and the two independent parameters of the main circle, the exterior earth pressure being a function of these parameters. For the determination of the 3 unknown quantities, we have the 3 equilibrium conditions for the earth mass bounded by the main circle and the wall which this circle touches.

Finally, the main rupture-line may run direct from one wall to another without touching the ground surface (Fig.36L, right). The main rupture-line may be of the type A or X, and at the foot of each wall it meets a secondary rupture-line. If the centre of the main circle is located below the wall, the secondary rupture will be a zone-rupture and, consequently, the exterior earth pressure will be independent of the actual position of the rotation centre. This allows an extreme-calculation to be carried out with a circle (or spiral) running between the walls only, the exterior earth pressures having been calculated as normal passive or active pressures respectively.

In the equilibrium-method, the unknown quantities may be the safety factor, one independent parameter of the main circle, and the boundary stress at one end of this circle. For their determination we have the 3 equilibrium conditions for the earth mass bounded by the main circle and the two walls.

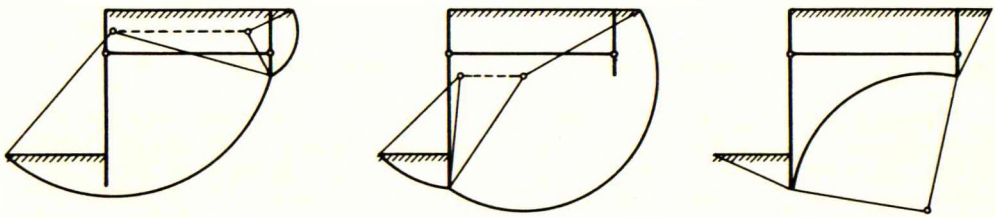

Fig.36L: Composite A-failures and X-failure

Example 36l: A sheet wall and an anchor slab, connected by anchor bars (Fig.36L). If we investigate a composite A-failure (Fig.36L, left or centre) we can find the unknown quantities as mentioned above. It should be noted, however, that, apart from the exterior earth pressure corresponding to the secondary rupture-line, we cannot determine the earth pressures on the individual walls, nor the anchor pull.

In order to determine the necessary anchor length, it will usually be necessary to investigate a composite X-failure (Fig.36L, right). On the exterior side of the anchor slab, we have ordinary active pressure, and on the exterior side of the sheet wall ordinary passive pressure. With a given safety factor we wish to find the smallest allowable anchor length. The other unknown quantities are the central angle of the circle and the stress in one end point.

As most other stability investigations, this is most easily made by means of the extreme-method, employing as main rupture-line a circle ($\varphi = 0$) or a logarithmic spiral ($\varphi \neq 0$). The necessary anchor length determined in this way will usually exceed the lower limit found as described in Example 36j.

365. Choice Between States of Failure

When an earth retaining structure is to be designed by means of a theory of rupture it will, as already mentioned, be necessary to base the calculation on an assumed state of failure. This state of failure must, of course, be kinematically and statically possible.

Simple structures can often fail in one way only, but for more complicated structures different possibilities may exist, as we have seen in Sections 362-64. The question is then, which of the possible states of failure should be chosen as the basis of the design.

It is evident that, if a structure is designed with an adequate safety against a certain type of failure, this failure will not occur under ordinary working conditions. But it is not equally evident that another type of failure, involving a smaller safety factor, might not occur.

However, it is a common feature of the behaviour of earth retaining structures that, when a part of the structure yields, the earth pressure on this part is decreased. At the same time, the pressures on the unyielding parts are usually increased somewhat, and this is definitely so for a part which is forced against the earth.

Therefore, if a structure, which is designed to fail in a certain way, should begin to yield in another way, this very movement will soon reduce the earth pressure on the yielding part to a smaller value than that for which it is designed. At the same time, the pressure on the part, which was designed to yield, will increase above the design value. The combined result of this pressure redistribution will be that the "unforeseen" yielding ceases and that, if the structure fails at all, it must do so in the manner assumed in its design.

Example 36m: An anchored sheet wall. As we have seen in the examples in Sections 362-64, such a structure may fail in several different ways. The earth in front of its foot may yield, making the wall rotate about the anchor point (Fig.36B) or a higher point (Fig.36J, right). The anchorage may yield, making the wall rotate about a point below the wall (Fig.36J, left) or about a higher point (Fig.36I).

If, for example, the anchored sheet wall is designed for earth pressures corresponding to a rotation about the anchor point (Fig.36B), it cannot fail in any other way. If the anchorage should start yielding, this will instantly reduce the pressure on the upper part of the wall, decreasing the anchor pull and thereby stopping the anchor yield. And if a yield hinge should begin to develop in the wall, this will reduce the pressure on the central part of the wall, decreasing the yield moment and thereby stopping the yield in the wall. Consequently, the assumed yielding of the earth in front of the wall is the only movement which will not be counteracted by a pressure redistribution, not envisaged in the design.

The above considerations are valid, as long as we consider only failures such as those used in earth pressure investigations, because we can then calculate all the individual earth pressures, for which we will find that they change with the movements of the structure in the general way described above.

However, in Section 364, we have seen that, in cases of stability failures, some of the earth pressures cannot be calculated, and therefore we do not know

how they will vary with the movements of the structure. Consequently, the possibility exists that, even if a structure is designed for the earth pressures corresponding to a certain state of failure, a stability failure of another type may be more critical (involve a smaller factor of safety).

Example 36n: A sheet wall and an anchor slab, connected by anchor bars. We presume that we have designed the sheet wall for rotation about the anchor point (Fig. 36B) and the anchor slab for a translation (Fig. 36D). The anchor bars are made of a length which will just keep the rupture-figures for the wall and the slab from touching each other (Fig. 36J).

It has already been mentioned in Example 36 l, that a stability failure of the composite X-type (Fig. 36L, right) will usually involve a smaller safety factor, unless the anchor length is increased.

However, also other stability failures may prove more critical than the design failure, e.g., the restrained A-failures (Fig. 36K, centre and right). This may be the case when the passive earth pressure in front of the wall increases rather slowly with the depth and when the anchor point is placed rather low. If, in such a case, we calculate the driving depth necessary for equilibrium, there will usually be two possible solutions, of which the one with the smaller driving depth will be unstable, because a stability failure of the A-type proves to be more critical.

As a result of the above considerations, we may state the following general rule: A safe design of an earth retaining structure can be made on the basis of any kinematically and statically possible state of failure, provided that a stability failure does not prove to be more critical. In the latter case the final design must, of course, be based on the most critical stability failure.

If soft layers are present below the structure, a stability investigation is definitely called for. Such an investigation is also necessary in order to find, for example, the safe distance between two walls in a composite structure (see Example 36 l).

Further, in many problems, especially in cases of low anchor points and slowly increasing passive pressures, there will be two possible solutions, one of which is actually unstable (see Example 36n). Fortunately, it will often be rather evident when an unstable solution has been obtained. If, for example, in the design of an anchored sheet wall a driving depth has been found, for which the active unit pressure at the foot exceeds the passive unit pressure, this is a strong indication that a stability failure may be more critical, because a somewhat longer wall would be unstable.

However, at least for single structures, stability failures are usually not considered, and in that case we can, according to the above-mentioned rule, in principle freely choose the state of failure, on which we wish to base our design. In practice, the choice will usually be decided by considerations regarding the permissibility of the necessary deformations and the economy of the design.

The movements and deformations necessary to produce a certain state of failure may be too great. Naturally, as a suitable safety against failure is provided for, the actual deformations will mostly be elastic and hence rather small. On the other hand, the assumed plastic deformations may often develop to some degree even under normal working conditions. This tendency is especially pronounced in the case of plastic clay. Consequently, a certain caution is called

for when designing a structure in clay on the basis of a theory of rupture, as this may lead to unallowable deformations.

Limited movements of a structure as a whole are not very harmful, but plastic deformations within the structure proper are more serious (especially in concrete structures). However, for certain structures (e.g. a fixed sheet wall) no state of failure can be indicated which does not involve at least one yield hinge, and for other structures (e.g. an anchored sheet wall) economical considerations may require the adoption of a state of failure involving a yield hinge.

Different states of failure lead, generally, to different designs and of these we must, of course, choose the one involving the lowest total cost. Usually, a cursory examination of the main possibilities will suffice to point out the most economical, but in special cases it may be necessary to make and compare full designs, based on different states of failure.

When a certain state of failure has been chosen, it must be used as a basis for the whole design, with the exception of such quantities, for which greater values are required in a stability investigation (e.g. the distance between a sheet wall and its anchor slab). It is not permissible to design different parts of the structure for different states of failure, each of which leads to the smallest possible dimensions of the part in question. If this was done the structure would not be safe, as no state of failure could be indicated, for which the structure would be in equilibrium.

In most earth pressure problems it is possible to indicate in advance the critical combination of loads, water levels and other variable factors. Therefore, it is usually only necessary to carry out one calculation. However, in certain cases it is not evident, which combination is the most critical one. In other cases, different combinations may be decisive for different parts of the structure. In such cases, two or more loading cases must be separately investigated.

The states of failure used in investigations of the same structure for different loading cases may, if statically possible, be identical, but they may also be different. Each part of the structure must be given the greatest of the dimensions found in the different calculations. The most economical design will usually be found by assuming identical states of failure.

So far, we have mainly dealt with design problems, which are the most common in engineering practice. If we wish to make a check computation of a given structure, we cannot freely choose the state of failure. Instead, we must try a probable state of failure and see, whether it is possible to fulfil all the statical conditions. Moreover, the safety factor is here an unknown quantity, which fact complicates the practical calculation considerably. However, the latter difficulty may be overcome by considering the yield moment in the wall as an unknown quantity instead of the safety factor.

Example 36o: An anchored wall with an unyielding anchorage. The possible states of failure for different driving depths are shown in Fig. 36M. The symbols for the corresponding figures of rupture at both sides of the wall are also indicated (for a smooth wall).

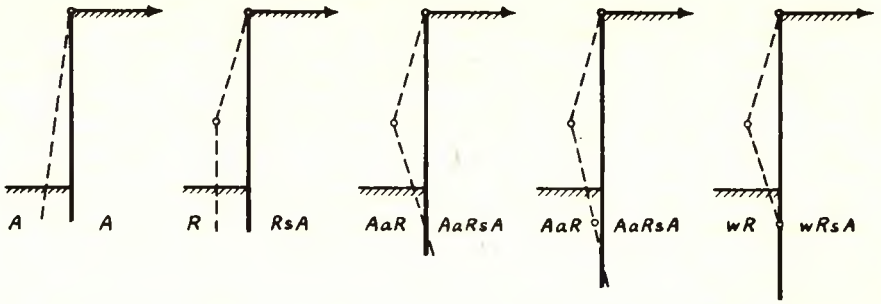

Fig.36M: Anchored sheet wall. States of failure for different driving depths, smooth wall.

If the driving depth is given, we must try a probable state of failure, e.g. the central one in Fig.36M, which is identical with the one shown in Fig.36I. As in Example 36i, the 6 unknown quantities are: A, N_2, M_2, S, h_3 and x_4. If a solution exists, we have then chosen the correct state of failure, and if the calculated values of A, N_2, M_2 and S do not exceed the permissible values, the structure is safe.

37. SOIL CONSTANTS AND SAFETY FACTORS

371. Determination of Soil Constants

In earth pressure theories based on the plasticity theory, to which also the author's method belongs, a soil is characterized exclusively by the three constants γ (effective unit weight), φ (apparent friction angle) and c (apparent cohesion).

The determination of the unit weight is done by simply weighing a sample and measuring its volume. For clay, the unit weight will usually range between 1.5 and 2.3 t/m^3, whereas dry sand will average 1.7 t/m^3, moist sand 1.8 t/m^3 and saturated sand 2.0 t/m^3. The submerged unit weight, which should be used for earth below the water table, is found by subtracting γ_w = 1.0 t/m^3 from the saturated unit weight.

The friction angle of cohesionless materials, such as sand and gravel, can, although with some uncertainty, be determined in situ, viz., by deep-sounding cone tests (Vermeiden 1948, Brinch Hansen 1951). If undisturbed samples are obtained, which, however, is extremely difficult (Bishop 1948), and if they are tested with their natural porosity, the friction angle can be found by means of shear box tests or triaxial tests.

In view of the uncertainties and difficulties connected with both the above-mentioned methods, it is often preferred to simply estimate the friction angle of sand or gravel. For sand, it lies generally between 30° and 40° (increasing with the density), and for gravel between 35° and 45°. The friction angle is practically the same above and below water level, provided that the density is the same.

In a shear test on sand the measured friction angle proves to be a function of the shear strain (Fig. 37A). For sand which is initially in a rather loose state, the friction angle increases steadily until the final value is reached. However, for sand which is initially in a rather dense state, the friction angle reaches first a maximum value and drops then slowly to approximately the same final value as found for loose sand.

Thus, for comparatively dense sand the question arises of whether the maximum or the final value should be employed (Tschebotarioff 1952). In zone-ruptures, the shear strains seldom reach any considerable magnitude, and it would therefore seem justifiable to use the maximum value of the friction angle here. Line-ruptures, on the other hand, often imply very great shear strains and are, moreover, progressive, so that here it would seem more appropriate to use the final value of the friction angle. However, for the sake of simplicity, no such distinction shall be made in the examples in the present work.

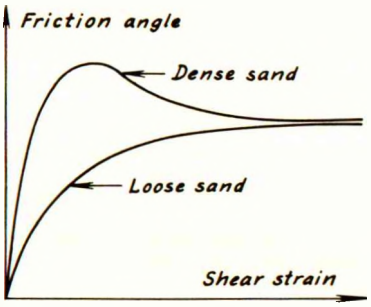

Fig. 37A: Stress-strain curves for sand

The apparent cohesion (actually the undrained shear strength) of a "frictionless" material, such as fully saturated clay, can be determined in situ by means of vane tests (Cadling and Odenstad 1950); this is probably the most reliable method known at present. For not too great depths and not too sensitive clays comparatively correct results can also be obtained by making unconfined compression tests or unconsolidated-undrained triaxial tests on undisturbed samples. The "cohesion" should then be assumed equal to half the compression strength.

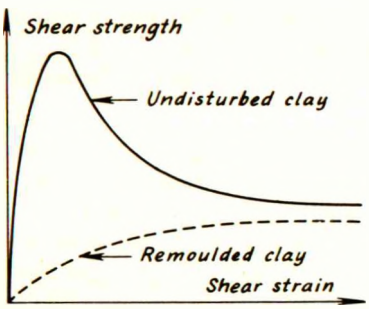

Fig. 37B: Stress-strain curves for clay

As the cohesion of clays may vary within very wide limits, no important earth pressure calculation should be based on merely estimated values.

In a shear test on undisturbed clay, the measured shear strength proves to be a function of the shear strain (Fig. 37B). It reaches first a maximum value and drops then slowly to a lower final value. The ratio between the maximum and the final value is known as the sensitivity of the clay.

As for sand, it might be argued that for clay also, the final value of the shear strength should be used, at least for a progressive line-rupture. However, due to the incompressibility of the clay, progressive failures are probably less apt to occur here than in sand. Moreover, experience has shown that many slopes in extra-sensitive clays are actually perfectly stable, although they would be definitely unstable if only the low final value of the shear strength could be counted on. For these reasons it is generally considered justifiable to reckon with the maximum shear strength of the clay in stability investigations and earth pressure calculations, provided that an adequate safety is secured.

With regard to soils other than fully saturated clays and cohesionless sands and gravels, we shall not discuss here the methods of determining the proper values of φ and c. A few indications have been given by Skempton and Bishop (1950).

372. Factors of Safety

In the design of earth-retaining structures by means of a theory of rupture it is necessary to introduce certain safety factors for the following reasons:

1) The actual loads may deviate from the specified or calculated values.

2) The actual strengths of the soils and the structural materials may deviate from the estimated or measured values.

3) The calculation as such involves a number of unavoidable inaccuracies, mainly due to simplifications, approximations, etc.

In order to take these facts into consideration the calculation is carried out with the specified loads multiplied by certain safety factors, and with the measured shear strengths of the soils divided by other safety factors. Finally, the structures are designed for the calculated forces and moments with "allowable" stresses equal to the measured strengths of the materials divided by suitable safety factors.

With regard to the loads, the most important ones, viz., the weights of the earth masses, can be determined with great accuracy by means of very simple tests. Therefore, it is proposed that no special safety factor be applied to these weights, i.e., to put $n_\gamma = 1$. This is also preferable from a practical point of view. For the weight of the structures proper it is likewise proposed that $n_\gamma = 1$ be assumed.

As regards the surcharges p these are, of course, rather uncertain. On the other hand it seems to be current practice to specify a surcharge so high that it will actually seldom, if ever, occur over any considerable area. For this reason it is proposed putting $n_p = 1$, but it will present no difficulties at all to reckon with $n_p \neq 1$, if required.

Water pressures can usually be calculated very accurately, but the fixing of the water levels may involve some inaccuracy. Therefore, a certain safety factor should be applied to water pressures, and it is proposed putting $n_w = 1.2$.

Summarizing the above, the following values are tentatively proposed for the main loads:

$$n_\gamma = 1 \qquad n_p = 1 \qquad n_w = 1.2 \qquad 3701\text{-}03$$

Suitable safety factors must also be applied to other exterior loads such as wave pressures, wind pressures, bollard pulls, impact forces from berthing ships, etc.

The actual shear strength of the soil under the prevailing conditions should always be determined by proper soil mechanics tests, as described in Section 371. It will usually be found that the internal friction of cohesionless materials (sand and gravel) can be determined with less uncertainty than the cohesion (= undrained shear strength) of frictionless materials (fully saturated clay). Therefore, it seems logical to apply a smaller safety factor to μ than to c. The following values are proposed:

$$n_\mu = 1.25 \qquad n_c = 1.5 \qquad 3704\text{-}05$$

The proposed value of $n_\mu = 1.25$ corresponds to the ratio between tan 36° and tan 30°. Therefore, if the actual friction angle of a soil is 36°, the calculations should be made with $\varphi = 30°$. In order to save time and space the tables in the Appendix have been prepared for $\varphi = 0°$ and $\varphi = 30°$ only, and the same applies to the earth pressure graphs in the Appendix. Thus, these tables and graphs can be used as they are, when the calculation is to be made with $\varphi = 0°$ or $\varphi = 30°$, i.e., when the actual friction angle is either 0° or 36° (provided that $n_\mu = 1.25$). The tables cannot be used for other friction angles, but by means of a simple correction (see Section 592), the graphs can be used for any friction angle.

The ultimate strengths of the structural materials should be determined experimentally, but deviations from the measured values must, of course, be expected, and these deviations are greater for concrete and timber than for steel. Therefore, a greater safety factor must be applied to concrete and timber than to steel. On the other hand, all these safety factors can be smaller than those usually specified for such materials, because we have already applied certain safety factors to the shear strength of the soil and to some of the exterior loads.

For steel, we find the "allowable" bending or tensile stress by dividing the yield stress by a safety factor n_σ^s. For concrete, we must divide the compression strength by a safety factor n_σ^c. Finally, for timber, the bending strength should be divided by n_σ^t. The following values are proposed:

$$n_\sigma^s = 1.2 \qquad n_\sigma^c = 2.5 \qquad n_\sigma^t = 2.5 \qquad 3706\text{-}08$$

It is, of course, also possible to design the structure in the conventional way with the usual allowable stresses, but in that case the forces and moments found by our calculations should first be divided by about 1.3. This procedure becomes necessary when, for example, the anchor pull from a sheet wall is transferred to a relieving platform, which should be designed in the conventional way.

4. CALCULATION OF EARTH PRESSURES

41. GENERAL PRINCIPLES AND FORMULAE

411. Introduction

We consider a wall with a height h, making an angle j with the vertical (Fig.41A). The earth, which may be stratified, is in each layer (height h_m measured along the wall) characterized by the constants γ_m, φ_m, c_m. The ground surface, as well as the internal boundaries are assumed to make a constant angle i with the horizon and to be loaded with vertical surcharges p_m. The surcharges on internal boundaries are usually zero; for i = 0, however, one of them may be a capillary pressure p_c.

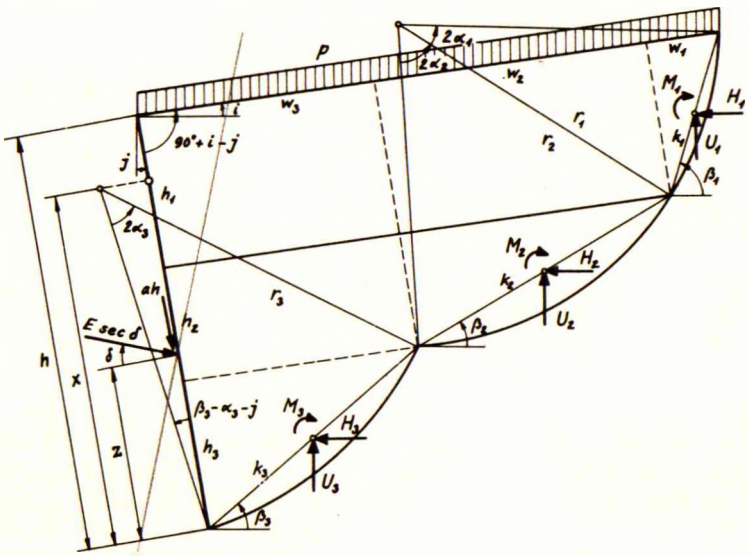

Fig.41A: Earth pressure calculation for composite rupture-line

Between the wall and each separate earth layer acts an earth pressure with a normal component E_m and a tangential component F_m. The latter is equal to:

$$F_m = E_m \tan \delta_m + a_m h_m \qquad 4101$$

From the ground surface to the foot of the wall runs a composite rupture-line, which is assumed to be a chain of N separate parts, viz., N_c circles and N_s straight lines. Each circle is characterized by the geometrical parameters α_n, β_n, k_n and each straight line by β_n, k_n. The corresponding heights h_n and widths w_n can be found by means of the formulae 3203-04.

The internal forces in the n' th rupture-line from the surface, as well as all surcharges and earth weights between two lines parallel to the wall through the end points of this rupture-line, are conveniently transferred to the middle point of the corresponding chord, giving a horizontal component H_n, a vertical component U_n and a moment M_n. H_n is the usual horizontal resultant of the internal forces in the rupture-line, whereas for U_n and M_n we find:

$$U_n = V_n - G_n - P_n - \sum_{1}^{n-1} (G_{xn} + P_{xn}) \qquad 4102$$

$$M_n = M_{Rn} + M_{Gn} + M_{Pn} + \sum_{1}^{n-1} (M_{Gxn} + M_{Pxn}) \qquad 4103$$

The mentioned forces can also be transferred to the foot of the wall, about which point we get the following moment for the n' th rupture-line:

$$M_n^f = M_n - H_n \left[\tfrac{1}{2} k_n \sin \beta_n + \sum_{n+1}^{N} k_x \sin \beta_x \right] - U_n \left[\tfrac{1}{2} k_n \cos \beta_n + \sum_{n+1}^{N} k_x \cos \beta_x \right] \qquad 4104$$

As explained in Section 346, we can only determine the stresses in the rupture-lines when φ has the same numerical value in all layers. In this case we have also the same δ for all layers, which we shall assume in the following.

412. Geometrical Parameters

The composite rupture-line through the foot of the wall involves altogether $3N_c + 2N_s$ geometrical parameters, and, if we are to be able to determine these, we must have a corresponding number of equations.

We consider first the forces acting upon the earth mass bounded by the ground surface, the wall and the composite rupture-line. By projection of all these forces on a line perpendicular to the forces $E_m \sec \delta_m$ (which are assumed to be parallel) we get:

$$\sin(\delta - j)\, \Sigma H_n - \cos(\delta - j)\, \Sigma U_n + \cos \delta\, \Sigma a_m h_m = 0 \qquad 4105$$

The summations in 4105 should be extended from 1 to N, and the same applies to all other equations in which no limits are indicated for the summations.

In 4105, δ and a_m are usually inserted with their maximum values, and with the same signs as φ_N and c_N (for the rupture-line next to the wall). From a kinematical consideration of Fig. 41B, it will be seen that this is correct, when the rotation centre for the wall is located in one of the sectors indicated by curved

arrows. If the rotation centre is located in one of the other two sectors, δ and a_m should be inserted with opposite signs of φ_N and c_N.

In the especially important case of a "normal" rotation, by which the rotation centre is located at the wall proper or its extensions, δ and a_m should have the same signs as φ_N and c_N when $\beta_N - \alpha_N - j > 0$, but the opposite signs when $\beta_N - \alpha_N - j < 0$.

However, it will sometimes be found that in neither of these cases can a possible solution be found, because in both cases the results will be contradictory to the assumptions. This can only mean that no tangential movement takes place between wall and earth, i.e., that the normal to the rupture-line at the foot of the wall goes through the rotation centre. In the case of a "normal" rotation this condition gives:

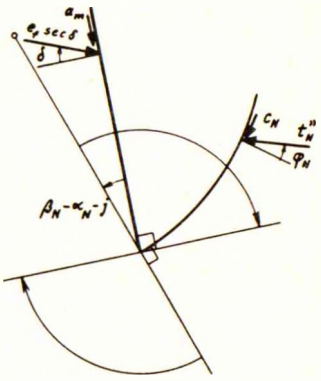

Fig.41B: Stresses at foot of wall

$$\beta_N - \alpha_N - j = 0 \qquad 4106$$

In this case 4106 must be used instead of 4105, which is useless here, because the actual values of δ and a_m are unknown.

For the further determination of the geometrical parameters we must either have a given rotation centre (x) or a given pressure centre (z). Usually, x is given, and we have then, provided that an elastic zone exists between the wall and the rupture-line next to it:

$$x = \xi h = \frac{k_N \cos(\beta_N - \alpha_N - j)}{2 \sin \alpha_N} \quad ; \quad \Gamma = \frac{k}{2 \sin\alpha} \qquad 4107$$

If z is given instead of x, equation 4107 cannot be used for the determination of the geometrical parameters, but may serve to indicate the location of the rotation centre. In its place we can find the following equation by taking the moments about the pressure centre:

$$z \cos j \, \Sigma H_n - z \sin j \, \Sigma U_n + \Sigma M_n^f = 0 \qquad 4108$$

A geometrical relation between the parameters is easily derived from Fig.41A:

$$\Sigma \, k_n \sin(\beta_n - i) = h \cos(j - i) \qquad 4109$$

Further, when two rupture-lines meet each other at an angle of 0° or 180° (f-rupture), we have an equation of the type:

$$\beta_{n+1} + \alpha_{n+1} = \beta_n - \alpha_n \qquad 4110$$

and when they meet at an angle of $90^\circ \pm \varphi$ (a-rupture) we have:

$$\beta_{n+1} + \alpha_{n+1} = \beta_n - \alpha_n + \varphi_n + 90^\circ \qquad 4111$$

Equations 4110-11 are, of course, not valid for rupture-lines meeting at the wall (w-ruptures) or at a "line of discontinuity" (see Section 345).

We have, in all, N - 1 equations of the types 4110-11. In addition we have 4105 or 4106, 4107 or 4108, and 4109, i.e., 3 more. Thus, in homogeneous earth we have altogether N + 2 equations for the determination of the $3N_c + 2N_s$ geometrical parameters.

It will be seen that for a single circle ($N = N_c = 1$, $N_s = 0$) the number of equations equals that of parameters. For $N > 1$, however, it is necessary to indicate a number of additional conditions in order to make the problem soluble.

In the case of stratified earth, we have for each separate layer an equation of the type 4109. Further, at each internal boundary 4110 must be satisfied, and the two rupture-lines meeting here must have the same radius:

$$\frac{k_{n+1}}{\sin \alpha_{n+1}} = \frac{k_n}{\sin \alpha_n} \qquad 4112$$

Consequently, although each new layer adds 3 geometrical parameters, we get also 3 new equations, so that a possible stratification does not affect the solubility of a problem, provided that we have the same φ (numerically) and the same δ for all the layers.

413. Total Earth Pressures

When the geometrical parameters have been determined, we can find the total earth pressures E and F, as well as the height z of the pressure centre, by means of the equilibrium conditions. By projection on a normal to the wall, by projection on the wall proper, and by taking the moments about the foot of the wall we get:

$$E = \cos j\, \Sigma H_n - \sin j\, \Sigma U_n \qquad F = \sin j\, \Sigma H_n + \cos j\, \Sigma U_n \qquad Ez = -\Sigma M_n^f \qquad 4113\text{-}15$$

When δ and a_m are known, it is often simpler to find E, F and z from the following equations, the first of which is obtained by projection on the horizon, whereas the last is found by taking the moments about the middle of the chord of the rupture-line next to the wall:

$$E = \left[\Sigma H_n - \sin j\, \Sigma a_m h_m\right] \cos\delta \sec(\delta - j) \qquad F = E \tan\delta + \Sigma a_m h_m \qquad 4116\text{-}17$$

$$Ez = \tfrac{1}{2} k_N \left[E \sin(\beta_N - j) + F \cos(\beta_N - j)\right] - \tfrac{1}{2} k_N \left[\sin\beta_N\, \Sigma H_n + \cos\beta_N\, \Sigma U_n\right] - \Sigma M_n^f \qquad 4118$$

The last two terms in 4118 can, in any given case, usually be written in a considerably simpler form.

In the case of no tangential movement between wall and earth, equations 4116-18 cannot be used. It should be investigated, however, whether F as found from 4114 is numerically smaller than the F determined by means of 4117 with the maximum values of δ and a_m. If so, it was correct to use 4106 instead of 4105.

In the case of homogeneous earth φ and c are numerically constant for all parts of the rupture-line, but may have different signs in different parts, according to our definitions in Sections 33-34. Inserting, for any φ_n and c_n, the numerical values φ and c, but with their proper signs, it will be found, by means of the pertaining formulae from Sections 32-34, that 4113-15 (or 4116-18) can be written in the following form:

$$E = \tfrac{1}{2}\gamma h^2 \lambda + ph\rho + ch\kappa \qquad Ez = \tfrac{1}{2}\gamma h^3 \lambda\eta + ph^2\rho\theta + ch^2\kappa\zeta \qquad 4119\text{-}20$$

$$F = E \tan \delta + ah \qquad 4121$$

The dimensionless constants λ, η, ρ, θ, κ, ζ are functions of i, j, φ, δ, a:c and the geometrical parameters. In equations such as 4119-21 the cohesion c should always be assumed positive, whereas for a and δ the sign rules indicated in Section 343 (p.66) are valid.

414. Unit Earth Pressures

In a similar way we can, by means of 3103, 3318 and the boundary formulae in Section 34, for homogeneous earth, find the following expressions for the unit normal and tangential earth pressures at a distance d from the top of the wall, provided that a rupture-line meets the wall at this point:

$$e_d = \gamma d\lambda_d + p\rho_d + c\kappa_d \qquad f_d = e_d \tan \delta + a \qquad 4122\text{-}23$$

The dimensionless constants λ_d, ρ_d, κ_d are functions of i, j, φ, δ, a:c and the geometrical parameters, as well as of the depth d. In equations such as 4122-23 (and 4124-25), the cohesion c should always be assumed positive, whereas for a and δ the sign rules indicated in Section 343 (p.66) are valid.

At the top and the foot of the wall we get for d = 0 and d = h respectively:

$$e_t = p\rho_t + c\kappa_t \qquad e_f = \gamma h\lambda_f + p\rho_f + c\kappa_f \qquad 4124\text{-}25$$

42. LINE-RUPTURES

421. Sloping Surface and Inclined Wall

Fig.42A shows a line-rupture A. As the rupture-line consists of a single circle, we have $3N_c + 2N_s = 3$ parameters, and $N + 2 = 3$ conditions, so that the problem is soluble without further assumptions or conditions.

When x is given, we have, for the determination of the 3 parameters, the equations 4105, 4107 and 4109. 4107 yields:

$$\xi = \frac{x}{h} = \frac{\cos(j-i)\,\cos(\beta-\alpha-j)}{2\sin\alpha\,\sin(\beta-i)} \qquad 4201$$

Solving 4201 with regard to β we find:

$$\cot(\beta-i) = 2\xi \sin\alpha \sec(\alpha+j-i) \sec(j-i) - \tan(\alpha+j-i) \qquad 4202$$

Further, equations 4109 and 4105 give:

$$k = h\,\frac{\cos(j-i)}{\sin(\beta-i)} \qquad 4203$$

$$H \sin(\delta-j) - (V-G-P)\cos(\delta-j) + ah\cos\delta = 0 \qquad 4204$$

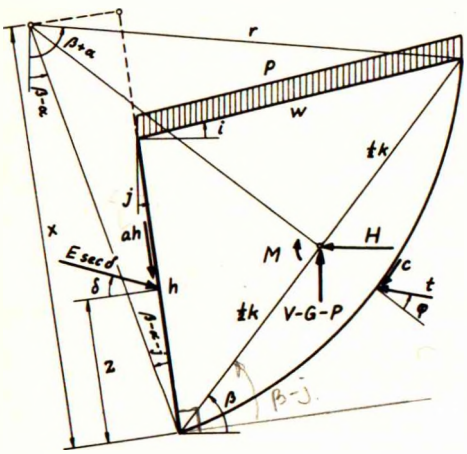

Fig.42A: Calculation of line-rupture

The procedure is now the following. With an estimated value of α we find the corresponding β from 4202, and then k from 4203. After insertion of 3206, 3208, 3325-26 and 3411 in 4204 it is then investigated whether 4204 is satisfied. If not, α must be changed and the calculation repeated, until satisfactory agreement is obtained.

The calculation is made for passive pressure with positive values of φ, c, δ and a, whereas negative values should be used for active pressure. Further, α should be positive for a rupture A, but negative for a rupture X.

When α and β have been found, it should be investigated, whether β-α-j > 0. If not, we must, instead of 4204, use 4106 which, when inserted in 4201, yields:

$$\cos(2\alpha+j-i) = \frac{\xi-1}{\xi}\cos(j-i) \qquad \beta = \alpha + j \qquad 4205\text{-}06$$

which then give α and β direct.

If z is given instead of x, the unknown angles α and β are determined either by 4108 and 4204, or by 4108 and 4106. ξ is then found from 4201.

When the geometrical parameters have been determined, we can find the unknown statical quantities by means of 4113-14 and 4118:

$$E = H\cos j - (V-G-P)\sin j \qquad F = H\sin j + (V-G-P)\cos j \qquad 4207\text{-}08$$

$$Ez = \tfrac{1}{2}k\left[E \sin(\beta-j) + F \cos(\beta-j)\right] - M_R - M_G - M_P \qquad 4209$$

If desired, the unit earth pressure e_f at the foot of the wall can be determined by means of 3411, 3318 and 3423. As, however, no other rupture-line meets the wall, the unit earth pressure cannot be determined at any other point. Therefore, the earth pressure distribution is, in principle, unknown.

Instead of starting the calculation with 4202-04 and investigating whether $\beta - \alpha - j > 0$ it is, of course, also possible to start with 4205-06, which is often simpler. The result will be correct, if the calculated F (from 4208) is numerically smaller than the greatest possible F (from 4117).

422. Horizontal Surface and Vertical Wall

For $i = j = 0$ the formulae 4201-04 and 4207-09 are reduced to the following:

$$\xi = \tfrac{1}{2}(1 + \cot\alpha \cot\beta) \qquad \cot\beta = (2\xi-1)\tan\alpha \qquad k = \frac{h}{\sin\beta} \qquad 4210\text{-}12$$

$$H \tan\delta - V + G + P + ah = 0 \qquad E = H \qquad F = V - G - P \qquad 4213\text{-}15$$

$$Ez = \tfrac{1}{2}h\,(E + F \cot\beta) - M_R - M_G - M_P \qquad 4216$$

With regard to the calculation method, see Section 421. Instead of estimating α and satisfying 4213, we can also start the calculation with 4205-06, which (for $j = 0$) give:

$$\cos 2\alpha = \frac{\xi-1}{\xi} \qquad \beta = \alpha \qquad 4217\text{-}18$$

As to the criteria for a correct solution, see Section 421.

Example 42a

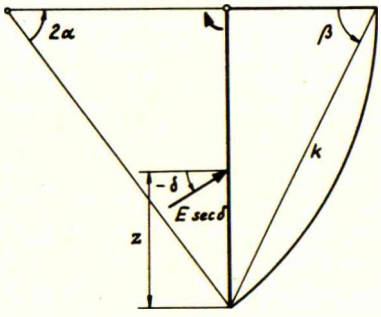

Fig. 42B: Rough wall rotating about its top

As an example we shall consider the following case (Fig. 42B) of active pressure on a rough wall rotating about its top (rupture A):

$$i = j = 0 \qquad p = c = a = 0 \qquad \varphi = \delta = -30^\circ$$

$$\gamma = 1 \qquad h = 1 \qquad \xi = 1$$

4211 gives at once the result: $\beta = 90^\circ - \alpha$. As 3413 yields $t' = 0$ we get, by insertion of 3223 and 3325-26 in 4213:

$$\left(G^{Yz} + \tfrac{1}{4}\sin 2\beta\right) - \left(V^{Yz} + V^{Yx}\sin(2\beta+2\varphi)\right) + \left[H^{Yz} + H^{Yy}\cos(2\beta+2\varphi)\right]\tan\delta = 0$$

With an estimated value of α we find the corresponding β as well as the G-, V- and H- functions (by means of Tables 1 and 3 in the Appendix). We investigate then whether the above equation is satisfied. After some trial we find with $\alpha = 26.5^\circ$ and $\beta = 63.5^\circ$:

$$0.079 + 0.25 \times 0.798 - 0.048 - 0.179 \times 0.920 - (0.184 - 0.179 \times 0.390) \times 0.577 = 0$$

We can now calculate E, F and z by means of 4214, 4121 and 4216, inserting 3326, 3335 and 3224, and using 4212 as well as Tables 1 and 3 in the Appendix:

$$k = 1 : 0.895 = 1.117 \qquad k^2 = 1.25 \qquad k^3 = 1.40$$

$$\underline{E} = 1.25\ (0.184 - 0.179 \times 0.390) = \underline{0.142} = \tfrac{1}{2}\lambda \qquad F = -0.142 \times 0.577 = -0.082$$

$$Ez = \tfrac{1}{2}\ (0.142 - 0.082 \times 0.499) - 1.40\ (0.008 \times 0.895 - 0.013 \times 0.446)$$
$$- 1.40\ (-0.080 \times 0.895 + 0.083 \times 0.895^3) = 0.064$$

$$\underline{z} = 0.064 : 0.142 = \underline{0.45} = \eta$$

43. ZONE-RUPTURES

431. Sloping Surface and Inclined Wall

Whereas the calculation of a line-rupture is "exact" under the given assumptions, because the rupture-line must be a circle, the calculation of a zone-rupture must generally be approximate only, as the actual shape of the rupture-lines is unknown. They shall here be approximated by a number of circles and straight lines, and, according to the number used, the calculation will give a more or less correct result.

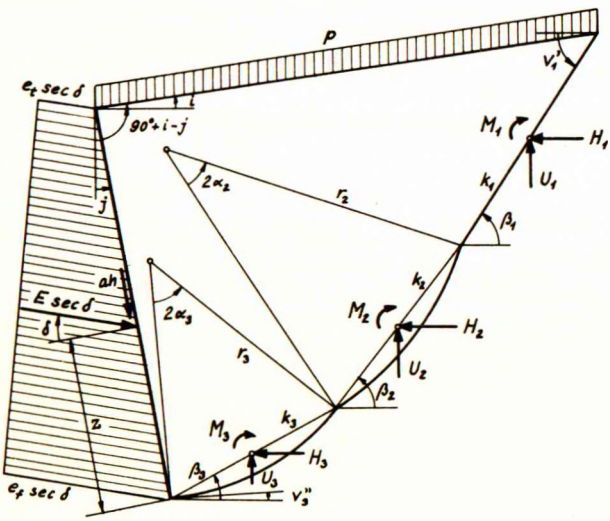

Fig.43A: Calculation of zone-rupture

In a zone-rupture a rupture-line meets the wall at any depth d. If we approximate such a line by N_c circles and N_s straight lines (Fig.43A), it will involve $3N_c + 2N_s$ geometrical parameters, viz., certain angles (α, β) and relative chord-lengths (k:d). When these parameters are known we can calculate the unit normal pressure e_d by means of 3411, 3318 and 3423. We get then for e_d an expression of the type 4122, in which the dimensionless quantities are functions of the said angles and relative chord-lengths.

It will be found, however, that ρ_d and $\varkappa_d$ depend only upon the angles v_1' and v_N'' at the surface and the wall respectively. As these two angles, which can be determined by means of 3405 and 3419 respectively, are independent of the depth d, the same must apply to ρ_d and $\varkappa_d$.

λ_d is generally not constant, however, because it depends upon all the angles and the relative chord-lengths in the rupture-line in question. It is actually only constant in the special cases of $\gamma = 0$ or $p = c = 0$. However, in order to carry out a comparatively simple calculation of a zone-rupture it is necessary to assume not only ρ_d and $\varkappa_d$ but also λ_d to be constant. This means that we assume the unit normal pressure to increase linearly from e_t (4124) at the top to e_f (4125) at the foot. In this case we need only consider the geometrical parameters of the lowest rupture-line as the unknown quantities.

According to the above-mentioned assumption we have:

$$E = \tfrac{1}{2}h\ (e_f + e_t) \qquad Ez = \tfrac{1}{6}h^2(e_f + 2e_t) \qquad 4301\text{-}02$$

As e_f and e_t are functions of the geometrical parameters for the lowest rupture-line, the same applies to E and z. There are, consequently, no other unknown quantities in the problem than these parameters. For their determination we have first equations 4109 and 4105, which always must be satisfied, if serious errors are to be avoided:

$$\Sigma\ k \sin(\beta - i) = h \cos(j - i) \qquad 4303$$

$$\sin(\delta - j)\ \Sigma H - \cos(\delta - j)\ \Sigma U + ah \cos\delta = 0 \qquad 4304$$

As the remaining two equilibrium conditions we choose 4116 and 4108:

$$E - (\Sigma H - ah \sin j) \cos\delta \sec(\delta - j) = 0 \qquad 4305$$

$$z\ (\cos j\ \Sigma H - \sin j\ \Sigma U) + \Sigma M^f = 0 \qquad 4306$$

Although the most accurate results are, of course, obtained by satisfying also 4305-06, it has been found that very good approximate results can be obtained by disregarding 4305 or 4306 or both.

For a zone-rupture with $N > 1$ it will be natural to have the rupture-line meet the surface and the wall at the statically correct angles. The corresponding angles v'_1 and v''_N are determined by means of 3405 and 3419 respectively. We have then:

$$\beta_1 + \alpha_1 = v'_1 \qquad \beta_N - \alpha_N = v''_N \qquad 4307\text{-}08$$

Moreover, when the rupture-line contains at least one circle ($N_c \geq 1$), we shall require the rupture-line to have a smooth contour. This means that we have $N - 1$ conditions of the type 4110:

$$\beta_{n+1} + \alpha_{n+1} = \beta_n - \alpha_n \qquad 4309$$

Finally, it will simplify the practical calculation, if we also require all circles to possess the same central angle. This gives $N_c - 1$ conditions of the type:

$$\alpha_n = \frac{v'_1 - v''_N}{2N_c} \qquad 4310$$

Adding up, we find that we have a minimum of 2 equations (4303-04) and a maximum of $2N_C + N_S + 4$ equations (4303-10). Comparing this with the $3N_C + 2N_S$ parameters, we get the result that the problem is soluble when $1 \leq N \leq 4$.

A rupture-line satisfying 4309 is "kinematically admissible" (Section 226) and gives, consequently, a somewhat too high value of E. On the other hand, a rupture-line consisting of straight lines only ($N_C = 0$, $N_S \geq 2$) is "statically admissible" and gives, therefore, a somewhat too low value of E. For such a rupture-line we cannot fulfil 4309, and 4310 has no meaning in this case. Instead, it will be practical to require that each pair of rupture-lines should meet each other at the same angle. This gives $N_S - 2$ conditions of the type:

$$\beta_n - \beta_{n+1} = \frac{v'_1 - v''_N}{N_S - 1} \qquad 4311$$

We have, in this case, a maximum of $N_S + 4$ equations (4303-08 and 4311) and, at the same time, $2N_S$ parameters. This leads to the result that the problem is soluble when $2 \leq N \leq 4$. (1 straight rupture-line is not statically but kinematically admissible).

Consequently, in order to calculate a zone-rupture, we must approximate the lowest rupture-line by means of 1 to 4 circles and/or straight lines.

With 1 straight line we can satisfy only 4303-04. The result is the same as obtained by means of Coulomb's method. It may be sufficiently correct for active pressures but is usually far too inaccurate for passive pressures.

With 1 circle we can fulfil one condition more, which must be 4306, as 4305 might give the result $\alpha = 0$, i.e., a straight line. However, the result is not very correct and the calculation rather troublesome, because α and β can only be determined by trial.

As soon as we have at least 2 circles and/or straight lines, we can fulfil 4303-04 and 4307-08 as well as 4309-10 or 4311. This means that all angles α and β are given from the start, so that the only remaining unknown parameters are the chord-lengths k. This gives, of course, the simplest calculations. With 2 circles and/or straight lines, the two chord-lengths may be determined by means of 4303-04. With 3 circles and/or straight lines, we must also use 4305, and with 4 circles and/or straight lines 4306 must be added as well.

When straight lines alone are used, it will usually be necessary to employ 3 of these in order to get a sufficiently reliable result. Circles alone should never be used, because the rupture-line is actually straight in the vicinity of the ground surface, and a better result will therefore be obtained by using a straight line here. The same applies to the vicinity of the wall, unless it is perfectly rough.

Consequently, when the wall is not perfectly rough, the rupture-line should be approximated by two straight lines with a circle in between. If the wall is perfectly rough, two circles and one straight line can be used for a very accurate calculation, but often it will be sufficient to use one circle and one straight line (see Example 43a).

When the geometrical parameters have been determined, we can calculate e_f and e_t (the latter with $k = 0$) by means of 3411, 3318 and 3423. E and z must then be found from 4301-02, whereas 4305-06 cannot be used for this purpose, as they will yield much too inaccurate results when they have been disregarded by the calculation of the parameters. However, in spite of this, 4301-02 may give very reliable results (see Example 43a).

δ and a should always have the same signs as φ and c (positive for passive pressure, and negative for active pressure). If we try to calculate a zone-rupture, in which δ and a are given the opposite signs of φ and c, the boundary condition will require that the wall should be a tangent to the rupture-lines. However, it seems impossible to find an approximate rupture-line of a comparatively simple shape, which fulfils the boundary conditions as well as the equilibrium conditions. Therefore, a zone-rupture can probably not occur, when δ and a have signs different from those of φ and c.

432. Horizontal Surface and Vertical Wall

For the statically correct angles v'_1 and v''_N we get from 3410 and 3421-22, with $i = j = 0$:

$$v'_1 = 45^\circ - \tfrac{1}{2}\varphi \qquad v''_{Ns} = 45^\circ - \tfrac{1}{2}\varphi \qquad v''_{Nr} = -\varphi \qquad 4312\text{-}14$$

where the subscripts s and r denote a smooth and a rough wall respectively. With the above values we find, further, from 3413 and 3425:

$$t'_1 = p\tan(45^\circ+\tfrac{1}{2}\varphi) + c \qquad e_s = (t''_N + c)\tan(45^\circ+\tfrac{1}{2}\varphi) \qquad e_r = t''_N \cos\varphi \qquad 4315\text{-}17$$

t''_N is derived from t'_1 by one or more applications of 3318. The formulae 4312-17 can, of course, only be used when we have chosen a rupture-line which meets the surface and the wall at the statically correct angles.

For $i = j = 0$, the formulae 4303-06 are reduced to the following:

$$\Sigma k \sin\beta = h \qquad \tan\delta\,\Sigma H - \Sigma U + ah = 0 \qquad 4318\text{-}19$$

$$E - \Sigma H = 0 \qquad z\,\Sigma H + \Sigma M^f = 0 \qquad 4320\text{-}21$$

The remaining formulae 4301-02 and 4307-11 are unchanged.

As to the calculation method see Section 431. It should be noted that E and z cannot be calculated with sufficient accuracy by means of 4320-21, but must be found from 4301-02.

Example 43a

As an example, we shall consider the following case of passive pressure on a rough wall (rupture P):

$$i = j = 0 \qquad p = c = a = 0$$

$$\varphi = \delta = +30^\circ \qquad \gamma = 1 \qquad h = 1$$

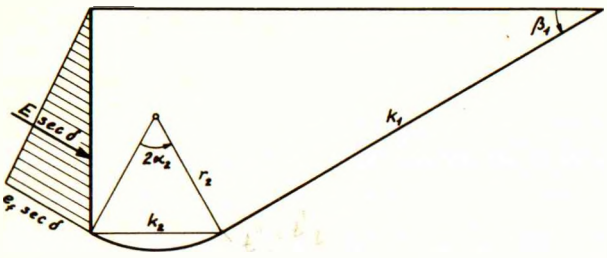

Fig.43B: Passive zone-rupture for rough wall

We choose here to approximate the lowest rupture-line by means of 1 straight line and 1 circle (Fig.43B). From 4312 and 4314 we get $v'_1 = 30^\circ$ and $v''_2 = -30^\circ$. As $\alpha_1 = 0^\circ$ we find from 4307-09 successively: $\beta_1 = 30^\circ$, $\alpha_2 = 30^\circ$ and $\beta_2 = 0^\circ$.

Next, 4318 gives $k_1 = 2$, so that k_2 is the only remaining unknown quantity. It shall be determined by means of 4319. As $t'_1 = 0$, we get, by means of 3318 and Table 2 in the Appendix:

$$t''_1 = 2\,(0.866 \times 0.5 + 0.5 \times 0.866) = 1.732 = t'_2$$

The forces G are determined by 3223 and 3227 with the aid of Table 1:

$$G_1 = 2^2 \times 0.25 \times 0.866 = 0.866 \qquad G_2 = k_2^2 \times 0.091 \qquad G_{12} = 1 \times k_2 = k_2$$

The forces V and H are found from 3325-26 by means of Table 2:

$$V_1 = 2^2 \times 0.25 \times 0.866 = 0.866 = G_1 \qquad H_1 = 2^2(0.25 + 0.25 \times 0.5) = 1.5$$

$$V_2 = k_2^2(0.170 + 0.397 \times 0.866) + k_2 \times 1.732 \times 1.782 \times 1 = 0.514\,k_2^2 + 3.086\,k_2$$

$$H_2 = k_2^2(0.377 - 0.397 \times 0.5) + k_2 \times 1.732 \times 0.793 \times 1 = 0.178\,k_2^2 + 1.375\,k_2$$

We can now insert into 4319, which gives:

$$0.577\,(1.5 + 0.178\,k_2^2 + 1.375\,k_2) - 0.866 - 0.514\,k_2^2 - 3.086\,k_2 + 0.866 + 0.091\,k_2^2 + k_2 =$$

$$0.320\,k_2^2 + 1.293\,k_2 - 0.866 = 0 \qquad \underline{k_2 = 0.59}$$

Then we find from 3318 and 4317, using Table 2:

$$t''_2 = 0.59 \times 1.147 + 1.732 \times 3.35 = 6.48 \qquad e_f = 6.48 \times 0.866 = \underline{5.61 = \lambda}$$

As we must have $e_t = 0$, we get, from 4301-02:

$$\underline{E} = \tfrac{1}{2} \times 5.61 = \underline{2.81} = \tfrac{1}{2}\lambda \qquad \underline{z = \tfrac{1}{3} = \eta}$$

If we use 4320-21, we find the less correct values $E = 2.39$ and $z = 0.29$. In spite of these considerable deviations, a more correct calculation, by means of 1 straight line and 2 circles, has shown that E, as found from 4301, is only about 1% out, as the correct value is $\lambda = 2E = 5.66$.

If 1 circle was used, we should satisfy 4318-19 and 4321 (with $z = \frac{1}{3}$). This would give $\alpha = 33.8^\circ$, $\beta = 25.2^\circ$ and $\lambda = 6.15$, which is about 8% out.

With 1 straight line, we would find $\beta = 13.4^\circ$ and $\lambda = 8.75$. With 2 straight lines, we have $\beta_1 = -\beta_2 = 30^\circ$, and by means of 4318-19, we would find $k_1 = 2.26$ and $k_2 = 0.26$, giving $\lambda = 4.45$. Finally, with 3 straight lines, we have $\beta_1 = -\beta_3 = 30^\circ$ and $\beta_2 = 0^\circ$, and by means of 4318-20, we would find $k_1 = 2.07$, $k_2 = 0.63$ and $k_3 = 0.07$, giving $\lambda = 5.35$. The latter result is only about 5% out.

It is worth noticing that 1 straight line, which is "kinematically admissible", gives a greater λ than the actual one, whereas 2 or 3 straight lines, which are "statically admissible", give smaller values of λ than the actual one.

433. Deformations

We shall now try to investigate which movements of the wall are compatible with the deformations of the earth in a plastic zone. Incidentally, when we speak of deformations in the plastic state, we actually mean rates of deformations.

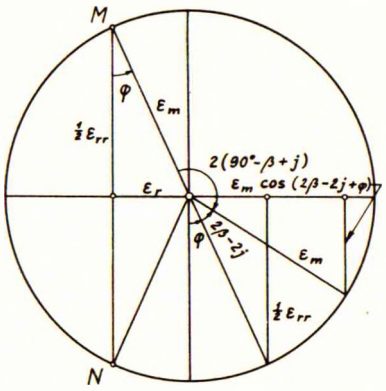

Fig.43C: Mohr's circle for deformations

First, we consider Mohr's circle for deformations (Fig.43C). As we assume incompressibility in the plastic state, the strains ε (positive when they indicate contractions) must be measured from the centre of the circle. Further, we assume that the principal strains ε_1 and ε_2 occur in the same lines as the principal stresses. To the rupture-lines proper correspond then the points M and N in Mohr's circle, and if we denote the maximum shortening by ε_m, we find in both rupture-lines the strain:

$$\varepsilon_r = \varepsilon_m \sin \varphi \qquad 4322$$

whereas the change of the angle between the rupture-lines is:

$$\varepsilon_{rr} = 2\varepsilon_m \cos \varphi = 2\varepsilon_r \cot \varphi \qquad 4323$$

which indicates also the change of the angle between a rupture-line and its normal.

As a result, we can state that by any plastic deformation with $\varphi \neq 0$, both rupture-lines must shorten and the sharp angle between them must increase.

The displacement of a small earth element is characterized by its velocity vector u, which, for the lowest rupture-line, must be tangential to this line. u is assumed positive when it is directed against the shear stress from below. When the arch length s is assumed positive in the same direction, we have:

$$\frac{du}{ds} = -\varepsilon_r \qquad 4324$$

A complete quantitative investigation of the movements and deformations in a plastic zone lies outside the scope of the present work. We shall, therefore, only make a few qualitative considerations. First, we consider the case of active pressure (Fig.43D).

At any point of the lowest rupture-line we must have $\varepsilon_{rr} \geq 0$ (increase of the sharp angle between the rupture-lines) and $u \geq 0$ (outward movement). As the rupture-line shortens, we must have $u'' < u'$. Therefore, one limiting condition is $u'' = 0$. The other is $\varepsilon'_{rr} = 0$, to which corresponds a certain (positive) value of ε''_{rr}.

For $u'' = 0$, the rotation centre of the wall will be situated at the foot (point U_2). To $\varepsilon''_{rr} = 0$ would correspond a rotation about the normal projection

on the wall of the centre of the osculating circle (point F_2). To $\varepsilon'_{rr} = 0$ corresponds a rotation centre (point F_1) above F_2. The actual rotation centre can, therefore, not be located between the points U_2 and F_1. As we shall see later, it must be located within one of the shaded areas in Fig. 43D.

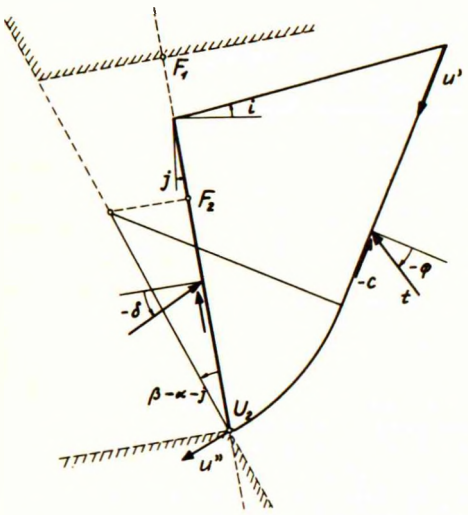

Fig. 43D: Rotation centres for active zone-rupture

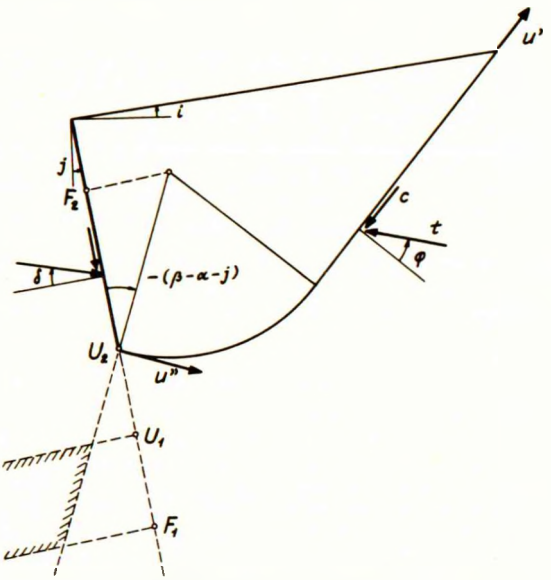

Fig. 43E: Rotation centres for passive zone-rupture

Turning now to the case of passive pressure (Fig. 43E), we must, at any point of the lowest rupture-line, have $\varepsilon_{rr} \geqslant 0$ (increase of the sharp angle between the rupture-lines) and $u \geqslant 0$ (inward movement). As the rupture-line shortens, we must have $u'' > u'$. Therefore, one limiting condition is $u' = 0$, to which corresponds a certain (positive) value of u". The other limiting condition is $\varepsilon'_{rr} = 0$, to which corresponds a certain (positive) value of ε''_{rr}.

For $u'' = 0$, the rotation centre of the wall would be situated at the foot (point U_2). To $u' = 0$ corresponds a rotation centre (point U_1) below U_2. To $\varepsilon''_{rr} = 0$ would correspond a rotation about the normal projection on the wall of the centre of the osculating circle (point F_2). To $\varepsilon'_{rr} = 0$ corresponds a rotation centre (point F_1), which is probably located below U_1. The actual rotation centre can, consequently, only be located between the points U_1 and F_1, and, as we shall see later, it must be located within the shaded area in Fig. 43E.

In the special case of the rupture-zone being one single R-zone, (i.e., when the statically correct angles v' and v" are equal), we can find the exact locations of the points U and F, because, for a straight rupture-line, we must have constant values of ε_r and ε_{rr}. As $r = \infty$, the points F_1 and F_2 must both be infinitely distant, so that for active pressure the wall can rotate about any point below its foot. For passive pressure we have, corresponding to $u' = 0$ (Fig. 43F):

$$u'' = k\varepsilon_r = h \frac{\cos(j-i)}{\sin(\beta-i)} \varepsilon_r \qquad 4325$$

$$k = h \frac{\cos(j-i)}{\sin(\beta-i)}$$

As the angle between wall and rupture-line is $90^\circ - \beta + j$, the decrease of this angle can, by means of Mohr's circle (Fig.43C), be found to be :

$$\varepsilon_{rw} = \tfrac{1}{2}\varepsilon_{rr} + \varepsilon_m \cos(2\beta - 2j + \varphi) = \frac{\varepsilon_r}{\sin\varphi}\left[\cos\varphi + \cos(2\beta - 2j + \varphi)\right] \qquad 4326$$

The location of the uppermost rotation centre U_1 can now be determined by:

$$\xi_1 = -\frac{u''\cos(\beta - j)}{h\varepsilon_{rw}} = -\frac{\sin\varphi\cos(j-i)}{2\sin(\beta - i)\cos(\beta + \varphi - j)} \qquad 4327$$

In another special case we can also indicate the exact location of the points U and F, viz., for frictionless earth ($\varphi = 0$), because in this case the rupture-lines do not change their lengths ($\varepsilon_r = 0$). This means that u is constant along the whole rupture-line, whereas ε_{rr} has different, but constant, values within each circular part of the rupture-line. However, the rotation of the pseudo-rupture-line , which is equal to ε_{rr} - u:r, is constant along the whole rupture-line. As we have $r_1 = \infty$ at the surface, the rotation of the wall, corresponding to $\varepsilon'_{rr} = 0$, must be zero, which means that the point F_1 is infinitely distant. Corresponding to u' = 0, we have also u" = 0, and the point U_1 coincides, therefore, with U_2 at the foot of the wall. The final result is that the wall can rotate about any point below its foot.

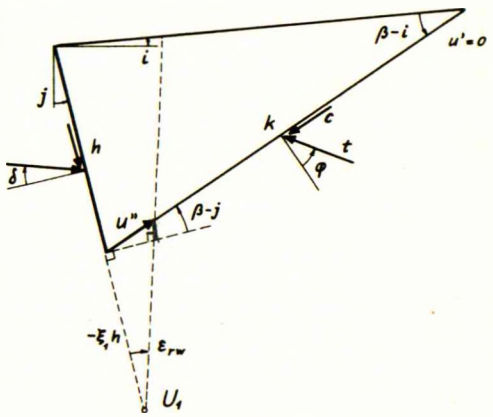

Fig.43F: Rotation centres for passive R-rupture

It has already been mentioned that δ and a should have the same signs as φ and c. This is only correct, however, if a corresponding tangential movement takes place between wall and earth.

For active pressure (Fig.43D), this movement has the correct direction when the rotation centre for the wall lies either above the normal to the wall through F_1 and to the right of the normal to the rupture-line through U_2, or below the normal to the wall through U_2 and to the left of the normal to the rupture-line through U_2. As we always have $\beta_N - \alpha_N - j \geq 0$ for active pressure, it will be seen that δ and a have the correct signs when the wall rotates "normally" only.

For passive pressure (Fig.43E), the movement has the correct direction when the rotation centre for the wall lies between the normals to the wall through U_1 and F_1 and to the left of the normal to the rupture-line through U_2. This means that when the wall rotates "normally" only, δ and a will only have the correct signs if $\beta_N - \alpha_N - j \geq 0$. The corresponding limiting value of δ is found by putting v"- j = 0 in 3419:

$$\cot\delta_o = 2\tan\varphi + \cot\varphi \qquad \text{or:} \qquad \delta_o = \psi - \varphi \qquad 4328$$

In the special case of frictionless earth ($\varphi = 0$), the limiting value of a is found by putting $v'' - j = 0$ in 3420. This gives $a_o = c$, so that a will always have the correct sign when the wall rotates "normally" only.

For $\delta < \delta_o$ we get the correct signs of δ and a, but for $\delta > \delta_o$, a contradiction exists, and this must mean that a passive zone-rupture cannot occur in this case. The actual rupture-figure is probably of the type XfP (see Fig.35E).

Even when $\delta < \delta_o$, we have seen that a passive zone-rupture can only occur when the rotation centre is located in the interval $U_1 - F_1$ (Fig.43E). If the rotation centre lies in the interval $U_2 - U_1$, the actual rupture-figure is probably of the type XfP, and if it lies below F_1 or above F_2 respectively, the actual rupture-figure is probably of the type XfPfA or AfPfA respectively (see Fig.35F).

44. RUPTURES LfR AND LaR

441. Sloping Surface and Inclined Wall

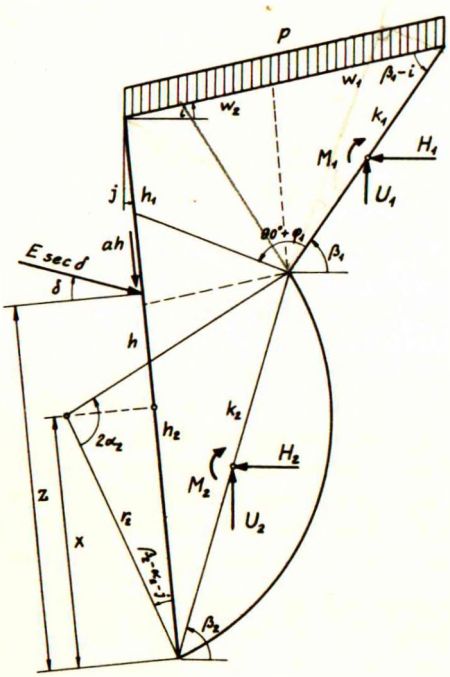

Fig.44A: Calculation of rupture LfR or LaR

We shall now proceed to show how an LfR- or LaR-rupture, with a straight R-line, can be calculated. These ruptures can occur for any roughness of the wall, as long as the R-zone does not touch the wall. In the special case of the statically correct angles v'_1 and v''_N being equal, the R-zone can have any extension.

Fig.44A shows, in principle, a rupture LfR or LaR. As $N_C = N_S = 1$, we have $3N_C + 2N_S = 5$ parameters and $N + 2 = 4$ conditions, so that we must add a new condition in order to make the problem soluble. It will be natural here to have the R-line meet the surface at the statically correct angle. We have then:

$$\alpha_1 = 0° \qquad \beta_1 = v'_1 \qquad 4401\text{-}02\ \surd$$

where v'_1 can be found from 3405. Further, 4110-11 give for an:

f-rupture: $\beta_2 = \beta_1 - \alpha_2$ 4403 √

a-rupture: $\beta_2 = \beta_1 - \alpha_2 + \varphi_1 + 90°$ 4404 √

When x is given, we get from 4107:

$$\xi = \frac{x}{h} = \frac{k_2 \cos(\beta_2-\alpha_2-j)}{2h \sin \alpha_2} \qquad \text{or:} \qquad k_2 = 2\xi h \sin \alpha_2 \sec(\beta_2-\alpha_2-j) \qquad 4405\text{-}06$$

Equations 4109 and 4105 give:

$$k_1 = \frac{h \cos(j-i) - k_2 \sin(\beta_2-i)}{\sin(\beta_1-i)} \qquad 4407$$

$$(H_1+H_2) \sin(\delta-j) - (U_1+U_2) \cos(\delta-j) + ah \cos \delta = 0 \qquad 4408$$

The procedure is now the following. α_1 and β_1 are given by 4401-02. With an estimated value of α_2, we find the corresponding β_2 from 4403 (f-rupture) or 4404 (a-rupture), and then k_2 and k_1 from 4406-07. After insertion of the pertaining formulae from Sections 32-34 in 4408, it is then investigated whether this equation is satisfied. If not, another value of α_2 is estimated and the procedure repeated.

It must be remembered that for an f-rupture we have $\varphi_1 = \varphi_2$ and $c_1 = c_2$, whereas for an a-rupture, we have $\varphi_1 = -\varphi_2$ and $c_1 = -c_2$. In both ruptures, δ and a should have the same signs as φ_2 and c_2. Finally, when the lower zone is an A-zone, α_2 should be positive, whereas α_2 should be negative for an X-zone.

If we find $\beta_2 - \alpha_2 - j < 0$, we must use, instead of 4408, equation 4106 which, when inserted in 4403-04, yields for an:

f-rupture: $\alpha_2 = \frac{1}{2}(\beta_1 - j)$ $\beta_2 = \alpha_2 + j$ 4409-10

a-rupture: $\alpha_2 = \frac{1}{2}(\beta_1 - j + \varphi_1 + 90^\circ)$ $\beta_2 = \alpha_2 + j$ 4411-12

which then give α_2 and β_2 direct.

If z is given instead of x, 4406 must be substituted by 4108.

When the geometrical parameters have been determined, we find the unknown statical quantities by means of 4113-14 and 4118:

$$E = (H_1+H_2)\cos j - (U_1+U_2)\sin j \qquad F = (H_1+H_2)\sin j + (U_1+U_2)\cos j \qquad 4413\text{-}14$$

$$Ez = \tfrac{1}{2}k_2\left[E \sin(\beta_2-j) + F \cos(\beta_2-j)\right] - M_1 - M_2 + \tfrac{1}{2}H_1(k_1 \sin \beta_1 + k_2 \sin \beta_2) + \tfrac{1}{2}U_1(k_1 \cos \beta_1 + k_2 \cos \beta_2) \qquad 4415$$

From Fig. 44A, it may be seen that the R-zone will just touch the top of the wall when:

$$\frac{w_1 + w_2}{\cos \varphi_1} = \frac{k_1}{\cos(\beta_1+\varphi_1-i)} \qquad 4416$$

$180 = \psi + \beta_1 - i + 90 + \varphi_1$

$\psi = 90 - (\beta_1 + \varphi_1 - i)$

This limiting condition can, by means of 3204 and 4406-07, be transformed to:

$$\xi_o = \frac{\sin(\beta_1+\varphi_1-j)\,\cos(\beta_2-\alpha_2-j)}{2\sin\alpha_2\,\cos(\beta_1-\beta_2+\varphi_1)} \qquad 4417$$

which indicates the lowest position of the rotation centre, for which the considered rupture can occur.

With regard to the deformations, it is evident that the R-line must shorten. For a rupture LaR, this agrees with the assumed direction of the shear stresses, if there is active pressure in the R-line, but not in the case of passive pressure. Therefore, strictly speaking, this rupture cannot occur with passive pressure in the R-line (except for $\varphi = 0$).

For a rupture LfR, the shortening of the R-line can also take place with passive pressure in this line, provided that the rotation centre for the wall lies below a certain point, the location of which can be found in a similar way as used in the investigation of the rupture R (see Section 433).

442. Horizontal Surface and Vertical Wall

When $i = j = 0$, it will be most practical to consider h_1 and h_2 as the unknown lengths. We find first by means of 4402, 4312 and 4315:

$$\beta_1 = 45^\circ - \tfrac{1}{2}\varphi_1 \qquad t_1' = p\tan(45^\circ+\tfrac{1}{2}\varphi_1) + c_1 \qquad 4418\text{-}19$$

Next, $t_2' = t_1''$ is calculated by means of 3339 and 3217:

$$t_2' = (p+\gamma h_1)\tan(45^\circ+\tfrac{1}{2}\varphi_1) + c_1 \qquad 4420$$

The formulae 4403-04 are unchanged.

With the above values of β_1 and t_1', it will be found, by means of 3221, 3223 and 3341, that $V_1 = G_1 + P_1$, i.e.: $U_1 = 0$.

Considering this and inserting $i = j = 0$, the formulae 4405-08 and 4413-15 are reduced to the following:

$$\xi = \frac{h_2}{2h}(1+\cot\alpha_2\cot\beta_2) \qquad h_2 = \frac{2\xi h}{1+\cot\alpha_2\cot\beta_2} \qquad h_1 = h - h_2 \qquad 4421\text{-}23$$

$$(H_1+H_2)\tan\delta - U_2 + ah = 0 \qquad E = H_1 + H_2 \qquad F = U_2 \qquad 4424\text{-}26$$

$$Ez = \tfrac{1}{2}h_2(E + F\cot\beta_2) + \tfrac{1}{2}hH_1 - M_1 - M_2 \qquad 4427$$

As to the calculation method, see Section 441. Instead of estimating α_2 and satisfying 4424, we can also start the calculation with 4409-10 (f-rupture) or 4411-12 (a-rupture), inserting $j = 0$. As to the criteria for a correct solution, see Section 421.

Example 44a

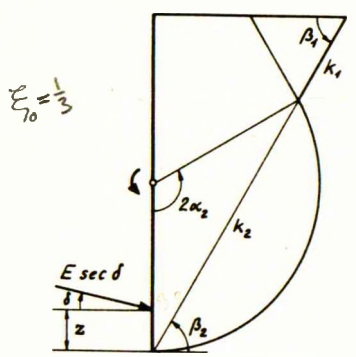

Fig.44B: Rough wall rotating about its middle point

As an example, we shall consider the following case (Fig. 44B) of a rough wall rotating about its middle point (rupture AaR):

$$i = j = 0 \qquad p = c = a = 0 \qquad \varphi_2 = -\varphi_1 = +30^\circ$$

$$\gamma = 1 \qquad h = 1 \qquad \xi = \tfrac{1}{2}$$

From 4401 and 4418-20 we get first:

$$\alpha_1 = 0^\circ \qquad \beta_1 = 60^\circ \qquad t'_1 = 0 \qquad t'_2 = 0.577\ h_1$$

We choose now to start the calculation with 4411-12. This gives:

$$\alpha_2 = \beta_2 = \tfrac{1}{2}\,(60^\circ - 30^\circ + 90^\circ) = 60^\circ$$

h_2 and h_1 are then found from 4422-23, after which 3217 yields k_2 and k_1:

$$h_2 = \sin^2 60^\circ = 0.75 \qquad h_1 = 1 - 0.75 = 0.25 \qquad t'_2 = 0.577 \times 0.25 = 0.144$$

$$k_2 = 0.75 : 0.866 = 0.866 \qquad k_2^2 = 0.75 \qquad k_2^3 = 0.649$$

$$k_1 = 0.25 : 0.866 = 0.288 \qquad k_1^2 = 0.083 \qquad k_1^3 = 0.024$$

Next, we find by means of 3223-24, 3227-28, 3325-26 and 3335, as well as Tables 1, 2 (lower rupture-line) and 3 (upper rupture-line) in the Appendix:

$$M_{G_1} = 0.024\ (-0.083 \times 0.866 + 0.083 \times 0.866^3) = -0.001$$

$$H_1 = 0.083\ (0.25 - 0.25 \times 0.5) = 0.010$$

$$M_{R_1} = 0.024\ (0.063 \times 0.866 - 0.036 \times 0.5) = 0.001$$

$$G_2 = 0.75\ (0.205 + 0.25 \times 0.866) = 0.316$$

$$M_{G_2} = 0.649\ (-0.059 \times 0.866 + 0.083 \times 0.866^3) = 0.002$$

$$G_{12} = 0.288 \times 0.866 \times 0.866 \times 0.5 = 0.108 \qquad M_{G_{12}} = 0$$

$$V_2 = 0.75\ (0.716 + 0.766 \times 0) + 0.144 \times 0.866\ (-0.516 \times 0.866 + 4.42 \times 0.5) = 0.758$$

$$H_2 = 0.75\ (0.447 + 0.766 \times 1) + 0.144 \times 0.866\ (4.42 \times 0.866 + 0.516 \times 0.5) = 1.418$$

$$M_{R_2} = 0.649\ (0.273 \times 0.866 + 0.424 \times 0.5) + 0.144 \times 0.75 \times 1.33 = 0.436$$

E, F and z are now found from 4425-27, using also 4102-03:

$$\underline{E} = 0.010 + 1.418 = \underline{1.43} = \tfrac{1}{2}\lambda \qquad F = 0.758 - 0.316 - 0.108 = 0.33 = \tfrac{1}{2}\lambda \tan\delta$$

$$Ez = 0.5 \times 0.75\ (1.43 + 0.33 \times 0.577) + 0.5 \times 0.010 + 0.001 - 0.001 - 0.002 - 0.436 = 0.175$$

$$\underline{z} = 0.175 : 1.43 = \underline{0.12} = \eta \qquad \underline{\tan\delta} = 0.33 : 1.43 = \underline{0.23}$$

As we find $\delta < \varphi$, it was thus correct to use 4411-12.

45. RUPTURES LfP AND LaP

451. Sloping Surface and Inclined Wall

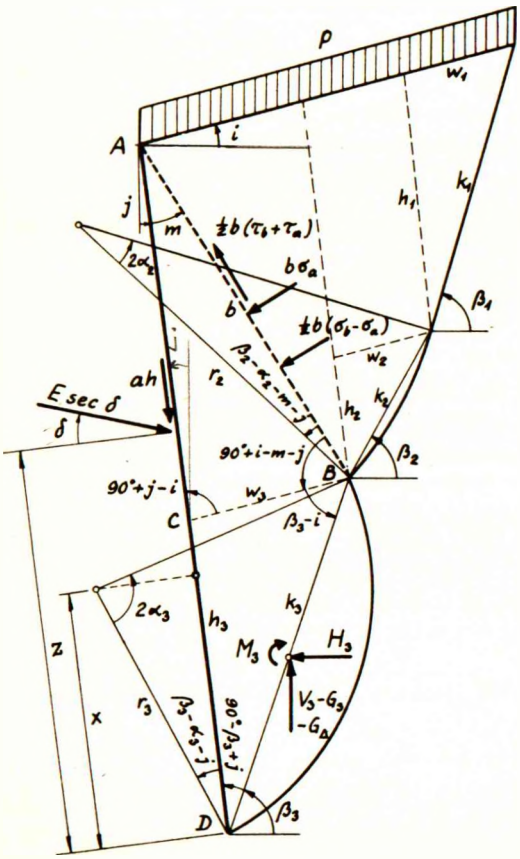

Fig.45A: Calculation of rupture LfP or LaP

In an LfP- or LaP-rupture, the exact shape of the plastic zone is not known. The lowest rupture-line may, as usual, be approximated by a number of circles and straight lines, but the boundary between the plastic and the elastic zones (which must be a rupture-line) is not straight, except in the special cases of $\gamma = 0$, or ~~$p = c$~~ $= 0$.

In order to overcome this difficulty and make a comparatively simple calculation possible, we shall assume that the plastic zone is shaped as a part of a complete P-rupture, corresponding to a wall height h°.

In the special cases of $\gamma = 0$, or $p = c = 0$, the shape of the complete P-rupture is independent of h°, but in the general case the shape varies with h°. However, this variation is not very great. Therefore, if we determine the shape of the complete P-rupture for an estimated value of h°, we need not correct this later, except if the actual h° should deviate very much from the estimated value.

Therefore, the first step is to estimate h° and carry out a calculation of the corresponding rupture P as described in Section 43. When this has been done, we know all the geometrical parameters of this rupture (denoted by the superscript 0). In the actual rupture LfP or LaP, the angles are the same, but the lengths should be multiplied by a factor K. Consequently, we have (Fig. 45A):

$$\alpha_1 = \alpha_1^\circ \qquad \beta_1 = \beta_1^\circ \qquad \beta_2 = \beta_2^\circ + \alpha_2^\circ - \alpha_2 \qquad k_1 = Kk_1^\circ \qquad 4501\text{-}04$$

$$w_2 + w_3 = K(w_2^\circ + w_3^\circ) \qquad r_2 = Kr_2^\circ \qquad h - h_2 - h_3 = K(h^\circ - h_2^\circ - h_3^\circ) \qquad 4505\text{-}07$$

Further, we get from 4110-11 for an:

f-rupture: $$\beta_3 = \beta_2 - \alpha_2 - \alpha_3 \qquad 4508$$

a-rupture: $$\beta_3 = \beta_2 - \alpha_2 - \alpha_3 + \varphi_2 + 90^\circ \qquad 4509$$

We draw now a straight line AB from the top of the wall to the point of intersection between the L- and the P-line (Fig.45A). This line has a length b and makes an angle m with the wall. The triangle ABC gives:

$$\frac{w_3}{\sin m} = \frac{h - h_3}{\cos(m+j-i)} = \frac{b}{\cos(j-i)} \qquad 4510$$

By means of 4505-07 and 3203-04, we find from 4510:

$$\cot m = \frac{h^\circ - h_2^\circ - h_3^\circ + 2r_2^\circ \sin\alpha_2 \sin(\beta_2-i) \sec(j-i)}{(w_2^\circ + w_3^\circ)\cos(j-i) - 2r_2^\circ \sin\alpha_2 \cos(\beta_2-j)} + \tan(j-i) \qquad 4511$$

Further, the triangle ABD gives:

$$\frac{k_3}{\sin m} = \frac{h}{\cos(\beta_3-m-j)} = \frac{b}{\cos(\beta_3-j)} \qquad 4512$$

When x is given, we get from 4107, by means of 4512:

$$\xi = \frac{x}{h} = \frac{\sin m \cos(\beta_3-\alpha_3-j)}{2 \sin\alpha_3 \cos(\beta_3-m-j)} \qquad 4513$$

Inserting 4508 (f-rupture) or 4509 (a-rupture) in 4513 and solving for α_3, we find an equation of the form:

$$\cot\alpha_3 = \xi(\cot m + \tan u) - \tan u - \sqrt{\xi^2(\cot m + \tan u)^2 + (1-2\xi)\sec^2 u} \qquad 4514$$

where the angle u has the following value for an:

f-rupture: $$u = \beta_2 - \alpha_2 - j \qquad 4515$$

a-rupture: $$u = \beta_2 - \alpha_2 - j + \varphi_2 + 90^\circ \qquad 4516$$

From 4505-06 we find, by means of 3204, 4510 and 4512:

$$K = \frac{h \sin m \cos(\beta_3-j) \sec(\beta_3-m-j)}{(w_2^\circ + w_3^\circ)\cos(j-i) - 2r_2^\circ \sin\alpha_2 \cos(\beta_2-j)} \qquad 4517$$

k_1 is given by 4504, and for k_2 and k_3 we obtain, by means of 3202, 4506 and 4512 the expressions:

$$k_2 = 2Kr_2^\circ \sin\alpha_2 \qquad k_3 = h \sin m \sec(\beta_3-m-j) \qquad 4518\text{-}19$$

The procedure is now the following. α_1 and β_1 are given direct by 4501-02. With an estimated value of α_2, we find β_2 from 4503 and m from 4511. Further, 4514 yields α_3, whereas β_3 is given by 4508 (f-rupture) or 4509 (a-rupture). K is then found from 4517 and k_1, k_2 and k_3 from 4504 and 4518-19. We now need only a statical equation to show whether α_2 has been correctly chosen.

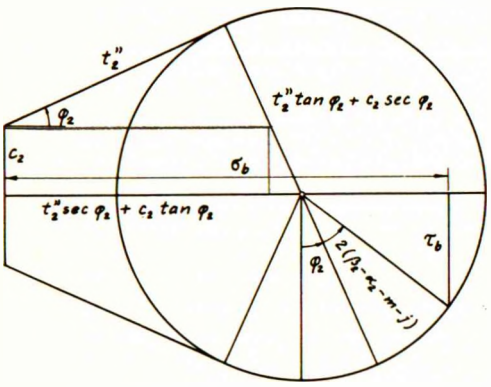

Fig.45B: Mohr's circle

We might, as in the previous sections, use 4105 for this purpose, but it is actually simpler, and at the same time more accurate, to consider the equilibrium of the earth mass bounded by the wall, the line AB and the L-line. In order to do this, we must first determine the forces acting upon the line AB. Its length is found from 4512:

$$b = h\cos(\beta_3-j)\sec(\beta_3-m-j) \qquad 4520\ \surd$$

At point B of the line AB act the stresses τ_b and σ_b, which can be calculated with the aid of Mohr's circle (Fig.45B), when the stress t_2'' has been determined by means of 3411 and 3318:

$$\tau_b = (t_2''\tan\varphi_2 + c_2\sec\varphi_2)\cos(2\beta_2-2\alpha_2-2m-2j+\varphi_2) \qquad 4521\ \surd$$

$$\sigma_b = (t_2''\tan\varphi_2 + c_2\sec\varphi_2)\sin(2\beta_2-2\alpha_2-2m-2j+\varphi_2) + (t_2''\sec\varphi_2 + c_2\tan\varphi_2) \qquad 4522\ \surd$$

The same equations can be used for determining the stresses τ_a and σ_a at point A of the line AB, when t_2'' is substituted by t_{2o}'', which is determined as t_2'', but with all chord-lengths equal to zero. Further, a linear variation of the stresses in AB is assumed.

For the weight of the triangular earth wedge ABC (Fig.45A) and its moment about the middle point of the chord k_3 we have:

$$G_\Delta = \tfrac{1}{2}\gamma w_3(h - h_3)\cos(j-i) \qquad 4523\ \surd$$

$$M_{G\Delta} = -G_\Delta\left[\tfrac{1}{3}(h - h_3)\sin j + \tfrac{2}{3}w_3\cos i - \tfrac{1}{2}k_3\cos\beta_3\right] \qquad 4524\ \surd$$

By projection on a line perpendicular to the force E sec δ we can now find:

$$H_3\sin(\delta-j) - (V_3 - G_3 - G_\Delta)\cos(\delta-j) + ah\cos\delta$$
$$+ \tfrac{1}{2}b(\sigma_b+\sigma_a)\sin(m+\delta) - \tfrac{1}{2}b(\tau_b+\tau_a)\cos(m+\delta) = 0 \qquad 4525$$

When this equation is satisfied, α_2 has been chosen correctly.

It must be remembered that, for an f-rupture we have $\varphi_1 = \varphi_2 = \varphi_3$ and $c_1 = c_2 = c_3$, whereas for an a-rupture, we have $\varphi_1 = \varphi_2 = -\varphi_3$ and $c_1 = c_2 = -c_3$.

In both ruptures, δ and a should have the same signs as φ_3 and c_3 (except in the initial calculation of the complete P-rupture, where they should have the same signs as φ_1 and c_1).

If we find $\beta_3 - \alpha_3 - j < 0$, we must, instead of 4525, use 4106 which, when inserted in 4508-09, yields for an:

f-rupture: $\alpha_3 = \frac{1}{2}(\beta_2 - \alpha_2 - j)$ $\beta_3 = \alpha_3 + j$ 4526-27

a-rupture: $\alpha_3 = \frac{1}{2}(\beta_2 - \alpha_2 - j + \varphi_2 + 90^\circ)$ $\beta_3 = \alpha_3 + j$ 4528-29

We start as usual with an estimated value of α_2, which is correct when 4513 is satisfied.

If z is given instead of x, equation 4514 must be substituted by the moment equation about the pressure centre.

When the geometrical parameters and the stresses in the line AB have been determined, we find the unknown statical quantities by projection on a normal to the wall, by projection on the wall, and by taking the moments about the middle point of the chord k_3 :

$$E = H_3 \cos j - (V_3 - G_3 - G_\Delta) \sin j + \tfrac{1}{2}b(\sigma_b+\sigma_a) \cos m + \tfrac{1}{2}b(\tau_b+\tau_a) \sin m \qquad 4530$$

$$F = H_3 \sin j + (V_3 - G_3 - G_\Delta) \cos j - \tfrac{1}{2}b(\sigma_b+\sigma_a) \sin m + \tfrac{1}{2}b(\tau_b+\tau_a) \cos m \qquad 4531$$

$$Ez = \tfrac{1}{2}k_3 \left[E \sin(\beta_3 - j) + F \cos(\beta_3 - j) \right] - M_{R_3} - M_{G_3} - M_{G\Delta} + \tfrac{1}{4}bh(\tau_b+\tau_a) \sin m + \tfrac{1}{4}bh(\sigma_b+\sigma_a) \cos m - \tfrac{1}{12}b^2(\sigma_b-\sigma_a) \qquad 4532$$

With regard to the deformations, similar remarks apply as those made in connection with the ruptures LfR and LaR (Section 441).

452. Horizontal Surface and Vertical Wall

For i = j = 0, the formulae 4511, 4513, 4517, 4523-25 and 4530-32 are reduced to the following:

$$\cot m = \frac{h^\circ - h_2^\circ - h_3^\circ + 2r_2^\circ \sin \alpha_2 \sin \beta_2}{w_2^\circ + w_3^\circ - 2r_2^\circ \sin \alpha_2 \cos \beta_2} \qquad 4533$$

$$\xi = \frac{\sin m \cos(\beta_3 - \alpha_3)}{2 \sin \alpha_3 \cos(\beta_3 - m)} \qquad K = \frac{h \sin m \cos \beta_3 \sec(\beta_3 - m)}{w_2^\circ + w_3^\circ - 2r_2^\circ \sin \alpha_2 \cos \beta_2} \qquad 4534\text{-}35$$

$$G_\Delta = \tfrac{1}{2}\gamma w_3 (h - h_3) \qquad M_{G\Delta} = -\tfrac{1}{6}w_3 G_\Delta \qquad 4536\text{-}37$$

$$H_3 \sin \delta - (V_3 - G_3 - G_\Delta - ah) \cos \delta + \tfrac{1}{2}b(\sigma_b+\sigma_a) \sin(m+\delta) - \tfrac{1}{2}b(\tau_b+\tau_a) \cos(m+\delta) = 0 \qquad 4538$$

$$E = H_3 + \tfrac{1}{2}b(\sigma_b+\sigma_a) \cos m + \tfrac{1}{2}b(\tau_b+\tau_a) \sin m \qquad 4539$$

$$F = V_3 - G_3 - G_\Delta - \tfrac{1}{2}b(\sigma_b+\sigma_a)\sin m + \tfrac{1}{2}b(\tau_b+\tau_a)\cos m \qquad 4540$$

$$Ez = \tfrac{1}{2}k_3(E\sin\beta_3 + F\cos\beta_3) - M_{R_3} - M_{G_3} - M_{G\Delta} + \tfrac{1}{4}bh(\tau_b+\tau_a)\sin m + \tfrac{1}{4}bh(\sigma_b+\sigma_a)\cos m - \tfrac{1}{12}b^2(\sigma_b-\sigma_a) \qquad 4541$$

The formulae 4501-03, 4508-09, 4514-16 and 4518-22 can be used as they are (with j = 0).

With regard to the calculation method see Section 451. Instead of using 4514 and satisfying 4538, we can also start the calculation with 4526-27 (f-rupture) or 4528-29 (a-rupture), putting j = 0 and satisfying 4534. As to the criteria for a correct solution, see Section 421.

Example 45a

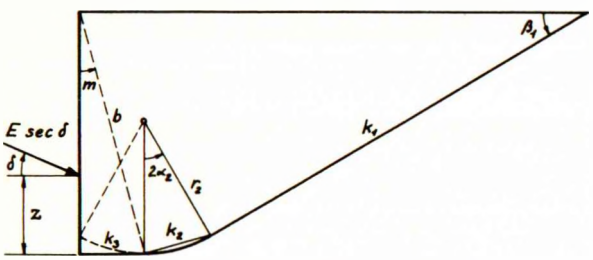

Fig.45C: Rough wall translating towards the earth

As an example, we shall consider the following case (Fig.45C) of passive pressure on a rough wall translating towards the earth (rupture SfP):

$$i = j = 0 \qquad p = c = a = 0$$

$$\varphi_3 = \varphi_2 = \varphi_1 = +30^\circ$$

$$\gamma = 1 \qquad h = 1 \qquad \xi = \infty$$

The corresponding complete rupture P has been calculated in Example 43a, where we have found:

$$\alpha_1^\circ = \beta_2^\circ = 0^\circ \qquad \alpha_2^\circ = \beta_1^\circ = 30^\circ \qquad h^\circ = 1 \qquad h_2^\circ = 0 \qquad k_1^\circ = 2 \qquad k_2^\circ = w_2^\circ = r_2^\circ = 0.59$$

We choose to start the calculation with 4527 which, when inserted in 4534 with $\xi = \infty$, immediately gives $\alpha_3 = \beta_3 = 0^\circ$. With this value, 4526 yields $\beta_2 = \alpha_2$, and 4503 gives then $\alpha_2 = \beta_2 = 15^\circ$.

As all quantities with superscript 0 and subscript 3 are non-existent in this case, we find from 4533 and 4535:

$$\cot m = \frac{1 + 2 \times 0.59 \times 0.259^2}{0.59 - 2 \times 0.59 \times 0.259 \times 0.965} = 3.66 \qquad m = 15.3^\circ$$

$$K = \frac{0.263 \times 1.036}{0.59 - 2 \times 0.59 \times 0.259 \times 0.965} = 0.927$$

We find now, by means of 4504 and 4518-20, that b = 1.036 and:

$$k_1 = 0.927 \times 2 = 1.855 \qquad k_2 = 2 \times 0.927 \times 0.59 \times 0.259 = 0.284$$

$$k_3 = 0.263 \times 1.036 = 0.273 \qquad k_3^2 = 0.074 \qquad k_3^3 = 0.020$$

As $t_1' = 0$, we can find by means of 3318 and Table 2 in the Appendix:

$$t_1'' = t_2' = 1.855\ (0.866 \times 0.5 + 0.5 \times 0.866) = 1.605$$

$$t_2'' = t_3' = 0.284\ (1.17 \times 0.259 + 0.718 \times 0.965) + 1.605 \times 1.83 = 3.23$$

We have, of course, $\tau_a = \sigma_a = 0$, whereas 4521-22 yield:

$$\tau_b = 3.23 \times 0.577 \times 1.000 = 1.87$$

$$\sigma_b = -\ 3.23 \times 0.577 \times 0.010 + 3.23 \times 1.155 = 3.71$$

As $\alpha_3 = \beta_3 = 0$, we have $G_3 = 0$ and $M_{G_3} = 0$ according to 3223-24. By means of 4536-37, 3325-26 and 3335, we get, using also Table 2 in the Appendix:

$$G_\Delta = 0.5 \times 0.273 \times 1 = 0.137 \qquad M_{G\Delta} = -\ 0.167 \times 0.273 \times 0.137 = -\ 0.006$$

$$V_3 = 0.074\ (0 + 0.25 \times 0.866) + 3.23 \times 0.273 \times 0.866 = 0.782$$

$$H_3 = 0.074\ (0.25 - 0.25 \times 0.5) + 3.23 \times 0.273 \times 0.5 = 0.452 \qquad M_{R_3} = 0.020 \times 0.036 = 0.001$$

We can now insert into 4539-41:

$$\underline{E} = 0.452 + 0.5 \times 1.036 \times 3.71 \times 0.963 + 0.5 \times 1.036 \times 1.87 \times 0.263 = \underline{2.57} = \tfrac{1}{2}\lambda$$

$$F = 0.782 - 0.137 - 0.5 \times 1.036 \times 3.71 \times 0.263 + 0.5 \times 1.036 \times 1.87 \times 0.963 = 1.07 = \tfrac{1}{2}\lambda \tan\delta$$

$$Ez = 0.5 \times 0.273 \times 1.07 - 0.001 + 0.006 + 0.25 \times 1.036 \times 1.87 \times 0.263$$
$$+ 0.25 \times 1.036 \times 3.71 \times 0.963 - 0.083 \times 1.036^2 \times 3.71 = 0.873$$

$$\underline{z} = 0.873 : 2.57 = \underline{0.34} = \eta \qquad \underline{\tan\delta} = 1.07 : 2.57 = \underline{0.42}$$

As we find $\delta < \varphi$, it was thus correct to use 4526-27.

46. OTHER COMPOSITE RUPTURES

461. Ruptures ZfL and ZaL

In order to calculate a ZfL- or ZaL-rupture we must assume, as in Section 45, that the plastic zone is shaped as a part of a complete rupture P (or R). Moreover, we have here $h^\circ = h$ and $K = 1$, so that all parameters of the complete plastic rupture (denoted by the superscript 0) are known. Consequently, we have (Fig.46A):

$$\alpha_3 = \alpha_3^\circ \qquad \beta_3 = \beta_3^\circ \qquad \beta_2 = \beta_2^\circ - \alpha_2^\circ + \alpha_2 \qquad 4601\text{-}03$$

$$k_3 = k_3^\circ \qquad r_2 = r_2^\circ \qquad h_1 + h_2 = h - h_3^\circ \qquad 4604\text{-}06$$

Further, we get from 4110-11 for an :

f-rupture: $\beta_1 = \beta_2 + \alpha_2 + \alpha_1$ 4607

a-rupture: $\beta_1 = \beta_2 + \alpha_2 + \alpha_1 + \varphi_2 - 90^\circ$ 4608

By means of 3202 and 4605-06 we can find:

$$k_2 = 2r_2^{\circ} \sin \alpha_2 \qquad k_1 = \frac{(h - h_3^{\circ}) \cos(j-i) - k_2 \sin(\beta_2 - i)}{\sin(\beta_1 - i)} \qquad 4609\text{-}10$$

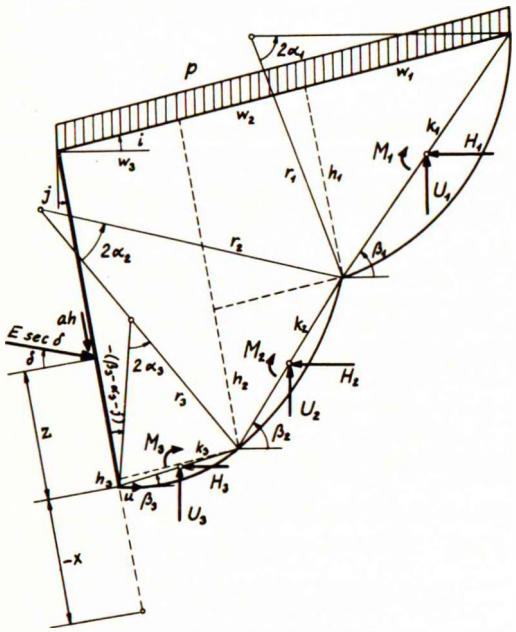

Fig.46A: Calculation of rupture ZfL or ZaL

If z is given, we must satisfy the equations 4105 and 4108, which can only be done by trial. We estimate values of α_1 and α_2, find β_2 from 4603, β_1 from 4607 (f-rupture) or 4608 (a-rupture) and k_1 and k_2 from 4609-10. We then investigate whether 4105 and 4108 are satisfied.

It must be remembered that, for an f-rupture we have $\varphi_3 = \varphi_2 = \varphi_1$, and $c_3 = c_2 = c_1$, whereas for an a-rupture, we have $\varphi_3 = \varphi_2 = -\varphi_1$ and $c_3 = c_2 = -c_1$. In both ruptures, δ and a should have the same signs as φ_3 and c_3.

If x is given, we are in general confronted with the difficulty of not being able to indicate a relation between the movement of the wall and that of the elastic zone without investigating in detail the deformations of the plastic zone.

However, in the special case of frictionless earth ($\varphi = 0$), we can solve the problem, because in this case we have found in Section 433 that the velocity vector u as well as the rotation of the pseudo-rupture-line ε_{rr} - u:r is constant along the whole P-line.

For an a-rupture, the velocity vectors in the P-line must be zero when $\varphi = 0$, which means that we can only have $x = 0$. For an f-rupture we get, as $\varepsilon_{rr_1} = 0$ in the elastic zone:

$$\varepsilon_{rr_3} - \frac{u}{r_3} = \varepsilon_{rr_2} - \frac{u}{r_2} = -\frac{u}{r_1} \qquad 4611$$

The decrease of the angle between wall and rupture-line can be found by putting $\varphi = 0$ and $\varepsilon_m = \frac{1}{2}\varepsilon_{rr}$ in 4326 and, at the same time, substituting β (for the straight rupture-line in Fig.43F) by $\beta_3 - \alpha_3$ (for the circular one in Fig.46A):

$$\varepsilon_{rw} = \varepsilon_{rr_3} \cos^2(\beta_3 - \alpha_3 - j) \qquad 4612$$

The rotation of the wall can now be expressed in two different ways (Fig. 46A), giving the equation:

$$\varepsilon_{rw} - \frac{u}{r_3} = \frac{u \cos(\beta_3 - \alpha_3 - j)}{-x} \qquad 4613$$

By elimination of ε_{rw} and ε_{rr_3} from 4611-13 we find:

$$\frac{1}{x} = \left[\frac{1}{r_1} + \frac{1}{r_3}\tan^2(\beta_3-\alpha_3-j)\right]\cos(\beta_3-\alpha_3-j) \qquad 4614$$

Using 3201 and inserting 4610 and 4607 in 4614, we get an equation, from which we can find:

$$\cos(2\alpha_1+\beta_2+\alpha_2-i) = \cos(\beta_2+\alpha_2-i) - \left[(h-h_3^\circ)\cos(j-i) - k_2\sin(\beta_2-i)\right]\cdot\left[\frac{1}{x}\sec(\beta_3-\alpha_3-j) - \frac{1}{r_3^\circ}\tan^2(\beta_3-\alpha_3-j)\right] \qquad 4615$$

When we have an f-rupture, frictionless earth and a given x, we estimate first a value of α_2. We find then β_2 from 4603 and k_2 from 4609. Next, 4615 gives the corresponding α_1, 4607 yields β_1 and 4610 k_1. We then investigate whether 4105 is satisfied. If not, α_2 must be changed and the calculation repeated.

When the geometrical parameters have been determined, we find the unknown statical quantities E, F and z by means of 4113-15 or 4116-18.

Example 46a

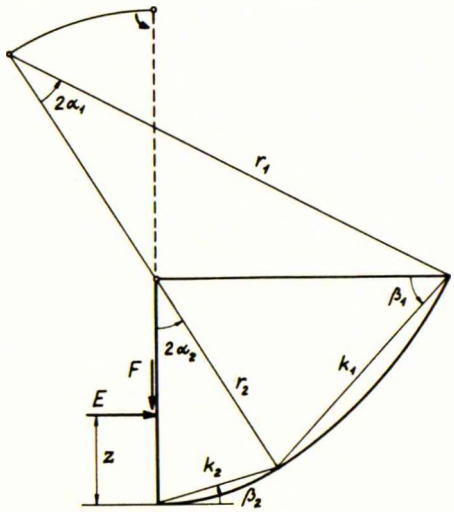

Fig.46B: Rupture PfA for frictionless earth

As an example, we shall consider the following case (Fig.46B) of passive pressure on a rough wall in frictionless earth (rupture PfA):

$$i = j = 0 \qquad p = 0 \qquad \gamma = 0 \qquad \varphi = \delta = 0$$

$$c = a = +1 \qquad h = 1 \qquad \xi = 2.2$$

From Prandtl's investigations (Section 223) it is known that the complete rupture P is as shown in Fig.35B (right). Consequently, we have:

$$\alpha_1^\circ = 0 \qquad \beta_1^\circ = 45^\circ \qquad \alpha_2^\circ = \beta_2^\circ = 22.5^\circ$$

$$r_2^\circ = 1 \qquad h_3^\circ = 0$$

After some trial we find that we must have $\alpha_2 = 16.3^\circ$. With this value 4603 gives $\beta_2 = 16.3^\circ$, whereas 4609 yields:

$$k_2 = 2 \times 1 \times 0.280 = 0.560 \qquad k_2^2 = 0.315$$

As in this case the rupture-line consists of two circles only, we must substitute β_3 and α_3 in 4615 by β_2 and α_2. We get then:

$$\cos(2\alpha_1 + 32.6^\circ) = 0.842 - (1 \times 1 - 0.560 \times 0.280) : 2.2 = 0.459 \qquad \alpha_1 = 15.0^\circ$$

Next, 4607 yields $\beta_1 = 47.6^\circ$, whereas 4610 gives:

$$k_1 = (1 \times 1 - 0.560 \times 0.280) : 0.739 = 1.140 \qquad k_1^2 = 1.300$$

We can now find, by means of 3414, 3350, 3353-54 and 3359, using Table 1 in the Appendix:

$$\sigma_1' = \cot(\beta_1+\alpha_1) = 0.517 \qquad \sigma_1'' = \sigma_2' = t_1^c + \sigma_1' = 1.045 + 0.517 = 1.562$$

$V_1 = 1.140\ (-0.954 \times 0.739 + 0.524 \times 0.673) + 1.140 \times 0.517 \times 0.673 = 0.00$

$H_1 = 1.140\ (\ 0.524 \times 0.739 + 0.954 \times 0.673) + 1.140 \times 0.517 \times 0.739 = 1.61$

$V_2 = 0.560\ (-0.946 \times 0.280 + 0.569 \times 0.959) + 0.560 \times 1.562 \times 0.959 = 1.00$

$H_2 = 0.560\ (\ 0.569 \times 0.280 + 0.946 \times 0.959) + 0.560 \times 1.562 \times 0.280 = 0.84$

$M_{R_1} = 1.300 \times 0.174 = 0.226$ $\qquad$ $M_{R_2} = 0.315 \times 0.188 = 0.059$

We can now show that 4105 is satisfied, as in this case it is reduced to:

$-V_1 - V_2 + ah = 0$ $\qquad$ $-0.00 - 1.00 + 1 \times 1 = 0$

Finally, we get, by means of 4113-14 and 4118:

$\underline{E} = H_1 + H_2 = 1.61 + 0.84 = \underline{2.45} = \varkappa$ $\qquad$ $F = V_1 + V_2 = 0.00 + 1.00 = 1.00 = a$

$Ez = \frac{1}{2}k_2(E \sin \beta_2 + F \cos \beta_2) - M_{R_1} - M_{R_2} + \frac{1}{2}V_1(k_1 \cos \beta_1 + k_2 \cos \beta_2) + \frac{1}{2}hH_1 =$

$0.5 \times 0.560\ (2.45 \times 0.280 + 1.00 \times 0.959) - 0.226 - 0.059 + 0.5 \times 1 \times 1.61 = 0.981$

$\underline{z} = 0.981 : 2.45 = \underline{0.40} = \zeta$

462. w-Ruptures

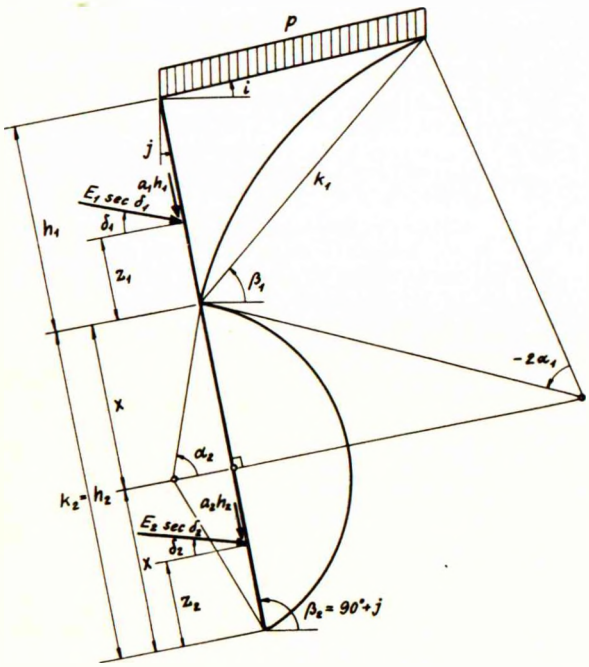

Fig.46C: Calculation of w-rupture

In an ordinary w-rupture the lower zone (subscript 2) is always an A-zone, whereas the upper zone (subscript 1) may be of the type R, P or X. In the last case, the centres of the two circles must be situated at the same normal to the wall (Fig.46C). We must always have $\varphi_1 = -\varphi_2$ and $c_1 = -c_2$. Further, δ_1 and a_1 should be given the same signs as φ_1 and c_1, whereas δ_2 and a_2 should have the same signs as φ_2 and c_2.

When x is given, we have at once $h_2 = k_2 = 2x$ and $h_1 = h - 2x$. The upper zone is now calculated first as an ordinary zone- or line-rupture, in the latter case with a given $\varepsilon_1 = -x : h_1$.

When this is done we can determine the stress t'_2 at the upper point of the lower rupture-line by means of 3428, provided

68

that we know δ_2 and a_2, which we do when $\alpha_2 \neq 90^\circ$. The lower zone is now calculated as a line-rupture with $\xi_2 = \frac{1}{2}$, and $\beta_2 = 90^\circ + j$. The total earth pressure on the wall is given by the equations:

$$E = E_1 + E_2 \qquad F = F_1 + F_2 \qquad Ez = E_1(z_1 + h_2) + E_2 z_2 \qquad 4616\text{-}18$$

Of the special w-ruptures (Section 355) shown in Fig. 35G, rupture wAw is kinematically impossible, whereas wA and wX cannot occur in homogeneous earth, with the exception of wX in the special case of the wall being a tangent to the circle. For the remaining ruptures there must, for kinematical reasons, always be passive pressure in the rupture-line. Finally, the centre of rotation for the wall is, for the ruptures wR and wP, located at the point where the lowest rupture-line meets the wall, whereas for the rupture Aw it is situated at the normal through the centre of the circle.

When x is given, we know, therefore, at once the height of the rupture-zone and can calculate it as an ordinary zone- or line-rupture. The only irregularity is presented by the rupture Aw, because here the rupture-line does not touch the surface but starts at the free earth front. This means that, in using the formulae from Section 342, we should not insert the actual values of i and p for the ground surface, but must put $i = 90^\circ + j$ and $p = 0$, corresponding to the free earth front. Further we have, of course, $\beta = 90^\circ + j$ in this rupture.

Example 46b

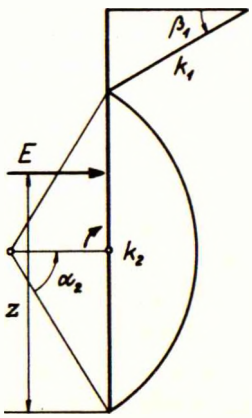

Fig. 46D: Rupture AwR for smooth wall

As an example, we shall consider the following case (Fig. 46D) of a smooth wall (rupture AwR):

$$i = j = 0 \qquad p = c = a = 0 \qquad \varphi_1 = -\varphi_2 = +30^\circ$$

$$\delta = 0 \qquad \gamma = 1 \qquad h = 1 \qquad \xi = 0.4$$

We find at once:

$$k_2 = h_2 = 2 \times 0.4 = 0.8 \qquad h_2^2 = 0.64 \qquad h_2^3 = 0.512$$

$$h_1 = 1 - 0.8 = 0.2 \qquad \beta_2 = 90^\circ \qquad \xi_2 = \tfrac{1}{2}$$

The upper zone is a Rankine-zone corresponding to ordinary passive pressure on a smooth wall (Fig. 22B, right). We have here:

$$\alpha_1 = 0^\circ \qquad \beta_1 = 45^\circ - \tfrac{1}{2}\varphi_1 = 30^\circ \qquad k_1 = 0.2 : 0.5 = 0.4$$

$$E_1 = \tfrac{1}{2}\gamma h_1^2 \tan^2(45^\circ + \tfrac{1}{2}\varphi_1) = 0.5 \times 0.2^2 \times 3 = 0.060 \qquad z_1 = \tfrac{1}{3}h_1 = 0.067$$

As $t_1' = 0$ we get by means of 3339 and 3428:

$$t_1'' = 1 \times 0.4 \times 0.866 = 0.346 \qquad t_2' = -0.346\,\frac{0.866\cos(\alpha_2+60^\circ)}{0.5\sin\alpha_2} = -0.6\,\frac{\cos(\alpha_2+60^\circ)}{\sin\alpha_2}$$

α_2 must be determined by trial, so as to satisfy 4213, which in this case is reduced to the simple form: $G_2 = V_2$. After some trial we find with $\alpha_2 = 58.6^\circ$, using 3223-24, 3325-26 and 3335 as well as Tables 1 and 3 in the Appendix:

$$t_2' = 0.6 \times 0.478 : 0.853 = 0.336$$

$G_2 = 0.64 \times 0.198 = 0.127$ $M_{G_2} = 0.512\ (-\ 0.060 + 0.083) = 0.012$

$V_2 = 0.64\ (0.075 + 0.116 \times 0.866) + 0.336 \times 0.8 \times 0.054 = 0.127$

$H_2 = 0.64\ (0.157 + 0.116 \times 0.5\ ) + 0.336 \times 0.8 \times 0.398 = 0.245$

$M_{R_2} = -\ 0.512 \times 0.039 - 0.336 \times 0.64 \times 0.118 = -\ 0.045$

As we find $G_2 = V_2$, α_2 has been chosen correctly. 4214 and 4216 give then:

$E_2 = 0.245$ $E_2 z_2 = 0.5 \times 0.8 \times 0.245 + 0.045 - 0.012 = 0.131$

Finally, we get by means of 4616 and 4618:

$$\underline{E} = 0.060 + 0.245 = \underline{0.305} = \tfrac{1}{2}\lambda$$

$Ez = 0.060\ (0.067 + 0.8) + 0.131 = 0.183$ $\underline{z} = 0.183 : 0.305 = \underline{0.60} = \eta$

463. s-Ruptures

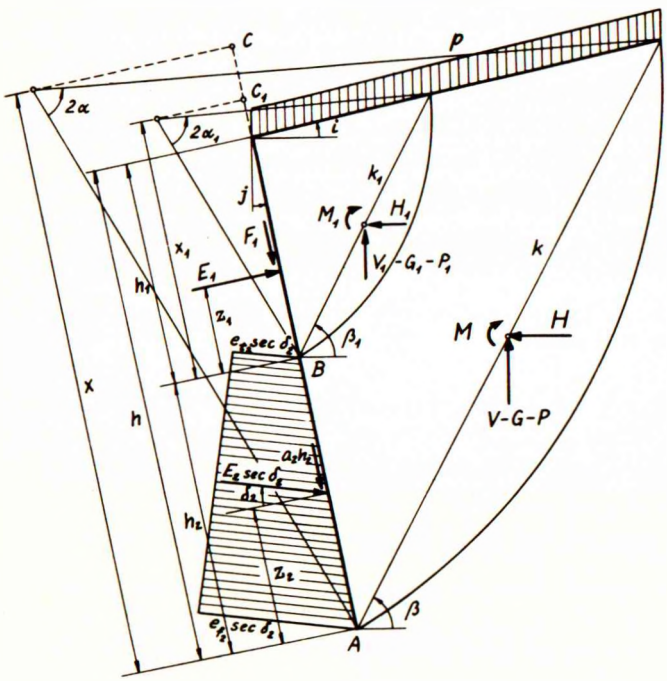

Fig.46E: Calculation of s-rupture

With two exceptions, which shall be mentioned later, the calculation of an s-rupture (Fig.46E) is only possible, when the heights h_1 and h_2 are given.

With the same exceptions it is kinematically necessary that the wall is provided with a hinge (actual or yield) between the two parts.

We shall first consider the simple case of an LsZ-rupture. The upper zone is calculated first as an ordinary zone-rupture. When this has been done we can calculate the whole rupture in principle as an ordinary line-rupture with a given $\xi = x:h$. The only difference is that the upper part of the earth front is acted upon by the known forces E_1 and F_1. Equation 4204 is in this case extended to:

$$E_1 \sin\delta_2 - (F_1 + a_2h_2)\cos\delta_2 - H\sin(\delta_2 - j) + (V-G-P)\cos(\delta_2 - j) = 0 \qquad 4619$$

This equation, together with 4202, determines α and β for the lowest rupture-line. If we find $\beta - \alpha - j < 0$, we must use 4205-06 instead. E, F and z (for the whole wall) are calculated by means of 4207-09, after which E_2, F_2 and z_2 (for the lower part only) can be found from 4616-18.

As regards the deformations, the rotation centre for the lower part of the wall must be located at the normal to the wall through the centre of the lower circle, i.e. for "normal" rotations at point C (Fig. 46E). The rotation centre for the upper part can be located anywhere between C and point B, where the upper circle meets the wall. It is here presumed that there is passive pressure in the one circle and active pressure in the other; if there is either passive or active pressure in both circles, the rotation centre for the upper part can be located anywhere except between points B and C.

Next, we shall investigate a ZsL-rupture, which is considerably more complicated. In this case we do not know the shape of the lower rupture-line nor that of the upper one, but if these were known we could calculate the total earth pressures E_1 and F_1 on the upper part as well as the unit pressures e_{t_2} and e_{f_2} at the top and foot of the lower part. We shall here as an approximation assume each of the mentioned rupture-lines to consist of one circle and we shall, moreover, assume a linear variation between e_{t_2} and e_{f_2}, which means that E_2 and z_2 are given by 4301-02 (with subscript 2).

Under these assumptions, the problem is soluble if the location of the upper pressure centre z_1 is given. The two parameters of the upper circle (α_1, β_1) can then be found as for a line-rupture with a given z, i.e. usually by means of 4108 and 4204. Those of the lower circle (α, β) can, after this, be determined by means of 4619 and the following equation, which corresponds to 4306:

$$E_1(z_1 - z_2 + h_2) + H(z_2 \cos j - \tfrac{1}{2}k \sin \beta) - (V-G-P)(z_2 \sin j + \tfrac{1}{2}k \cos \beta) + M_R + M_G + M_P = 0 \qquad 4620$$

From 4619-20 we must find α and β by trial. We estimate a value of α, find the corresponding β from 4619 and investigate whether 4620 is satisfied. If not, α must be changed and the calculation repeated. In the case of active pressure a very good approximation is obtained by assuming a straight lower rupture-line, in which case we disregard 4620 and find β from 4619 with $\alpha = 0$; for homogeneous earth, this gives the same β and e_{f_2} as found in Coulomb's theory.

When α and β have been determined, E_2 and z_2 must be found from 4301-02, as otherwise serious errors may be introduced. E, F and z for the whole wall are calculated finally by means of 4616-18.

As regards the deformations, the rotation centre for the lower part of the wall may, as described in Section 433, be located within a certain interval below the foot of the wall (passive pressure) and possibly also in an interval above the top of the wall (active pressure). The limits of these intervals, as well as the actual location of the rotation centre for the upper part, cannot be indicated without a detailed investigation of the deformations in the plastic zone.

Such an investigation is, strictly speaking, also necessary if we are to calculate a rupture ZsL with a given rotation centre for the upper part. In order to circumvent this difficulty, we shall assume that the upper rotation centre is situated at point C_1 (Fig. 46E), but this is evidently an approximation only.

Under this assumption we calculate first the two parameters of the upper circle (α_1, β_1) as for a line-rupture with a given $\xi_1 = x_1 : h_1$, i.e. usually by means of 4202 and 4204. Those of the lower circle (α, β) are then found from 4619-20, after which 4301-02 give E_2 and z_2, whereas 4616-18 yield E, F and z.

Example 46c

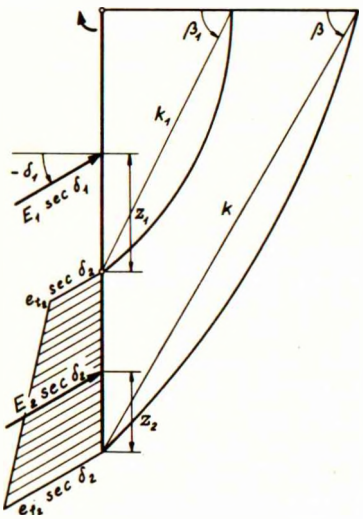

Fig. 46F: Rupture PsA for rough wall

As an example, we shall consider the following case (Fig. 46F) of active pressure on a rough wall, in which a yield hinge has developed (rupture PsA):

$$i = j = 0 \qquad p = c = a = 0 \qquad \varphi = \varphi_1 = \delta_1 = \delta_2 = -30^\circ$$

$$\gamma = 1 \qquad h = 1.7 \qquad h_1 = 1 \qquad h_2 = 0.7 \qquad \xi_1 = 1$$

The rupture A corresponding to the upper zone has been calculated in Example 42a, where we have found:

$$\alpha_1 = 26.5^\circ \qquad \beta_1 = 63.5^\circ \qquad k_1 = 1.117$$

$$E_1 = 0.142 \qquad F_1 = -0.082 \qquad z_1 = 0.45$$

e_{t_2} is then determined by means of 3318 (with $t_1' = 0$) and 3423, using also Table 3 in the Appendix:

$$t_1'' = 1.117\ (0.506 \times 0.895 - 0.350 \times 0.446) = 0.332$$

$$e_{t_2} = 0.332 \times 0.866 \times 0.799 : 0.920 = 0.250$$

As regards the circle bounding the lower zone, α and β should satisfy 4619-20, which in this case are reduced to:

$$V - G - H \tan\delta = 0 \qquad E_1(z_1 - z_2 + h_2) + H(z_2 - \tfrac{1}{2}h) - \tfrac{1}{2}h(V-G)\cot\beta + M_R + M_G = 0$$

The former of these give, after insertion of 3223 and 3325-26:

$$(V^{YX} - \tfrac{1}{4}\cos 2\varphi)\sin(2\beta + 2\varphi) + (-H^{Yy}\tan\delta + \tfrac{1}{4}\sin 2\varphi)\cos(2\beta + 2\varphi) + (V^{YZ} - H^{YZ}\tan\delta - G^{YZ}) = 0$$

After some trial we find with $\alpha = 15.0^\circ$, using Tables 1 and 3 in the Appendix:

$$(0.206 - 0.25 \times 0.5)\sin(2\beta - 60^\circ) + (-0.206 \times 0.577 - 0.25 \times 0.866)\cos(2\beta - 60^\circ)$$
$$+ (0.033 + 0.207 \times 0.577 - 0.044) = 0.081\sin(2\beta - 60^\circ) - 0.335\cos(2\beta - 60^\circ) + 0.109 = 0$$

which, with the aid of 3406-07, yields $\beta = 59.0^\circ$. With this value we find:

$$k = 1.7 : 0.857 = 1.98 \qquad k^2 = 3.94 \qquad k^3 = 7.80$$

We get now, by means of 3318, 3423 and 4301-02 (with subscript 2):

$$t'' = 1.98\ (0.640 \times 0.857 - 0.392 \times 0.515) = 0.685$$

$e_{f_2} = 0.685 \times 0.866 \times 0.719 : 0.960 = 0.445$ $\underline{E_2} = 0.5 \times 0.7\ (0.445 + 0.250) = \underline{0.243}$

$E_2 z_2 = 0.167 \times 0.7^2 (0.445 + 2 \times 0.250) = 0.077$ $\underline{z_2} = 0.077 : 0.243 = \underline{0.32}$

Further we find, using 3223-24, 3325-26 and 3335:

$$G = 3.94\ (0.044 + 0.25 \times 0.883) = 1.04$$

$$M_G = 7.80\ (-0.082 \times 0.857 + 0.083 \times 0.857^3) = -0.14$$

$$V = 3.94\ (0.033 + 0.206 \times 0.848) = 0.82$$

$$H = 3.94\ (0.207 - 0.206 \times 0.530) = 0.39$$

$$M_R = 7.80\ (0.029 \times 0.857 - 0.020 \times 0.515) = 0.12$$

We can now show that 4620, as indicated above, is satisfied:

$$0.142\ (0.45 - 0.32 + 0.7) + 0.39\ (0.32 - 0.5 \times 1.7)$$
$$- 0.5 \times 1.7\ (0.82 - 1.04)\ 0.601 + 0.12 - 0.14 = 0$$

If we had put $\alpha = 0$, 4619 would have given $\beta = 54.4^\circ$ (the Coulomb value). To this would correspond $e_{f_2} = 1.7 \times 0.257 = 0.437$, which deviates only slightly from the value found above (0.445).

There are two special cases, in which the location of the rotation centre (for a rigid wall) and the heights h_1 and h_2 are not given, but are found by the calculation proper. Both cases concern earth with cohesion, allowing part of the earth front to stand unsupported, while the wall moves away from it.

The first of these cases concerns the rupture ZsL with an unsupported upper earth front. We have then $E_1 = F_1 = 0$, in which case the equations 4207-09 give:

$$H_1 = 0 \qquad V_1 - G_1 - P_1 = 0 \qquad M_{R_1} + M_{G_1} + M_{P_1} = 0 \qquad 4621\text{-}23$$

From these equations it is possible to find α_1, β_1 and k_1. The plastic zone is then calculated as described above. The rotation centre for the rigid wall can be located in the usual intervals found for a zone-rupture (compare Section 433).

The second case concerns the rupture LsZ with an unsupported lower earth front. We have then $E_2 = F_2 = 0$, in which case equations 4207-09 and 4616-18 give:

$$E_1 - H \cos j + (V-G-P) \sin j = 0 \qquad F_1 - H \sin j - (V-G-P) \cos j = 0 \qquad 4624\text{-}25$$

$$E_1 (z_1 + h_2) - \tfrac{1}{2} k \left[E_1 \sin(\beta - j) + F_1 \cos(\beta - j) \right] + M_R + M_G + M_P = 0 \qquad 4626$$

In general, we must start by estimating a value of h_1 and calculating the corresponding values of E_1, F_1 and z_1 as for an ordinary zone-rupture. α and β for the line-rupture are then found from 4624-25 and it is finally investigated whether 4626 is satisfied. If not, h_1 must be changed and the calculation repeated. The rotation centre for the rigid wall can be located anywhere between the points B and C (Fig. 46E).

47. EARTH PRESSURE DISTRIBUTION

471. Introduction

As already pointed out in several instances, we can calculate the unit earth pressure e at any point, where a rupture-line meets the wall, but not at any other point.

In a zone-rupture, a rupture-line meets the wall at any point and we can, therefore, in principle, determine the earth pressure distribution completely. In practice, we usually calculate e_f (at the foot) and e_t (at the top) only and assume a linear variation.

For e_d (at an arbitrary depth d) we have the formal equation 4122, and, by means of 3318 and the boundary conditions, it will be possible to determine the constants λ_d, ρ_d and κ_d in any given case. However, as these constants are functions of the geometrical parameters which, in turn, depend upon the ratio p : c : γh, the said constants will vary with this ratio. This means that the law of superposition is usually not valid in earth pressure calculations.

In a line-rupture only one rupture-line meets the wall, viz. at the foot. Although we can thus calculate e_f, this is of no great advantage, as we cannot find e at any other point. The same difficulty exists in most composite ruptures, at least for a part of the wall. We know, however, the total earth pressure E and the height z of its pressure centre.

For E and Ez, we have the formal equations 4119-20, and by means of two suitable equilibrium conditions, it will be possible to determine the 6 constants λ, ρ, κ, η, θ and ζ in any given case. However, for the same reasons as given above, these constants will vary with the ratio p : c : γh, and even for a given ratio the solution is not unique, because other equilibrium conditions will give a different set of constants. Therefore, we know actually only E and z (as well as e_f).

As long as we are concerned only with the stability of a structure, we need not know the distribution of the earth pressure, but if we are to investigate the stresses in the structure proper, we must know the earth pressure distribution, at least approximately.

Although this problem cannot be solved by means of the plasticity theory, we shall in the following indicate a simple, tentative pressure distribution, which may be used as an approximation in the absence of more exact information.

472. Signs for Rotations and Shear Constants

In Section 331 (p. 58) we have defined the concepts of passive and active pressure in a rupture-line and have decided to use positive values of φ and c for passive pressure and negative values for active pressure.

In the case of a line-rupture, a zone-rupture, or a composite f-rupture, we have either passive or active pressure in the whole rupture-line. Therefore, in these cases we can also speak of passive or active pressure on the wall without giving rise to any misunderstanding.

However, in the case of a composite a- or w-rupture, we have passive pressure in one part of the rupture-line and active pressure in another. Consequently, we cannot speak of passive or active earth pressure on the whole wall in these cases.

Instead, we shall introduce a new concept, viz. positive or negative rotation of the wall. A positive rotation is one in which the angle (through the earth) between the wall and the original ground surface is increased. In a negative rotation this angle is decreased. Further we decide that c, when used in equations such as 4119-25, should always be assumed positive.

473. Pressure Diagrams for Rigid Walls

A general earth pressure diagram must, of course, fulfil the condition that, in the limiting cases of passive and active zone-ruptures respectively, the correct pressure distributions are obtained. For these zone-ruptures we have, respectively:

$$e_d^p = \gamma d\lambda^p + p\rho^p + c\kappa^p = \gamma d\lambda^p + e_t^p \qquad 4701$$

$$e_d^a = \gamma d\lambda^a + p\rho^a + c\kappa^a = \gamma d\lambda^a + e_t^a \qquad 4702$$

Further, the area of the normal pressure diagram must be equal to E, and its pressure centre must be located at the height z above the foot of the wall. As previously mentioned, we also know the actual e_f, but it would not make the pressure diagram as a whole appreciably more correct to compel it to give the correct value of e_f, and it is much simpler to disregard this requirement.

Consequently, the pressure diagram should involve 2 variables only. The simplest diagram, which fulfils this requirement and conforms also to both limiting cases, is the one shown in Fig.47A for positive rotation (left) and negative rotation (right). The wall is shown vertical, but may as well be inclined.

The pressure diagram is constructed as follows: First we draw two straight lines corresponding to the passive and active zone-ruptures respectively, and intersecting each other at a point 0.

Now, a pressure jump is assumed to occur at a height $y = \omega h$ above the foot of the wall. Above this point we have , as a rule, ordinary passive pressure $e^x = e^p$ (positive rotation) or active pressure $e^x = e^a$ (negative rotation). Below the point we have a kind of active pressure e^y (positive rotation) or passive pressure e^y (negative rotation), varying in such a way that the corresponding contour line of the diagram passes through point 0. Thus we have, above and below the pressure jump respectively:

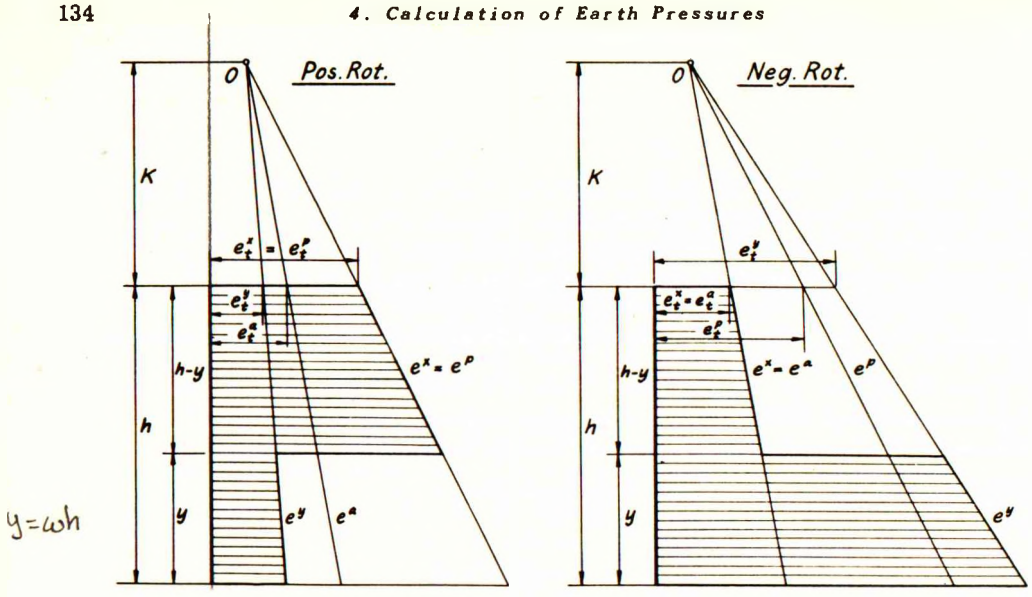

Fig.47A: Tentative earth pressure diagrams for rigid walls

$$e_d^x = \gamma d\lambda^x + p\rho^x + c\kappa^x = \gamma d\lambda^x + e_t^x \qquad 4703$$

$$e_d^y = \gamma d\lambda^y + p\rho^y + c\kappa^y = \gamma d\lambda^y + e_t^y \qquad 4704$$

where λ^x, ρ^x, κ^x and e_t^x are usually identical with λ^p, ρ^p, κ^p and e_t^p in the case of positive rotation, and with λ^a, ρ^a, κ^a and e_t^a in the case of negative rotation. (An exception is made in Section 511, however).

Point 0 is situated at a height K above the top of the wall, determined by:

$$K = \frac{e_t^p - e_t^a}{\gamma\,(\lambda^p - \lambda^a)} = \frac{e_t^x - e_t^y}{\gamma\,(\lambda^x - \lambda^y)} \qquad 4705$$

As the pressure diagram should give the correct values of E and z, we must have:

$$E = he_t^y + (h-y)(e_t^x - e_t^y) + \tfrac{1}{2}\gamma h^2\lambda^y + \tfrac{1}{2}\gamma(h-y)^2(\lambda^x - \lambda^y) \qquad 4706$$

$$Ez = \tfrac{1}{2}h^2e_t^y + \tfrac{1}{2}(h^2-y^2)(e_t^x - e_t^y) + \tfrac{1}{6}\gamma h^3\lambda^y + \tfrac{1}{6}\gamma(h-y)^2(h+2y)(\lambda^x - \lambda^y) \qquad 4707$$

Eliminating e_t^y and λ^y from 4705-07, we can find the following second-degree equation in the unknown quantity h - y + K:

$$(h-y+K)^2 + \tfrac{1}{2}(h-y+K+h+K)\,\frac{E(3z-h-K) - he_t^x(\frac{1}{2}h-K) + \frac{1}{2}\gamma h^2\lambda^x K}{E - he_t^x - \frac{1}{2}\gamma h^2\lambda^x} = 0 \qquad 4708$$

When y has been found from 4708, we can calculate λ^y by means of 4705-06 (eliminating e_t^y) and, finally, e_t^y by means of 4705:

$$\lambda^y = \lambda^x + \frac{E - he_t^x - \frac{1}{2}\gamma h^2\lambda^x}{\gamma y\ (h - \frac{1}{2}y + K)} \qquad e_t^y = e_t^x + \gamma K\ (\lambda^y - \lambda^x) \qquad 4709\text{-}10$$

In the special cases $\gamma = 0$ or $\lambda^p = \lambda^a$ the preceding formulae cannot be used direct, because 4705 gives $K = \infty$. However, as point 0 is infinitely distant, we must have: $\lambda^x = \lambda^y = \lambda^p = \lambda^a$. Further we find, from 4706-07:

$$y = \frac{2Ez - h^2e_t^x - \frac{1}{3}\gamma h^3\lambda^x}{E - he_t^x - \frac{1}{2}\gamma h^2\lambda^x} \qquad e_t^y = e_t^x + \frac{1}{y}(E - he_t^x - \frac{1}{2}\gamma h^2\lambda^x) \qquad 4711\text{-}12$$

A pressure diagram of the proposed type can be determined for most of the simple ruptures, such as R, P, A, AaR, AaP, AwR and PfA, which are most commonly used. However, for some other ruptures (e.g. X, XfP and AwXfP) it cannot always be used, as 4708 may give values of y outside the possible interval $0 \leq y \leq h$.

Example 47a

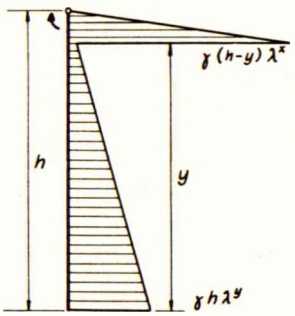

Fig.47B: Pressure diagram for rough, rigid wall

In Example 42a we have found, for a case of positive rotation of a rough wall (rupture A): $E = 0.142$ and $Ez = 0.064$.

The corresponding passive zone-rupture has been calculated in Example 43a, where we have found $\lambda^p = 5.61$ and $e_t^p = 0$. We have not calculated λ^a, but we know that $e_t^a = 0$. With these values 4705 gives $K = 0$, and we have: $\lambda^x = 5.61$, $e_t^x = e_t^y = 0$.

For $\gamma = 1$ and $h = 1$ we find, from 4708-09:

$$(1-y)^2 + \tfrac{1}{2}(1-y+1)\,\frac{3 \times 0.064 - 0.142}{0.142 - 0.5 \times 5.61} =$$

$$(1-y)^2 - 0.010\ (1-y) - 0.010 = 0 \qquad y = 0.895$$

$$\lambda^y = 5.61 + \frac{0.142 - 0.5 \times 5.61}{0.895\ (1 - 0.5 \times 0.895)} = 0.22$$

The corresponding pressure diagram is shown to scale in Fig.47B.

474. Pressure Diagrams for Hinged Walls

When a yield hinge develops in a wall, the rupture-figure will usually be of the s-type, and in that case the tentative pressure diagrams described above must be modified somewhat.

We shall first consider a rupture LsZ (Fig.47C). Above the hinge we have ordinary passive or active pressure, and below the hinge, a pressure diagram similar to the one described in Section 473. The latter diagram, which should correspond to E_2 and z_2, is determined by means of the formulae 4705 and 4708-10 (or in special cases 4711-12) with subscripts 2. The pressures e_{t_2} should, of course, correspond to the depth h_1 below the ground surface.

Another method of solving this problem approximately, will be to assume the ground surface to pass through the hinge but to retain its correct slope. The weight of the earth above this imaginary surface is then considered as an additional surcharge. In this case the pressure diagram for the lower part is determined as for an ordinary rigid wall with height h_2.

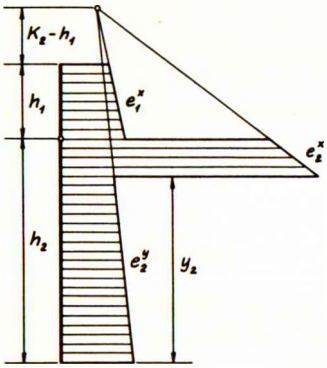

Fig.47C: Pressure diagram for rupture LsZ

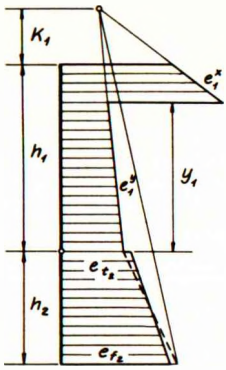

Fig.47D: Pressure diagram for rupture ZsL

Turning now to the rupture ZsL (Figs. 46E and 47D) it is evident that the pressure diagram for the upper part should be determined as for an ordinary rigid wall with the height h_1. As regards the lower part, we have shown in Section 463, how the actual pressures e_{t_2} and e_{f_2} can be calculated.

However, we shall now indicate a much simpler method of determining the pressures on the lower part with sufficient accuracy. We simply assume e_{t_2} to be equal to $e^y_{f_1}$ for the upper part, and further e_{f_2} to be equal to the corresponding value for a complete zone-rupture. Between these values a linear variation is assumed (the dotted line in Fig. 47D).

Example 47b

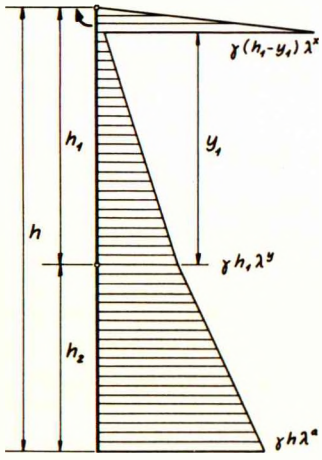

Fig.47E: Pressure diagram for rough, hinged wall

In Example 46c, we have found, for a case of a rough wall with a yield hinge (rupture PsA): $E_2 = 0.243$ and $z_2 = 0.32$.

The upper part of the wall has been calculated in Example 42a, and the corresponding pressure distribution has been determined in Example 47a, where we have found $\lambda^y = 0.22$. Consequently we have, as $\gamma = 1$ and $h_1 = 1$:

$$e_{t_2} = e^y_{f_1} = 0.22 \times 1 \times 1 = 0.22$$

The complete active zone-rupture for a rough wall has not yet been calculated but, as shall be shown in Section 523, we find for $\varphi = \delta = -30^\circ$ the value $\lambda^a = 0.266$. This gives, as $h = 1.7$:

$$e_{f_2} = 0.266 \times 1 \times 1.7 = 0.45$$

For the total earth pressure on the lower part of the wall, we find:

$$\underline{E_2} = 0.5 \times 0.7\,(0.45 + 0.22) = \underline{0.235}$$

$$E_2 z_2 = 0.167 \times 0.7^2 (0.45 + 2 \times 0.22) = 0.073$$

$$\underline{z_2} = 0.073 : 0.235 = \underline{0.31}$$

which is a sufficiently close approximation. The pressure diagram is shown to scale in Fig. 47E.

5. THE SIMPLEST CASES

51. MAIN CASES AND MODEL TESTS

511. Most Important Cases

In the present Section 5 we shall consider exclusively the simple but important special case of a vertical wall ($j = 0$) and a horizontal surface ($i = 0$). Further, we shall take $h = 1$, in which case we will have $x = \xi$ and $y = \omega$.

The main object of the investigation is to determine the earth pressure on the wall for any possible location of the rotation centre. With regard to the relative roughness of the wall we shall consider the two extreme cases of a perfectly smooth wall ($\delta = 0$, $a = 0$) and a perfectly rough wall ($\delta = \varphi$, $a = c$). In the latter case we shall, however, consider "normal" rotations only, i.e. rotation centres located at the wall proper or its extensions.

In the general case the earth has a friction angle φ, a cohesion c, an effective unit weight γ and a surcharge p. However, we shall here consider the following special cases separately:

1) Frictionless Earth ($\varphi = 0$, $c = 1$, $\gamma = 0$, $p = 0$). From 4119-21 it will be seen that we have then $E = \kappa$, $z = \zeta$ and $F = a$.

2) Weightless Earth ($\varphi \neq 0$, $c = 0$, $\gamma = 0$, $p = 1$). From 4119-21 it will be seen that we have then $E = \rho$, $z = \overset{\circ}{\theta}$ and $F = \rho \tan \delta^{p}$.

3) Cohesionless, Unloaded Earth ($\varphi \neq 0$, $c = 0$, $\gamma = 1$, $p = 0$). From 4119-21 it will be seen that we have then $E = \frac{1}{2}\lambda$, $z = \eta$ and $F = \frac{1}{2}\lambda \tan \delta^{\gamma}$.

All formulae shall be developed so that they can be used in principle for any value of φ, but in the numerical calculations in this section we shall consider mainly the special values $\varphi = 0^{\circ}$ and $\varphi = 30^{\circ}$, for which the Tables in the Appendix can be used. The results of the calculations for $\varphi = 0^{\circ}$ and $\varphi = 30^{\circ}$ are recorded on Graphs 1-6 and 7-18 respectively in the Appendix, but, by means of Graphs 19-20, these results can also be used approximately for other friction angles.

Although in a theory of plasticity the law of superposition is, strictly speaking, not valid except in special cases, it shall be shown later that a very good approximation will generally be obtained by assuming this law to be valid. Thus, for $i = j = 0$, the case of frictionless earth may be superposed on a case of "hydrostatic" pressure, and the cases of weightless earth and cohesionless,

unloaded earth may be superposed on each other when the friction angle is the same.

In order to facilitate such superpositions in practice, it is convenient to have the same ω for weightless earth as for cohesionless, unloaded earth. Therefore, whereas in the latter case we assume (as described in Section 47) λ^x to be given and determine ω and λ^y, for weightless earth we shall assume ω to be given (as the value obtained for cohesionless, unloaded earth with the same ξ) and determine ρ^x and ρ^y.

For cohesionless, unloaded earth we have $e_t = 0$ and $K = 0$ (see 4705), and find then from 4708-09 the following equations, the first of which is a second-degree equation in $1 - \omega$:

$$(1 - \omega)^2 + (1 - \omega + 1)\frac{\lambda\,(3\eta - 1)}{2\,(\lambda - \lambda^x)} = 0 \qquad \lambda^y = \lambda^x + \frac{\lambda - \lambda^x}{\omega\,(2 - \omega)} \qquad 5101\text{-}02$$

For weightless earth we have $\gamma = 0$, $e_t^x = \rho^x$ and $e_t^y = \rho^y$ and find then from 4706-07:

$$\rho^x = \rho\,\frac{2\theta - \omega}{1 - \omega} \qquad \rho^y = \rho\,\frac{1 + \omega - 2\theta}{\omega} \qquad 5103\text{-}04$$

Finally, for frictionless earth we have $\gamma = 0$, $e_t^x = \varkappa^x$ and $e_t^y = \varkappa^y$ and find then from 4711-12:

$$\omega^\circ = \frac{2\varkappa\zeta - \varkappa^x}{\varkappa - \varkappa^x} \qquad \varkappa^y = \varkappa^x + \frac{\varkappa - \varkappa^x}{\omega} \qquad 5105\text{-}06$$

512. Small-Scale Model Tests

In order to study the shape of actual rupture-figures in sand, the author carried out a number of small-scale model tests in an apparatus devised for this purpose.

The wall was 15 cm wide and 15 cm high. Two different walls were used, one of polished glass and one of aluminium with the back covered with sandpaper. The latter can be considered perfectly rough, but the former is far from being perfectly smooth. Both walls were so rigid that their elastic deformations may be disregarded.

The earth was clean, dry sand in a rather loose state ($\gamma = 1.6$ t/m^3) as no attempt was made to compact it. It contained grains up to 2 mm, but the main part of the grains were smaller than 0.5 mm. Its friction angle in the loose state was about 32° (measured as the angle of repose), and it possessed no cohesion.

In all the tests the ground surface was horizontal and the wall vertical (in the middle of the test). The following procedure was used: A rotation centre was fixed and the wall was given a slow continuous rotation about the corresponding horizontal axis. The sand-papered wall was prevented from rising vertically, whereas the glass wall was allowed to rise freely.

During the rotation the movements of the sand grains were recorded on a photographic plate, but the exposure was not commenced until a state of rupture had developed in the earth. This procedure was chosen in order to record, as far as possible, only the plastic deformations and not the elastic ones.

A number of such photographs are reproduced in the following sections. The rotation centre is indicated by a small circle, and the direction of the rotation by arrows. Two arrows and no rotation centre indicate a translation.

In a few cases, tests were made with an aluminium wall provided with a horizontal hinge in the centre. The upper and lower free edges were kept in position, while the hinge was moved outwards or inwards.

Originally, provisions were made for measuring the total earth pressure on the wall (in two horizontal lines), but this was given up, as too large errors were introduced through the friction against the side walls of the rather narrow test box. However, this side friction did not greatly influence the shape of the rupture-figure, as the distance from the wall to the point where the lowest rupture-line met the ground surface, was only slightly smaller at the side walls than in the middle of the box.

It has been deliberated whether or not to show in the photographs the theoretical rupture-lines as determined by the following calculations. However, as these calculations are made for $\varphi = 30^\circ$ and perfectly rough or smooth walls only, whereas the actual friction angle in the tests was 32° and the glass wall, at least, was neither perfectly rough nor smooth, the author decided to let the photographs speak for themselves.

52. RUPTURES R AND P

521. Frictionless Earth

With $\varphi = \delta = \gamma = p = 0$, $h = 1$ and $c = 1$, we find from 4315 and 3350-51:

$$\sigma_1' = 1 \qquad \sigma_N'' = 1 + 2\,(v_1' - v_N'') \qquad 5201\text{-}02$$

For the rupture R (smooth wall) we get, by means of 4312-13, 4316 and 4301-02:

$$\kappa_S = 2 \qquad \zeta_S = \tfrac{1}{2} \qquad 5203\text{-}04$$

For the rupture P (rough wall) we get, by means of 4312, 4314, 4317 and 4301-02:

$$\kappa_r = 1 + \tfrac{1}{2}\pi = 2.57 \qquad \zeta_r = \tfrac{1}{2} \qquad 5205\text{-}06$$

As explained in Section 433, the wall can rotate about any point below its foot.

522. Weightless Earth

With $\gamma = c = a = 0$, $h = 1$ and $p = 1$ we find from 4315 and 3318-19:

$$t'_1 = \tan(45^\circ + \tfrac{1}{2}\varphi) \qquad t''_N = e^{2\mu(v'_1 - v''_N)} \tan(45^\circ + \tfrac{1}{2}\varphi) \qquad 5207\text{-}08$$

For the rupture R (smooth wall) we get, by means of 4312-13, 4316 and 4301-02:

$$\rho_S = \tan^2(45^\circ + \tfrac{1}{2}\varphi) \qquad \theta_S = \tfrac{1}{2} \qquad 5209\text{-}10$$

For the rupture P (rough wall) we get, by means of 4312, 4314, 4317 and 4301-02:

$$\rho_r = e^{\mu(\frac{1}{2}\pi + \varphi)} \cos\varphi \, \tan(45^\circ + \tfrac{1}{2}\varphi) \qquad \theta_r = \tfrac{1}{2} \qquad 5211\text{-}12$$

Values of ρ for different friction angles are given in a table in Section 523.

The possible locations of the rotation centre have been discussed in Section 433. We shall here, as an approximation, assume that the active ruptures R and P, as well as the passive rupture R, will occur for any rotation centre below the foot of the wall, whereas the passive rupture P will occur only for $\xi = 0$.

523. Cohesionless, Unloaded Earth

With $p = c = a = 0$, $h = 1$ and $\gamma = 1$, we find from 4315 that $t'_1 = 0$.

We shall first consider the rupture R (smooth wall). 4312-13 show that one straight rupture-line satisfies all the statical boundary conditions. Therefore we have:

$$\alpha = 0^\circ \qquad \beta = 45^\circ - \tfrac{1}{2}\varphi \qquad k = 1 : \sin\beta \qquad 5213\text{-}15$$

With these values 3318, 4316 and 4301-02 yield:

$$\lambda_S = \tan^2(45^\circ + \tfrac{1}{2}\varphi) = \rho_S \qquad \eta_S = \tfrac{1}{3} \qquad 5216\text{-}17$$

The correctness of this result should be checked by investigating whether the equilibrium conditions 4319-21 are satisfied, but it will be found that this condition is fulfilled in the present case.

The rupture P (rough wall) can be calculated very accurately by approximating the lowest rupture-line by means of 1 straight line and 2 circles (Fig. 52A). By means of 4307-10, 4312 and 4314 we find:

$$\alpha_1 = 0^\circ \qquad \alpha_2 = \alpha_3 = 11.25^\circ + \tfrac{1}{8}\varphi \qquad 5218\text{-}19$$

$$\beta_1 = 45^\circ - \tfrac{1}{2}\varphi \qquad \beta_2 = 33.75^\circ - \tfrac{5}{8}\varphi \qquad \beta_3 = 11.25^\circ - \tfrac{7}{8}\varphi \qquad 5220\text{-}22$$

The unknown quantities are k_1, k_2 and k_3, and for their determination we have the equations 4318-20. The solution is obtained in the following way:

First, 4318 is used to eliminate k_1 from 4319-20, leaving two second-degree equations in k_2 and k_3. They are solved by eliminating the second power of k_3, obtaining thus a first-degree-equation in k_3. Finally, this is used to eliminate k_3 from one of the equations, giving a fourth-degree-equation in k_2 alone. When k_1, k_2 and k_3 have been determined, $e = \lambda$ is found by means of 3318 and 4317.

Example 52a

With $\varphi = +30^\circ$ (passive pressure) a calculation as outlined above has given the following results:

$\alpha_1 = 0^\circ$ $\beta_1 = 30^\circ$ $\alpha_2 = \alpha_3 = \beta_2 = -\beta_3 = 15^\circ$

$k_1 = 1.581$ $k_2 = 1.025$ $k_3 = 0.215$ $\lambda_r^p = 5.66$ $\eta_r^p = \frac{1}{3}$

A check is obtained by calculating $\dot{z} = \eta$ by means of 4321, which gives $\eta = 0.339$. Fig. 52A (left) is drawn to scale corresponding to $\varphi = +30^\circ$.

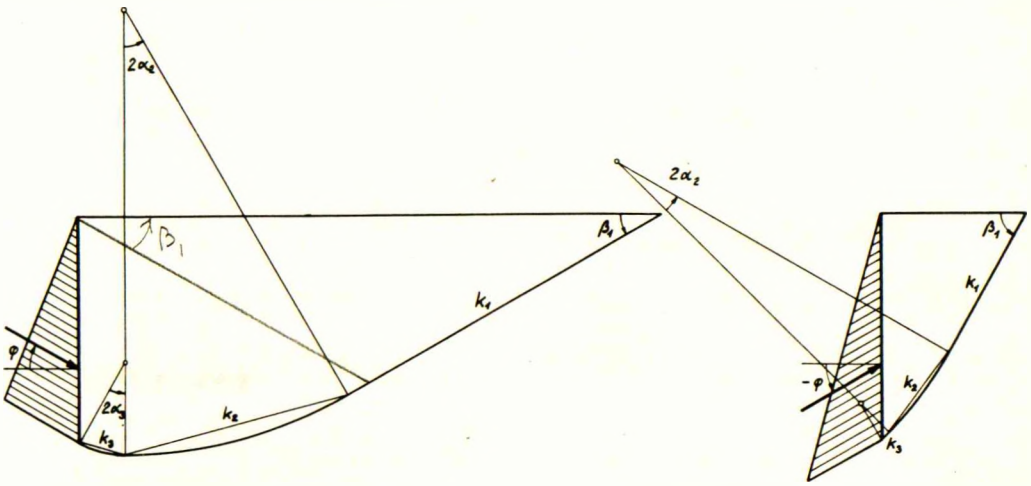

Fig. 52A: Calculation of passive and active P-ruptures

With $\varphi = -30^\circ$ (active pressure) a corresponding calculation has given:

$\alpha_1 = 0^\circ$ $\alpha_2 = \alpha_3 = 7.5^\circ$ $\beta_1 = 60^\circ$ $\beta_2 = 52.5^\circ$ $\beta_3 = 37.5^\circ$

$k_1 = 0.720$ $k_2 = 0.441$ $k_3 = 0.045$ $\lambda_r^a = 0.266$ $\eta_r^a = \frac{1}{3}$

By means of 4321, we find $\eta = 0.333$ which is exact. Fig. 52A (right) is drawn to scale corresponding to $\varphi = -30^\circ$.

For λ_r no simple, exact formula can be indicated, such as 5211 for ρ_r. However, the author has developed the following simple, empirical formula:

$$\lambda_r = \rho_r + 0.007\,(e^{9 \sin \varphi} - 1) \qquad \eta_r = \tfrac{1}{3} \qquad 5223\text{-}24$$

As all other formulae in Sections 522-23, equation 5223 is valid for passive pressures with a positive φ, and for active pressures with a negative φ. It involves errors of less than $\frac{1}{2}\%$ and is thus considerably more accurate than the empirical formula developed by Kerisel (1939), quite apart from the fact that the Kerisel formula can be used for passive pressures only. 5223 may also be used for an imperfectly rough wall when φ is substituted by δ.

In the following table some values of ρ_s (5209), ρ_r (5211), λ_s (5216) and λ_r (5223) are indicated:

φ	$\rho_s^p = \lambda_s^p$	$\rho_s^a = \lambda_s^a$	ρ_r^p	ρ_r^a	λ_r^p	λ_r^a
0	1.00	1.000	1.00	1.000	1.00	1.000
5	1.19	0.840	1.26	0.802	1.27	0.798
10	1.42	0.704	1.60	0.646	1.63	0.641
15	1.70	0.589	2.06	0.522	2.12	0.516
20	2.04	0.490	2.70	0.422	2.84	0.415
25	2.46	0.406	3.63	0.340	3.93	0.333
30	3.00	0.333	5.03	0.273	5.66	0.266
35	3.69	0.271	7.25	0.218	8.46	0.211
40	4.60	0.218	11.02	0.172	13.29	0.165
45	5.83	0.172	18.01	0.134	22.07	0.127
	$K_{q\sigma,max}$	$K_{q\sigma,min}$	$K_{q\tau,max}$	$K_{q\tau,min}$	$K_{\sigma\tau,max}$	$K_{\sigma\tau,min}$

With regard to the possible locations of the rotation centre for the ruptures R and P, the same remarks apply as made at the end of Section 522.

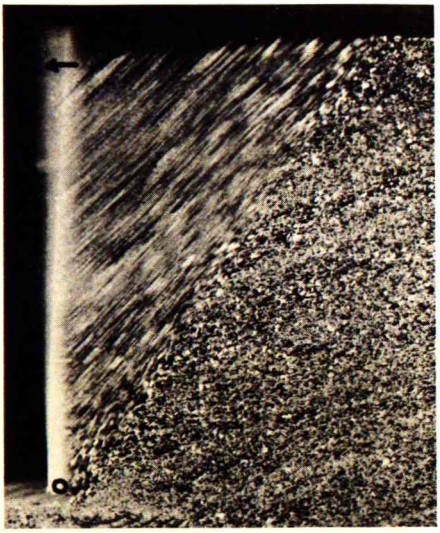

Fig.52B: Actual Rupture R

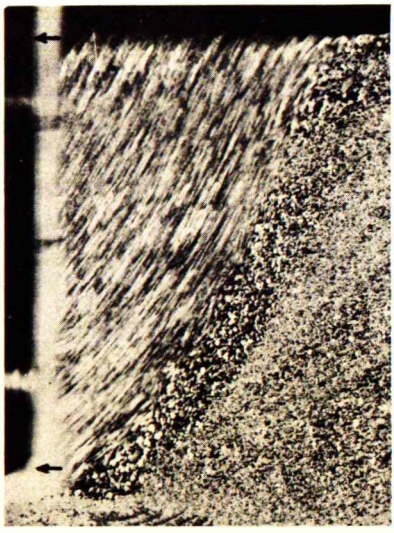

Fig.52C: Actual Rupture P

Fig. 52B shows an actual rupture R, corresponding to $\xi = 0$ and negative rotation (glass wall). Fig. 52C shows an actual rupture P, corresponding to $\xi = \infty$ and outward movement (sand-papered wall).

53. RUPTURE A

531. Frictionless Earth

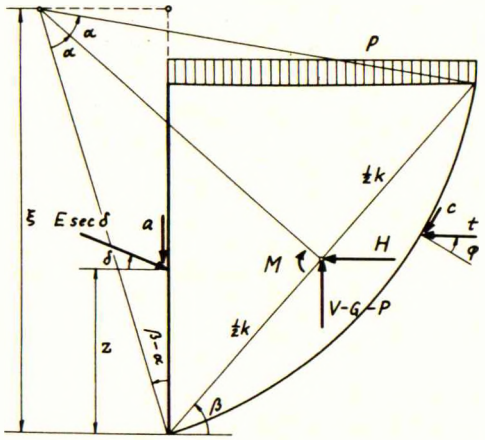

Fig.53A: Rupture A

A rupture A for i = j = 0 is shown in Fig.53A. We have here φ = δ = γ = 0, p = 0, h = 1 and c = 1 (neg. rot.). We find then from 3414:

$$\sigma' = \cot(\beta+\alpha) \qquad 5301$$

By insertion of 5301 in 3353, and of this in 4213, we find an equation which can be transformed to the following:

$$V^{cy}\sin(2\beta+\alpha) + (1-V^{cx}+a)\cos(2\beta+\alpha)$$
$$+ V^{cy}\sin\alpha + (1+V^{cx}-a)\cos\alpha = 0 \qquad 5302$$

In the case of a smooth wall (a=0), we choose an arbitrary value of α and insert in 5302, taking the V-functions from Table 1 in the Appendix. The angle $\beta + \frac{1}{2}\alpha$ can then be found by means of 3406-07. Next, we find ξ from 4210, as well as κ = E and ζ = z from 4214 and 4216 (after insertion of 3354, 3359 and 5301). Further, we determine $\kappa_f = e_f$ with the aid of 3350 and 3426. Finally, ω° and κ^y are calculated by means of 5105-06 with κ^x = -2 (neg. rot.). The results of a number of such calculations are given in the following table:

α	β	ξ	κ	ζ	κ_f	ω°	κ^y
0	45.0	∞	2.000	0.500	2.00	1.000	2.00
5	45.3	6.155	1.989	0.442	2.03	0.942	2.23
10	46.2	3.224	1.961	0.386	2.10	0.887	2.46
15	47.6	2.207	1.916	0.333	2.21	0.837	2.68
20	49.5	1.675	1.858	0.285	2.34	0.793	2.87
25	51.8	1.344	1.793	0.241	2.49	0.755	3.03
30	54.5	1.117	1.722	0.200	2.65	0.723	3.15
35	57.6	0.952	1.648	0.163	2.82	0.695	3.25
40	61.1	0.830	1.568	0.126	2.98	0.671	3.32
45	64.8	0.736	1.480	0.087	3.14	0.649	3.36
50	68.8	0.663	1.377	0.041	3.28	0.626	3.39
55	73.1	0.606	1.239	-0.024	3.38	0.599	3.41
58.5	76.5	0.574	1.103	-0.099	3.41	0.574	3.41

In the case of a rough wall, we choose an arbitrary value of α and assume β = α. Next, we find ξ, κ and ζ as described above, whereas 4213 gives the average value of a. When a is known, we can also find κ_f, assuming a to be constant along the wall. Finally, ω° and κ^y are calculated with κ^x = - 2.57 (neg. rot.). The results are given in the following table:

$\alpha = \beta$	$\xi = a$	κ	ζ	κ_f	ω^o	κ^y
45	1.000	2.142	0.267	3.14	0.788	3.41
50	0.852	1.959	0.205	3.32	0.745	3.51
55	0.745	1.797	0.152	3.48	0.714	3.55
60	0.667	1.638	0.098	3.61	0.687	3.55
65	0.609	1.457	0.032	3.70	0.661	3.52
67.5	0.586	1.346	-0.015	3.71	0.646	3.49

532. Weightless Earth

We have here $\gamma = c = a = 0$, $h = 1$ and $p = 1$. We find then from 3413:

$$t' = \frac{\sin(\beta+\alpha+\varphi)}{\sin(\beta+\alpha)} \qquad 5303$$

By insertion of 5303 in 3325-26, and of these as well as 3221 in 4213, we find an equation which can be transformed to the following:

$$(V^{tx}\tan\delta + V^{ty} - \cos\varphi)\sin(2\beta+\alpha+\varphi) + (V^{ty}\tan\delta - V^{tx} + \sin\varphi)\cos(2\beta+\alpha+\varphi)$$
$$+ \left[V^{tx}\cos(\alpha+\varphi-\delta) + V^{ty}\sin(\alpha+\varphi-\delta)\right]\sec\delta - \sin\alpha = 0 \qquad 5304$$

In the case of a smooth wall ($\delta = 0$) we choose an arbitrary value of α and insert in 5304, taking the V-functions from Table 2 ($\varphi = +30^\circ$, neg. rot.) or Table 3 ($\varphi = -30^\circ$, pos. rot.) in the Appendix. The angle $\beta + \frac{1}{2}\alpha + \frac{1}{2}\varphi$ can then be found by means of 3406-07. Next, we find ξ from 4210, as well as $\rho = E$ and $\theta = z$ from 4214 and 4216 (after insertion of 3222, 3326, 3335 and 5303). Further, we determine $\rho_f = e_f$ with the aid of 3318 and 3425. Finally, we find from the tables in Section 533 (by interpolation) the value of ω corresponding to the given ξ, and can then determine ρ^x and ρ^y by means of 5103-04.

The results for $\varphi = +30^\circ$ (neg. rot.) are given in the following table:

α	β	ξ	ρ	θ	ρ_f	ω	ρ^x	ρ^y
0	30.0	∞	3.000	0.500	3.00	1.000	-	3.00
5	30.4	10.22	2.977	0.434	3.06	0.705	1.640	3.53
10	31.7	5.085	2.924	0.374	3.20	0.586	1.145	4.18
15	33.9	3.279	2.844	0.324	3.43	0.497	0.855	4.86
20	36.8	2.335	2.756	0.287	3.74	0.427	0.706	5.50
25	40.5	1.757	2.669	0.260	4.12	0.373	0.629	6.10
30	44.7	1.375	2.591	0.241	4.57	0.332	0.582	6.63
35	49.4	1.113	2.523	0.228	5.08	0.301	0.559	7.09
40	54.4	0.927	2.460	0.218	5.63	0.278	0.539	7.45
45	59.5	0.794	2.388	0.209	6.13	0.260	0.509	7.73
50	64.7	0.698	2.279	0.201	6.49	0.244	0.476	7.86
52.6	67.4	0.659	2.192	0.198	6.56	0.238	0.454	7.77

The results for $\varphi = -30^\circ$ (pos. rot.) are given below:

α	β	ξ	ρ	θ	ρ_f	ω	ρ^x	ρ^y
0	60.0	∞	0.333	0.500	0.333	1.000	-	0.333
5	60.2	3.769	0.336	0.566	0.327	0.907	0.85	0.287
10	60.9	2.076	0.342	0.627	0.313	0.873	1.03	0.242
15	62.0	1.492	0.352	0.678	0.292	0.849	1.18	0.204
20	63.3	1.190	0.365	0.719	0.270	0.830	1.30	0.172
25	64.9	1.002	0.380	0.750	0.246	0.813	1.40	0.146
30	66.7	0.873	0.397	0.772	0.223	0.800	1.48	0.127
35	68.6	0.780	0.416	0.788	0.201	0.788	1.55	0.112
40	70.7	0.709	0.437	0.799	0.181	0.777	1.61	0.101
45	72.9	0.654	0.461	0.806	0.163	0.767	1.67	0.093
50	75.2	0.611	0.489	0.810	0.148	0.759	1.74	0.088
55	77.8	0.576	0.524	0.813	0.135	0.751	1.84	0.087
60	80.8	0.547	0.570	0.815	0.125	0.743	1.97	0.087
65.2	84.8	0.521	0.651	0.816	0.120	0.734	2.20	0.091

In the case of a rough wall we can, for $\varphi = -30^\circ$ and $\alpha < 61.1^\circ$, employ the same procedure as above, assuming $\delta = \varphi$. In the remaining cases we must, however, assume $\beta = \alpha$ and find the average δ from 4213. When δ is known, we can also find ρ_f, assuming δ to be constant along the wall. Finally, ρ^x and ρ^y are determined as described above.

The results for $\varphi = +30^\circ$ (neg. rot.) are given in the following table:

α = β	ξ	tan δ^p	ρ	θ	ρ_f	ω	ρ^x	ρ^y
40	1.210	0.221	3.214	0.233	6.33	0.378	0.455	7.75
45	1.000	0.217	3.100	0.218	7.01	0.331	0.487	8.38
50	0.852	0.218	3.007	0.206	7.71	0.300	0.481	8.90
55	0.745	0.219	2.899	0.197	8.30	0.277	0.469	9.24
60	0.667	0.220	2.721	0.188	8.57	0.259	0.429	9.28

The results for $\varphi = -30^\circ$ (pos. rot.) are given below:

α	β	ξ	tan δ^p	ρ	θ	ρ_f	ω	ρ^x	ρ^y
25	55.3	1.242	-0.577	0.295	0.653	0.245	0.918	1.39	0.197
30	56.1	1.083	-0.577	0.310	0.691	0.233	0.903	1.53	0.179
35	56.8	0.967	-0.577	0.326	0.719	0.220	0.892	1.65	0.166
40	57.7	0.877	-0.577	0.343	0.738	0.208	0.883	1.74	0.159
45	58.5	0.807	-0.577	0.362	0.751	0.197	0.875	1.82	0.154
50	59.3	0.749	-0.577	0.382	0.758	0.187	0.867	1.86	0.155
55	60.2	0.701	-0.577	0.404	0.761	0.180	0.862	1.93	0.159
60	60.9	0.660	-0.577	0.429	0.760	0.175	0.856	1.98	0.168
61.1	61.1	0.652	-0.577	0.434	0.760	0.174	0.854	1.98	0.170
65	65	0.609	-0.454	0.475	0.783	0.146	0.848	2.24	0.158
70	70	0.566	-0.338	0.537	0.798	0.125	0.839	2.53	0.155
75	75	0.536	-0.261	0.625	0.806	0.115	0.832	2.90	0.165

533. Cohesionless, Unloaded Earth

We have here $p = c = a = 0$, $h = 1$ and $\gamma = 1.3413$ gives then $t' = 0$, and by insertion of 3223 and 3325-26 in 4213, we find an equation which can be transformed to the following:

$$(V^{\gamma x} - \tfrac{1}{4}\cos 2\varphi)\sin(2\beta+2\varphi) + (V^{\gamma x}\tan\delta + \tfrac{1}{4}\sin 2\varphi)\cos(2\beta+2\varphi) + (V^{\gamma z} - H^{\gamma z}\tan\delta - G^{\gamma z}) = 0 \qquad 5305$$

In the case of a smooth wall ($\delta = 0$) we choose an arbitrary value of α and insert in 5305, taking the G-function from Table 1 in the Appendix, and the V- and H-functions from Table 2 ($\varphi = +30^\circ$, neg. rot.) or Table 3 ($\varphi = -30^\circ$, pos. rot.). The angle $\beta + \varphi$ can then be found by means of 3406-07. Next, we find ξ from 4210, as well as $\lambda = 2E$ and $\eta = z$ from 4214 and 4216 (after insertion of 3224, 3326 and 3335). Further, we determine $\lambda_f = e_f$ with the aid of 3318 and 3425. Finally, ω and λ^y are calculated by means of 5101-02 with $\lambda^x = \frac{1}{3}$ (neg. rot.) or $\lambda^x = 3$ (pos. rot.).

The results for $\varphi = +30^\circ$ (neg. rot.) are given in the following table:

α	β	ξ	λ	η	λ_f	ω	λ^y
0	30.0	∞	3.000	0.333	3.00	1.000	3.00
5	31.9	9.664	2.982	0.292	3.03	0.697	3.25
10	34.2	4.670	2.946	0.257	3.09	0.570	3.54
15	36.9	2.987	2.898	0.227	3.20	0.477	3.87
20	40.0	2.140	2.843	0.204	3.34	0.410	4.18
25	43.5	1.632	2.781	0.187	3.51	0.360	4.48
30	47.3	1.298	2.721	0.174	3.71	0.323	4.74
35	51.5	1.068	2.665	0.164	3.93	0.296	4.96
40	56.0	0.902	2.614	0.156	4.17	0.275	5.15
45	60.6	0.781	2.565	0.150	4.41	0.258	5.31
50	65.4	0.692	2.514	0.145	4.64	0.243	5.44
52.3	67.7	0.659	2.488	0.143	4.73	0.238	5.48

The results for $\varphi = -30^\circ$ (pos. rot.) are given below:

α	β	ξ	λ	η	λ_f	ω	λ^y
0	60.0	∞	0.333	0.333	0.333	1.000	0.333
5	61.8	3.560	0.335	0.378	0.331	0.904	0.310
10	63.9	1.890	0.339	0.415	0.324	0.867	0.291
15	66.1	1.326	0.345	0.448	0.314	0.839	0.274
20	68.6	1.039	0.353	0.475	0.302	0.817	0.261
25	71.2	0.864	0.363	0.498	0.289	0.798	0.250
30	74.0	0.748	0.373	0.516	0.276	0.783	0.243
35	77.0	0.665	0.385	0.530	0.264	0.769	0.237
40	80.1	0.604	0.397	0.541	0.252	0.757	0.234
45	83.4	0.558	0.410	0.550	0.241	0.746	0.232
50	86.9	0.523	0.425	0.558	0.231	0.735	0.230
54.2	90.0	0.500	0.439	0.564	0.224	0.725	0.230

In the case of a rough wall we can, for $\varphi = -30^\circ$, use the same procedure as above, assuming $\delta = \varphi$. For $\varphi = +30^\circ$ we must, however, assume $\beta = \alpha$ and find the average δ from 4213. When δ is known, we can also find λ_f, assuming δ to be constant along the wall. Finally, ω and λ^y are calculated with $\lambda^x = 0.266$ (neg. rot.) or $\lambda^x = 5.66$ (pos. rot.).

The results for $\varphi = +30^\circ$ (neg. rot.) are given in the following table:

$\alpha = \beta$	ξ	$\tan \delta^Y$	λ	η	λ_f	ω	λ^y
40	1.210	0.288	3.824	0.185	5.35	0.378	6.07
45	1.000	0.268	3.611	0.168	5.56	0.331	6.32
50	0.852	0.256	3.458	0.156	5.81	0.300	6.53
55	0.745	0.248	3.340	0.147	6.08	0.277	6.71
60	0.667	0.243	3.236	0.140	6.33	0.259	6.85

The results for $\varphi = -30^\circ = \delta$ (pos. rot.) are given below:

α	β	ξ	λ	η	λ_f	ω	λ^y
20	60.9	1.264	0.274	0.412	0.258	0.920	0.239
25	62.9	1.048	0.282	0.448	0.251	0.900	0.228
30	65.0	0.903	0.292	0.477	0.244	0.886	0.221
35	67.2	0.800	0.302	0.500	0.235	0.874	0.216
40	69.6	0.722	0.313	0.518	0.226	0.864	0.213
45	72.0	0.663	0.325	0.532	0.217	0.856	0.212
50	74.5	0.616	0.337	0.542	0.208	0.849	0.213
55	77.2	0.580	0.350	0.551	0.200	0.842	0.215
60	80.0	0.551	0.364	0.558	0.192	0.836	0.217
65	83.0	0.528	0.378	0.564	0.184	0.830	0.221
66.2	83.8	0.524	0.382	0.565	0.183	0.828	0.222

150

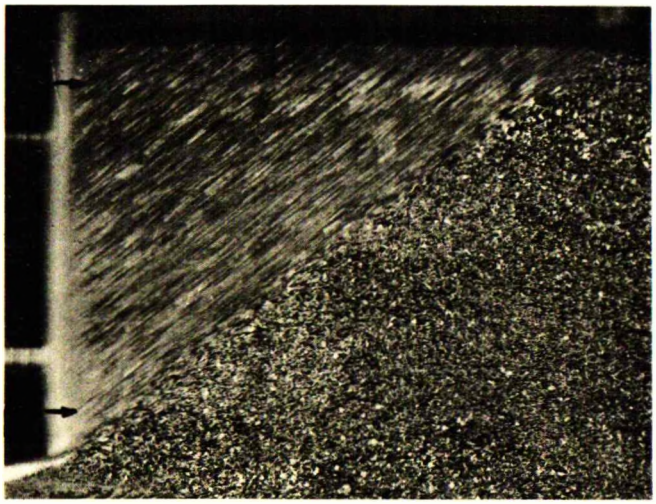

Fig.53B: Actual Rupture S

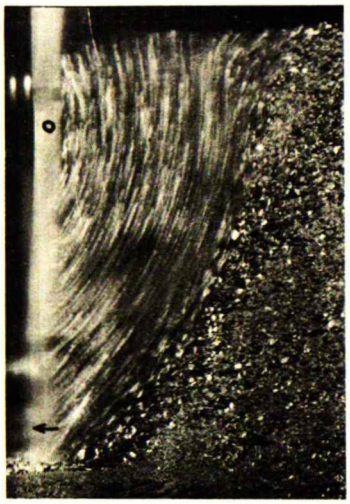

Fig.53C: Actual Rupture A

Fig.53B shows an actual rupture S, corresponding to $\xi = \infty$ and inward movement (glass wall). Due to the fact that the exterior pressure was not quite horizontal, the inclination of the rupture-line does not agree with Coulomb's theory. Fig.53C shows an actual rupture A, corresponding to $\xi = 0.78$ and positive rotation (sand-papered wall).

54. RUPTURE AaR

541. Frictionless Earth

A rupture AaR for i = j = 0 is shown in Fig.54A. We have here $\varphi = \delta = \gamma = 0$, p = 0, h = 1 and $c_2 = -c_1 = 1$ (neg. rot.). We find then from 4401, 4404 and 4418-20:

$$\alpha_1 = 0^\circ \qquad \beta_1 = 45^\circ \qquad \beta_2 = 135^\circ - \alpha_2 \qquad \sigma_1' = \sigma_2' = -1 \qquad 5401\text{-}04$$

By insertion of 5403-04 in 3353, and of this in 4424, we find the following equation:

$$V_2^{cx} + (V_2^{cy} - 1)\cot(135^\circ - \alpha_2) - \frac{a}{h_2} = 0 \qquad 5405$$

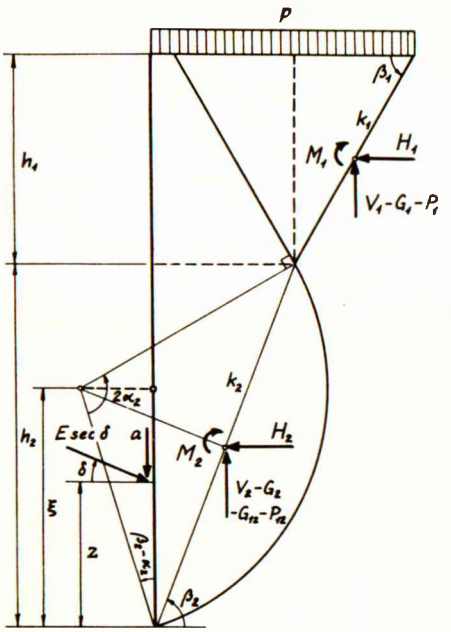

Fig.54A: Rupture AaR

In the case of a smooth wall (a = 0) equation 5405 enables the determination of α_2 (by trial) independently of h_2. This gives $\alpha_2 = 58.5^\circ$ and $\beta_2 = 76.5^\circ$. Next, we choose an arbitrary value of h_2 and find ξ from 4421, as well as $\kappa = E$ and $\zeta = z$ from 4425 and 4427. Finally, κ_f, ω° and κ^y are found as described in Section 531, which gives $\kappa_f = 3.41$, $\omega^\circ = \xi$ and $\kappa^y = 3.41$. The remaining results are given in the following table (neg. rot.):

h_2	$\xi = \omega^\circ$	κ	ζ
1.0	0.574	1.103	-0.099
0.9	0.516	0.793	-0.352
0.8	0.459	0.483	-0.891
0.75	0.430	0.328	-1.524
0.7	0.402	0.172	-3.271
0.645	0.370	0.000	∞
0.6	0.344	-0.138	4.925
0.5	0.287	-0.448	1.734
0.4	0.230	-0.759	1.131
0.3	0.172	-1.069	0.861
0.2	0.115	-1.379	0.699
0.1	0.057	-1.690	0.587
0.0	0.000	-2.000	0.500

In the case of a rough wall we assume $\beta_2 = \alpha_2$, with which 5403 gives $\alpha_2 = \beta_2 = 67.5^\circ$. Next, we find ξ, κ and ζ as described above, whereas 5405 gives the average value of a. Finally, κ_f, ω° and κ^y are calculated as described in Section 531, which gives $\kappa_f = 3.71$. The remaining results are given in the following table (neg. rot.):

h_2	$\xi = a$	κ	ζ	ω°	κ^y
1.0	0.586	1.346	-0.015	0.646	3.49
0.9	0.527	1.012	-0.204	0.603	3.37
0.8	0.469	0.677	-0.551	0.562	3.21
0.75	0.439	0.510	-0.880	0.543	3.10
0.707	0.414	0.366	-1.393	0.528	2.99

542. Weightless Earth

We have here $\gamma = c = a = 0$, $h = 1$ and $p = 1$. We find then from 4401, 4404, 4418-20 and 5209:

$$\alpha_1 = 0^\circ \qquad \beta_1 = 45^\circ - \tfrac{1}{2}\varphi_1 \qquad \beta_2 = 135^\circ + \tfrac{1}{2}\varphi_1 - \alpha_2 \qquad 5406\text{-}08$$

$$t'_1 = t'_2 = \tan(45^\circ + \tfrac{1}{2}\varphi_1) \qquad H_1 = h_1 \tan^2(45^\circ + \tfrac{1}{2}\varphi_1) \qquad 5409\text{-}10$$

By insertion of 5407-09 in 3325-26, and of these as well as 5410 and 3221 in 4424, we find the following equation:

$$V_2^{tx} + (V_2^{ty} - \tan\beta_1)\cot\beta_2 - \left[V_2^{ty} - V_2^{tx}\cot\beta_2 + (\frac{1}{h_2}-1)\cot\beta_1\right]\tan\delta = 0 \qquad 5411$$

In the case of a smooth wall ($\delta = 0$) equation 5411, in connection with 5407-08, enables the determination of α_2 (by trial) independently of h_2. Next, we choose an arbitrary value of h_2 and find ξ from 4421, as well as $\rho = E$ and $\theta = z$ from 4425 and 4427. Finally, ρ_f, ρ^x and ρ^y are calculated as described in Section 532.

With $\varphi_2 = -\varphi_1 = +30^\circ$ (neg. rot.) we find $\alpha_2 = 52.6^\circ$, $\beta_2 = 67.4^\circ$ and $\rho_f = 6.56$. The remaining results are given in the following table:

h_2	ξ	ρ	θ	ω	ρ^x	ρ^y
1.0	0.659	2.192	0.198	0.238	0.454	7.77
0.9	0.593	2.006	0.191	0.221	0.415	7.60
0.8	0.527	1.820	0.185	0.203	0.381	7.45
0.7	0.461	1.634	0.182	0.182	0.363	7.32
0.6	0.396	1.449	0.181	0.159	0.350	7.21
0.5	0.330	1.263	0.185	0.135	0.343	7.12
0.4	0.264	1.077	0.194	0.109	0.337	7.04
0.3	0.198	0.891	0.214	0.083	0.335	6.97
0.2	0.132	0.705	0.252	0.056	0.334	6.91
0.1	0.066	0.519	0.326	0.028	0.333	6.86
0.0	0.000	0.333	0.500	0.000	0.333	6.82

With $\varphi_2 = -\varphi_1 = -30^\circ$ (pos. rot.) we find $\alpha_2 = 65.2^\circ$, $\beta_2 = 84.8^\circ$ and $\rho_f = 0.120$. The remaining results are given below:

h_2	ξ	ρ	θ	ω	ρ^x	ρ^y
1.0	0.521	0.651	0.816	0.734	2.20	0.091
0.9	0.469	0.886	0.807	0.705	2.73	0.114
0.8	0.417	1.121	0.785	0.647	2.94	0.133
0.7	0.365	1.356	0.756	0.573	2.98	0.144
0.6	0.313	1.591	0.724	0.495	3.00	0.153
0.5	0.260	1.826	0.689	0.413	3.00	0.153
0.4	0.208	2.061	0.653	0.330	3.00	0.153
0.3	0.156	2.295	0.616	0.248	3.00	0.153
0.2	0.104	2.530	0.578	0.164	3.00	0.153
0.1	0.052	2.765	0.539	0.083	3.00	0.153
0.0	0.000	3.000	0.500	0.000	3.00	0.153

In the case of a rough wall we assume $\beta_2 = \alpha_2$ and use 5408. Further, 5411 gives the average δ. Otherwise, the procedure is the same as before.

With $\varphi_2 = -\varphi_1 = +30^\circ$ (neg. rot.) we find $\alpha_2 = \beta_2 = 60^\circ$. The remaining results are given in the following table:

h_2	ξ	$\tan\delta^p$	ρ	θ	ρ_f	ω	ρ^x	ρ^y
1.0	0.667	0.220	2.721	0.188	8.57	0.259	0.429	9.28
0.9	0.600	0.216	2.482	0.179	8.55	0.242	0.380	9.07
0.8	0.533	0.213	2.243	0.172	8.53	0.222	0.352	8.87
0.7	0.467	0.208	2.005	0.167	8.51	0.201	0.334	8.65
0.6	0.400	0.203	1.766	0.165	8.48	0.179	0.322	8.37
0.5	0.333	0.195	1.527	0.165	8.45	0.157	0.313	8.04

With $\varphi_2 = -\varphi_1 = -30^\circ$ (pos. rot.) we find $\alpha_2 = \beta_2 = 75^\circ$. The remaining results are given below:

h_2	ξ	$\tan \delta^p$	ρ	θ	ρ_f	ω	ρ^x	ρ^y
1.00	0.536	-0.261	0.625	0.806	0.115	0.832	2.90	0.165
0.95	0.509	-0.208	0.743	0.808	0.110	0.822	3.31	0.186
0.90	0.482	-0.170	0.862	0.804	0.108	0.810	3.62	0.215
0.866	0.464	-0.150	0.943	0.798	0.106	0.791	3.63	0.233

543. Cohesionless, Unloaded Earth

We have here $p = c = a = 0$, $h = 1$ and $\gamma = 1$. We find then from 4401, 4404, 4418-20 and 5216:

$$\alpha_1 = 0^\circ \qquad \beta_1 = 45^\circ - \tfrac{1}{2}\varphi_1 \qquad \beta_2 = 135^\circ + \tfrac{1}{2}\varphi_1 - \alpha_2 \qquad 5412\text{-}14$$

$$t'_1 = 0 \qquad t'_2 = h_1 \tan(45^\circ + \tfrac{1}{2}\varphi_1) \qquad H_1 = \tfrac{1}{2}h_1^2 \tan^2(45^\circ + \tfrac{1}{2}\varphi_1) \qquad 5415\text{-}17$$

By insertion of 5413-16 in 3325-26, and of these as well as 5417, 3223 and 3227 in 4424, we find a second-degree-equation in h_2, the coefficients of which are functions of α_2, β_2, β_1 and δ.

In the case of a smooth wall ($\delta = 0$) equation 4424 is reduced to a first-degree-equation in h_2, which can be solved when we insert a chosen value of α_2 and the corresponding β_2 (from 5414). However, the values of α_2 which give usable values of h_2 ($0 \leq h_2 \leq 1$) lie usually within a very narrow interval. When h_2 has been determined, we find ξ from 4421, as well as $\lambda = 2E$ and $\eta = z$ from 4425 and 4427. Finally, λ_f, ω and λ^y are calculated as described in Section 533.

For $\varphi_2 = -\varphi_1 = +30^\circ$ (neg. rot.) we know that α_2 must lie between 52.3° (Section 533) and about 52.6° (Section 542). The results of the calculations are given in the following table:

α_2	β_2	h_2	ξ	λ	η	λ_f	ω	λ^y
52.30	67.70	1.000	0.659	2.488	0.143	4.73	0.238	5.48
52.34	67.66	0.937	0.617	2.444	0.139	4.84	0.227	5.57
52.39	67.61	0.830	0.546	2.342	0.133	5.04	0.209	5.71
52.43	67.57	0.732	0.482	2.217	0.128	5.22	0.189	5.84
52.47	67.53	0.626	0.412	2.048	0.121	5.41	0.165	5.98
52.51	67.49	0.503	0.332	1.808	0.116	5.64	0.136	6.15
52.55	67.45	0.364	0.240	1.479	0.113	5.89	0.100	6.34
52.58	67.42	0.247	0.163	1.157	0.120	6.11	0.069	6.49
52.60	67.40	0.162	0.106	0.893	0.139	6.26	0.046	6.61
52.61	67.39	0.118	0.077	0.749	0.158	6.34	0.033	6.67
52.62	67.38	0.071	0.047	0.589	0.193	6.43	0.020	6.72
52.63	67.37	0.021	0.014	0.409	0.272	6.52	0.006	6.77
52.64	67.36	0.000	0.000	0.333	0.333	6.56	0.000	6.82

For $\varphi_2 = -\varphi_1 = -30^\circ$ (pos. rot.) we know that β_2 must lie between 90° (Section 533) and 84.8° (Section 542). Consequently, α_2 must lie between 60° and 65.2°. The results of the calculations are given below:

α_2	β_2	h_2	ξ	λ	η	λ_f	ω	λ^y
60.0	90.0	0.727	0.364	0.719	0.604	0.185	0.572	0.209
60.5	89.5	0.667	0.335	0.822	0.599	0.179	0.530	0.203
61.0	89.0	0.605	0.305	0.944	0.588	0.172	0.484	0.198
61.5	88.5	0.540	0.274	1.088	0.572	0.165	0.435	0.192

α_2	β_2	h_2	ξ	λ	η	λ_f	ω	λ^y
62.0	88.0	0.473	0.241	1.257	0.551	0.158	0.383	0.187
62.5	87.5	0.404	0.207	1.451	0.525	0.152	0.329	0.181
63.0	87.0	0.333	0.171	1.673	0.495	0.145	0.272	0.176
63.5	86.5	0.259	0.134	1.926	0.462	0.139	0.212	0.171
64.0	86.0	0.183	0.095	2.211	0.426	0.133	0.150	0.165
64.5	85.5	0.105	0.054	2.530	0.387	0.127	0.086	0.160
65.2	84.8	0.000	0.000	3.000	0.333	0.120	0.000	0.153

In the case of a rough wall we can, for $\varphi_2 = -30^\circ$, use the same procedure as above, assuming $\delta = \varphi_2$. The only difference is that 4424 is a second-degree-equation in this case. For $\varphi_2 = +30^\circ$ we must, however, assume $\beta_2 = \alpha_2$ and use 5414. The remaining calculation is then carried out with an arbitrary value of h_2, and 4424 gives the average δ.

With $\varphi_2 = -\varphi_1 = +30^\circ$ (neg. rot.) we find $\alpha_2 = \beta_2 = 60^\circ$. The remaining results are given in the following table:

h_2	ξ	$\tan \delta^y$	λ	η	λ_f	ω	λ^y
1.0	0.667	0.243	3.236	0.140	6.33	0.259	6.85
0.9	0.600	0.239	3.114	0.134	6.55	0.242	6.97
0.8	0.533	0.235	2.955	0.127	6.77	0.222	7.07
0.7	0.467	0.231	2.758	0.120	6.99	0.201	7.15
0.6	0.400	0.226	2.524	0.113	7.20	0.179	7.19
0.5	0.333	0.220	2.253	0.107	7.40	0.157	7.14

The results for $\varphi_2 = -\varphi_1 = -30^\circ = \delta$ (pos. rot.) are given below:

α_2	β_2	h_2	ξ	λ	η	λ_f	ω	λ^y
66.2	83.8	1.000	0.524	0.382	0.565	0.183	0.828	0.222
67.0	83.0	0.967	0.509	0.397	0.571	0.177	0.822	0.225
68.3	81.7	0.923	0.488	0.425	0.578	0.168	0.812	0.233

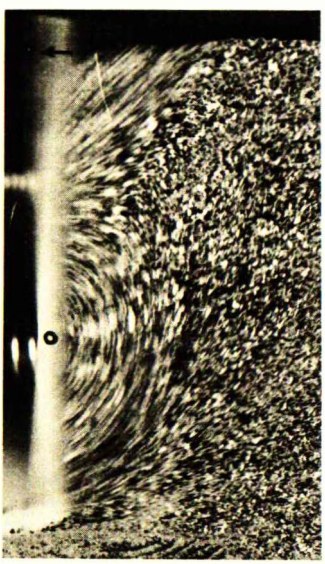

Fig.54B: Actual Rupture AaR

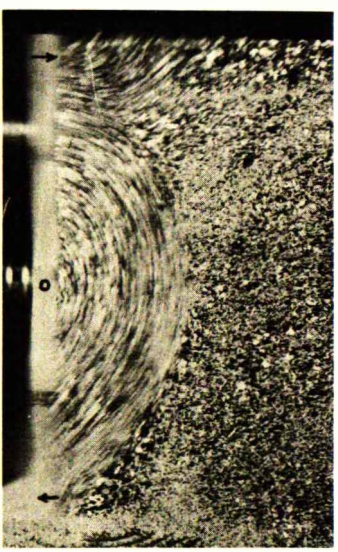

Fig.54C: Actual Rupture AaR

Fig.54B shows an actual rupture AaR, corresponding to $\xi = 0.38$ and negative rotation (glass wall). Fig.54C shows another actual rupture AaR, corresponding to $\xi = 0.50$ and positive rotation (sand-papered wall).

55. RUPTURE AaP

551. Frictionless Earth

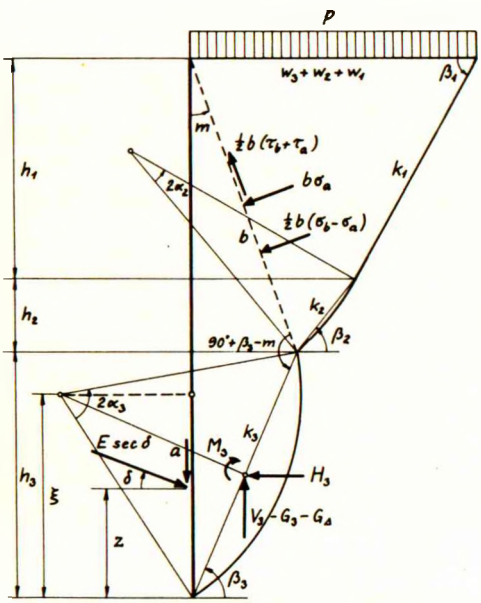

Fig.55A: Rupture AaP

A rupture AaP for $i = j = 0$ is shown in Fig.55A. We have here $\varphi = \delta = \gamma = p = 0$ and $c_3 = -c_2 = -c_1 = 1$ (neg. rot.). σ'_1 and σ'_2 are given by 5404, and 3350 yields then:

$$\sigma'_3 = \sigma''_2 = -1 - t_2^C \qquad 5501$$

As the pseudo-rupture-lines in the plastic zone are, in this case, straight lines through the top of the wall, we have:

$$m = \beta_3+\alpha_3-90^\circ \qquad \alpha_2 = \tfrac{1}{2}(45^\circ-m) \qquad 5502\text{-}03$$

From 4519-22 we find, with $h = 1$, $j = 0$, and $\varphi = 0$:

$$k_3 = \sin m \sec(\beta_3-m) \qquad 5504$$

$$b = \cos\beta_3 \sec(\beta_3-m) \qquad 5505$$

$$\tau_b = \tau_a = -1 \qquad \sigma_b = \sigma_a = \sigma''_2 \qquad 5506\text{-}07$$

The rupture AaP occurs only for a rough wall. In this case we choose an arbitrary value of α_3 and assume $\beta_3 = \alpha_3$. Next, we determine successively m, α_2, σ'_3, k_3, b, τ_b and σ_b by means of 5501-07. We can then find ξ from 4534, as well as $\kappa = E$ and $\zeta = z$ from 4539 and 4541. The average $a = F$ is found from 4540. Finally, κ_f, ω° and κ^y are calculated as described in Section 531. The results are given in the following table (neg. rot.):

$\alpha_3 = \beta_3$	ξ	a	κ	ζ	κ_f	ω°	κ^y
67.50	0.414	0.414	0.366	-1.393	3.71	0.528	2.99
66.75	0.408	0.377	0.256	-2.169	3.61	0.517	2.90
66.00	0.401	0.338	0.147	-4.088	3.50	0.505	2.81
65.00	0.391	0.286	0.000	∞	3.36	0.488	2.69
63.75	0.378	0.218	-0.178	4.075	3.19	0.467	2.55
62.50	0.365	0.147	-0.356	2.227	3.01	0.445	2.40
60.00	0.333	0.000	-0.705	1.297	2.67	0.398	2.12
57.50	0.297	-0.155	-1.044	0.978	2.35	0.346	1.84
55.00	0.255	-0.316	-1.373	0.810	1.97	0.289	1.57
50.00	0.148	-0.653	-1.997	0.621	1.27	0.158	1.04
45.00	0.000	-1.000	-2.571	0.500	0.57	0.000	0.53

552. Weightless Earth

We have here $\gamma = c = a = 0$, $h = 1$ and $p = 1$. t'_1 and t'_2 are given by 5409, and 3318 yields then:

$$t'_3 = t''_2 = t^t_2 \tan(45^\circ + \tfrac{1}{2}\varphi_1) \qquad 5508$$

As the pseudo-rupture-lines in the plastic zone are straight lines through the top of the wall in this case also, the formulae 5502 and 5504-05 are valid for m, k_3 and b. Instead of 5503 and 5506-07 we find, however:

$$\alpha_2 = \tfrac{1}{2}(45^\circ + \tfrac{1}{2}\varphi_1 - m) \qquad \tau_b = \tau_a = t''_2 \sin\varphi_2 \qquad \sigma_b = \sigma_a = t''_2 \cos\varphi_2 \qquad 5509\text{-}11$$

As the wall is rough, we choose an arbitrary value of α_3 and assume $\beta_3 = \alpha_3$. Next, we determine successively m, α_2, t'_3, k_3, b, τ_b and σ_b by means of 5502, 5509, 5508, 5504-05 and 5510-11. We can then find ξ from 4534, as well as $\rho = E$ and $\theta = z$ from 4539 and 4541. The average δ can be found by means of 4540. Finally, ρ_f, ρ^x and ρ^y are calculated as described in Section 532.

With $\varphi_3 = -\varphi_2 = -\varphi_1 = +30^\circ$ (neg. rot.) we find the results indicated in the following table:

$\alpha_3 = \beta_3$	ξ	$\tan\delta^p$	ρ	θ	ρ_f	ω	ρ^x	ρ^y
60.00	0.333	0.195	1.527	0.165	8.45	0.157	0.313	8.04
58.75	0.316	0.170	1.341	0.171	7.51	0.151	0.302	7.18
57.50	0.297	0.141	1.175	0.178	6.62	0.143	0.292	6.46
56.25	0.277	0.108	1.027	0.187	5.90	0.133	0.286	5.85
55.00	0.255	0.069	0.897	0.199	5.21	0.121	0.282	5.33
53.75	0.231	0.025	0.781	0.213	4.59	0.108	0.279	4.88
52.50	0.206	-0.027	0.678	0.232	4.03	0.096	0.277	4.48
51.25	0.178	-0.087	0.587	0.256	3.52	0.082	0.275	4.11
50.00	0.148	-0.157	0.507	0.286	3.07	0.068	0.274	3.76
48.75	0.115	-0.238	0.437	0.323	2.66	0.053	0.273	3.42
47.50	0.080	-0.333	0.375	0.369	2.29	0.037	0.273	3.08
46.25	0.042	-0.445	0.321	0.427	1.97	0.020	0.273	2.74
45.00	0.000	-0.577	0.273	0.500	1.67	0.000	0.273	2.40

With $\varphi_3 = -\varphi_2 = -\varphi_1 = -30^\circ$ (pos. rot.) the following results are obtained:

$\alpha_3 = \beta_3$	ξ	$\tan\delta^p$	ρ	θ	ρ_f	ω	ρ^x	ρ^y
75.0	0.464	-0.150	0.943	0.798	0.106	0.791	3.63	0.233
72.5	0.450	-0.099	1.119	0.788	0.126	0.778	4.02	0.290
70.0	0.434	-0.046	1.321	0.775	0.150	0.765	4.41	0.371
67.5	0.414	0.008	1.549	0.761	0.177	0.733	4.56	0.446
65.0	0.391	0.064	1.806	0.746	0.210	0.691	4.68	0.520
62.5	0.365	0.121	2.093	0.728	0.249	0.644	4.78	0.610
60.0	0.333	0.179	2.412	0.707	0.295	0.588	4.86	0.714
57.5	0.297	0.240	2.764	0.684	0.350	0.525	4.91	0.829
55.0	0.255	0.302	3.149	0.657	0.416	0.451	4.95	0.956
52.5	0.206	0.366	3.569	0.626	0.493	0.364	4.98	1.100
50.0	0.148	0.433	4.022	0.590	0.584	0.261	5.00	1.250
47.5	0.080	0.504	4.509	0.549	0.692	0.141	5.02	1.410
45.0	0.000	0.577	5.026	0.500	0.820	0.000	5.03	1.580

553. Cohesionless, Unloaded Earth

We have here $p = c = a = 0$, $h = 1$ and $\gamma = 1$. t'_1 and t'_2 are given by 5415-16 and we find then by means of 3318, 4503 and 4509:

$$t'_3 = t''_2 = h_2(t_2^{\gamma x} + t_2^{\gamma y}\cot\beta_2) + t'_2 t_2^{t} \qquad 5512$$

$$\alpha_2 = \tfrac{1}{2}(\beta_2^0 + \alpha_2^0 - \beta_3 - \alpha_3 + \varphi_2 + 90^\circ) \qquad \beta_2 = \beta_2^0 + \alpha_2^0 - \alpha_2 \qquad 5513\text{-}14$$

As the wall is rough, we choose an arbitrary value of α_3 and assume $\beta_3 = \alpha_3$. 5513-14 give then α_2 and β_2, after which we find successively m, K, k_1, k_2, k_3, t'_3, b, τ_b and σ_b from 4533, 4535, 4504, 4518-19, 5512 and 4520-22. τ_a and σ_a are, of course, equal to zero. When this is done we can find ξ from 4534, as well as $\lambda = 2E$ and $\eta = z$ from 4539 and 4541. The average δ is calculated by means of 4540. Finally, λ_f, ω and λ^y are determined as described in Section 533.

For $\varphi_3 = -30^\circ$ (pos. rot.) and $\beta_3 > 71.8^\circ$ we cannot use this procedure but must assume $\delta = \varphi_3$. We choose then a set of values of α_2 and α_3, and find β_2 from 4503 and β_3 from 4509. We proceed then as above, but must change α_2 or α_3 until 4538 is satisfied.

For the complete rupture P (superscript 0) we use the values calculated in Example 52a. However, as we have here approximated the P-line by means of two circles with different radii, the quantities found by a direct calculation for the rupture AaP will not exhibit a smooth variation. Therefore, the results given in the following two tables have been adjusted somewhat, mainly by assuming that ω should be approximately proportional to ξ.

For $\varphi_3 = -\varphi_2 = -\varphi_1 = +30^\circ$ (neg. rot.) the adjusted results are:

$\alpha_3 = \beta_3$	ξ	$\tan\delta^\gamma$	λ	η	λ_f	ω	λ^y
60.00	0.305	0.217	2.127	0.104	7.51	0.147	7.08
59.25	0.282	0.204	1.939	0.103	7.22	0.135	6.89
58.50	0.258	0.189	1.750	0.102	6.92	0.123	6.69
57.75	0.234	0.171	1.562	0.102	6.60	0.110	6.48
57.00	0.208	0.149	1.377	0.103	6.25	0.097	6.26
56.25	0.182	0.121	1.196	0.106	5.87	0.084	6.02
55.50	0.155	0.086	1.020	0.113	5.47	0.071	5.76
54.75	0.126	0.039	0.851	0.124	5.04	0.058	5.48
54.00	0.097	-0.026	0.692	0.142	4.57	0.045	5.18
53.25	0.067	-0.118	0.545	0.172	4.07	0.031	4.86
52.50	0.036	-0.258	0.411	0.223	3.54	0.017	4.52
45.00	0.000	-0.577	0.266	0.333	1.63	0.000	4.09

For $\varphi_3 = -\varphi_2 = -\varphi_1 = -30^\circ$ (pos. rot.) the adjusted results are:

α_3	β_3	ξ	$\tan\delta^\gamma$	λ	η	λ_f	ω	λ^y
68.7	81.3	0.481	-0.577	0.434	0.580	0.165	0.809	0.236
69.3	76.7	0.459	-0.577	0.506	0.590	0.145	0.786	0.258
71.8	71.8	0.428	-0.577	0.615	0.587	0.120	0.761	0.309
70.5	70.5	0.415	-0.465	0.693	0.599	0.120	0.735	0.318
69.0	69.0	0.396	-0.336	0.816	0.608	0.121	0.700	0.336
67.5	67.5	0.374	-0.212	0.977	0.610	0.122	0.660	0.362

α_3	β_3	ξ	tan δY	λ	η	λ_f	ω	λ^y
66.0	66.0	0.347	-0.093	1.188	0.605	0.132	0.613	0.398
64.5	64.5	0.315	0.021	1.470	0.591	0.144	0.557	0.447
63.0	63.0	0.276	0.130	1.865	0.568	0.167	0.488	0.515
61.5	61.5	0.228	0.234	2.420	0.533	0.205	0.403	0.625
60.0	60.0	0.170	0.333	3.200	0.481	0.270	0.300	0.830
57.0	57.0	0.138	0.388	3.650	0.453	0.320	0.244	0.960
54.0	54.0	0.105	0.440	4.123	0.424	0.400	0.186	1.095
51.0	51.0	0.072	0.489	4.610	0.396	0.525	0.127	1.235
48.0	48.0	0.037	0.535	5.125	0.364	0.695	0.065	1.380
45.0	45.0	0.000	0.577	5.664	0.333	0.925	0.000	1.530

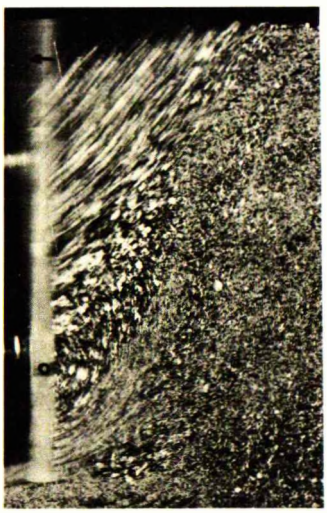

Fig.55B: Actual Rupture AaP

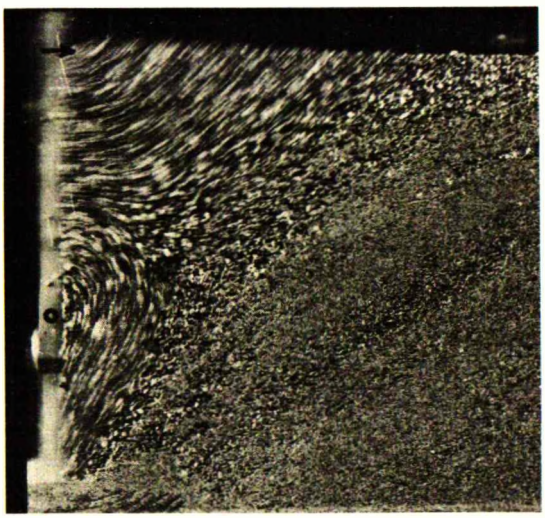

Fig.55C: Actual Rupture AaP

Fig.55B shows an actual rupture AaP, corresponding to $\xi = 0.25$ and negative rotation (sand-papered wall). Fig.55C shows another rupture AaP, corresponding to $\xi = 0.39$ and positive rotation (sand-papered wall).

56. RUPTURES XfP AND AwXfP

561. Introduction

We have seen in Section 433, that when $\varphi \neq 0$, the passive rupture P cannot occur for a "normal" rotation of the wall. We have also seen that the passive rupture R cannot occur for negative values of ξ between 0 and ξ_1 (4327). Similar remarks apply to ruptures AaP and AaR with passive pressure in the plastic zone.

Instead of ruptures P and R, the rupture XfP (Fig.35E) may occur, and, instead of ruptures AaP and AaR, the rupture AwXfP (Fig.35F).

The above remarks do not apply to frictionless earth, as in this case the ruptures P and R are kinematically possible.

562. Weightless Earth

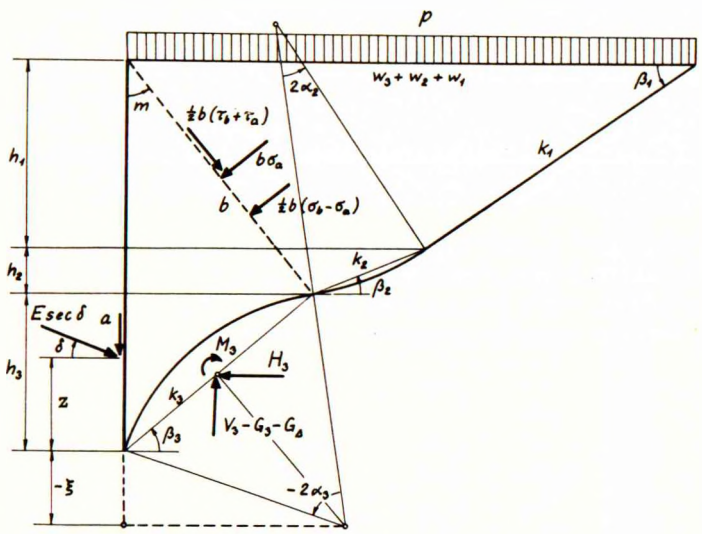

Fig.56A: Rupture XfP

The rupture XfP can be calculated according to the principles indicated in Section 45. Moreover, all formulae given in Sections 551-52 for the rupture AaP are also valid for the rupture XfP, with the exception that 5502 must be substituted by (Fig. 56A):

$$m = \beta_3 + \alpha_3 + \varphi_2 \qquad 5601$$

When the wall is rough, we choose an arbitrary negative value of α_3 and assume $\beta_3 = \alpha_3$. Next, we determine successively m, α_2, t'_3, k_3, b, τ_b and σ_b by means of 5601, 5509, 5508, 5504-05 and 5510-11. We can then find ξ from 4534, as well as $\rho = E$ and $\theta = z$ from 4539 and 4541. The average δ can be found by means of 4540, after which we can calculate ρ_f with the aid of 3318 and 3425.

With $\varphi_3 = \varphi_2 = \varphi_1 = +30^\circ$ (pos. rot.) we get the results indicated in the following table:

$\alpha_3 = \beta_3$	ξ	$\tan \delta^p$	ρ	θ	ρ_f
-15.0	-0.000	0.577	5.03	0.500	5.49
-12.5	-0.211	0.529	4.98	0.503	5.27
-10.0	-0.532	0.485	4.91	0.505	5.09
- 7.5	-1.073	0.445	4.84	0.506	4.93
- 5.0	-2.165	0.409	4.76	0.505	4.79
- 2.5	-5.462	0.376	4.67	0.503	4.68
- 0.0	- ∞	0.346	4.58	0.500	4.58

Considering the slight variation of θ, we shall, for the sake of simplicity, assume a constant $\theta = \frac{1}{2}$, in which case we have $\omega = 0$ and $\rho^X = \rho$. It should be noted that for $\xi = -\infty$ we have $\rho = \rho_f$ and $\delta = \psi - \varphi$ (compare 4328).

When the wall is smooth ($\delta = 0$), we choose a set of values of α_2 and α_3, and find the corresponding β_2 from 4503 and β_3 from 4508. We proceed then as above, but must change α_2 or α_3 until 4538 is satisfied.

As an example of such a calculation we can indicate the following result for $\varphi_3 = \varphi_2 = \varphi_1 = +30^\circ$ (pos. rot.):

α_3	β_3	ξ	ρ	θ	ρ_f
-40.0	50.0	0	2.46	0.639	0

Such a calculation can be carried out for any negative value of ξ, but if we determine ρ_f by means of 3425 with $\delta = 0$, we find negative values of ρ_f when $\beta_3 - \alpha_3 > 90^\circ - \varphi$. For $\beta_3 - \alpha_3 = 90^\circ - \varphi$, we find even $\rho_f = \infty$. As these results are meaningless, we shall not use the rupture XfP for a smooth wall but shall in its place (as an approximation) use the rupture R, in spite of the fact that it is not kinematically possible for $\xi_1 < \xi < 0$.

From the above example it will be seen that, although ρ is considerably smaller, and θ considerably greater than for the rupture R ($\rho = 3$, $\theta = \frac{1}{2}$), the moment $E(z-x) = \rho\theta$ about the rotation centre is only about 5% higher for rupture XfP than for rupture R. It is, therefore, approximately correct and on the safe side, to use the rupture R instead of XfP for a smooth wall.

Corresponding to the rupture XfP for $-\infty < \xi < 0$ we might, for $0 < \xi < \frac{1}{2}$, have the rupture AwXfP (Fig. 35F). This rupture could theoretically be calculated as a w-rupture (Section 462), using the boundary condition 3428. However, certain complications arise indicating that the method is hardly applicable to this case.

For a smooth wall we have already seen that a calculation of the rupture XfP leads to meaningless results when $\beta_3 - \alpha_3 > 90^\circ - \varphi$, and the same applies, of course, to the corresponding rupture AwXfP.

For a rough wall with "normal" rotation we must first remark, as mentioned in Section 344, that 3428 may not be valid when $\delta_1 \neq \delta_2$. Moreover, one or both of the rupture-lines will usually meet the wall at right angles, in which case we do not know δ at all.

We shall, consequently, not use the rupture AwXfP, but (as approximations) the ruptures AaR and AaP, even in such cases when they are, strictly speaking, kinematically impossible.

563. Cohesionless, Unloaded Earth

For the rupture XfP the formulae indicated in Section 553 are valid, with the exception that 5513 must be substituted by:

$$\alpha_2 = \tfrac{1}{2}(\beta_2^\circ + \alpha_2^\circ - \beta_3 - \alpha_3) \qquad 5602$$

When the wall is rough, we choose an arbitrary negative value of α_3 and assume $\beta_3 = \alpha_3$. 5602 and 5514 give then α_2 and β_2. Next, we determine successively m, K, k_1, k_2, k_3, t'_3, b, τ_b and σ_b from 4533, 4535, 4504, 4518-19, 5512 and 4520-22. τ_a and σ_a are equal to zero. After this we find ξ from 4534, as well as $\lambda = 2E$ and $\eta = z$ from 4539 and 4541. The average δ is calculated by means of 4540, after which we can find λ_f with the aid of 3318 and 3425. For the complete rupture P (superscript 0) we use the values calculated in Example 52a.

With $\varphi_3 = \varphi_2 = \varphi_1 = +30^\circ$ (pos. rot.) we get the results indicated in the following table:

$\alpha_3 = \beta_3$	ξ	$\tan \delta Y$	λ	η	λ_f
-15.0	-0.000	0.577	5.66	0.333	6.20
-12.0	-0.094	0.566	5.62	0.336	6.05
- 9.0	-0.251	0.537	5.56	0.339	5.90
- 6.0	-0.565	0.496	5.47	0.340	5.65
- 3.0	-1.506	0.449	5.34	0.340	5.40
- 0.0	- ∞	0.399	5.16	0.338	5.15

Considering the slight variation of η, we shall for the sake of simplicity assume a constant $\eta = \frac{1}{3}$, in which case we have $\omega = 0$ and $\lambda^X = \lambda$.

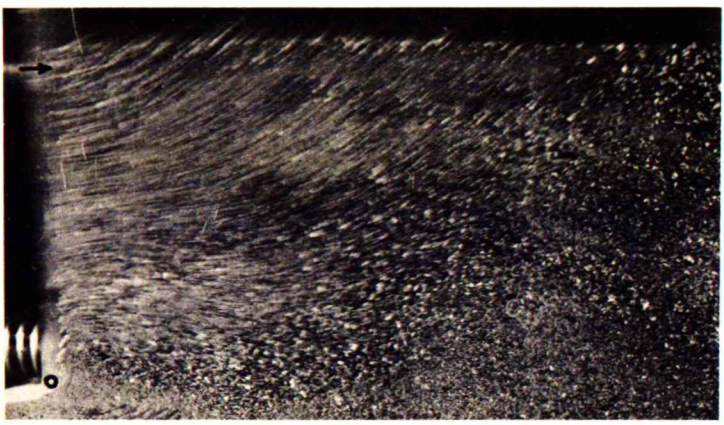

Fig.56B: Actual Rupture XfP

Fig.56B shows an actual rupture XfP, corresponding to $\xi = 0$ and positive rotation (sand-papered wall). It should be noted, however, that the X-line does not meet the wall at 90° as assumed above, but at approximately 0°. Fig.56C shows the special rupture SfP, corresponding to $\xi = \infty$ and inward movement (sand-papered wall).

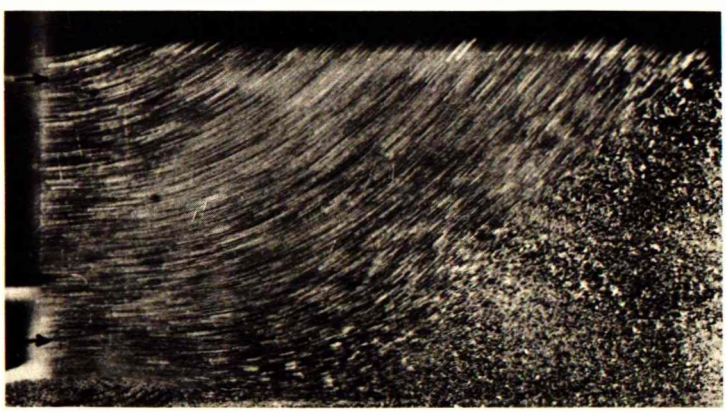

Fig.56C: Actual Rupture SfP

When the wall is smooth ($\delta = 0$), we choose a set of values of α_2 and α_3, and find the corresponding β_2 from 4503 and β_3 from 4508. We proceed then as above, but must change α_2 or α_3, until 4538 is satisfied.

As an example of such a calculation we can indicate the following result for $\varphi_3 = \varphi_2 = \varphi_1 = +30^\circ$ (pos. rot.):

α_3	β_3	ξ	λ	η	λ_f
-38.6	51.4	0	2.28	0.484	0

The moment $E(z\text{-}x) = \frac{1}{2}\lambda\eta$ about the rotation centre is only 10% greater than for the rupture R ($\lambda = 3$, $\eta = \frac{1}{3}$).

Concerning the rupture XfP for a smooth wall, as well as the rupture AwXfP for both smooth and rough walls, the same remarks apply as made in Section 562.

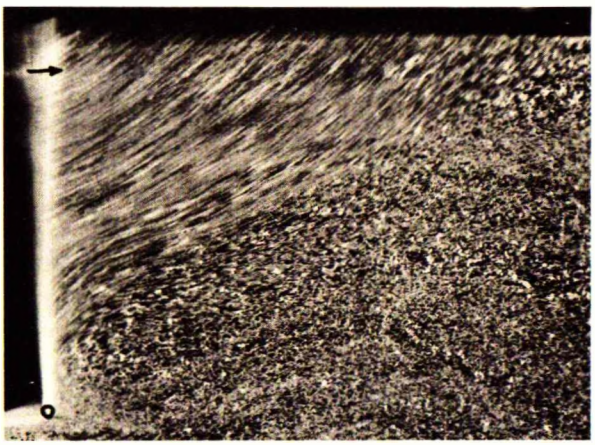

Fig.56D: Actual Rupture XfP

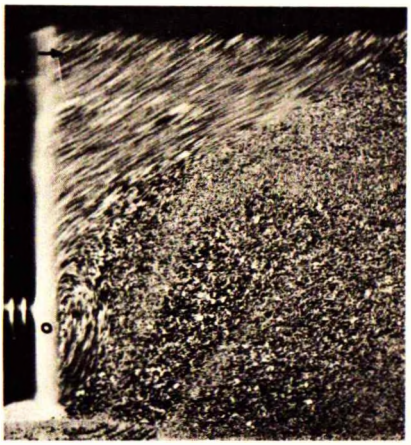

Fig.56E: Actual Rupture AwXfP

In spite of the theoretical difficulties ruptures XfP and AwXfP seem to occur in nature. Fig.56D shows an actual rupture XfP, corresponding to $\xi = 0$ and positive rotation (glass wall). Its contour agrees very well with the values calculated above. Fig.56E shows a rupture AwXfP, corresponding to $\xi = 0.20$ and positive rotation (glass wall).

57. RUPTURES AwR AND PfA

571. Rupture AwR

Whereas there is usually no gap between the ruptures A and AaR, such a gap exists in the case of cohesionless, unloaded earth for positive rotation of a smooth wall, viz. in the interval $0.364 < \xi < 0.5$. This gap is filled by the rupture AwR (Fig.57A), which can be calculated as described in Section 462.

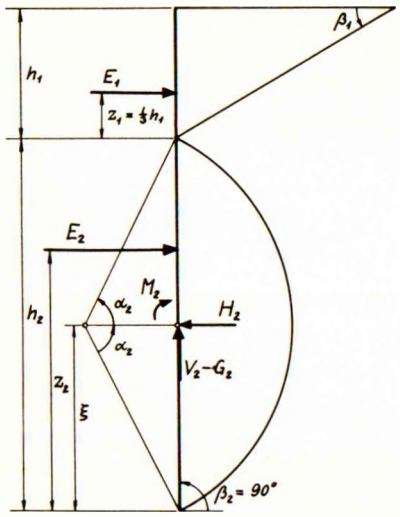

Fig.57A: Rupture AwR

As we are only interested in the special case mentioned above, we have $p = c = a = \delta = 0$, $h = 1$ and $\gamma = 1$. The heights are then given by:

$$h_2 = 2\xi \qquad h_1 = 1 - 2\xi \qquad 5701\text{-}02$$

For the R-rupture in the upper zone the formulae 5412-13 and 5415-17 are valid. Further we have:

$$E_1 = H_1 \qquad z_1 = \tfrac{1}{3}h_1 \qquad 5703\text{-}04$$

The stress at the lower point of the R-line is given by 5416, and the stress at the upper point of the A-line can then be found from 3428 with $\beta_2 = 90°$, $\alpha_1 = 0°$ and $j = 0$:

$$t'_2 = (1-h_2)\,\frac{\sin(\alpha_2-\varphi_1)}{\sin\alpha_2}\,\tan^2(45° + \tfrac{1}{2}\varphi_1) \qquad 5705$$

We can now calculate the A-zone as described in Section 422. By insertion of $\beta_2 = 90°$ and 5705 in 3223 and 3325, and of these in 4213, we get with $\delta = 0$:

$$\frac{1}{h_2} = \frac{(G_2^{YZ} - V_2^{YZ} - V_2^{YX}\sin 2\varphi_1)\,\sin\alpha_2}{V_2^{tX}\,\sin(\alpha_2-\varphi_1)\,\tan^2(45° + \tfrac{1}{2}\varphi_1)} + 1 \qquad 5706$$

With an arbitrary value of α_2 we find the corresponding h_2 from 5706. Next, we find ξ from 5701, h_1 from 5702, $E_1 = H_1$ from 5417 and z_1 from 5704. Further, when t'_2 has been calculated by means of 5705, we can find $E_2 = H_2$ from 4214 and z_2 from 4216. $\lambda = 2E$ and $\eta = z$ are then given by 4616 and 4618. Finally, λ_f, ω and λ^y are determined as described in Section 533 (with $\lambda^x = 3$).

For $\varphi_2 = -\varphi_1 = -30°$ (pos. rot.) we know that α_2 must lie between 54.2° (Section 533) and 60° (Section 543). The results of the calculations are given in the following table:

α_2	h_2	ξ	λ	η	λ_f	ω	λ^y
54.2	1.000	0.500	0.439	0.564	0.224	0.725	0.230
55.5	0.945	0.473	0.464	0.574	0.215	0.708	0.228
57.0	0.878	0.439	0.518	0.590	0.205	0.674	0.223
58.5	0.806	0.403	0.601	0.601	0.195	0.628	0.216
60.0	0.727	0.364	0.719	0.604	0.185	0.572	0.209

572. Rupture PfA

As explained in Section 461, we can only calculate a rupture PfA with a given x in the case of frictionless earth. This special case, which only occurs for a rough wall, is shown in Fig.57B, where we have $\varphi = \delta = \gamma = p = 0$, $h = 1$ and $c = a = 1$ (neg. rot.).

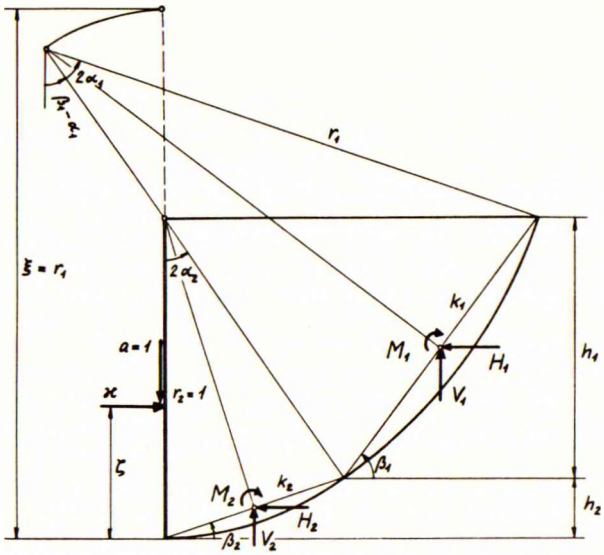

Fig.57B: Rupture PfA

As one set of the rupture-lines in the plastic zone consists of circles, with the top of the wall as centre, we have:

$$\beta_2 = \alpha_2 = \tfrac{1}{2}(\beta_1 - \alpha_1) \qquad 5707$$

$$h_1 = \cos(\beta_1 - \alpha_1) \qquad 5708$$

$$h_2 = 1 - \cos(\beta_1 - \alpha_1) \qquad 5709$$

The normal stresses at the starting points of the two circles are determined by 3414 and 3350:

$$\sigma_1' = \cot(\beta_1 + \alpha_1) \qquad 5710$$

$$\sigma_2' = \sigma_1'' = \sigma_1' + t_1^c \qquad 5711$$

The height of the rotation centre for the wall is determined by 4614 with $j = 0$ and $\beta_3 = \alpha_3$, which gives $\xi = r_1$. Further we find, by means of 3218 and 5708:

$$\xi = r_1 = \tfrac{1}{2}\,(1 + \cot\alpha_1 \cot\beta_1) \qquad 5712$$

By insertion of 3353 in 4105 we get, with $j = 0$, $\delta = 0$ and $a = 1$:

$$h_1\left[V_1^{cx} + (V_1^{cy} + \sigma_1')\cot\beta_1\right] + h_2\left[V_2^{cx} + (V_2^{cy} + \sigma_2')\cot\beta_2\right] = 1 \qquad 5713$$

After having eliminated, by means of 5707-11, all quantities but α_1 and β_1 from 5713, it will be found that the resulting relation between α_1 and β_1 is exactly the same as the relation 5302 (with $a = 0$) between α and β for the rupture A in the case of a smooth wall.

We can therefore use the values of α and β calculated in Section 531 for a smooth wall. A comparison of 4210 and 5712 will show that ξ is also the same. After a calculation of α_2, β_2, h_1, h_2, σ_1' and σ_2' by means of 5707-11 we can find $\kappa = E$ and $\zeta = z$ from 4113 and 4115 (with $j = 0$). Finally, κ_f, ω^o and κ^y are determined as described in Section 531 (with $\kappa^x = -2.57$).

The results of these calculations are given in the following table (neg. rot.):

α_1	β_1	ξ	κ	ζ	κ_f	ω^o	κ^y
0	45.0	∞	2.571	0.500	2.57	1.000	2.57
5	45.3	6.155	2.557	0.472	2.59	0.972	2.70
10	46.2	3.224	2.519	0.438	2.63	0.939	2.85
15	47.6	2.207	2.459	0.400	2.70	0.902	3.00
20	49.5	1.675	2.384	0.362	2.80	0.867	3.15
25	51.8	1.344	2.298	0.324	2.92	0.834	3.27
30	54.5	1.117	2.206	0.289	3.05	0.805	3.36
33.4	56.6	1.000	2.142	0.267	3.14	0.788	3.41

58. OTHER RUPTURES

581. More Complicated Ruptures

As we have seen in the preceding sections, the new method enables calculations to be carried out for the simpler ruptures, such as R, P, A, AaR, AaP and AwR.

However, we have already met with certain inconsistencies (notably for a smooth wall and low negative values of ξ) as regards the rupture XfP, which show that the application of the method is limited. For the rupture AwXfP, it seems hardly possible to use the method at all.

Another difficulty occurs in the calculation of the rupture PfA, where the location of the rotation centre cannot be determined without a detailed investigation of the deformations in the plastic zone. Only in the case of frictionless earth is this possible by simple methods.

Moreover, the rupture PfA (as calculated in Section 572 for $\varphi = 0$) is actually statically impossible, as Kötter's equation is not satisfied for the pseudo-rupture-lines in the plastic zone. In spite of this fact the rupture PfA may provide a good approximation, but the actual rupture is probably of the type AfPfA (compare Fig. 35F).

A rupture AfPfA occurs probably also for $\varphi \neq 0$ when the wall is rough. At least, this seems the logical rupture to fill the gap between the ruptures A and SfP, as the rupture AfP is kinematically impossible (Section 354). Unfortunately, the rupture AfPfA is too complicated for practical calculation, but, as we shall see in Section 591, the results can be estimated with sufficient accuracy.

The author's small-scale model tests, as recorded on the photographs in the present Section 5 show that most of the simple ruptures calculated in the preceding sections actually occur in nature too. However, they also show that in some cases more complicated ruptures will occur. A few examples shall be mentioned.

Fig. 58A shows an actual rupture, corresponding to $\xi = 0.37$ and positive rotation (glass wall). In this case we would expect a rupture AaP or AwXfP. Actually, both these rupture-figures occur at the same time, so that we may term this rupture AaP + AwXfP (compare Fig. 35F). Fig. 58B shows a similar rupture, corresponding to $\xi = 0.26$ and negative rotation (glass wall).

Fig. 58C shows another actual rupture, corresponding to $\xi = 0.58$ and positive rotation (glass wall). In this case we would expect the simple rupture A. Actually, the rupture-figure is of a far more complicated type, probably AfX + AwX (compare Fig. 35F). It will be seen, however, that in the main the deviations from the simple rupture A are not very great.

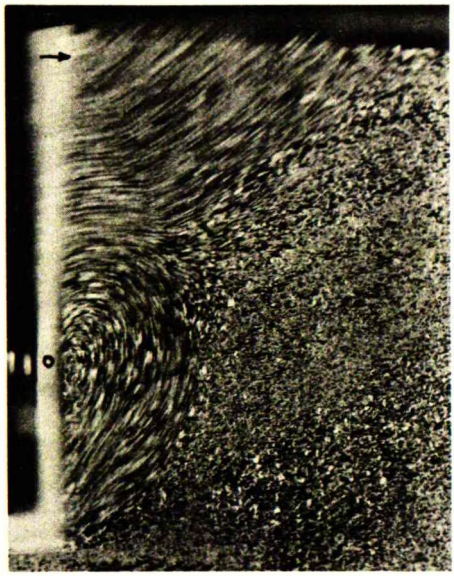

Fig.58A: Actual Rupture AaP + AwXfP

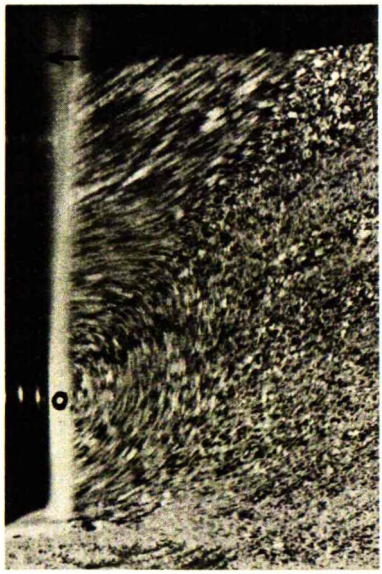

Fig.58B: Actual Rupture AaP + AwXfP

More important deviations are found by negative rotation. Fig.58D shows an actual rupture, corresponding to $\xi = 1$ and negative rotation (glass wall). According to the theory we should have a rupture A, but actually it is probably of the type AfAsR (compare Fig.35F). Instead of intersecting the surface at 90° (Terzaghi & Peck 1948), the lowest rupture-line makes an angle of about 45° with the surface. Moreover, at the surface it could be observed that a plastic zone of limited extension occurred at some distance from the wall.

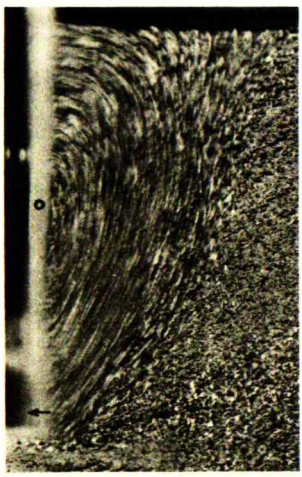

Fig.58C: Actual Rupture AfX + AwX (?)

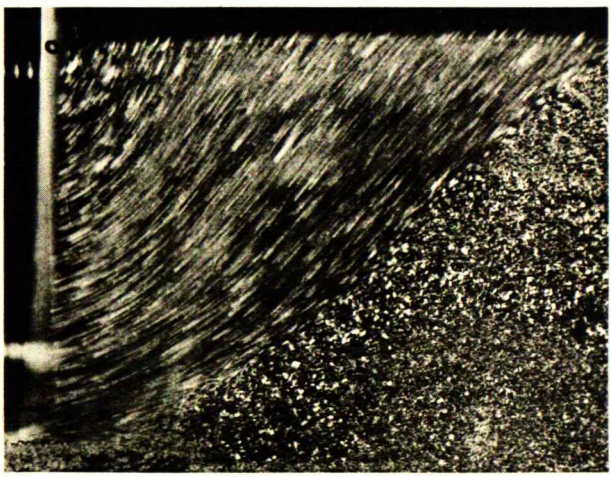

Fig.58D: Actual Rupture AfAsR (?)

However, all the more complicated rupture-figures mentioned above are far too difficult for practical calculation. We shall therefore use exclusively, as approximations, the simple rupture-figures calculated in the preceding sections and, in addition, the rupture AfPfA, for which we can estimate the results. By means of these rupture-figures we can cover the complete interval $-\infty \leqslant \xi \leqslant +\infty$, as shall be shown in Section 591.

582. Less Critical Ruptures

In addition to the ruptures calculated in the preceding sections, other comparatively simple ruptures have been investigated but have been found to be less critical, as they involve greater work having to be done by the earth pressure acting upon the earth (see Section 357). Naturally, only such ruptures can be compared which correspond to the same rotation centre (ξ) or the same pressure centre (ζ, θ or η).

As an example may be mentioned that for negative values of ξ and a smooth wall it has been found that the rupture X is less critical than XfP, which again is less critical than R. Correspondingly, for low positive values of ξ and a smooth wall, the rupture AwX is less critical than AwXfP, which again is less critical than AwR, which is still less critical than AaR.

583. s-Ruptures

In the preceding part of Section 5 we have dealt exclusively with rupture-figures corresponding to the movement of a rigid wall without yield hinges. As soon as a yield hinge develops in a rigid wall, the rupture-figure in the earth will usually be of the s-type.

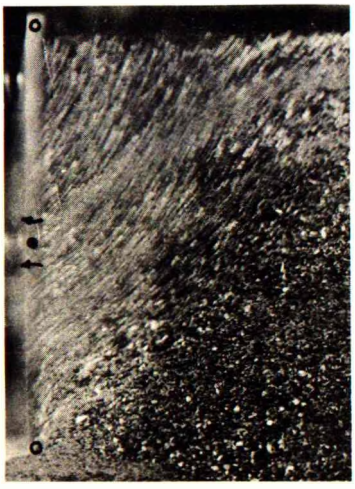

Fig.58E: Actual Rupture PsA

Fig.58F: Actual Rupture XfPsAfAsR (?)

In Section 463, we have seen how s-ruptures can be calculated. However, in Section 474, it has also been shown that, at least for active ZsL-ruptures, a very good approximation may be obtained in a much simpler way (see p. 136), making use of our tentative pressure diagrams.

The author has also made a few model tests with hinged walls. Fig. 58E shows an actual rupture PsA (compare Fig. 35D), corresponding to $\xi_1 = 1$ and $\xi_2 = 0$ and outward movement of the hinge (aluminium wall). Fig. 58F shows the corresponding rupture for inward movement of the hinge; it is probably of the type XfPsAfAsR, i.e. a combination of a rupture XfP (Fig. 35E and Fig. 56B) for the lower part and a rupture AfAsR (Fig. 35F and Fig. 58D) for the upper part.

59. EARTH PRESSURE GRAPHS

591. Friction Angles 0° and 30°

The results of the calculations carried out in the preceding sections have been put together in Graphs 1-18 in the Appendix. Graphs 1-6 concern frictionless earth ($\varphi = 0^\circ$), Graphs 7-10 and 17-18 weightless earth ($\varphi = 30^\circ$) and Graphs 11-16 cohesionless, unloaded earth ($\varphi = 30^\circ$).

The dimensionless earth pressure constants indicated in the graphs are defined by the equations 4119-21 and 4703-04. So far, these constants have only been determined for the 3 special cases mentioned in Section 511, but in Section 61 it shall be shown, that it is usually a very good approximation to assume the law of superposition to be valid, provided that the friction angle is the same.

With the exception of Graphs 3, 9 and 13, in which the earth pressure factor is given as a function of the location of the pressure centre, all the dimensionless constants are given as functions of the location of the rotation centre (ξ).

In all the graphs, excepting Graphs 4, 10 and 14, which concern rough walls only, two sets of curves are given, one for a perfectly smooth, and one for a perfectly rough wall. In cases of imperfectly rough walls it should be possible to interpolate. Further, in Graphs 7-18 ($\varphi = 30^\circ$) curves are given both for positive and for negative rotation (see Section 472).

In Graphs 7-18 ($\varphi = 30^\circ$) we have, for the interval $1.25 < \xi < \infty$ and rough walls, assumed the rupture AfPfA to occur (indicated by dotted lines). We have first estimated the values of ρ, λ, λ^y and ρ^y (Graphs 7, 11, 16 and 18), which evidently cannot involve any important errors. On the basis of these values we have then found successively ω from 5904, η from 5905, θ from 5906 and ρ^x from 5103. Finally, the values of $\tan\delta$ (Graphs 10 and 14) have been estimated.

For the constants ρ, ρ^x, ρ^y and λ, λ^x, λ^y a logarithmic scale is used, enabling the determination of these constants with the same relative accuracy, independent of their absolute values.

For the quantities which may become infinite, i.e., ξ and ζ, a sort of "semi-inverse" scale is used (B. Jakobsson 1947). The two central quarters of

the axis represent the interval 0 to + 1 (points on the wall proper). The left quarter represents the interval + 1 to + ∞ (points above the wall) in such a way that, taking the distance 0-1 as the unit, the distance from the point + ∞ to a point ξ (> 1) is equal to $0.25 : (\xi - \frac{1}{2})$. Correspondingly, the right quarter represents the interval 0 to - ∞ (points below the wall) in such a way that the distance from the point - ∞ to a point ξ (< 0) is equal to $- 0.25 : (\xi - \frac{1}{2})$. Such a scale has the property that two parts of a smooth curve, which meet each other at a point corresponding to $\xi = 0$ or $\xi = 1$, will have the same tangent at this point.

592. Other Friction Angles

For friction angles other than 0° or 30° the earth pressure constants can be calculated by means of the methods and formulae indicated in the previous sections. This is rather troublesome, however, and we shall therefore in the following indicate a much simpler method, by means of which approximate results can be obtained by applying a simple correction to the values found from the graphs for $\varphi = 30°$.

When the passive and the active zone-ruptures are denoted by the superscripts p and a respectively, then the following approximate formulae are assumed to apply:

$$\log \frac{\rho}{\rho^a} = K \log \frac{\rho_{30}}{\rho^a_{30}} \qquad \log \frac{\lambda}{\rho^a} = K \log \frac{\lambda_{30}}{\rho^a_{30}} \qquad K = \log \frac{\rho^p}{\rho^a} : \log \frac{\rho^p_{30}}{\rho^a_{30}} \qquad 5901\text{-}03$$

ρ^p is given by 5209 (smooth wall) or 5211 (rough wall), assuming φ positive. ρ^a can be found by means of the same formulae, assuming φ negative. Some values are indicated in a table in Section 523. In the following table some values of the constants ρ^a and K are given. The subscripts s and r denote a smooth and a rough wall respectively.

φ	ρ^a_s	K_s	ρ^a_r	K_r
0	1.000	0.000	1.000	0.000
5	0.840	0.159	0.802	0.154
10	0.704	0.319	0.646	0.310
15	0.589	0.482	0.522	0.471
20	0.490	0.649	0.422	0.637
25	0.406	0.821	0.340	0.813
30	0.333	1.000	0.273	1.000
35	0.271	1.188	0.218	1.204
40	0.218	1.389	0.172	1.429
45	0.172	1.605	0.134	1.684

The procedure is now the following. Corresponding to the given value of ξ the constants ρ_{30}, ρ^x_{30}, ρ^y_{30} and λ_{30}, λ^x_{30}, λ^y_{30} are found from the graphs for $\varphi = 30°$. Further, for the given value of φ the constants ρ^a and K are taken from the table above. The same applies to ρ^a_{30}.

The constants ρ, ρ^x, ρ^y and λ, λ^x, λ^y are then calculated by means of 5901-02, which are assumed to be valid for all the above-mentioned constants. They can also be found by means of Graph 19 (smooth wall) or Graph 20 (rough wall).

Next, ω, η and θ are determined successively by means of the following equations, which are derived from 5101-04:

$$\omega = 1 - \sqrt{\frac{\lambda - \lambda^y}{\lambda^x - \lambda^y}} \qquad \eta = \tfrac{1}{3} + \tfrac{2}{3}\omega \, \frac{\lambda - \lambda^y}{\lambda} \qquad \theta = \tfrac{1}{2} + \tfrac{1}{2}\omega \, \frac{\rho - \rho^y}{\rho} \qquad 5904\text{-}06$$

Finally, if required, δ^p or δ^γ can be calculated approximately by means of the equation:

$$\tan \delta = \sqrt{3} \, \tan|\varphi| \, \tan \delta_{s0} \qquad 5907$$

Example 59a

As an example we shall consider the following case of positive rotation, active pressure and a rough wall (rupture A):

$i = j = 0$ $\quad p = c = a = 0$ $\quad \gamma = 1$ $\quad h = 1$ $\quad \varphi = \delta = -20^\circ$ $\quad \xi = 0.578$

Corresponding to this value of ξ, but for $\varphi = 30^\circ$, we find from Graphs 11 and 16 in the Appendix:

$$\lambda_{s0} = 0.350 \qquad \lambda^x_{s0} = 5.66 \qquad \lambda^y_{s0} = 0.215$$

From the table in Section 592 we find, for $\varphi = 20^\circ$ and a rough wall:

$$K_r = 0.637 \qquad \rho^a_r = 0.422 \qquad \rho^a_{s0} = 0.273$$

We get now, by means of equation 5902 (or Graph 20):

$$\log \frac{\lambda}{0.422} = 0.637 \log \frac{0.350}{0.273} = 0.069 \qquad \lambda = \underline{0.495}$$

$$\log \frac{\lambda^x}{0.422} = 0.637 \log \frac{5.66}{0.273} = 0.840 \qquad \lambda^x = \underline{2.92}$$

$$\log \frac{0.422}{\lambda^y} = 0.637 \log \frac{0.273}{0.215} = 0.066 \qquad \lambda^y = \underline{0.362}$$

Finally, equations 5904-05 give:

$$\omega = 1 - \sqrt{\frac{0.495 - 0.362}{2.92 - 0.362}} = \underline{0.773} \qquad \eta = \tfrac{1}{3} + \tfrac{2}{3} \times 0.773 \, \frac{0.495 - 0.362}{0.495} = \underline{0.472}$$

A correct calculation, carried out as described in Section 422, will give the following results, when λ^x is taken from the table in Section 523:

$\psi = -36.05^\circ$ $\quad \alpha = 60.0^\circ$ $\quad \nu = 0.218$ $\quad \beta = 74.95^\circ$ $\quad k = 1.036$

$\lambda = 0.501$ $\quad \eta = 0.484$ $\quad \lambda^x = 2.84$ $\quad \omega = 0.757$ $\quad \lambda^y = 0.351$

It will be seen that the agreement is fully satisfactory for practical purposes.

6. MORE COMPLICATED CASES

61. SUPERPOSITION

611. Frictionless Earth

In Section 5 we have, for frictionless earth ($\varphi = \delta = 0$), also assumed $\gamma = p = 0$. We shall now investigate what takes place when $\gamma \neq 0$ and $p \neq 0$. In the case of a horizontal ground surface ($i = 0$) equations 3414 and 3350 give:

$$\sigma' = p + c \cot(\beta+\alpha) \qquad \sigma'' = p + \gamma h + c \cot(\beta+\alpha) + ct^c \qquad 6101\text{-}02$$

This shows that the normal pressure has a "hydrostatic" component ($p + \gamma h$) and a component which is proportional to c. The latter we have investigated in Section 5.

If we consider the rupture-line, for which equilibrium exists when $\gamma = 0$ and $p = 0$, it is evident that equilibrium also exists when $\gamma \neq 0$ and $p \neq 0$, because when $i = 0$, the hydrostatic pressures in any line are in equilibrium with the loads G and P above the line, provided that corresponding hydrostatic pressures act between the wall and the earth. Therefore, we must have:

$$E = \tfrac{1}{2}\gamma h^2 + ph + ch\kappa \qquad Ez = \tfrac{1}{6}\gamma h^3 + \tfrac{1}{2}ph^2 + ch^2\kappa\zeta \qquad 6103\text{-}04$$

where κ and ζ have the values calculated in Section 5. By comparison with the general equations 4119-20 it will be seen that for $i = 0$ and $\varphi = 0$, we have $\lambda = \rho = 1$, $\eta = \frac{1}{3}$ and $\theta = \frac{1}{2}$.

It should be noted that this simple superposition of the γ-, p- and c-terms is only exact in the case of $i = 0$ and $\varphi = 0$.

612. Weightless Earth

In Section 5 we have, for weightless earth ($\gamma = 0$), also assumed $c = 0$. We shall now investigate what takes place when $c \neq 0$. In the case of a horizontal ground surface ($i = 0$), equations 3413 and 3318 give:

$$t' = (p + c \cot \varphi) \frac{\sin(\beta+\alpha+\varphi)}{\sin(\beta+\alpha)} - \frac{c}{\sin \varphi} \qquad 6105$$

$$t'' = (p + c \cot \varphi) \frac{\sin(\beta+\alpha+\varphi)}{\sin(\beta+\alpha)} t^t - \frac{c}{\sin \varphi} \qquad 6106$$

The corresponding normal and shear stresses are found by means of 3312-13:

$$\sigma'' = (p + c \cot \varphi) \frac{\sin(\beta+\alpha+\varphi)}{\sin(\beta+\alpha)} t^t \cos \varphi - c \cot \varphi \qquad 6107$$

$$\tau'' = (p + c \cot \varphi) \frac{\sin(\beta+\alpha+\varphi)}{\sin(\beta+\alpha)} t^t \sin \varphi \qquad 6108$$

This shows that the normal pressure has a constant component $-c \cot \varphi$ and a component which is proportional to $(p + c \cot \varphi)$. The shear stress has only the latter component. This component we have investigated in Section 5.

When $p = 1$ and $c = 0$, we know that, for a certain rupture-line, equilibrium exists between the surface load $h \cot \beta$, the normal earth pressure ρh, the tangential earth pressure $\rho h \tan \delta$ and the corresponding internal stresses in the rupture-line. Equilibrium still exists when all these loads and stresses are multiplied by $(p + c \cot \varphi)$, and also when $c \cot \varphi$ is subtracted from all the normal pressures. As, however, we get in this way the surface load $ph \cot \beta$, and the internal stresses defined by 6107-08, we have proved that equilibrium exists for the same rupture-line, also when $c \neq 0$. Consequently, we have:

$$E = \rho h (p + c \cot \varphi) - ch \cot \varphi \qquad Ez = \rho\theta h^2 (p + c \cot \varphi) - \tfrac{1}{2} ch^2 \cot \varphi \qquad 6109\text{-}10$$

$$F = \rho h (p + c \cot \varphi) \tan \delta^p \qquad 6111$$

In the above equations, c and φ should be assumed positive for passive pressure and negative for active pressure (p.58). However, as c and φ only occur in the product $c \cot \varphi$, we could as well assume them to be always positive. Comparing equations 6109-11 with the general expressions 4119-21, in which c is always positive (p.103), we find then the following relations:

$$\kappa = (\rho - 1) \cot|\varphi| \qquad \kappa\zeta = (\rho\theta - \tfrac{1}{2}) \cot|\varphi| \qquad 6112\text{-}13$$

$$\zeta = (\rho\theta - \tfrac{1}{2}) : (\rho - 1) \qquad a = c \cot \varphi \tan \delta^p \qquad 6114\text{-}15$$

By means of 6112-15 the quantities κ, ζ, a (for $\varphi \neq 0$) can be found from the values of ρ, θ, δ^p, calculated in Section 5 and indicated in the graphs. With regard to the tentative pressure diagram (Section 47) it is evident that, as we multiply the normal pressures with a constant factor and subtract a constant amount, ω does not change, whereas we get:

$$\kappa^x = (\rho^x - 1) \cot|\varphi| \qquad \kappa^y = (\rho^y - 1) \cot|\varphi| \qquad 6116\text{-}17$$

In the equations 6112-17, both φ and c should always be assumed positive, whereas δ^p and a may be positive or negative, according to the direction of the tangential earth pressure.

It should be noted that this simple superposition of the p- and c-terms is only exact in the case of $i = 0$ and $\gamma = 0$.

613. General Case

In the general case a superposition of the separately calculated γ-, p- and c-terms is only exact, if we have found the same rupture-line in each case. This condition is generally not fulfilled, except when we have $\beta = \alpha$ in each separate case.

However, in spite of this it is usually (for $i = 0$) a very good approximation, and on the safe side, to superpose the separately calculated γ-, p- and c-terms according to the following formulae (compare 4119-21 and 4703-04):

$$E = \tfrac{1}{2}\gamma h^2 \lambda + ph\rho + ch\kappa \qquad Ez = \tfrac{1}{2}\gamma h^3 \lambda\eta + ph^2\rho\theta + ch^2\kappa\zeta \qquad 6118\text{-}19$$

$$F = \tfrac{1}{2}\gamma h^2 \lambda \tan \delta^{\gamma} + (ph\rho + ch\kappa) \tan \delta^{p} + ah \qquad 6120$$

$$e_d^x = \gamma d\lambda^x + p\rho^x + c\kappa^x \qquad e_d^y = \gamma d\lambda^y + p\rho^y + c\kappa^y \qquad y = \omega h \qquad 6121\text{-}23$$

For $\varphi = 30^\circ$ the quantities λ, λ^x, λ^y, η, δ^{γ} and ρ, ρ^x, ρ^y, θ, δ^p can be taken from Graphs 7-18 in the Appendix, and the same applies to ω. The quantities κ, κ^x, κ^y, ζ, a cannot be taken from Graphs 1-6, which are valid for $\varphi = 0^\circ$ only, but must be calculated by means of 6112-17.

When $0^\circ \neq \varphi \neq 30^\circ$ we determine first the quantities λ, λ^x, λ^y, δ^{γ} and ρ, ρ^x, ρ^y, δ^p for $\varphi = 30^\circ$ (by means of the graphs), and then the corresponding values as well as η, θ, ω for the actual φ (by means of 5901-07). Finally, we calculate κ, κ^x, κ^y, ζ, a (by means of 6112-17).

Example 61a

As an example we shall consider the following case of positive rotation, active pressure and a rough wall (rupture A):

$i = j = 0$ $\qquad \varphi = \delta = -30^\circ$ $\qquad c = a = -0.5\ t/m^2$

$\gamma = 1\ t/m^3$ $\qquad p = 7\ t/m^2$ $\qquad h = 10\ m$ $\qquad \xi = 1$

By means of Graphs 7-18, and the formulae 6112-17 (with φ positive), we find the following constants:

$\lambda = 0.285$	$\eta = 0.455$	$\omega = 0.895$	$\lambda^x = 5.66$	$\lambda^y = 0.225$
$\rho = 0.320$	$\theta = 0.710$		$\rho^x = 1.60$	$\rho^y = 0.170$
$\kappa = -1.18$	$\zeta = 0.400$		$\kappa^x = 1.04$	$\kappa^y = -1.44$

With these values the formulae 6118-19 yield the following results (assuming c positive):

$$E = \tfrac{1}{2} \times 1 \times 10^2 \times 0.285 + 7 \times 10 \times 0.320 - 0.5 \times 10 \times 1.18 = \underline{30.7\ t/m}$$

$$Ez = \tfrac{1}{2} \times 1 \times 10^3 \times 0.285 \times 0.455 + 7 \times 10^2 \times 0.320 \times 0.710 - 0.5 \times 10^2 \times 1.18 \times 0.400 = \underline{200\ tm/m}$$

A correct calculation, carried out as described in Section 422, will give the following results:

$\alpha = 30^\circ$ $\beta = 60^\circ$ $k = 11.55$ m $E = 30.7$ t/m $Ez = 206$ tm/m

It will be seen that the agreement is very good in this case.

62. EFFECT OF WATER PRESSURES

621. Hydrostatic Water Pressures

If a ground water table is present, and if the same water level occurs at both sides of the wall, then the only effect of the water pressures will be to produce an uplift on the submerged parts of the soil and the wall. The water pressures proper on the two sides of a thin wall will cancel each other. In the calculation of the earth pressures the ground water table must be considered as an internal boundary, below which the effective weight of the earth should be equal to the submerged unit weight, i.e., reduced for uplift.

We denote by γ_w the specific gravity of the water ($\gamma_w = 1$ t/m^3), and by γ_s the specific gravity of the solid particles (usually $\gamma_s = 2.65$ t/m^3). Further, the porosity n is defined as the ratio between the volume of the voids and the total volume of the soil. We have then:

Total unit weight of dry earth:	$\gamma_{s+a} = (1-n)\gamma_s = \gamma$	6201
Total unit weight of saturated earth:	$\gamma_{s+w} = (1-n)\gamma_s + n\gamma_w = \gamma$	6202
Submerged unit weight of saturated earth:	$\gamma_{s+w-u} = (1-n)(\gamma_s-\gamma_w) = \gamma'$	6203

When different water levels exist on the two sides of the wall we must distinguish between hydrostatic and hydrodynamic water pressures. If the wall and its foundation are impermeable, the water pressures are hydrostatic, as in this case no ground water movements take place.

In the case of hydrostatic water pressures we can calculate the water pressures and the earth pressures (with submerged unit weights under the water table) separately and add the results. In the design of a structure both kinds of pressures must, of course, be considered together. If, for example, a sheet wall is to be designed for a differential water pressure, this pressure must be entered into the equilibrium conditions governing the design of the wall.

In fine-grained soils the capillary forces will cause the water to rise to a certain height h_c above the hydrostatic water table. We can, also in this case, consider the water pressures and the earth pressures separately, when the following facts are taken into account.

Above the normal ground water table negative water pressures occur, starting with zero and ending with $-\gamma_w h_c$ at the upper boundary of the zone of capillary water. In the calculation of the earth pressures the submerged unit weight should be used, not only below the ground water table but also in the whole zone

of capillary water. In addition, the effect of the capillary forces on the earth pressures must be considered by assuming a surcharge $p_c = \gamma_w h_c$ acting at the upper boundary of the zone of capillary water.

In coarse sand and gravel the problem of capillary rise can be disregarded completely, because h_c is very small. For fine sand and silt, however, it may be necessary to reckon as described above, when the soil is partly submerged.

In clay, considered as a frictionless material, the outlined method leads to exactly the same results as a simpler method consisting in assuming, above the normal ground water table, full unit weight and no water pressures. We can also disregard the water pressures below the water table when we reckon with the full unit weight of the soil, but in that case a possible water pressure on the other side of the wall must, of course, be taken into consideration.

622. Hydrodynamic Water Pressures

When different water levels exist at the two sides of a wall, and when the wall or its foundation is more or less permeable, ground water movements will occur, resulting in hydrodynamic water pressures.

In this case the water pressures can be determined by the construction of a flow net (Terzaghi 1947, Taylor 1948). Each small earth element will then, in addition to the gravity force and the hydrostatic uplift, which are both vertical, be subjected to a force proportional to the pressure gradient and acting in the direction of this gradient. As the latter force is generally neither constant nor vertical, this means that, strictly speaking, we cannot use any of our formulae, because they are all based on Kötter's equation, which presumes the mass forces to be constant and vertical.

However, many problems involving hydrodynamic water pressures can be solved approximately by means of the methods and formulae developed in the present work. For this purpose we need only assume that the pressure gradient is constant and vertical. As this is usually a rather crude approximation there would be no point in calculating the corresponding water pressures very accurately. Therefore, the approximate calculation is proposed to take place in the following way.

By means of a rough flow net we determine an approximate value of the average hydraulic gradient for each side of the wall. The gradient i is assumed positive when it is directed downwards, otherwise negative. Further, this gradient is assumed to have two effects when, as usual, we consider water pressures and earth pressures separately. First, it increases the effective unit weight of the soil proper by an amount $i\gamma_w$ and, second, it decreases the effective unit weight of the water in the ground by the same amount $i\gamma_w$. Thus we have:

Effective unit weight of earth: $$\gamma_{s+w-u+i} = (1-n)(\gamma_s-\gamma_w) + i\gamma_w = \gamma'' \qquad 6204$$

Effective unit weight of water: $$\gamma_{w-i} = (1-i)\gamma_w = \gamma''_w \qquad 6205$$

In clay, considered as a frictionless material, the two above-mentioned effects will cancel each other. Here we can, therefore, disregard the hydrodyna-

mic water pressures and reckon either with hydrostatic water pressures and submerged unit weight of the soil or (as explained in Section 621) with no water pressures at all but full unit weight of the soil.

63. STRATIFIED EARTH

631. Line-Rupture

We shall now investigate the case of stratified or layered earth. In the present Section 63, we shall consider horizontal layers and a vertical wall, but, in principle, similar investigations can be made for layers and walls with any inclination.

Fig.63A shows a simple line-rupture through two different layers. The upper layer is characterized by the constants γ_1, c_1, a_1, and the lower layer by γ_2, c_2, a_2. On top of the upper layer acts a surcharge p_1, and at the internal boundary may act, in the case of capillary pressures (Section 621), another surcharge $p_2 = \gamma_w h_c$.

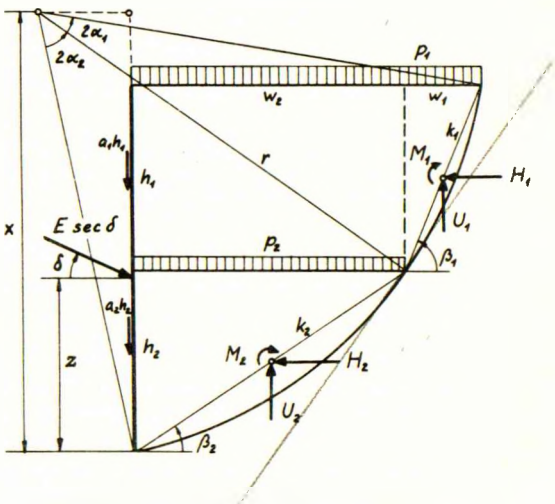

Fig.63A: Line-rupture in stratified earth

We have seen in Section 346, that we can only solve the problem when all layers have the same friction angle. We assume, therefore, that we have $\varphi_1 = \varphi_2 = \varphi$ and $\delta_1 = \delta_2 = \delta$. At the point where the rupture-line intersects the internal boundary the boundary condition 3437 must be used.

From Fig.63A the following geometrical relations may be derived:

$$\cot \beta_2 = \left[\frac{2x}{h_2} - 1\right] \tan \alpha_2 \qquad \beta_1 = \beta_2 + \alpha_2 + \alpha_1 \qquad 6301\text{-}02$$

$$\cos(2\alpha_1+\beta_2+\alpha_2) = \cos(\beta_2+\alpha_2) - \frac{2h_1}{h_2} \sin \alpha_2 \sin \beta_2 \qquad 6303$$

h_1, h_2 and x are given quantities. With a chosen value of α_2 we find successively β_2 from 6301, α_1 from 6303 and β_1 from 6302. k_1 and k_2 are as usual determined by 3217, whereas w_1 and w_2 are found by means of 3219.

As we do not know the stresses in the internal boundary, we have only 3 statical equilibrium conditions, viz. for the whole earth mass above the rupture-line. We have already one unknown quantity (α_2) and can consequently determine only two more, viz. the magnitude of the total earth pressure (E) and the loca-

tion of its pressure centre (z). We use the equations 4105 and 4116-18 which, with j = 0, yield:

$$(H_1 + H_2) \tan \delta - U_1 - U_2 + a_1 h_1 + a_2 h_2 = 0 \qquad 6304$$

$$E = H_1 + H_2 \qquad F = E \tan \delta + a_1 h_1 + a_2 h_2 \qquad 6305\text{-}06$$

$$Ez = \tfrac{1}{2} h_2 (E + F \cot \beta_2) + \tfrac{1}{2} H_1 (h_1 + h_2) + \tfrac{1}{2} U_1 (w_1 + w_2) - M_{G_1} - M_{G_2} - M_{R_1} - M_{R_2} \qquad 6307$$

U_1 and U_2 are defined by 4102. When 6304 is satisfied, α_2 has been chosen correctly and we find then E, F and z from 6305-07. If $\beta_2 - \alpha_2 < 0$, we must, instead of satisfying 6304, assume $\beta_2 = \alpha_2$, in which case this angle is found direct from 6301. 6306 is then useless, whereas 4114 yields F.

The described procedure is somewhat cumbersome, and we shall therefore in the following show that the effects of the stratification can be taken into account in a much simpler, although approximate way, viz. by a modification of our tentative pressure diagram. The correctness of this procedure shall be investigated by means of examples.

632. Frictionless Layers

In Section 611 it has been shown that for i = 0 and $\varphi = 0$ the pressures corresponding to $\gamma = p = 0$ can simply be added to the "hydrostatic" pressures ($\gamma h + p$). This result is evidently also correct when the earth consists of horizontal layers with different unit weights but with the same cohesion.

Our tentative pressure diagram for $\varphi = 0$ is normally constructed by adding to the hydrostatic pressure an amount $c\kappa^x$ above a point at the height $y = \omega^o h$, and an amount $c\kappa^y$ below this point. In the case of layers with different cohesions it is proposed to do exactly the same, but to use in the different layers the respective values of c (see Fig. 63B). In the n' th layer from the surface we have thus either the pressure:

$$e_n^x = \sum_1^{n-1} \gamma_m h_m + \gamma_n d_n + \sum_1^n p_m + \kappa^x c_n \qquad 6308$$

or a pressure e_n^y, which is determined by 6308 with superscripts y. The depth d_n is measured from the surface of the n' th layer.

The pressures e^x occur above, and e^y below, a pressure jump, which is located at a distance $y = \omega^o h$ from the foot of the wall. Other pressure jumps will occur at the boundaries between the different layers, unless the cohesion is constant.

If the cohesion c varies with the depth according to a certain theoretical or empirical law, the pressure diagram is constructed by adding to the hydrostatic pressure at any depth, the value of c at this depth multiplied by κ^x or κ^y respectively.

It is easy to show that the proposed procedure leads to the correct result in the special case of an R- or S-rupture and a smooth wall, but in general it is an approximation only.

Example 63a

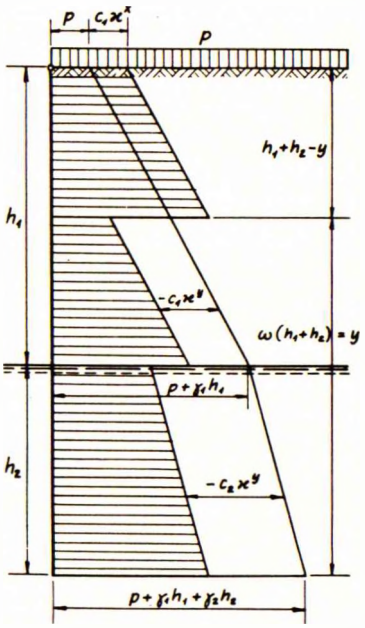

Fig.63B: Stratified frictionless earth

As an example we shall consider the following case of positive rotation, active pressure and a smooth wall rotating about its top (rupture A):

$h_1 = 5.3$ m $\quad \gamma_1 = 1.6$ t/m^3 $\quad c_1 = 1.0$ t/m^2

$h_2 = 3.7$ m $\quad \gamma_2 = 0.8$ t/m^3 $\quad c_2 = 1.6$ t/m^2

$p_1 = 2$ t/m^2 $\quad p_2 = 0$ $\quad a = 0$ $\quad \varphi = 0$ $\quad \xi = 1$

By means of Graphs 5-6 we find for $\xi = 1$ and a smooth wall:

$\omega^o = 0.705$ $\quad \kappa^x = 2$ $\quad \kappa^y = -3.22$

The corresponding pressure diagram is shown to scale in Fig. 63B. We find by means of 6123 and 6308:

$$y = 0.705\ (5.3 + 3.7) = 6.35 \text{ m}$$

$$e_1^x = 1.6\ d_1 + 2 + 2 \times 1.0 = 1.6\ d_1 + 4 \quad (t/m^2)$$

$$e_1^y = 1.6\ d_1 + 2 - 3.22 \times 1.0 = 1.6\ d_1 - 1.22 \quad (t/m^2)$$

$$e_2^y = 1.6 \times 5.3 + 0.8\ d_2 + 2 - 3.22 \times 1.6 = 0.8\ d_2 + 5.33 \quad (t/m^2)$$

For this pressure diagram we find:

E = 55.1 t/m $\quad$ Ez = 232 tm/m

If a correct calculation is carried out as described in Section 631, we get:

$\alpha_1 = \alpha_2 = 16^o$ $\quad \beta_1 = 74^o$ $\quad \beta_2 = 42^o$ $\quad k_1 = k_2 = 5.52$ m

E = 57.9 t/m $\quad$ Ez = 239 tm/m

The agreement may be considered satisfactory for practical purposes.

633. Layers with the Same Friction Angle

In the case of i = 0 and p = c = 0 our tentative pressure diagram is normally constructed by multiplying the hydrostatic pressure by a factor λ^x above a point at the height y = ωh, and by a factor λ^y below this point. In the case of layers with different unit weights, but with the same friction angle, it is proposed to do exactly the same (see Fig. 63C).

If surcharges p are present they are multiplied by the factor ρ^x or ρ^y, whereas the remaining part of the hydrostatic pressure is multiplied by λ^x or λ^y.

If the layers have also different cohesions, these are taken into account in the same way as for frictionless earth, but the corresponding factors κ^x and κ^y must be found from 6116-17. In the n'th layer from the surface we have thus either the pressure:

$$e_n^x = \lambda^x \left[\sum_1^{n-1} \gamma_m h_m + \gamma_n d_n \right] + \rho^x \sum_1^n p_m + \kappa^x c_n \qquad 6309$$

or a corresponding pressure e_n^y. The main pressure jump is located at a distance $y = \omega h$ from the foot of the wall.

It is easy to show that the proposed procedure leads to the correct result in the special case of an R- or S-rupture and a smooth wall, but in general it is an approximation only.

Example 63b

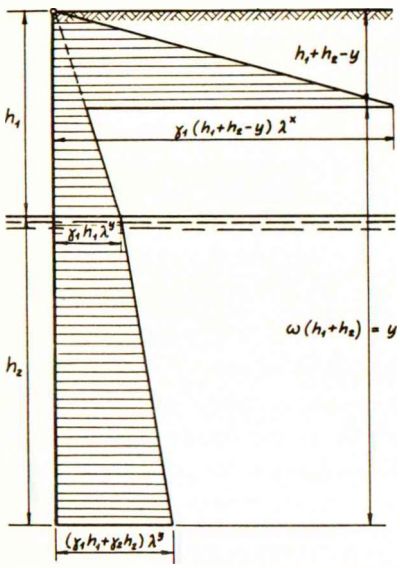

Fig.63C: Stratified cohesionless earth

As an example we shall consider the following case of positive rotation, active pressure and a smooth wall rotating about its top (rupture A) :

$h_1 = 3.7$ m $\quad \gamma_1 = 1.8$ t/m^3 $\quad \varphi = 30^\circ$ $\quad \xi = 1$

$h_2 = 5.5$ m $\quad \gamma_2 = 1.0$ t/m^3 $\quad p = c = a = \delta = 0$

By means of Graphs 15-16 we find for $\xi = 1$ and a smooth wall:

$\omega = 0.815$ $\quad \lambda^x = 3$ $\quad \lambda^y = 0.260$

The corresponding pressure diagram is shown to scale in Fig.63C. We find by means of 6123 and 6309:

$$y = 0.815\ (3.7 + 5.5) = 7.50 \text{ m}$$

$$e_1^x = 3 \times 1.8\ d_1 = 5.4\ d_1 \ (\text{t/m}^2)$$

$$e_1^y = 0.260 \times 1.8\ d_1 = 0.468\ d_1 \ (\text{t/m}^2)$$

$$e_2^y = 0.260\ (1.8 \times 3.7 + 1.0\ d_2)$$
$$= 0.260\ d_2 + 1.73 \ (\text{t/m}^2)$$

For this pressure diagram we find:

E = 23.8 t/m $\qquad$ Ez = 113 tm/m

If a correct calculation is carried out as described in Section 631, we get:

$\alpha_1 = 8^\circ$ $\quad \alpha_2 = 13.5^\circ$ $\quad \beta_1 = 82^\circ$ $\quad \beta_2 = 60.5^\circ$ $\quad k_1 = 3.75$ m $\quad k_2 = 6.30$ m

E = 23.0 t/m $\qquad$ Ez = 110 tm/m

The agreement will suffice for practical purposes.

634. Layers with Different Friction Angles

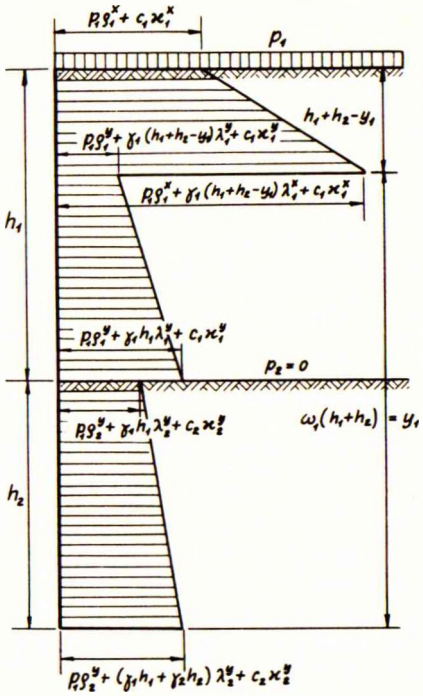

Fig.63D: General case of stratified earth

In the case of layers with different friction angles it is not possible to carry out an "exact" calculation by means of the present theory. The reason is explained in Section 346. However, as this case is often encountered in practice, the following tentative solution is proposed (see Fig. 63D).

A pressure diagram is constructed by multiplying the hydrostatic pressures by λ^x or λ^y (for the γ-terms) respectively by ρ^x or ρ^y (for the p-terms). Possible cohesions are multiplied by κ^x or κ^y and are added. For each separate layer the respective values of the different constants are used. In the n'th layer from the surface we have thus, either the pressure:

$$e_n^x = \lambda_n^x \left[\sum_1^{n-1} \gamma_m h_m + \gamma_n d_n \right] + \rho_n^x \sum_1^n p_m + \kappa_n^x c_n \qquad 6310$$

or a pressure e_n^y, which is determined by 6310 with superscripts y. The depth d_n is measured from the surface of the n'th layer.

The pressures e^x occur above, and e^y below a pressure jump, which is located at a distance y from the foot of the wall. In order to determine y we first calculate the different values $y_n = \omega_n h$, all corresponding to the same $\xi = x : h$, but to the different friction angles φ_n. Only such pressure jumps, which prove to be located in the layer to which the corresponding φ and ω belong, are assumed to actually occur.

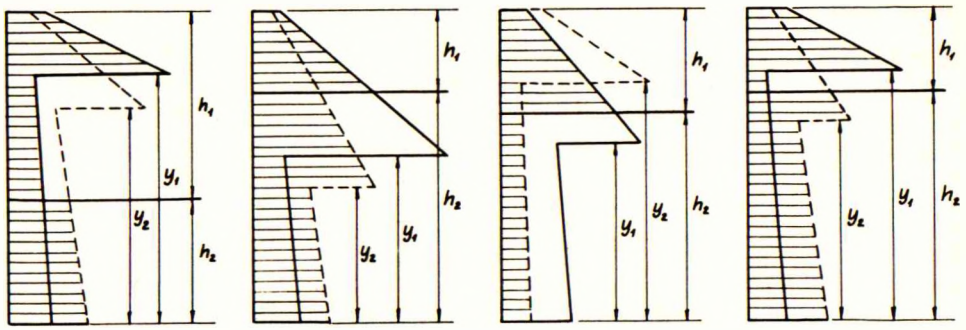

Fig.63E: Different pressure diagrams for stratified earth

Usually, only one pressure jump fulfils this condition, but in special cases two may occur, or none at all. Fig.63E illustrates these possibilities for the case of two different layers. The pressure diagrams corresponding to the constants of the upper layer are shown in unbroken lines, whereas those corresponding to the constants of the lower layer are shown in dotted lines. In addition to the pressure jumps mentioned above, other pressure jumps will occur at the boundaries between the different layers, unless φ and c are constant.

64. PARTLY UNSUPPORTED EARTH FRONT

641. General

In Section 5 it has been assumed that the earth particles next to the wall must have the same normal movements as the wall, although they may have other tangential movements. This assumption is evidently correct for cohesionless earth, but for earth with cohesion the possibility exists that part of the earth front can stand unsupported while the wall moves away from it.

However, there is some evidence that this is a theoretical possibility only, and that actually the earth will follow the wall completely, even when it has cohesion (Tschebotarioff 1948). Therefore, we shall generally consider it a sufficiently good approximation to use the results found in Section 5, also in the case of earth with cohesion. In order to be on the safe side we shall, however, disregard possible negative pressures between wall and earth.

On the other hand, when the earth is able to stand unsupported to a considerable height, it may be of interest to investigate the special ruptures which will occur when part of the earth front does not follow the wall.

If the upper part of the wall moves away from the earth (neg. rot.), we may get ruptures of the types RsA, PsA (Fig. 35D), Aw (Fig. 35G) or AwRsA, AwPsA, AaRsA, AaPsA (Fig. 35F).

If the lower part of the wall moves away from the earth (pos. rot.), we may get ruptures of the types AsR, AsP (Fig. 35D) or wR, wP (Fig. 35G).

A rupture RsA, PsA, AsR or AsP can, if required, be calculated as described in Section 463. The ruptures AaRsA, AaPsA, AwRsA and AwPsA can in principle be dealt with in a similar way as the simpler ruptures AaR, AaP, AwR and AwP. However, in all these cases the result of the calculation will, to a considerable extent, depend on the actual relation between γh, p and c, as the law of superposition is not even approximately valid for cases of unsupported earth fronts.

Only for the ruptures wR, wP and Aw can general results be derived. We will therefore investigate these ruptures, but shall for the sake of simplicity confine ourselves to the case of frictionless earth, a vertical wall and a horizontal ground surface.

642. Ruptures wR and wP

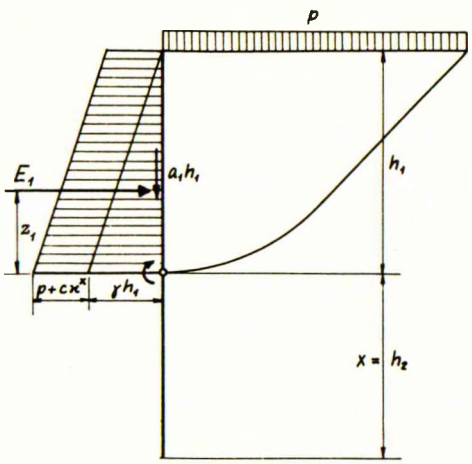

Fig.64A: Rupture wZ

A rupture wZ is shown in Fig.64A. It occurs only for positive rotation and $0 < \xi < 1$. The rupture wR occurs when the wall is smooth, and the rupture wP when it is rough. We have:

$$h_2 = x \qquad h_1 = h - x \qquad 6401\text{-}02$$

On the lower part of the wall the earth pressure is zero, and for the upper part we have:

$$e_d^x = \gamma d + p + c\kappa^x \qquad 6403$$

$$E_1 = \tfrac{1}{2}\gamma h_1^2 + ph_1 + ch_1\kappa^x \qquad 6404$$

$$E_1 z_1 = \tfrac{1}{6}\gamma h_1^3 + \tfrac{1}{2}ph_1^2 + \tfrac{1}{2}ch_1^2\kappa^x \qquad 6405$$

where $\kappa^x = 2$ for rupture wR (smooth wall), whereas $\kappa^x = 2.57$ for rupture wP (rough wall). The pressure distribution is shown in Fig.64A.

643. Rupture Aw

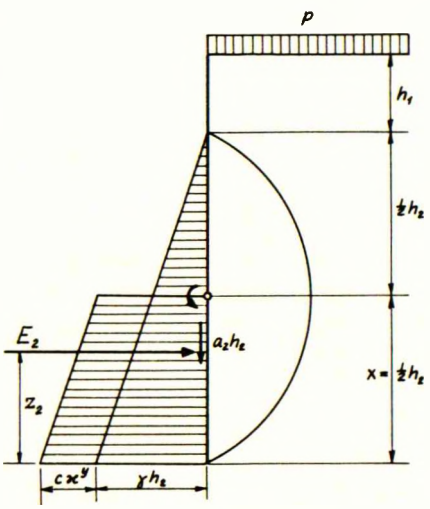

Fig.64B: Rupture Aw

The rupture Aw is shown in Fig.64B. It occurs only for negative rotation and $0 < \xi < \frac{1}{2}$. (Actually, the upper limit must be lower than $\xi = \frac{1}{2}$, as for small values of h_1 the tensile strength of the material will be exceeded between the ground surface and the upper part of the rupture-circle.) We have:

$$h_2 = 2x \qquad h_1 = h - 2x \qquad 6406\text{-}07$$

On the upper part of the wall the earth pressure is zero, and on the lower part we can calculate it as for a line-rupture. However, as mentioned in Section 462, we must assume $p = 0$, $i = 90^\circ$ and $\beta_2 = 90^\circ$, because the A-line ends at the free vertical earth front. We get then from 3412:

$$\sigma_2 = c \cot \alpha_2 \qquad 6408$$

By insertion of 6408 in 3353, and of this as well as 3208 in 4204 we get (with $j = \delta = 0$ and $i = \beta_2 = 90^\circ$):

$$c\, V_2^{cx} - a_2 = 0 \qquad 6409$$

For a smooth wall ($a_2 = 0$) 6409 gives $\alpha_2 = 66.8^\circ$, with which 4207-09 yield:

$$E_2 = \tfrac{1}{2}\gamma h_2^2 + 2.76\, ch_2 \qquad E_2 z_2 = \tfrac{1}{6}\gamma h_2^3 + 0.690\, ch_2^2 \qquad 6410\text{-}11$$

For a rough wall ($a_2 = c$) 6409 gives $\alpha_2 = 90^\circ$, with which 4207-09 yield:

$$E_2 = \tfrac{1}{2}\gamma h_2^2 + 3.14\, ch_2 \qquad E_2 z_2 = \tfrac{1}{6}\gamma h_2^3 + 0.785\, ch_2^2 \qquad 6412\text{-}13$$

The above results correspond to a pressure distribution as shown in Fig. 64B. We have, above and below the rotation centre respectively:

$$e_d^x = \gamma(d - h_1) \qquad e_d^y = \gamma(d - h_1) + c\kappa^y \qquad 6414\text{-}15$$

where $\kappa^y = 5.52$ for a smooth wall and $\kappa^y = 6.28$ for a rough wall.

65. SLOPING SURFACE AND INCLINED WALL

651. Rupture P

In the case of a sloping surface (angle i with the horizon) and/or an inclined wall (angle j with the vertical), a zone-rupture is generally of the type P. Only in special cases may we get the rupture R, viz., when v' from 3405 is equal to v'' from 3419.

If the lowest rupture-line is approximated by one straight line, we get, for cohesionless earth, the usual formulae 2105-06 from Coulomb's theory. However, this is somewhat (for passive pressures, considerably) on the unsafe side, and in the general case $c \neq 0 \neq \varphi$ the results become rather complicated.

When the rupture-line is approximated by two straight lines with a circle in between, we can find rather reliable results in any separate case (Section 431), but general formulae cannot be derived. Therefore, we shall develop in another way a set of general and comparatively simple formulae, which are approximate but more accurate than Coulomb's and usually on the safe side.

The actual rupture-line makes, with the horizon, an angle v' at the surface, and an angle v'' at the wall. These angles are in the general case determined by 3405 and 3419 respectively.

The stress t' at the surface is determined by 3411 (with $\beta + \alpha = v'$), and the stress t'' at the wall can be found by one or more applications of 3318, if the chord lengths in the rupture-line are known. Finally, e_f can be calculated from t'' by means of 3423 (with $\beta - \alpha = v''$). In this way we get the following equation for e_f:

$$e_f = \frac{\cos\delta\cos(v''-j)}{\cos(v''+\varphi+\delta-j)}\left[\gamma K + \frac{c(t^t-1)}{\sin\varphi}\right] + \frac{\cos\delta\sin(v''+\varphi-j)}{\cos(v''+\varphi+\delta-j)}(c+a)$$

$$+ \frac{t^t\cos\delta\cos(v''-j)}{\cos(v''+\varphi+\delta-j)\sin(v'-i)}\left[p\sin(v'+\varphi) + c\cos(v'+\varphi-i)\right] \qquad 6501$$

where K is a function of the geometrical parameters of the rupture-line.

Comparing 6501 with 4125 (in which c is always positive) and using 3418 as well as 3319 (with $2\alpha = v' - v''$) we can find the following general formulae:

$$\rho = \frac{\cos\delta\sin(v'+\varphi)\cos(v''-j)}{\sin(v'-i)\cos(v''+\varphi+\delta-j)}\, e^{2\mu(v'-v'')} \qquad 6502$$

$$\kappa = \left[\rho\frac{\sin(v'+\varphi-i)}{\sin(v'+\varphi)} - 1\right]\cot|\varphi| \qquad 6503$$

As the exponential function in 6502 is equal to t^t (3319), it can, for $\varphi = \pm 30^\circ$, be taken from Tables 2-3 in the Appendix, assuming $\alpha = \frac{1}{2}(v'-v'')$.

Equations 6502-03 are exact, apart from the possible approximation involved in using 3418. However, as we do not know the chord lengths in the rupture-line, we cannot find an exact general expression for λ.

In the simple case of one straight rupture-line, we would have $v' = v'' = \beta$, $t^t = 1$ and $K = k\sin(\beta+\varphi)$. Using also 3202 we find, by comparing 6501 with 4125, the following relation, which is exact for a straight rupture-line, and may be used as an approximation, when the rupture-line is not straight:

$$\lambda = \rho\cos(j-i) \qquad 6504$$

In order to obtain an idea of the error involved in using 6504, we note that this equation yields $\lambda = \rho$ for $i = j = 0$. In Sections 522-23 we have, for $\varphi = 30^\circ$ and a rough wall, found $\rho^a = 0.273$ and $\lambda^a = 0.266$, as well as $\rho^p = 5.03$ and $\lambda^p = 5.66$. This shows that the error is insignificant for active pressures, whereas it is of the order of 10% (on the safe side) for passive pressures. For comparison it may be mentioned that Coulomb's formula (2106) yields $\rho^a = \lambda^a = 0.257$ and $\rho^p = \lambda^p = 8.75$.

In the special case of cohesionless earth ($c = a = 0$), the angles v' and v'' are determined by 3408 and 3419:

$$\cos(2v'+\varphi-i) = -\frac{\sin i}{\sin\varphi} \qquad \cos(2v''+\varphi+\delta-2j) = \frac{\sin\delta}{\sin\varphi} \qquad 6505\text{-}06$$

In the special case of frictionless earth ($\varphi = \delta = 0$) the angles v' and v'' are determined by 3409 and 3420, whereas 6502-03 are transformed as follows:

$$\cos(2v'-2i) = -\frac{p}{c}\sin i \qquad \cos(2v''-2j) = \frac{a}{c} \qquad 6507\text{-}08$$

$$\rho^o = \frac{\sin v'}{\sin(v'-i)} \qquad \pm\kappa^o = 2(v'-v'') + \cot(v'-i) + \sin(2v''-2j) \qquad 6509\text{-}10$$

In all the above equations 6501-10, positive values of μ, φ, δ, c and a should be used for passive zone-ruptures (pos. rot.), whereas negative values must be used for active zone-ruptures (neg. rot.). Only in 6503 is the last φ, as indicated, always to be assumed positive. Of the double sign in 6510 the upper one is valid for passive pressure, and the lower one for active pressure.

As for other zone-ruptures, we may assume that we have $\eta = \frac{1}{3}$ and $\theta = \zeta = \frac{1}{2}$.

652. Rupture SfP

This rupture may occur for a "normal" translation of a rough wall, but for passive pressure only. If we assume that we have, as for a zone-rupture, $\eta = \frac{1}{3}$ and $\theta = \zeta = \frac{1}{2}$ (compare Sections 562-63), the actual value of δ is equal to $\psi - \varphi$ (4328). In order to calculate ρ, κ and λ for the rupture SfP, we need then only insert this value of δ in 3419 and 6502-04.

However, a still simpler, and probably also more accurate, solution may be obtained, if we are interested in λ only. For $i = j = 0$, $p = c = 0$ and $\varphi = 30^\circ$ we have investigated the rupture XfP (Section 563) and have found that λ for rupture SfP (5.16) is very nearly equal to ρ for rupture P (5.03). We shall assume this to be approximately correct for other values of i, j and φ also, but according to 6504 we shall multiply by cos(j-i). Consequently, λ for rupture SfP may be determined approximately by 6502 and 6504 with $\delta = \varphi$.

Example 65a

As an example we shall, for a sloping surface, determine λ corresponding to a translation of a rough wall (passive rupture SfP). The given quantities are:

$$i = -20^\circ \qquad j = 0 \qquad \varphi = 30^\circ \qquad p = c = 0 \qquad \xi = \infty$$

We find, by means of 6505-06 with $\delta = \varphi$:

$$\cos(2v' + 30^\circ + 20^\circ) = 0.342 : 0.5 = 0.684 \qquad v' = -1.5^\circ$$

$$\cos(2v'' + 30^\circ + 30^\circ) = 1 \qquad v'' = -30^\circ$$

Finally, 6502 and 6504 give, with $\delta = \varphi$:

$$\rho = \frac{0.866 \times 0.477 \times 0.866}{0.317 \times 0.866} e^{2 \times 0.577 \times 28.5 \times \pi : 180} = 2.32$$

$$\underline{\lambda} = 2.32 \times 0.940 = \underline{2.18} \qquad \eta = \tfrac{1}{3}$$

7. PRACTICAL EARTH PRESSURE PROBLEMS

71. RETAINING WALLS

711. General

We consider here the general case of a retaining wall with an inclined back which makes an angle j with the vertical (Fig. 71A). The ground has a sloping surface, making an angle i with the horizon, and is loaded by a vertical surcharge p per unit area of the sloping surface. i and j should be given their proper signs; in Fig. 71A they are both positive.

A retaining wall, which is founded direct on the ground, will, as explained in Example 36f, in the state of failure rotate about a point below its base. The same will usually be the case, if the wall is founded on piles. This means that the rupture-figure in the backfill will usually be of the type P or, in special cases, R. As the pressure is active, we have the following expressions for the earth pressures on the back of the wall (homogeneous earth):

$$e_d^a = \gamma d\lambda^a + p\rho^a + c\kappa^a \qquad f_d^a = e_d^a \tan \delta^a + a^a \qquad 7101\text{-}02$$

$$E^a = \tfrac{1}{2}\gamma h^2\lambda^a + ph\rho^a + ch\kappa^a \qquad F^a = E^a \tan \delta^a + ha^a \qquad 7103\text{-}04$$

$$E^a z^a = \tfrac{1}{6}\gamma h^3\lambda^a + \tfrac{1}{2}ph^2\rho^a + \tfrac{1}{2}ch^2\kappa^a \qquad 7105$$

Earth with cohesion is able to stand unsupported to a certain critical height h^c, which can be determined approximately by putting $E^a = 0$ in 7103 and using the constants for a smooth wall:

$$h^c = -\frac{p\rho_s^a + c\kappa_s^a}{\tfrac{1}{2}\gamma\lambda_s^a} \qquad 7106$$

According to 7101, negative pressures may be found on the upper part of the wall to a depth d°, which is determined by putting $e_d^a = 0$ in 7101:

$$d^\circ = -\frac{p\rho^a + c\kappa^a}{\gamma\lambda^a} \qquad 7107$$

In order to be on the safe side, it is recommended that such negative pressures be disregarded, in which case we find (for homogeneous earth):

$$E^a = \tfrac{1}{2}\gamma\lambda^a(h-d^o)^2 \qquad z^a = \tfrac{1}{3}(h-d^o) \qquad F^a = E^a \tan\delta^a + a^a(h-d^o) \qquad 7108\text{-}10$$

In the formulae 7101-10, the cohesion c should be assumed positive, whereas κ^a, δ^a and a^a are negative. For a smooth wall we must put $\delta^a = a^a = 0$, and for a rough wall $\delta^a = -|\varphi|$ and $a^a = -|c|$. For an imperfectly rough wall intermediate values may be used.

If the inclination of the back of the wall exceeds the inclination of the pseudo-rupture-lines in a Rankine zone, an elastic zone will occur immediately behind the wall, and behind this zone we will have an R-zone bounded by two straight rupture-lines through the lower rear edge of the wall. In this case we consider the elastic zone as a part of the wall and calculate the earth pressure on its rear boundary as for a perfectly rough wall.

In cohesive earth, the tensile stresses in the upper layers may cause the formation of open cracks in the earth or between the wall and the earth. If surface water enters such a crack, the wall will be subjected to water pressures, for which it is usually not designed. In order to avoid this, suitable drainage should be provided behind the wall, or the ground surface should be covered with an impervious layer.

In a rational design, the foundation of the wall also should be investigated for the state of failure, and in that case the earth pressures on the wall should be calculated with values of φ and c, to which appropriate safety factors have been applied as described in Section 372.

However, as foundation pressure problems are not dealt with in the present work, they must, for the time being, be treated by means of the conventional methods, and in that case the earth pressures on the wall should be calculated with the actual values of φ and c. Correspondingly, ordinary allowable stresses should be used in the design of the wall sections.

712. Sloping Surface and Inclined Back

In the general case of $i \neq 0 \neq j$ the procedure is to determine first v' and v'' by means of 3405-07 and 3419. The constants ρ^a, κ^a and λ^a are then calculated by means of 6502-04.

In the special case of frictionless earth ($\varphi = 0$), the formulae 6507-10 are used, and in the other special case of cohesionless earth ($c = 0$), the formulae 6505-06, together with 6502 and 6504.

As the pressure is active, negative values of μ, φ, δ, c and a should be inserted in all these formulae, and in 6510 the lower one of the double signs should be used.

Example 71a

As an example, we shall consider an angle-shaped retaining wall with counterforts as shown in Fig. 71A. The earth between the counterforts will follow the wall in its movements and must, therefore, be considered as a part of the wall. Correspondingly, we must consider a plane

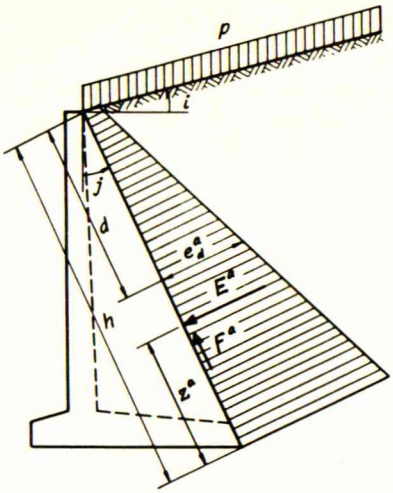

Fig.71A: Retaining wall

through the back of the counterforts as the "back" of the wall. As this plane goes mainly through earth it must be assumed perfectly rough. The fill is clayey sand with a friction angle of 25° and a cohesion of 0.5 t/m^2. The given quantities are:

$h = 5$ m $\quad i = 15^\circ \quad j = 25^\circ \quad p = 2$ t/m^2

$\gamma = 1.8$ t/m^3 $\quad \varphi = \delta = -25^\circ \quad c = a = -0.5$ t/m^2

Equation 3405 yields:

$$-0.5 \times 0.906 \times 0.259 \sin(2v' - 25^\circ - 15^\circ) + 2 \times 0.259$$
$$+ (-2 \times 0.422 - 0.5 \times 0.906 \times 0.965) \cos(2v' - 25^\circ - 15^\circ) =$$
$$-0.117 \sin(2v' - 40^\circ) - 1.281 \cos(2v' - 40^\circ) + 0.518 = 0$$

By means of 3406-07 we find $v' = 55.8^\circ$. For a perfectly rough wall 3419 is reduced to 3422 which yields $v'' = 50^\circ$. We get then successively from 6502-04:

$$\rho^a = \frac{0.906 \times 0.512 \times 0.906}{0.653 \times 0.906} e^{-2 \times 0.466 \times 5.8 \times \pi : 180} = \underline{0.645}$$

$$\kappa^a = \left[\frac{0.645 \times 0.273}{0.512} - 1\right] \times 2.14 = \underline{-1.40} \qquad \lambda^a = 0.645 \times 0.985 = \underline{0.635}$$

The corresponding unit earth pressures are found from 7101-02 (with c positive):

$$e_d^a = 1.8 \times d \times 0.635 + 2 \times 0.645 - 0.5 \times 1.40 = 1.14\, d + 0.59 \ (t/m^2)$$

$$f_d^a = -(1.14\, d + 0.59) \times 0.466 - 0.5 = -0.53\, d - 0.77 \ (t/m^2)$$

whereas 7103-05 give: $\underline{E^a = 17.2 \text{ t/m}} \qquad \underline{F^a = -10.5 \text{ t/m}} \qquad \underline{z^a = 1.81 \text{ m}}$

For comparison it may be mentioned, that a graphical extreme-calculation according to Coulomb's method has given $E^a = 17.6$ t/m.

713. Horizontal Surface and Vertical Back

For the case of $i = j = 0$, the constants $\rho_s = \lambda_s$ (smooth wall) are given by 5209 or 5216, whereas ρ_r and λ_r (rough wall) are given by 5211 and 5223 respectively. For active pressure, negative values of φ must be used in these formulae. Some values of the constants are given in a table in Section 523. If required, κ can be calculated by means of 6112.

For the critical height h^c of a vertical bank, we find by inserting 5209, 5216 and 6112 in 7106 (and changing the sign of φ) the equation:

$$h^c = \frac{1}{\gamma}\left[4c \tan(45^\circ + \tfrac{1}{2}\varphi) - 2p\right] \qquad 7111$$

in which positive values of φ and c should be used.

In the special case of frictionless earth ($\varphi = 0$) we have $\rho^a = \lambda^a = 1$ and $\kappa_s^a = -2$ or $\kappa_r^a = -2.57$ respectively (see 5203 and 5205). For the critical height, we find by putting $\varphi = 0$ in 7111:

$$h^c = \frac{1}{\gamma}(4c - 2p) \qquad 7112$$

where c should be assumed positive. In the special case of p = 0, equation 7112 gives $h^c = 4c : \gamma$. A more correct value can, however, be found by means of the first table in Section 531. The pressure component proportional to c can only cancel the hydrostatic pressure when $\zeta = \frac{1}{3}$, and this is found for $\alpha = 15^\circ$. To this corresponds $\varkappa = 1.916$, giving $h^c = 3.83\ c : \gamma$.

Example 71b

In this example we shall calculate the active earth pressure on the back of an anchor slab (see Fig. 72C), which shall be designed in Example 72b. The slab is vertical, rough and partly submerged, and the ground surface is horizontal. The fill consists of coarse sand with an actual friction angle of 36°. Applying a safety factor 1.25 to μ, we find that the calculation should be made with $\varphi = 30^\circ$. The given quantities are (compare Fig. 72C):

$i = j = 0$	$h_1 = 2$ m	$\gamma_1 = 1.8$ t/m³	$\varphi = \delta = -30^\circ$
$p = 1$ t/m²	$h_2 = 0.15$ m	$\gamma_2 = 1.0$ t/m³	$c = a = 0$

From the table in Section 523 we find, for $\varphi = 30^\circ$ and a rough wall, $\rho_r^a = 0.273$ and $\lambda_r^a = 0.266$. Then we get, using 6309 and calculating the hydrostatic earth pressure by assuming first full height (h_1+h_2) and full unit weight (γ_1), and subtracting later an amount corresponding to the submerged height (h_2) and the differential unit weight $(\gamma_1-\gamma_2)$:

$$E^a = \tfrac{1}{2}(1.8 \times 2.15^2 - 0.8 \times 0.15^2) \times 0.266 + 1 \times 2.15 \times 0.273 = \underline{1.70\ t/m}$$

$$E^a z^a = \tfrac{1}{6}(1.8 \times 2.15^3 - 0.8 \times 0.15^3) \times 0.266 + \tfrac{1}{2} \times 1 \times 2.15^2 \times 0.273 = \underline{1.42\ tm/m}$$

$$F^a = -1.70 \times 0.577 = \underline{-0.98\ t/m}$$

For comparison it may be mentioned, that a calculation with the Coulomb values $\rho_r^a = \lambda_r^a = 0.257$ would give $E^a = 1.62$ t/m.

72. ANCHOR SLABS

721. General

Fig. 72A shows the general case of an inclined anchor slab (angle j with the vertical) below a sloping ground surface (angle i with the horizon). It should be noted that, according to our definitions, i and j have different signs on the two sides of the slab. In Fig. 72A they are positive on the "passive" side, negative on the "active".

In order to be on the safe side we assume the surface in front of the slab to be unloaded, whereas behind the slab it is loaded with a vertical surcharge p. The slab is acted upon by an anchor pull, having a component A normal to the slab, and making an angle g with the horizon (positive when the pull is directed downwards).

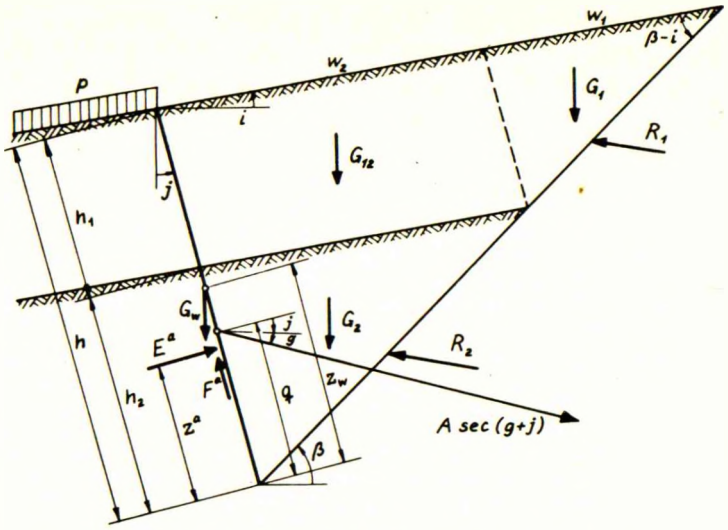

Fig.72A: Anchor slab in stratified earth

From the surface to the depth h_1 (measured along the slab) the earth has the unit weight γ_1, but below this depth the unit weight is γ_2. However, both layers are assumed to possess the same friction angle φ and cohesion c. The boundary between the two layers is assumed to be parallel to the ground surface.

For economical reasons the anchor point should be placed at such a level that the greatest possible passive pressure is obtained. Graphs 3 and 13 in the Appendix show that this would imply the development of a rupture P in front of a rough slab. However, a passive rupture P with $\delta = \varphi$ cannot occur here, because the equilibrium conditions require the tangential component of the passive pressure to be equal to the sum of the corresponding components of the anchor pull, the weight of the slab and the active pressure on its back (Th. Rasmussen, 1948).

Apart from the rupture P, the rupture SfP is the one which gives the greatest passive pressure (see Graph 13), and to this rupture corresponds a translation of the slab in the state of failure.

For this movement we have behind the slab an active rupture P, i.e. ordinary active pressure as on a retaining wall. E^a, F^a and z^a are consequently calculated as described in Section 71, but with reversed signs of i and j. In frictionless earth it will usually be found that the depth d° (7107) exceeds h, and in that case we must put $E^a = F^a = 0$ (we presume that care is taken to prevent surface water from entering a possible crack between slab and earth or in the earth proper).

722. Sloping Surface and Inclined Slab

With regard to the passive rupture SfP, the difficulty exists that we neither know the actual values of δ and a, nor the inclination β of the S-line. However, we have seen in Section 56, that a rupture SfP gives practically the

same value of z as a zone-rupture, which means that it could just as well have been calculated as such, if δ and a had been known. Moreover, as the actual values of δ and a are usually comparatively small, the actual rupture-line cannot deviate much from a straight line.

Consequently, we shall calculate this rupture SfP as a zone-rupture, using a straight rupture-line. However, instead of considering the "passive" earth wedge alone and projecting on a line perpendicular to the force E sec δ (the direction of which is unknown here), we shall consider this earth wedge plus the slab, and project on a line perpendicular to the direction of the anchor pull. We get then (see Fig. 72A):

$$R_1^g + R_2^g - (G_1 + G_2 + G_{12} + G_w) \cos g + E^a \sin(g+j) + F^a \cos(g+j) = 0 \qquad 7201$$

After insertion of 3208 (with $G^{YZ} = 0$), 3214, 3339-40 and 3411 (with $p = 0$ and $\alpha = 0$), equation 7201 is found to have the following solution:

$$\cot(\beta-i) = \tan(\varphi+g+i) + \sec(\varphi+g+i) \sqrt{1 + \frac{K_4}{K_5} \cos(\varphi+g+i)} \qquad 7202$$

in which the quantities K_4 and K_5 are determined by the equations:

$$K_1 = \tfrac{1}{2}\gamma_1 (h_1 + h_2)^2 \qquad K_2 = \tfrac{1}{2}(\gamma_1 - \gamma_2) h_2^2 \qquad K_3 = c(h_1 + h_2) \qquad 7203\text{-}05$$

$$K_4 = (K_1 - K_2) \sin(g+j-i) + \left[G_w \cos g - E^a \sin(g+j) - F^a \cos(g+j) \right] \sec(j-i) \qquad 7206$$

$$K_5 = (K_1 - K_2) \cos(j-i) \sin(\varphi+i) + K_3 \cos \varphi \qquad 7207$$

When β has been determined by means of 7202-07 we should, according to the theory in Section 431, find E^p by calculating the passive unit pressures by means of 3423. However, this would be somewhat complicated, because δ and a are still unknown. Fortunately, in the case of one straight rupture-line, the result can actually be obtained in a much simpler way, viz. by projecting the forces acting on the earth wedge, on a normal to the slab:

$$E^p = - R_1^{90^\circ - j} - R_2^{90^\circ - j} + (G_1 + G_2 + G_{12}) \sin j \qquad 7208$$

By insertion of 3208 (with $G^{YZ} = 0$), 3214, 3339-40 (with $g = 90^\circ - j$) and 3411 (with $p = 0$ and $\alpha = 0$) we find for E^p an expression of the form:

$$E^p = (K_1 - K_2) \lambda^p + K_3 \kappa^p \qquad \text{where:} \qquad \kappa^p = \frac{\cos(j-i)}{\sin^2(\beta-i)} \cos \varphi \sin(2\beta+\varphi-i-j) \qquad 7209\text{-}10$$

$$\lambda^p = \frac{\cos(j-i)}{\sin^2(\beta-i)} \left[\cos(j-i) \sin(\beta+\varphi) \sin(\beta+\varphi-j) + \sin j \sin(\beta-i) \cos(\beta-j) \right] \qquad 7211$$

Next, the normal component of the anchor pull is found by projecting the forces, acting on the slab proper, on a normal to the slab:

$$A = E^p - E^a + G_w \sin j \qquad 7212$$

As the rupture SfP is approximately a zone-rupture, the distribution of the passive pressure E^p may be assumed to be "hydrostatical". This means that the pressure centres of the components $K_1\lambda^p$, $K_2\lambda^p$ and $K_3\kappa^p$ are located at the distances $\frac{1}{3}(h_1+h_2)$, $\frac{1}{3}h_2$ and $\frac{1}{2}(h_1+h_2)$ respectively, from the foot of the slab. Consequently, we get, by taking the moments about the foot of the slab, the following equation:

$$Aq = \tfrac{1}{3}(h_1+h_2)K_1\lambda^p - \tfrac{1}{3}h_2K_2\lambda^p + \tfrac{1}{2}(h_1+h_2)K_3\kappa^p - E^a z^a + G_w z_w \sin j \qquad 7213$$

which determines the proper location (q) of the anchor point.

So far, we have assumed that the anchor slab reaches the surface with its top (Fig.72A). In practice, this will usually not be the case, but theory as well as experiments have shown that the resistance of a "buried" anchor slab at shallow depth is very nearly the same as for a slab reaching the surface.

Consequently, the calculation can be made as described above, and when the necessary depth h has been determined (by trial) so as to give the required value of A, the actual height s of the anchor slab can be chosen more or less arbitrarily. s should, however, never be smaller than $\frac{1}{2}$h or 1.5 q and should preferably be about $\frac{2}{3}$h or 2q.

In order to find the transverse moments in the slab, the total normal pressure A is assumed to have a trapezoidal distribution over the actual height s of the slab. In that case we find the greatest moment:

$$M = 2Aq^2(s-q)^2 : s^3 \qquad 7214$$

Example 72a

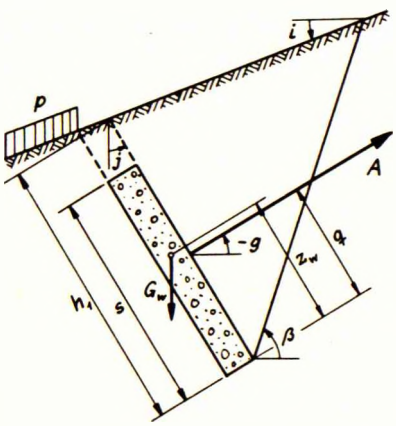

Fig.72B: Inclined anchor slab in clay with sloping surface

As an example, we shall consider the following case of an inclined anchor slab in homogeneous clay with a sloping surface (Fig.72B):

$i = 20^\circ$ $\quad j = 30^\circ$ $\quad g = -30^\circ$ $\quad \varphi = 0$

$h_1 = 2.5$ m $\quad h_2 = 0$ $\quad p = 2$ t/m^2

$\gamma_1 = 1.6$ t/m^3 $\quad c = 4.5 : 1.5 = 3$ t/m^2

where we have divided the actual cohesion by a safety factor 1.5. The indicated values of i and j are valid for the "passive" side; for the "active" side their signs should be reversed.

If the depth d° is calculated by means of 7107, ~~it~~ it is found to exceed h_1. Consequently, we can put $E^a = p^a = 0$.

In order to find the weight of the slab, we estimate that it should be 2.0 m high, 0.3 m thick and made of reinforced concrete (unit weight 2.5 t/m^3). As we must include the earth on top of the slab we get:

$$G_W = 0.3\ (0.5 \times 1.6 + 2.0 \times 2.5) = 1.74\ \text{t/m}$$

$$G_W z_W = 0.3\ (0.5 \times 1.6 \times 2.25 + 2.0 \times 2.5 \times 1.0) = 2.04\ \text{tm/m}$$

By means of 7203-07 we can now find the following quantities:

$$K_1 = \tfrac{1}{2} \times 1.6 \times 2.5^2 = 5 \qquad K_2 = 0 \qquad K_3 = 3 \times 2.5 = 7.5$$

$$K_4 = -5 \times 0.342 + 1.74 \times 0.866 \times 1.015 = -0.18 \qquad K_5 = 5 \times 0.985 \times 0.342 + 7.5 \times 1 = 9.19$$

With these values 7202 yields:

$$\cot(\beta - 20^\circ) = -0.176 + 1.015 \sqrt{1 - \frac{0.18}{9.19} \times 0.985} = 0.830 \qquad \underline{\beta = 70.3^\circ}$$

Next, we calculate κ^p and λ^p from 7210-11:

$$\kappa^p = \frac{0.985}{0.770^2} \times 1 \times 0.999 = 1.66$$

$$\lambda^p = \frac{0.985}{0.770^2}\ (0.985 \times 0.942 \times 0.647 + 0.5 \times 0.770 \times 0.763) = 1.48$$

Finally we get, from 7209 and 7212-13:

$$E^p = 5 \times 1.48 + 7.5 \times 1.66 = 19.9\ \text{t/m} \qquad \underline{A} = 19.9 + 1.74 \times 0.5 = \underline{20.8\ \text{t/m}}$$

$$Aq = \tfrac{1}{3} \times 2.5 \times 5 \times 1.48 + \tfrac{1}{2} \times 2.5 \times 7.5 \times 1.66 + 2.04 \times 0.5 = 22.8\ \text{tm/m}$$

$$\underline{q} = 22.8 : 20.8 = \underline{1.09\ \text{m}}$$

We give the slab an actual height $\underline{s = 2.00\ \text{m}}$, and find then from 7214:

$$\underline{M} = 2 \times 20.8 \times 1.09^2\ (2.00 - 1.09)^2 : 2.00^3 = \underline{5.11\ \text{tm/m}}$$

For this moment the slab should be designed with "allowable" stresses of, for example:

$$\sigma_c = \frac{300}{2.5} = 120\ \text{kg/cm}^2 \qquad \sigma_s = \frac{2400}{1.2} = 2000\ \text{kg/cm}^2$$

723. Horizontal Surface and Vertical Slab

In the important special case of $i = j = 0$ the equations 7203-05, 7209 and 7214 are unchanged, whereas the remaining formulae are reduced to the following:

$$\cot\beta = \tan(\varphi+g) + \sec(\varphi+g) \sqrt{1 + \frac{K_4}{K_5} \cos(\varphi+g)} \qquad 7215$$

$$K_4 = (K_1 - K_2 - E^a) \sin g + (G_W - F^a) \cos g \qquad 7216$$

$$K_5 = (K_1 - K_2) \sin\varphi + K_3 \cos\varphi \qquad 7217$$

$$\kappa^p = \frac{\cos\varphi \sin(2\beta+\varphi)}{\sin^2\beta} \qquad \lambda^p = \frac{\sin^2(\beta+\varphi)}{\sin^2\beta} \qquad 7218\text{-}19$$

$$A = E^p - E^a \qquad Aq = \tfrac{1}{3}(h_1+h_2)K_1\lambda^p - \tfrac{1}{3}h_2K_2\lambda^p + \tfrac{1}{2}(h_1+h_2)K_3\kappa^p - E^a z^a \qquad 7220\text{-}21$$

Example 72b

In this example, we shall design the anchor slab which is necessary for anchoring the sheet wall designed in Example 74c (Fig. 74E). The fill is coarse sand with an actual friction angle of 36°. Applying a safety factor 1.25 to μ we find that the calculation should be made with $\varphi = 30°$. In Example 74c we have found A = 13.3 t/m and, after some preliminary trial, we find that the anchor slab should be partly submerged and have $h_2 = 0.15$ m (see Fig. 72C). Thus, the given quantities are:

$i = j = g = 0$ $\quad h_1 = 2$ m $\quad \gamma_1 = 1.8$ t/m³ $\quad \varphi = 30°$

$p = 1$ t/m² $\quad h_2 = 0.15$ m $\quad \gamma_2 = 1.0$ t/m³ $\quad c = 0$

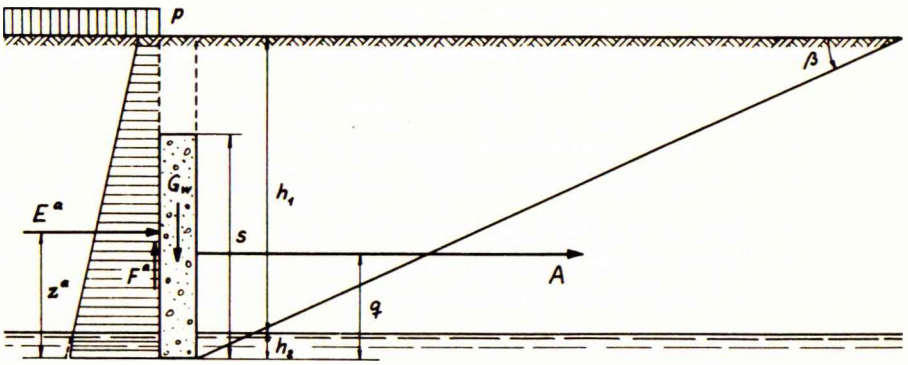

Fig. 72C: Partly submerged anchor slab in sand

The active pressures on the back of the slab have been calculated in Example 71b where we have found:

$E^a = 1.70$ t/m $\qquad E^a z^a = 1.42$ tm/m $\qquad F^a = -0.98$ t/m

In order to find the weight of the slab we estimate that it should be 1.5 m high, 0.25 m thick and made of reinforced concrete (unit weight 2.5 t/m³). Subtracting the uplift and adding the weight of the earth on top of the slab we get:

$$G_w = 0.25\ (0.65 \times 1.8 + 1.35 \times 2.5 + 0.15 \times 1.5) = 1.20 \text{ t/m}$$

By means of 7203-05 and 7216-17, we can now find the following quantities:

$K_1 = \frac{1}{2} \times 1.8 \times 2.15^2 = 4.15 \qquad K_2 = \frac{1}{2} \times 0.8 \times 0.15^2 = 0.01 \qquad K_3 = 0$

$K_4 = (1.20 + 0.98) \times 1 = 2.18 \qquad K_5 = (4.15 - 0.01) \times 0.5 = 2.07$

With these values 7215 yields:

$$\cot \beta = 0.577 + 1.155\sqrt{1 + \frac{2.18}{2.07} \times 0.866} = 2.17 \qquad \underline{\beta = 24.7°}$$

Next, we calculate λ^p by means of 7219:

$$\lambda^p = \frac{0.815^2}{0.418^2} = 3.81$$

Finally we get, from 7209 and 7221-22:

$$E^p = (4.15 - 0.01) \times 3.81 = 15.8 \text{ t/m} \qquad \underline{A} = 15.8 - 1.70 = \underline{14.1 \text{ t/m}}$$

$$A_q = \tfrac{1}{3} \times 2.15 \times 4.15 \times 3.81 - \tfrac{1}{3} \times 0.15 \times 0.01 \times 3.81 - 1.42 = 10.0 \text{ tm/m}$$

$$\underline{q} = 10.0 : 14.1 = \underline{0.71 \text{ m}}$$

We give the slab an actual height $\underline{s = 1.50 \text{ m}}$, and find then from 7214:

$$\underline{M} = 2 \times 14.1 \times 0.71^2 (1.50 - 0.71)^2 : 1.50^3 = \underline{2.63 \text{ tm/m}}$$

The same "allowable" stresses can be used as in Example 72a.

The calculated anchor pull is somewhat greater than the required 13.3 t/m, as it should be, because the anchorage is assumed unyielding in Example 72c. The value found for q shows that the anchor point should be located 1.44 m below the surface. As the anchor point of the sheet wall lies 1.5 m below the surface (Example 72c), we will very nearly have g = 0 as assumed.

The above calculation shows that in the case considered, the greatest attainable value of λ^p is 3.81. For comparison it may be mentioned that a calculation according to Coulomb's method (with $\varphi = 30^\circ$) would give $\lambda^p = 3.00$ for $\delta = 0$, and $\lambda^p = 4.80$ for $\delta = \frac{1}{2}\varphi$. The Danish Rules (1952) require for $\delta = \frac{1}{2}\varphi$, a safety factor of 2.0, but it will be seen that this would give an actual safety of about 1.6 only. As we have a safety factor of 1.25 on μ for the earth pressures on the anchor slab as well as those on the sheet wall, the "total" safety is about 1.7.

73. FREE SHEET WALLS

731. General

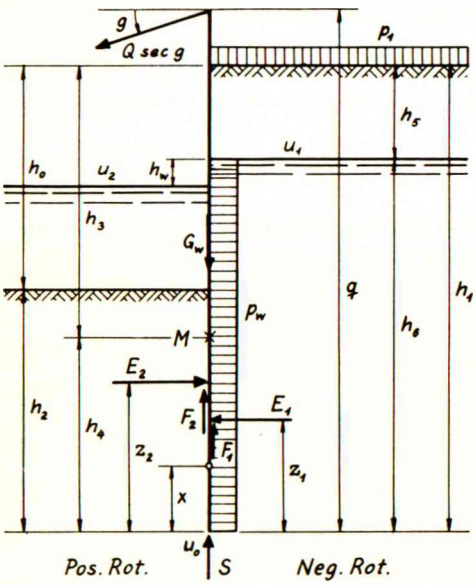

Fig.73A: Free sheet wall

A free sheet wall is a wall which has no anchorage or bracing, but owes its stability exclusively to the fact that it is supported by earth on both sides. We shall here consider a vertical wall and horizontal ground surfaces which, however, may lie at different levels at the two sides of the wall (Fig. 73A).

The wall is assumed to be partly submerged, the water level on the active side dividing the height h_1 in the parts h_5 and h_6. The corresponding effective unit weights are γ_5 and γ_6 but φ and c are assumed to be the same above and below the water level. They may, however, have different values on the two sides of the wall.

If the water levels on the two sides of the wall exhibit a small difference h_w, a differential water pressure with a maximum intensity $p_w = \gamma_w h_w$ will occur. For

the sake of simplicity we shall assume a uniform pressure p_w over the entire height h_6 and, as this is somewhat on the safe side, we may, on the other hand, disregard the effects of the small hydraulic gradients on the effective unit weights of the soil (see Section 622). However, if the difference h_w is considerable, a more correct calculation must be made (see Section 734).

The wall proper has a weight G_w and may be acted upon by an exterior force with a horizontal component Q (Fig.73A). This force must, of course, be of such a nature that it does not restrain the movements of the wall. Finally, the foot of the wall is supported by a vertical point resistance S.

If no yield hinge develops, the free sheet wall must, in the state of failure, rotate about a point above its foot. This point is located at the unknown height x, and we have:

$$\xi_1 = x : h_1 \qquad \xi_2 = x : h_2 \qquad 7301\text{-}02$$

For the right side of the wall in Fig.73A the rotation is negative, and for the left side it is positive. At both sides the rupture-figure is, for cohesionless earth, of the type AaR (smooth wall) or AaP (rough wall).

For the forces acting upon the wall proper we get by vertical projection, by horizontal projection and by taking the moments about the pressure centre of Q:

$$S = G_w - F_1 - F_2 + Q \tan g \qquad Q = E_2 - E_1 - p_w h_6 \qquad 7303\text{-}04$$

$$q(E_1 - E_2) - E_1 z_1 + E_2 z_2 + p_w h_6 (q - \tfrac{1}{2} h_6) = 0 \qquad 7305$$

$$E_1 (q - z_1) - E_2 (q - z_2) + p_w h_6 (\tfrac{1}{2} h_6 + q - h_6) = 0$$

Equation 7303 is not of primary importance to the main problem, but it can be used to investigate whether the wall will rise vertically, viz. when 7303 gives a negative S. In this case the curves for a rough wall in the graphs cannot be used, as they presume horizontal movements only.

E, Ez and F are given by the general expressions 6118-20, which can be used direct in the case of homogeneous earth. In cases of partly submerged or stratified earth, pressure diagrams must be constructed according to the principles indicated in Sections 62-63.

If the dimensions (including q) are given, we can find x from 7305 by trial, because E and Ez are functions of ξ, and both ξ's are functions of x. When x has been determined, Q may be found from 7304.

If Q and h_0 are given, the problem may be solved by trial, viz. by estimating a value of h_2 and calculating the corresponding Q. h_2 must then be changed and the calculation repeated until the calculated Q attains the required value. This is rather involved however and we shall, therefore, in Section 735 indicate a much simpler, although approximate method.

In the special case of $Q = 0$, $p_w = 0$ and a given h_0 we must consider h_2 and x as the unknown quantities. They can be determined by means of 7304-05 which, in this case, are simplified to:

$$E_1 = E_2 \qquad z_1 = z_2 \qquad 7306\text{-}07$$

The greatest moment in the wall occurs at the point where the transversal force is zero. This point divides the height h_1 in two parts h_3 and h_4 (Fig. 73A). The location of this point as well as the corresponding moment can, of course, be determined by means of analytical expressions, but in general it is simpler to use the pressure diagrams direct.

732. Frictionless Earth.

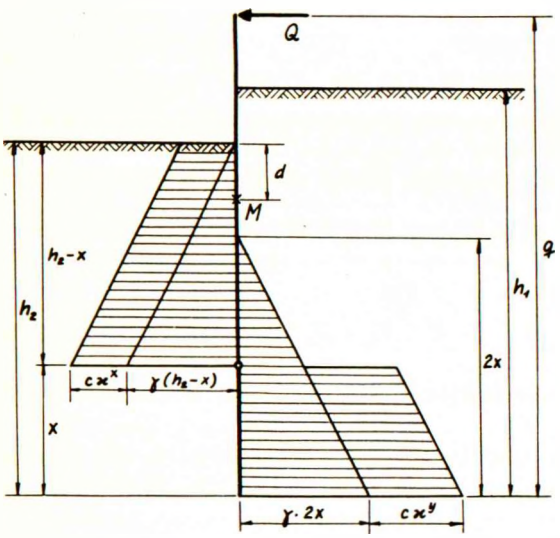

Fig.73B: Free sheet wall in clay

Free sheet walls can seldom be made very high. Consequently, in frictionless earth, the cases of partly unsupported earth fronts will usually occur (Section 64). This means that on one side (neg. rot.) we will get a rupture Aw, and on the other side (pos. rot.) a rupture wR (smooth wall) or wP (rough wall).

These ruptures, which are shown in Fig. 35G, have been calculated in Section 64. The corresponding pressure diagrams are shown in Fig. 73B. It will be seen that h_1 is actually unimportant, as long as we have $2x < h_1 < 2x + h^C$, where h^C is defined by 7106.

By taking the moments about the pressure centre of the force Q we get the following equation:

$$\tfrac{1}{6}\gamma(h_2 - x)^2(3q - h_2 - 2x) - \tfrac{1}{6}\gamma(2x)^2(3q - 2x) + \tfrac{1}{2}c\varkappa^x(h_2 - x)(2q - h_2 - x) - \tfrac{1}{2}c\varkappa^y x(2q - x) = 0 \qquad 7308$$

which can be transformed to:

$$6\gamma x^3 + 3\left[c(\varkappa^x + \varkappa^y) - \gamma(3q - h_2)\right]x^2 - 6q\left[c(\varkappa^x + \varkappa^y) + \gamma h_2\right]x + h_2\left[3c\varkappa^x(2q - h_2) + \gamma h_2(3q - h_2)\right] = 0 \qquad 7309$$

From this equation x can be found. Q is then determined by horizontal projection:

$$Q = \tfrac{1}{2}\gamma(h_2 - x)^2 - 2\gamma x^2 + c\varkappa^x(h_2 - x) - c\varkappa^y x \qquad 7310$$

Example 73a

As an example we shall consider the following case of a smooth sheet wall in clay, subjected to an exterior, horizontal force (compare Fig. 73B which, however, is not to scale):

$$h_1 = h_2 = 5\text{ m} \qquad q = 10\text{ m} \qquad \gamma = 1.5\text{ t/m}^3 \qquad \varphi = \delta = a = 0 \qquad c = 4.5 : 1.5 = 3\text{ t/m}^2$$

where we have divided the actual cohesion by a safety factor 1.5.

According to Section 64 we have for a smooth wall: $\varkappa^x = 2$ and $\varkappa^y = 5.52$. Equation 7309 gives now:

$$6 \times 1.5 \times x^3 + 3\,(3 \times 7.52 - 1.5 \times 25)\,x^2 - 6 \times 10\,(3 \times 7.52 + 1.5 \times 5)\,x$$
$$+ 5\,(3 \times 3 \times 2 \times 15 + 1.5 \times 5 \times 25) = 9\,x^3 - 45\,x^2 - 1804\,x + 2288 = 0 \qquad \underline{x = 1.24\text{ m}}$$

If we use 7112 we find $h^c = 4 \times 3 : 1.5 = 8\text{ m} > h_1 - 2x = 2.52\text{ m}$, which shows that is correct to employ the rupture Aw.

Next, the corresponding value of Q is found from 7310:

$$\underline{Q} = \tfrac{1}{2} \times 1.5 \times 3.76^2 - 2 \times 1.5 \times 1.24^2 + 3 \times 2 \times 3.76 - 3 \times 5.52 \times 1.24 = \underline{8.0\text{ t/m}}$$

The depth d (see Fig. 73B), at which the transversal force is zero, is determined by the equation:

$$\tfrac{1}{2}\gamma d^2 + cd\varkappa^x - Q = \tfrac{1}{2} \times 1.5 \times d^2 + 3 \times d \times 2 - 8.0 = 0 \qquad \underline{d = 1.16\text{ m}}$$

The corresponding maximum moment in the sheet wall is numerically:

$$-\underline{M} = Q(q - h_1 + d) - \tfrac{1}{6}\gamma d^3 - \tfrac{1}{2}cd^2\varkappa^x = 8.0 \times 6.16 - \tfrac{1}{6} \times 1.5 \times 1.16^3 - \tfrac{1}{2} \times 3 \times 1.16^2 \times 2 = \underline{45\text{ tm/m}}$$

For a sheet wall of steel 37 the "allowable" stress is 2400 : 1.2 = 2000 kg/cm^2. The necessary section modulus is therefore:

$$\underline{W} = 4500000 : 2000 = \underline{2250\text{ cm}^3/\text{m}}$$

733. Cohesionless Earth

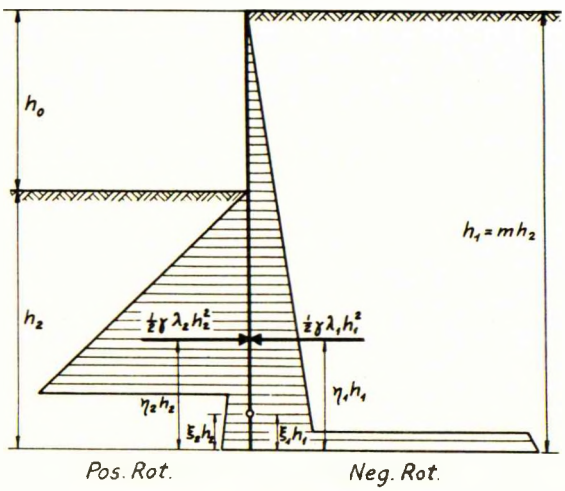

Fig. 73C: Free sheet wall in sand

In cohesionless earth a correct calculation becomes rather laborious, when h_1 and h_2 are not given, because we must estimate h_2 and x independently of each other and change them until both 7304 and 7305 are satisfied. Therefore, a simple, approximate method shall be indicated in Section 735.

The exact calculation is somewhat easier in the special case of $c = p = p_w = Q = 0$ (Fig. 73C). We get here from 7301-02, 7306-07 and 6118-19 the conditions:

$$m = \frac{h_1}{h_2} = \frac{\xi_2}{\xi_1} = \frac{\eta_2}{\eta_1} = \sqrt{\frac{\lambda_2}{\lambda_1}} \qquad 7311$$

For $\varphi = 30^\circ$ the problem can be solved in a relatively simple way, viz. by means of Graphs 11-12 in the Appendix. Through the point ($\xi = 0$, $\eta = 0$) in Graph 12 an arbitrary straight line is drawn. It will intersect the curve for negative rotation in a point (ξ_1, η_1) and the curve for positive rotation in a point (ξ_2, η_2), satisfying 7311. The corresponding values of λ_1 and λ_2 are now found from Graph 11 and we must then investigate whether 7311 is fully satisfied. If not, the procedure must be repeated with another straight line, until satisfactory agreement is obtained.

Example 73b

We shall determine the critical ratio m for the case of $Q = 0$ and $\varphi = 30^\circ$ (compare Fig. 73C which, however, is not to scale). We assume first that the wall is perfectly smooth, and find then after some trial that the following values satisfy 7311:

$\xi_1 = 0.038$ $\eta_1 = 0.205$ $\lambda_1 = 0.57$

$\xi_2 = 0.076$ $\eta_2 = 0.410$ $\lambda_2 = 2.28$

$$\frac{h_1}{h_2} = 2.00 = m_s$$

We then assume that the wall is perfectly rough and find:

$\xi_1 = 0.060$ $\eta_1 = 0.185$ $\lambda_1 = 0.51$

$\xi_2 = 0.154$ $\eta_2 = 0.470$ $\lambda_2 = 3.35$

$$\frac{h_1}{h_2} = 2.57 = m_r$$

734. Hydrodynamic Water Pressures

In the case of hydrodynamic water pressures (Section 622) the potentials and gradients can be found by the construction of a flow net. However, for a sheet wall in homogeneous earth, sufficiently correct results can usually be obtained by means of the following approximate formulae.

If u_1 and u_2 are the potentials at the respective water levels at the two sides of the wall, and if h_1 and h_2 are the corresponding heights of the submerged earth layers, then the actual potential at the foot of the wall is approximately:

$$u_o = \frac{u_2\sqrt{h_1} + u_1\sqrt{h_2}}{\sqrt{h_1} + \sqrt{h_2}} \qquad 7312$$

Now, at the foot of the wall a pressure jump is assumed to occur, with a magnitude of $0.3\ \gamma_w(u_1-u_2) = 0.3\ \gamma_w h_w$. The average hydraulic gradients at the two sides of the wall are then:

$$i_1 = 0.7\,\frac{u_1 - u_o}{h_1} = \frac{0.7\ h_w}{h_1 + \sqrt{h_1 h_2}} \qquad i_2 = 0.7\,\frac{u_2 - u_o}{h_2} = \frac{-\ 0.7\ h_w}{h_2 + \sqrt{h_1 h_2}} \qquad 7313\text{-}14$$

The corresponding effective unit weights of the earth and the water are given by 6204-05. As h_1 and h_2 in 7312-14 should be the submerged heights of the respective layers, we must, for a case such as shown in Fig. 73A, substitute h_1 by h_6.

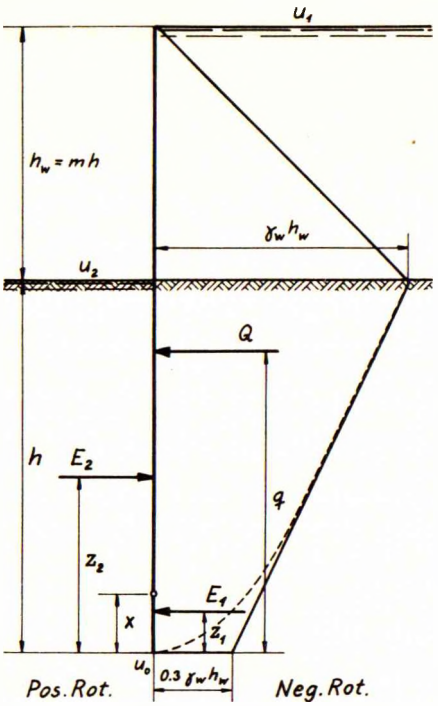

Fig. 73D: Hydrodynamic pressures on free sheet wall

In the special case shown in Fig. 73D we have $h_1 = h_2 = h$ and $h_w = mh$. Consequently, we find from 7313-14, the gradients $i_1 = -i_2 = 0.35\ m$, and then, by means of 6204-05:

$$\begin{matrix}\gamma_1 \\ \gamma_2\end{matrix} = \gamma \mp 0.35\, m\gamma_w \qquad 7315$$

$$\begin{matrix}\gamma_{w_1} \\ \gamma_{w_2}\end{matrix} = (1 \mp 0.35\, m)\gamma_w \qquad 7316$$

According to the above-mentioned approximation, the differential water pressure on the buried part of the wall decreases linearly from $\gamma_w h_w$ at ground level, to $0.3\ \gamma_w h_w$ at the foot of the wall. We get, therefore, the following expressions for the total water pressure and its moment about the foot of the wall:

$$Q = \tfrac{1}{2}h^2 m(m + 1.3)\gamma_w \qquad 7317$$

$$Qq = \tfrac{1}{6}h^3 m(m^2 + 3m + 2.3)\gamma_w \qquad 7318$$

The unknown quantities are m and x. For their determination we have the equations 7304-05, in which we must put $p_w = 0$ and insert the general formulae 6118-19 with $p = c = 0$:

$$Q = \tfrac{1}{2}h^2(\gamma_2\lambda_2 - \gamma_1\lambda_1) \qquad Qq = \tfrac{1}{2}h^3(\gamma_2\lambda_2\eta_2 - \gamma_1\lambda_1\eta_1) \qquad 7319\text{-}20$$

From 7317-20, the following equations can be derived by elimination of Q and q and insertion of 7315:

$$m^2 + 0.35(3.71 + \lambda_1 + \lambda_2)m + \frac{\gamma}{\gamma_w}(\lambda_1 - \lambda_2) = 0 \qquad 7321$$

$$\tfrac{1}{3}m^3 + m^2 + 0.35(2.19 + \lambda_1\eta_1 + \lambda_2\eta_2)m + \frac{\gamma}{\gamma_w}(\lambda_1\eta_1 - \lambda_2\eta_2) = 0 \qquad 7322$$

In order to solve these equations we must estimate a value of ξ and find the corresponding constants λ_1 and η_1 (neg. rot.) as well as λ_2 and η_2 (pos. rot.) from Graphs 11-12. We compute then m from 7321 and investigate, whether 7322 is satisfied.

Example 73c

We shall determine the critical ratio m for the following case of a free sheet wall in cohesionless sand (Fig. 73D):

$$\varphi = 30^\circ \qquad p = c = 0 \qquad \gamma = \gamma_w = 1\ t/m^3$$

We first assume the wall to be perfectly smooth and find then, after some trial, that $\xi = 0.085$ is the correct value, giving:

$$\lambda_1 = 0.82 \quad \eta_1 = 0.145 \quad \lambda_1\eta_1 = 0.119 \quad \lambda_2 = 2.20 \quad \eta_2 = 0.425 \quad \lambda_2\eta_2 = 0.935$$

With these values we get from equations 7321-22:

$$m^2 + 0.35(3.71 + 0.82 + 2.20)m + 1(0.82 - 2.20) = m^2 + 2.36\,m - 1.38 = 0 \qquad m_s = 0.48$$

$$\tfrac{1}{3} \times 0.48^3 + 0.48^2 + 0.35(2.19 + 0.119 + 0.935) \times 0.48 + 1(0.119 - 0.935) = 0$$

If the wall is assumed to be perfectly rough, we find for $\xi = 0.155$:

$$\lambda_1 = 1.02 \quad \eta_1 = 0.110 \quad \lambda_1\eta_1 = 0.112 \quad \lambda_2 = 3.45 \quad \eta_2 = 0.470 \quad \lambda_2\eta_2 = 1.62$$

With these values equations 7321-22 yield:

$$m^2 + 0.35(3.71 + 1.02 + 3.45)m + 1(1.02 - 3.45) = m^2 + 2.87\,m - 2.43 = 0 \qquad m_r = 0.68$$

$$\tfrac{1}{3} \times 0.68^3 + 0.68^2 + 0.35(2.19 + 0.112 + 1.62) \times 0.68 + 1(0.112 - 1.62) = 0$$

Fig.73D is drawn to scale corresponding to the case of a rough wall. The theoretically exact water pressure diagram is shown with a dotted line, and it will be seen that the proposed approximation (unbroken line) is a very close one in this case.

735. Approximate Solution

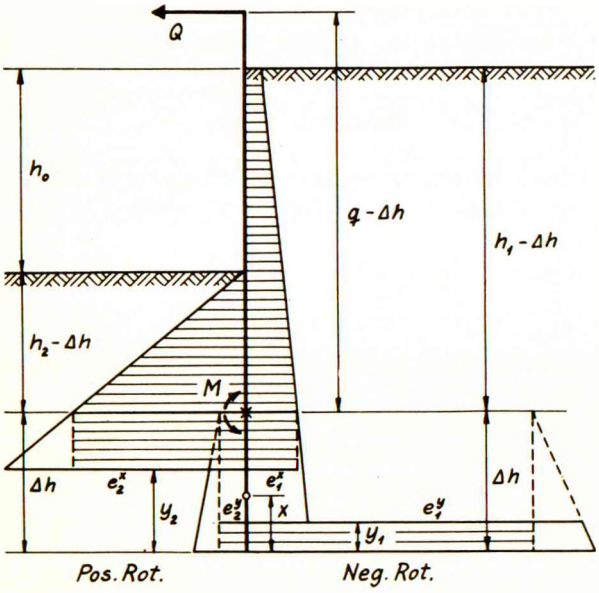

Fig.73E: Approximate calculation of free sheet wall

In the general case of a given h_o and a given Q, an exact calculation requires that h_2 and x be estimated independently of each other and altered until both 7304 and 7305 are satisfied. This procedure is rather laborious, however, and we shall therefore now indicate a much simpler, although approximate method (Fig.73E).

We determine first the location of the point where the transversal force is zero. This is easily done, as we have $e = e^x$ above this point, and these pressures are practically independent of the actual (unknown) values of ξ, when these are small (see Graphs 6 and 16-17).

When we have located the point of zero transversal force, which lies at the unknown height Δh (= h_4 in Fig.73A) above the foot of the wall, we know the heights $h_1 - \Delta h$, $h_2 - \Delta h$ and

q - Δh, and can then calculate the greatest moment M (negative, because it produces compression in the outer side of the wall).

Below the point of zero transversal force the usual pressure diagrams will give the pressure distribution shown in unbroken lines in Fig. 73E (p_w is not shown). However, we shall simplify this by assuming the distribution shown by dotted lines. According to this we reckon with a differential pressure, which is zero between the two pressure jumps, whereas it has the following numerical values above the upper pressure jump and below the lower pressure jump respectively:

$$\Delta e^x = e_2^x - e_1^x - p_w \qquad \Delta e^y = e_1^y - e_2^y + p_w \qquad 7323\text{-}24$$

The different unit pressures in 7323-24 should all correspond to the depth at which the transversal force in the wall is zero. The equilibrium conditions for the lower part of the wall give then:

$$y_1 \Delta e^y = (\Delta h - y_2)\Delta e^x \qquad \tfrac{1}{2}(\Delta h + y_2 - y_1) y_1 \Delta e^y = - M \qquad 7325\text{-}26$$

From the Graphs 5 and 15 in the Appendix, it will be seen that for small values of ξ there is a direct proportionality between ω and ξ. Therefore we have:

$$K_1 = \frac{\omega_1}{\xi_1} = \frac{y_1}{x} \qquad K_2 = \frac{\omega_2}{\xi_2} = \frac{y_2}{x} \qquad 7327\text{-}28$$

By means of Graphs 5 and 15 we find the following values for $\varphi = 0^\circ$ and $\varphi = 30^\circ$. For other values of φ a rough interpolation or extrapolation must be made.

	Smooth Wall		Rough Wall	
	Neg. Rot.	Pos. Rot.	Neg. Rot.	Pos. Rot.
$\varphi = 0^\circ$	$K_1 = 1.0$	$K_2 = 1.0$	$K_1 = 1.1$	$K_2 = 1.1$
$\varphi = 30^\circ$	$K_1 = 0.4$	$K_2 = 1.6$	$K_1 = 0.5$	$K_2 = 1.8$

By insertion of 7327-28 in 7325-26 we get two equations in x and Δh, from which we can find:

$$\frac{1}{x^2} = \frac{K_1 \Delta e^y}{-2M}\left[2K_2 + K_1\left(\frac{\Delta e^y}{\Delta e^x} - 1\right)\right] \qquad \Delta h = x\left(K_2 + K_1 \frac{\Delta e^y}{\Delta e^x}\right) \qquad 7329\text{-}30$$

The only remaining difficulty is that, as we do not know the actual values of ξ_1 and ξ_2, we cannot calculate e_1^y and e_2^y. However, as ξ is small, no serious errors will be committed by calculating e_1^y and e_2^y corresponding to $\xi_1 = 0$ and $\xi_2 = 0$ (compare Graphs 6, 16 and 18). When this has been done, and K_1 and K_2 have been found as described above, we use, successively, the equations 7323-24, 7329 and 7330. It should be noted that a negative M must be inserted in 7329.

Example 73d

As an example we shall apply the described approximate method to the smooth wall dealt with in the first part of Example 73b. We assume here:

$h_o = 2$ $\gamma = 1$ $\varphi = 30^o$ $\delta = 0$ $c = p = p_w = 0$ $Q = 0$

We get then from Graph 16, corresponding to $\xi_1 = \xi_2 = 0$:

$$\lambda_1^x = \tfrac{1}{3} \qquad \lambda_1^y = 6.8 \qquad \lambda_2^x = 3 \qquad \lambda_2^y = 0.16$$

As $h_1 = 2 + h_2$, we can now find $h_2 - \Delta h$ from the following equation, which expresses that the transversal force should be zero:

$$\tfrac{1}{2}(h_2 - \Delta h)^2 \times 3 - \tfrac{1}{2}(2 + h_2 - \Delta h)^2 \times \tfrac{1}{3} = \tfrac{4}{3}(h_2 - \Delta h)^2 - \tfrac{2}{3}(h_2 - \Delta h) - \tfrac{2}{3} = 0 \qquad h_2 - \Delta h = 1 \qquad h_1 - \Delta h = 3$$

The corresponding moment is:

$$M = \tfrac{1}{6} \times 1^3 \times 3 - \tfrac{1}{6} \times 3^3 \times \tfrac{1}{3} = -1.00$$

Further, we get for the different unit pressures:

$$e_1^x = 3 \times \tfrac{1}{3} = 1.00 \qquad e_2^x = 1 \times 3 = 3.00 \qquad \Delta e^x = 2.00$$

$$e_1^y = 3 \times 6.8 = 20.40 \qquad e_2^y = 1 \times 0.16 = 0.16 \qquad \Delta e^y = 20.24$$

For a smooth wall and $\varphi = 30^o$ we have $K_1 = 0.4$ and $K_2 = 1.6$, with which we find from 7329-30:

$$\frac{1}{x^2} = \frac{0.4 \times 20.24}{2 \times 1.00}\left[2 \times 1.6 + 0.4\left(\frac{20.24}{2.00} - 1\right)\right] = 27.6 \qquad x = 0.190$$

$$\Delta h = 0.190\left(1.6 + 0.4\,\frac{20.24}{2.00}\right) = 1.07 \qquad h_1 = 4.07 \qquad h_2 = 2.07 \qquad \underline{m_s = \frac{4.07}{2.07} = 1.97}$$

As the calculation in Example 73b has given $m_s = 2.00$, it will be seen that the approximate method is on the safe side and actually rather accurate.

If a similar calculation is made for the rough wall considered in the latter part of Example 73b, we find $\underline{m_r = 2.47}$ by means of the approximate method, whereas the correct value is 2.57.

74. ANCHORED SHEET WALLS

741. Design With No Yield Hinge

Fig. 74A shows an anchored sheet wall. The wall is assumed vertical and the ground surfaces horizontal, at least on the active side. On this side a surcharge p_1 may occur. The wall is also assumed to be partly submerged, and may be acted upon by a differential water pressure p_w. Further, the wall has a weight G_w and may be loaded by a vertical force L at its top. Its foot is supported by a vertical point resistance S.

As explained in Section 36, the wall may be designed for any chosen state of failure which is kinematically possible. However, the smallest possible driving depth is obtained when we assume that, in the state of failure, the wall rotates about the anchor point. This will usually lead to the most economical design, when the wall is driven into soft clay or into a slope. In the considered state of failure we have $x = q$ and:

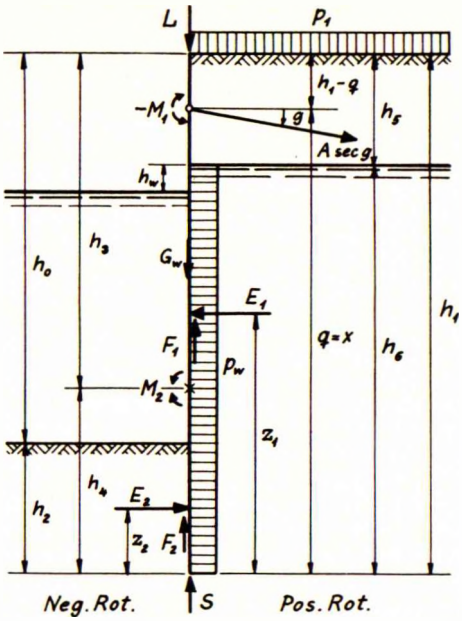

Fig.74A: Anchored sheet wall with no yield hinge

$$\xi_1 = q : h_1 \qquad \xi_2 = q : h_2 \qquad 7401\text{-}02$$

On the active side the rotation is positive, and the corresponding rupture-figure must be of the type A. On the passive side, the rotation is negative, and the corresponding rupture-figure is assumed to be of the type A (smooth wall) or AfPfA (rough wall).

The heights h_0, h_5 and h_1-q are given, whereas the driving depth h_2, the horizontal component A of the anchor pull and the moments in the wall shall be determined by the calculation.

For the forces acting on the wall proper we get by vertical projection, by horizontal projection and by taking the moments about the anchor point:

$$S = L + G_W - F_1 - F_2 + A \tan g \qquad 7403$$

$$A = E_1 - E_2 + p_w h_6 \qquad 7404$$

$$q(E_1 - E_2) - E_1 z_1 + E_2 z_2 + p_w h_6 (q - \tfrac{1}{2} h_6) = 0 \qquad 7405$$

Equation 7403 is not of primary importance to the main problem, but it can be used to investigate whether the wall (considered as a row of point-bearing piles) can carry the vertical forces acting upon it.

In the case of homogeneous earth we have, for E and Ez, the general expressions 6118-19. When the earth is partly submerged or stratified, corresponding analytical equations can be made. They become rather involved, however, and it is therefore usually simpler to construct the pressure diagrams according to the principles indicated in Sections 62-63.

The calculation proceeds now in the following way. We estimate a value of h_2 and calculate the corresponding values of h_1, h_6 and q. 7401-02 give then ξ_1 and ξ_2, for which we can find the earth pressure constants by means of the graphs in the Appendix. After this, the pressure diagrams are constructed, E_1, $E_1 z_1$, E_2 and $E_2 z_2$ are calculated, and it is investigated whether 7405 is satisfied. If not, we must change h_2 and repeat the calculation until satisfactory agreement is obtained. 7404 gives then the horizontal anchor pull A.

The greatest positive moment M_2 occurs at the point where the transversal force in the wall is zero. The height h_4 of this point (above the foot of the wall), as well as the corresponding moment, is determined by the aid of the pressure diagrams. The same applies to the greatest negative moment M_1 which, of course, occurs at the anchor point.

It should be noted that, when we have applied adequate safety factors to c and tan φ, the driving depth found by the calculation is fully sufficient as regards the stability of the wall. It may, however, be necessary to increase the calculated driving depth, if extra safety against scour is required, or if it proves necessary to increase the bearing capacity of the wall, considered as a row of piles. However, in such cases a more economical design can usually be obtained by using the method in Section 742 or Section 743.

Example 74a

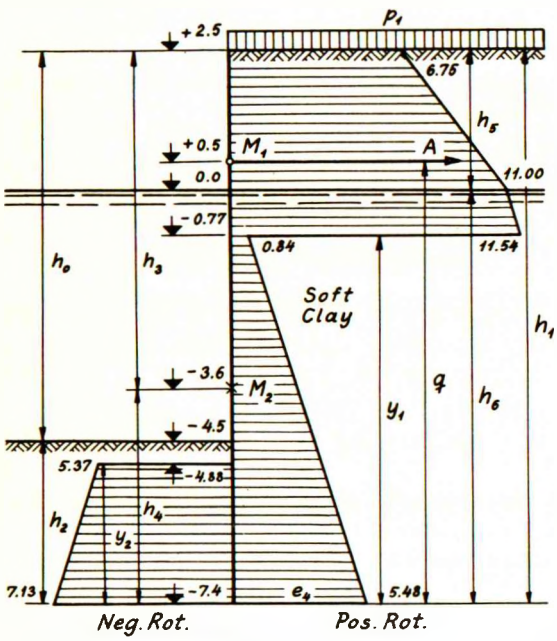

Fig.74B: Anchored sheet wall in soft clay

As an example, we shall consider the following case of a smooth sheet wall in soft clay (Fig.74B):

$h_0 = 7$ m $h_1 - q = 2$ m $h_5 = 2.5$ m

$\gamma_5 = 1.7$ t/m³ $\gamma_6 = \gamma_2 = 0.7$ t/m³

$p_1 = 2.75$ t/m² $p_w = 0$ $\varphi = \delta = 0$

$c = 3 : 1.5 = 2$ t/m² $a = 0$

where we have applied a safety factor 1.5 to the actual cohesion.

After some trial we find that we must assume:

$h_2 = 2.9$ m $h_1 = 7 + 2.9 = 9.9$ m

$q = 9.9 - 2 = 7.9$ m $h_6 = 7.4$ m

$\xi_1 = \frac{7.9}{9.9} = 0.80$ $\xi_2 = \frac{7.9}{2.9} = 2.7$

For these values of ξ we find from Graphs 5 and 6:

$\omega_1^0 = 0.67$ $\kappa_1^x = 2$ $\kappa_1^y = -3.35$

$\omega_2^0 = 0.87$ $\kappa_2^x = -2$ $\kappa_2^y = 2.55$

The heights y in the approximate pressure diagrams are :

$y_1 = 0.67 \times 9.9 = 6.63$ m $y_2 = 0.87 \times 2.9 = 2.52$ m

and the pressures are determined by the general formula 6308, from which we find the following results for the active side (pos. rot.):

At level	+2.5 m:	$2.75 + 2 \times 2$	$= 6.75$ t/m²
At level	0.0 m:	$6.75 + 1.7 \times 2.5$	$= 11.00$ t/m²
Above level	-0.77 m:	$11.00 + 0.7 \times 0.77$	$= 11.54$ t/m²
Below level	-0.77 m:	$11.54 - (3.35 + 2) \times 2$	$= 0.84$ t/m²
At level	-7.4 m:	$0.84 + 0.7 \times 6.63$	$= 5.48$ t/m²

For the passive side (neg. rot.) we get, disregarding negative pressures:

At level -4.88 m: $0.7 \times 0.38 + 2.55 \times 2 = 5.37$ t/m^2
At level -7.4 m: $5.37 + 0.7 \times 2.52 = 7.13$ t/m^2

The pressure diagrams are shown to scale in Fig. 74B. With the aid of these we can now calculate:

$$E_1 = \tfrac{1}{2} \times 2.5 \times 6.75 + \tfrac{1}{2} \times 2.5 \times 11.00 + \tfrac{1}{2} \times 0.77 \times 11.00 + \tfrac{1}{2} \times 0.77 \times 11.54 + \tfrac{1}{2} \times 6.63 \times 0.84 + \tfrac{1}{2} \times 6.63 \times 5.48 = 8.43 + 13.75 + 4.24 + 4.44 + 2.79 + 18.20 = 51.9 \text{ t/m}$$

$$E_1 z_1 = 8.43 \times 9.07 + 13.75 \times 8.23 + 4.24 \times 7.14 + 4.44 \times 6.88 + 2.79 \times 4.42 + 18.20 \times 2.21 = 303 \text{ tm/m}$$

$$E_2 = \tfrac{1}{2} \times 2.52 \times 5.37 + \tfrac{1}{2} \times 2.52 \times 7.13 = 6.77 + 8.99 = 15.8 \text{ t/m}$$

$$E_2 z_2 = 6.77 \times 1.68 + 8.99 \times 0.84 = 19.0 \text{ tm/m}$$

We can then show that 7405 is satisfied:

$$7.9(51.9 - 15.8) - 303 + 19.0 = 0$$

The horizontal component of the anchor pull is now determined by 7404:

$$\underline{A} = 51.9 - 15.8 = \underline{36.1 \text{ t/m}}$$

The transversal force is zero at a height h_4, which may be determined by the equation:

$$e_4 h_4 - \tfrac{1}{2}\gamma_6 h_4^2 - E_2 = 5.48\, h_4 - \tfrac{1}{2} \times 0.7\, h_4^2 - 15.8 = 0 \qquad h_4 = 3.8 \text{ m} \qquad h_3 = 6.1 \text{ m}$$

The corresponding maximum moment is:

$$\underline{M_2} = \tfrac{1}{2} e_4 h_4^2 - \tfrac{1}{3}\gamma_6 h_4^3 - E_2 z_2 = \tfrac{1}{2} \times 5.48 \times 3.8^2 - \tfrac{1}{3} \times 0.7 \times 3.8^3 - 19.0 = \underline{7.9 \text{ tm/m}}$$

whereas the minimum moment (at anchor level) is:

$$\underline{M_1} = -\tfrac{1}{2} \times 6.75 \times 2^2 - \tfrac{1}{6} \times 1.7 \times 2^3 = \underline{-15.8 \text{ tm/m}}$$

If the sheet wall, as well as the anchors, are made of steel 37 with a yield stress of about 2400 kg/cm^2, the "allowable" stress is 2400 : 1.2 = 2000 kg/cm^2. Consequently, the necessary anchor section (T), and the necessary section modulus (W) of the wall, will be:

$$\underline{T} = 36100 : 2000 = \underline{18.05 \text{ cm}^2/\text{m}} \qquad \underline{W} = 1580000 : 2000 = \underline{790 \text{ cm}^3/\text{m}}$$

Example 74b

As a more complicated example, we shall consider the following case concerning a smooth sheet wall in stratified earth (Fig. 74C). Moreover, this case shows the way to deal with variable cohesions and friction angles other than 30°.

The upper layer is sand fill with an actual friction angle of 30°. Applying a safety factor 1.25 to μ, we find that the calculation should be made with $\varphi = 25°$.

The lower layer is a boulder clay with an actual cohesion (undrained shear strength) of $0.21\,d + 2.55$ (t/m^2), where d is the depth (m) below the natural surface of the clay layer. Applying a safety factor of 1.5, we find that the calculation should be made with $c = 0.14\,d + 1.7$. The given quantities are then:

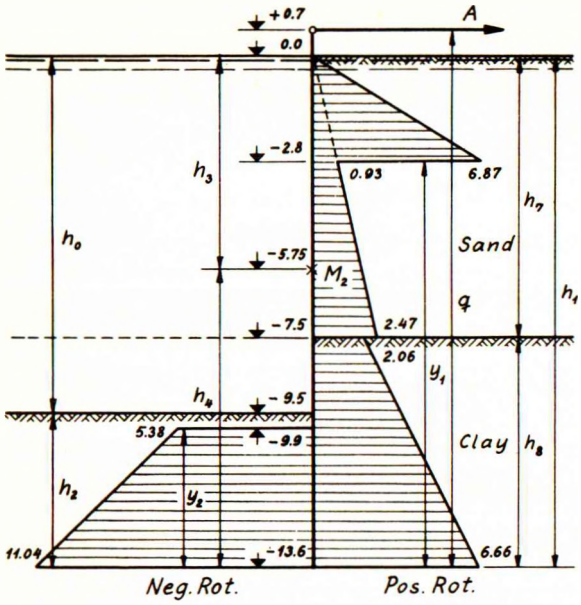

Fig.74C: Anchored sheet wall in stratified earth

$h_0 = 9.5$ m $q - h_1 = 0.7$ m

$h_7 = 7.5$ m $p_1 = p_w = 0$

$\gamma_7 = 1.0$ t/m^3 $\varphi_7 = 25^\circ$ $c_7 = 0$

$\gamma_8 = \gamma_2 = 1.2$ t/m^3 $\varphi_8 = \varphi_2 = 0$

$c_8 = c_2 = 0.14\,d + 1.7$ t/m^2

After some trial we find that we must assume:

$\underline{h_2 = 4.1 \text{ m}}$ $h_1 = 9.5 + 4.1 = 13.6$ m

$q = 13.6 + 0.7 = 14.3$ m $h_8 = 6.1$ m

$\xi_1 = \frac{14.3}{13.6} = 1.05$ $\xi_2 = \frac{14.3}{4.1} = 3.5$

For these values of ξ we find from Graphs 5, 6, 11, 15 and 16 for $\varphi = 0^\circ$ and $\varphi = 30^\circ$ respectively:

$\omega_2^0 = 0.90$ $\kappa_2^y = 2.40$

$\omega_8^0 = 0.71$ $\kappa_8^y = -3.20$

$\lambda_{30} = 0.35$ $\lambda_{30}^x = 3$ $\lambda_{30}^y = 0.26$

By means of Graph 19 and equation 5904, we get now for $\varphi = 25^\circ$:

$\lambda_7 = 0.42$ $\lambda_7^x = 2.45$ $\lambda_7^y = 0.33$ $\omega_7 = 1 - \sqrt{\frac{0.42 - 0.33}{2.45 - 0.33}} = 0.795$

As both ω_8^0 and ω_7 correspond to a pressure jump within h_7, ω_7 is valid (Section 634), and we get:

$y_1 = 0.795 \times 13.6 = 10.8$ m $y_2 = 0.90 \times 4.1 = 3.7$ m

By means of 6308-09, we can now calculate the unit pressures on the <u>active</u> side:

Above level - 2.8 m: $2.45 \times 1.0 \times 2.8 = 6.87$ t/m^2
Below level - 2.8 m: $0.33 \times 1.0 \times 2.8 = 0.93$ t/m^2
Above level - 7.5 m: $0.33 \times 1.0 \times 7.5 = 2.47$ t/m^2
Below level - 7.5 m: $1.0 \times 7.5 - 3.20 \times 1.7 = 2.06$ t/m^2
At level -13.6 m: $2.06 + 1.2 \times 6.1 - 3.20 \times 0.14 \times 6.1 = 6.66$ t/m^2

and on the <u>passive</u> side, disregarding negative pressures:

At level - 9.9 m: $1.2 \times 0.4 + 2.40\ (0.14 \times 2.4 + 1.7) = 5.38$ t/m^2
At level -13.6 m: $1.2 \times 4.1 + 2.40\ (0.14 \times 6.1 + 1.7) = 11.04$ t/m^2

The pressure diagrams are shown to scale in Fig.74C. With the aid of these we can now calculate:

$$E_1 = \tfrac{1}{2} \times 7.5 \times 2.47 + \tfrac{1}{2} \times 2.8\ (6.87 - 0.93) + \tfrac{1}{2} \times 6.1 \times 2.06 + \tfrac{1}{2} \times 6.1 \times 6.66 =$$
$$9.25 + 8.31 + 6.28 + 20.35 = 44.2 \text{ t/m}$$

$$E_1 z_1 = 9.25 \times 8.6 + 8.31 \times 11.73 + 6.28 \times 4.07 + 20.35 \times 2.03 = 245 \text{ tm/m}$$

$$E_2 = \tfrac{1}{2} \times 3.7 \times 5.38 + \tfrac{1}{2} \times 3.7 \times 11.04 = 9.95 + 20.45 = 30.4 \text{ t/m}$$

$$E_2 z_2 = 9.95 \times 2.47 + 20.45 \times 1.23 = 50 \text{ tm/m}$$

We can then show that 7405 is satisfied:

$$14.3\ (44.2 - 30.4) - 245 + 50 = 0$$

The horizontal component of the anchor pull is now determined by 7404:

$$\underline{A} = 44.2 - 30.4 = \underline{13.8 \text{ t/m}}$$

The depth h_3, at which the transversal force is zero, may be determined by the equation:

$$\tfrac{1}{2} \times 1.0 \times h_3^2 \times 0.33 + \tfrac{1}{2} \times 2.8\ (6.87 - 0.93) - 13.8 = 0 \qquad h_3 = 5.75 \text{ m} \qquad h_4 = 7.85 \text{ m}$$

The corresponding maximum moment is:

$$\underline{M_2} = 13.8 \times 6.45 - \tfrac{1}{6} \times 1.0 \times 5.75^3 \times 0.33 - 8.31 \times 3.88 = \underline{46 \text{ tm/m}}$$

For anchors of steel 52 and a sheet wall of steel 55-60, the "allowable" stress is about 3300 : 1.2 = 2750 kg/cm^2. Consequently, we find the necessary anchor section and wall section modulus at:

$$\underline{T} = 13800 : 2750 = \underline{5.0 \text{ cm}^2\text{/m}} \qquad \underline{W} = 4600000 : 2750 = \underline{1670 \text{ cm}^3\text{/m}}$$

742. Design with One Yield Hinge

The design method described in Section 741 will yield the smallest possible driving depth, and will also give moderate moments in the wall, but the necessary anchor pull will usually be rather high.

A considerably smaller anchor pull can be obtained, at the expense of a somewhat increased driving depth, by designing the wall on the assumption that a yield hinge develops in the state of failure. This method will usually give the most economical design, when the wall is driven into sand or firm clay with a horizontal surface.

The yield hinge is assumed to develop at a point which divides the height h_1 in two parts, h_3 and h_4 (Fig.74D). Otherwise, the exterior conditions are the same as in Fig.74A.

In the state of failure the upper part of the wall rotates about the anchor point, whereas the lower part is assumed to undertake a translation. When the design is made on this basis, it can be shown that no other movement is possible.

If the lower part should show a tendency to rotate about some point below itself, this will not affect the active pressure materially, but it will at once decrease the passive pressure and raise its pressure centre (compare the calculation of rupture XfP for a smooth wall in Section 56). This will reduce the moment in the yield hinge, stopping the yield here until the assumed translation takes place again.

If the lower part should show a tendency to rotate about some point above itself, this will raise the resultant of the active pressure and lower the re-

sultant of the passive pressure. This will tend to increase the moment in the yield hinge, causing an increased yield here until the assumed translation takes place again.

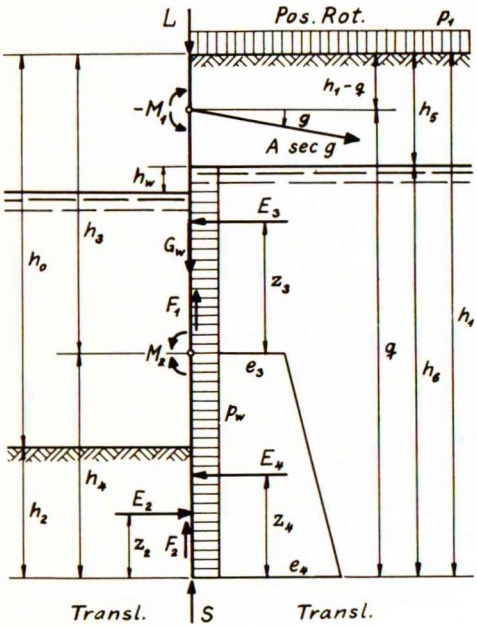

Fig.74D: Anchored sheet wall with one yield hinge

We have, consequently, for the upper and the lower part of the wall respectively:

$$\xi_3 = 1 - \frac{h_1 - q}{h_3} \qquad \xi_4 = \xi_2 = \infty \qquad 7406\text{-}07$$

On the passive side of the wall we have a rupture S (smooth wall) or SfP (rough wall). On the active side, the rupture must be of the type RsA (smooth wall) or PsA (rough wall). The latter ruptures, which are shown in Fig.35D, can be calculated as described in Section 463. However, we shall here use the approximation indicated in Section 474, according to which the pressures on the upper part of the wall are the same as for an active rupture A ($\xi = \xi_3$), whereas for the lower part they increase linearly from e_3 (at the yield hinge) to a value e_4 (at the foot of the wall) which corresponds to an active rupture Z ($\xi = \xi_4 = \infty$).

If the earth is stratified, with an internal boundary within h_4, two straight pressure lines are determined for h_4, one corresponding to the constants of the upper layer, and the other to those of the lower layer. In each layer the respective part of the corresponding pressure line is then used.

As the transversal force in the yield hinge is zero, the conditions of equilibrium for the two parts of the wall give, provided that $h_4 < h_6$ (or $p_w = 0$):

$$E_2 - E_4 - p_w h_4 = 0 \qquad M_2 = E_4 z_4 - E_2 z_2 + \tfrac{1}{2} p_w h_4^2 \qquad 7408\text{-}09$$

$$A = E_3 + p_w(h_6 - h_4) \qquad M_2 = E_3(q - h_4) - E_3 z_3 + \tfrac{1}{2} p_w (h_6 - h_4)(2q - h_6 - h_4) \qquad 7410\text{-}11$$

Whereas E_3 and $E_3 z_3$ are best determined by means of the pressure diagram, because general analytical expressions become too involved, we find for E_2, $E_2 z_2$, E_4 and $E_4 z_4$:

$$E_2 = \tfrac{1}{2}\gamma_2 \lambda_2 h_2^2 + c_2 \kappa_2 h_2 \qquad E_2 z_2 = \tfrac{1}{6}\gamma_2 \lambda_2 h_2^3 + \tfrac{1}{2} c_2 \kappa_2 h_2^2 \qquad 7412\text{-}13$$

$$E_4 = \tfrac{1}{2} h_4 (e_3 + e_4) \qquad E_4 z_4 = \tfrac{1}{6} h_4^2 (2e_3 + e_4) \qquad 7414\text{-}15$$

where:
$$e_3 = \left[\gamma_5 h_5 + \gamma_6 (h_3 - h_5)\right] \lambda_3^{\gamma} + p_1 \rho_3^{\gamma} + c_6 \kappa_3^{\gamma} \qquad 7416$$

and:
$$e_4 = (\gamma_5 h_5 + \gamma_6 h_6) \lambda_4^{\gamma} + p_1 \rho_4^{\gamma} + c_6 \kappa_4^{\gamma} \qquad 7417$$

As $h_6 = h_3+h_4-h_5$ and $h_2 = h_3+h_4-h_0$ we find, by insertion of 7416-17 in 7414, and of this as well as 7412 in 7408, the following equation in h_4:

$$0 = h_4^2(\gamma_2\lambda_2 - \gamma_6\lambda_4^y) + (h_0-h_3)\left[\gamma_2\lambda_2(h_0-h_3) - 2c_2\kappa_2\right]$$
$$- h_4\left[2\gamma_2\lambda_2(h_0-h_3) - 2c_2\kappa_2 + \gamma_5 h_5\lambda_4^y + \gamma_6(h_3-h_5)\lambda_4^y + p_1\rho_4^y + c_6\kappa_4^y + e_3 + 2p_w\right] \quad 7418$$

The calculation proceeds now in the following way. We estimate a value of h_3 and find the corresponding ξ_3 from 7406. As we know also $\xi_4 = \xi_2 = \infty$, the graphs in the Appendix will supply all the constants necessary for determining the complete pressure diagrams corresponding to any driving depth.

Next, we find e_3 from 7416 and can now, by means of 7418, calculate the value of h_4 which corresponds to the estimated h_3. When this has been done, we determine all the earth pressures and investigate then whether 7409 and 7411 yield the same positive moment M_2. If the difference is small, the average value can be used, but if it is considerable, h_3 must be altered and the whole calculation repeated until the agreement is satisfactory.

When this has been obtained we can, finally, calculate the anchor pull A by means of 7410 and the greatest negative moment M_1 (at anchor level) by means of the pressure diagram.

Example 74c

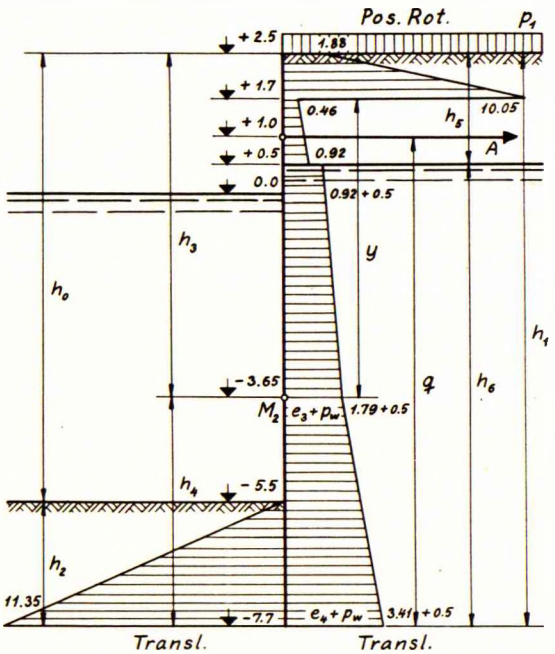

Fig.74E: Anchored sheet wall in sand

As an example we shall consider the following case of a rough sheet wall in coarse sand with an actual friction angle of 36°. Applying a safety factor of 1.25 to μ we find that the calculation should be made with $\varphi = 30°$. In addition to the active earth pressure a differential water pressure shall be taken into account. The given quantities are (see Fig. 74E):

$h_0 = 8$ m $h_1 - q = 1.5$ m $h_5 = 2$ m

$\gamma_5 = 1.8$ t/m³ $\gamma_6 = \gamma_2 = 1.0$ t/m³

$p_1 = 1$ t/m² $p_w = 0.5$ t/m² $\varphi = 30°$

After some preliminary calculations we find that we must assume:

$h_3 = 6.15$ m $\xi_3 = 1 - 1.5 : 6.15 = 0.75$

For $\xi_3 = 0.75$ and $\xi_4 = \xi_2 = \infty$ we get from Graphs 11 and 15-18 in the Appendix:

$\lambda_2 = 5.16$ $\omega_3 = 0.87$

$\rho_3^x = 1.88$ $\rho_3^y = 0.16$ $\rho_4^y = 0.273$

$\lambda_3^x = 5.66$ $\lambda_3^y = 0.21$ $\lambda_4^y = 0.266$

We will now first calculate e_3 from 7416:

$$e_3 = (1.8 \times 2 + 1.0 \times 4.15) \times 0.21 + 1 \times 0.16 = 1.79 \text{ t/m}^2$$

and we find then by means of 7418:

$$h_4^2 (1.0 \times 5.16 - 1.0 \times 0.266) + 1.85 \times 1.0 \times 5.16 \times 1.85$$
$$- h_4 (2 \times 1.0 \times 5.16 \times 1.85 + 1.8 \times 2 \times 0.266 + 1.0 \times 4.15 \times 0.266 + 1 \times 0.273 + 1.79 + 2 \times 0.5)$$
$$= 4.89 h_4^2 - 24.2 h_4 + 17.7 = 0 \qquad \underline{h_4 = 4.05 \text{ m}}$$

The remaining heights can now be calculated:

$$h_1 = 6.15 + 4.05 = 10.2 \text{ m} \qquad \underline{h_2} = 10.2 - 8 = \underline{2.2 \text{ m}} \qquad h_6 = 10.2 - 2 = 8.2 \text{ m}$$

$$q = 10.2 - 1.5 = 8.7 \text{ m} \qquad y_3 = 0.87 \times 6.15 = 5.35 \text{ m}$$

Next, we find the following unit earth pressures on the <u>active</u> side:

At level + 2.5 m: $1.88 \times 1 = 1.88 \text{ t/m}^2$
Above level + 1.7 m: $1.88 + 5.66 \times 1.8 \times 0.8 = 10.05 \text{ t/m}^2$
Below level + 1.7 m: $0.16 \times 1 + 0.21 \times 1.8 \times 0.8 = 0.46 \text{ t/m}^2$
At level + 0.5 m: $0.46 + 0.21 \times 1.8 \times 1.2 = 0.92 \text{ t/m}^2$
At level - 3.65 m: $0.92 + 0.21 \times 1.0 \times 4.15 = 1.79 \text{ t/m}^2$
At level - 7.7 m: $0.273 \times 1 + 0.266 (1.8 \times 2 + 1.0 \times 8.2) = 3.41 \text{ t/m}^2$

and on the <u>passive</u> side:

At level - 7.7 m: $5.16 \times 1.0 \times 2.2 = 11.35 \text{ t/m}^2$

The pressure diagrams (including the differential water pressures) are shown to scale in Fig. 74E. With their aid we can calculate:

$$E_2 = \tfrac{1}{2} \times 2.2 \times 11.35 = 12.5 \text{ t/m} \qquad E_2 z_2 = 12.5 \times 0.73 = 9.2 \text{ tm/m}$$

$$E_3 = \tfrac{1}{2} \times 0.8 \times 1.88 + \tfrac{1}{2} \times 0.8 \times 10.05 + \tfrac{1}{2} \times 1.2 \times 0.46 + \tfrac{1}{2} \times 1.2 \times 0.92 + \tfrac{1}{2} \times 4.15 \times 0.92$$
$$+ \tfrac{1}{2} \times 4.15 \times 1.79 = 0.75 + 4.02 + 0.28 + 0.55 + 1.91 + 3.72 = 11.2 \text{ t/m}$$

$$E_3 z_3 = 0.75 \times 5.88 + 4.02 \times 5.62 + 0.28 \times 4.95$$
$$+ 0.55 \times 4.55 + 1.91 \times 2.77 + 3.72 \times 1.38 = 41.3 \text{ tm/m}$$

$$E_4 = \tfrac{1}{2} \times 4.05 \times 1.79 + \tfrac{1}{2} \times 4.05 \times 3.41 = 3.62 + 6.90 = 10.5 \text{ t/m}$$

$$E_4 z_4 = 3.62 \times 2.70 + 6.90 \times 1.35 = 19.1 \text{ tm/m}$$

We can now find the <u>maximum moment</u> M_2 from 7409 and 7411:

$$M_2 = 19.1 - 9.2 + \tfrac{1}{2} \times 0.5 \times 4.05^2 = 14.0 \text{ tm/m}$$

$$M_2 = 11.2 (8.7 - 4.05) - 41.3 + \tfrac{1}{2} \times 0.5 \times 4.15 (2 \times 8.7 - 8.2 - 4.05) = 16.0 \text{ tm/m}$$

The agreement is sufficiently good, and the design should be based on the average value <u>$M_2 = 15.0$ tm/m.</u> The horizontal <u>anchor pull</u> is given by 7410:

$$\underline{A} = 11.2 + 0.5 \times 4.15 = \underline{13.3 \text{ t/m}}$$

The minimum moment (at anchor level) is found by means of the pressure diagram:

$$M_1 = -0.75 \times 1.23 - 4.02 \times 0.97 - \tfrac{1}{2} \times 0.46 \times 0.7^2 - \tfrac{1}{6} \times 0.21 \times 1.8 \times 0.7^3 = -5.0 \text{ tm/m}$$

With anchors and sheet wall of steel 37 the "allowable" stress is 2000 kg/cm², so that we find:

$$T = 13300 : 2000 = 6.65 \text{ cm}^2/\text{m} \qquad W = 1500000 : 2000 = 750 \text{ cm}^3/\text{m}$$

The corresponding anchor slab has been designed in Example 72b (see Fig. 72C).

In the following table, the results found by the author's methods are compared with results obtained by some empirical design methods. The driving depths, the anchor sections and the wall section moduli are comparable direct, but not the anchor pulls and wall moments as the safety factors are introduced in different ways.

Design according to:	Driving Depth m	Anchor Pull t/m	Anchor Stress kg/cm²	Anchor Section cm²/m	Max. Moment tm/m	Wall Stress kg/cm²	Wall Modulus cm³/m
Section 741	2.1	18.1	2000	9.05	12.7	2000	635
Section 742	2.2	13.3	2000	6.65	15.0	2000	750
Section 743	4.1	11.0	2000	5.5	10.6	2000	530
Danish Rules	~~2.0~~ 1.8	8.0	1300	6.2	~~10.5~~ 9.0	1600	~~655~~ 565
Tschebotarioff	3.5	8.5	1400	6.1	13.2	1870	705
Rowe	3.3	7.8	1260	6.2	8.9	1260	700
Terzaghi	3.2	8.8	1400	6.3	14.5	1600	900

With increasing driving depth (and unyielding anchors) the possible state of failure changes as indicated in Fig. 36M. At the extreme left is shown the state, on which the calculations in Section 741 are based, and at the centre left the state assumed in the present Section 742.

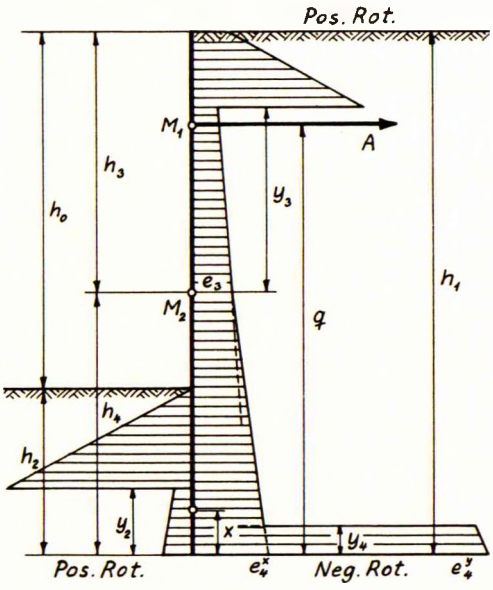

Fig. 74F: Anchored sheet wall partly fixed in ground

When the driving depth is made somewhat greater than necessary according to the calculation in Section 742, a certain reduction of the moments and the anchor pull can be obtained by making a new calculation, based on the state of failure shown in the centre of Fig. 36M. The corresponding rupture-figures are, on the passive side, of the type AaR (smooth wall) or AaP (rough wall), and on the active side, of the type AaRsA (smooth wall) or AaPsA (rough wall). The latter rupture is shown in Fig. 35F. We have then (see Fig. 74F):

$$\xi_3 = \frac{q - h_4}{h_3} \qquad \xi_4 = \frac{x}{h_1} \qquad \xi_2 = \frac{x}{h_2} \qquad 7419\text{-}21$$

If x is known, the pressures on the passive side can easily be determined, corresponding to ξ_2 and positive rotation. On the upper part h_3 of the active side, the pressures correspond to

ξ_3 and positive rotation, and at the foot of the wall we can calculate e_4^x and e_4^y approximately, corresponding to ξ_4 and negative rotation. Between e_3 and e_4^x a linear variation is assumed, and we have $y_4 = \omega_4 h_1$. Apart from the earth pressures a differential water pressure p_w may occur (not shown in Fig. 74F).

The given quantities are here h_1, h_2 and q, whereas we shall determine x, h_4, M_2 and A by means of 7408-11.

The calculation may now proceed in the following way. First, we estimate ξ_3 and draw a line corresponding to e_3^y. Next, we estimate x, calculate ξ_4 and ξ_2 and draw the diagram for the passive side as well as the part corresponding to e_4^y. h_4 is now fixed in such a way that 7408 is satisfied, and ξ_3 is checked and the necessary adjustments made. Next, the remaining part of the active pressure diagram is drawn, and it is investigated whether 7409 and 7411 give the same M_2. If not, x must be changed and the calculation repeated. Finally, 7410 gives A.

This calculation is made on the correct basis as long as the negative moments in the buried part of the wall prove to be numerically smaller than M_2. Otherwise, the method indicated in Section 743 must be used.

743. Design with Two Yield Hinges

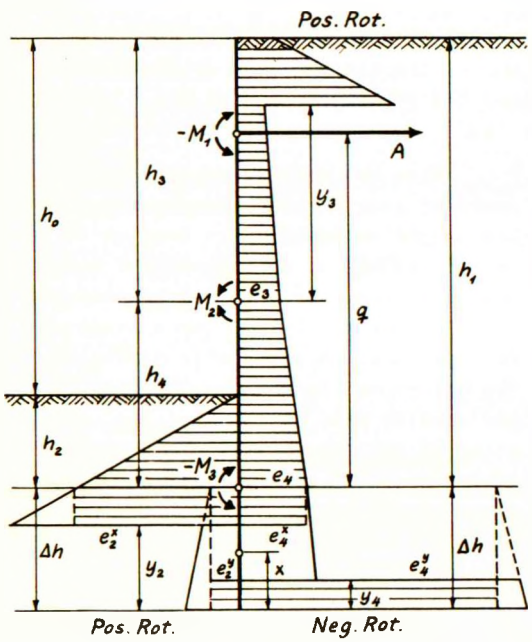

Fig.74G: Anchored sheet wall with two yield hinges

When the driving depth is sufficiently great, a second yield hinge will develop, viz. in the buried part of the wall, at the point where the transversal force is zero. If the driving depth is just sufficient to produce a negative yield moment M_3, numerically equal to the positive yield moment M_2, the state of failure will be as shown in Fig. 36M, centre right. If the driving depth is still greater, the state shown at the extreme right will occur. The following calculation method is valid for both these cases.

In the first part of the calculation, we consider only the pressures acting above the level of the lower yield hinge (see Fig. 74G). These pressures correspond approximately to :

$$\xi_3 = 1 - \frac{h_1 - q}{h_3} \qquad \xi_4 = \xi_2 = 0 \qquad 7422\text{-}23$$

Between the active pressures e_3 and e_4 a linear variation is assumed. Apart from the earth pressures a differential water pressure p_w may occur (not shown in Fig. 74G).

Of the 4 equations of equilibrium for the parts h_3 and h_4, the 3 are identical with 7408 and 7410-11, but 7409 must be substituted by:

$$M_2 - M_3 = E_4 z_4 - E_2 z_2 + \tfrac{1}{2} p_w h_4^2 \qquad 7424$$

The calculation proceeds exactly as described in the first part of Section 742, except that the criterion for a correct choice of h_3 is that $M_2 - M_3$ (from 7424) should be equal to twice M_2 (from 7411).

In the second part of the calculation, we must consider the pressures below the level of the lower yield hinge in order to find the necessary increase Δh of the calculated depth h_2. This is most simply done by means of the approximate method described in Section 735. We can use the formulae 7323-24 and 7329-30 direct, when e_1 is substituted by e_4, and M by M_3.

75. FIXED SHEET WALLS

751. Design With One Yield Hinge

Fig.75A shows a sheet wall, the top of which is fixed in an unyielding superstructure. Apart from this, the exterior conditions are the same as for the anchored sheet wall in Fig.74A.

For a fixed sheet wall no state of failure is possible, which does not involve the formation of at least one yield hinge in the wall. If only one yield hinge develops, this will generally be located at the top of the wall. A design based on this state of failure will lead to the smallest possible driving depth, and this will usually give the most economical design, when the wall is driven into soft clay or into a slope.

The moment in the top yield hinge can actually be chosen arbitrarily, provided that the wall is designed accordingly, but the most economical design will be obtained, when the fixing moment is numerically equal to the greatest positive moment.

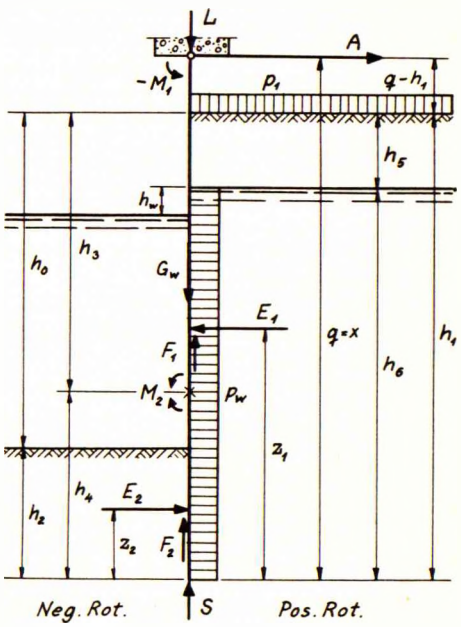

Fig.75A: Fixed sheet wall with one yield hinge

When the safety factor for the positive moments equals or exceeds that for the fixing moment, the wall must, in the state of failure, rotate about the top yield hinge. When the design is made on this basis, no other state of failure is

possible, as explained in Section 36. In the considered state of failure we have $x = q$ and:

$$\xi_1 = q : h_1 \qquad \xi_2 = q : h_2 \qquad 7501\text{-}02$$

The rupture-figures in the earth will be the same as those mentioned in Section 741.

The fixing moment at the top is denoted M_1 and is negative. The greatest positive moment M_2 occurs at the point where the transversal force is zero. The heights h_0, h_5 and $q\text{-}h_1$ are given, whereas the driving depth h_2, the anchor pull A and the moments M_1 and M_2 shall be determined by the calculation.

Considering the wall as a whole, as well as the lower part (h_4) separately, we get the following conditions of equilibrium:

$$S = L + G_W - F_1 - F_2 \qquad A = E_1 - E_2 + p_W h_6 \qquad 7503\text{-}04$$

$$-M_1 = q(E_1 - E_2) - E_1 z_1 + E_2 z_2 + p_W h_6 (q - \tfrac{1}{2} h_6) \qquad 7505$$

$$E_2 - E_4 - p_W h_4 = 0 \qquad M_2 = E_4 z_4 - E_2 z_2 + \tfrac{1}{2} p_W h_4^2 \qquad 7506\text{-}07$$

The calculation proceeds now as follows. We estimate a value of h_2 and calculate the corresponding values of h_1, h_6 and q. 7501-02 give then ξ_1 and ξ_2, for which we can find the earth pressure constants by means of the graphs in the Appendix. After this, we construct the pressure diagrams according to the principles indicated in Sections 62-63, and determine the height h_4, at which the transversal force is zero (7506). Next, we calculate $-M_1$ from 7505 and M_2 from 7507. If these two moments are not approximately equal, we must change h_2 and repeat the calculation until satisfactory agreement is obtained. 7504 gives then the anchor pull A.

Example 75a

We shall here consider a sheet wall (Fig. 75B), the top of which is fixed at the rear of a relieving platform supported on piles (not shown). The ground surface is horizontal on the active side, whereas on the passive side, a sloping surface is present, making a negative angle i_2 with the horizon.

We assume a rotation of the wall about a yield hinge at its top. In this case, where the wall proper does not reach the ground surface, the rupture on the active side must be of the type AsR (smooth back of superstructure) or AsP (rough back of superstructure), because an active zone-rupture must develop above the wall behind the superstructure. However, as mentioned in Section 474, we may simplify the calculation by reckoning with a rupture A as usual and considering the earth above anchor level simply as an additional surcharge.

On the passive side, where the surface slopes, the rupture is probably of the type A (smooth wall) or AfPfA (rough wall). However, for the sake of simplicity, we shall assume this rupture to be either of the type P (smooth wall) or SfP (rough wall). For both these ruptures general approximate formulae have been indicated in Section 65.

In the example considered the wall is assumed to be rough, and the earth on both sides to consist of coarse sand with an actual friction angle of 36°. Applying a safety factor 1.25 to μ we find that the calculation should be made with $\varphi = 30^\circ$. The given quantities are then:

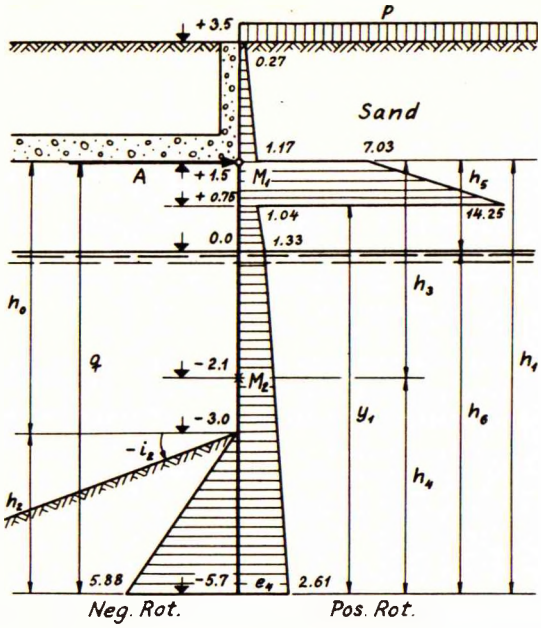

Fig.75B: Fixed sheet wall at rear of relieving platform

$h_0 = 4.5$ m $q - h_1 = 0$ $h_5 = 1.5$ m

$\gamma_5 = 1.7$ t/m^3 $\gamma_6 = \gamma_2 = 1.0$ t/m^3

$p = 1$ t/m^2 $p_w = 0$ $c = 0$ $\varphi = 30^\circ$

$j = 0$ $i_1 = 0$ $i_2 = -20^\circ$

The effective "surcharge" at anchor level is, including the weight of the earth, above this level:

$$p_1 = 1 + 1.7 \times 2.0 = 4.4 \text{ t/m}^2$$

For the active side we have $\xi_1 = 1$, and find then by means of Graphs 15-18:

$\omega_1 = 0.895$ $\lambda_1^x = 5.66$ $\lambda_1^y = 0.225$ $\rho_1^x = 1.60$ $\rho_1^y = 0.17$

The pressure constants for the passive side have already been calculated in Example 65a, where we have found:

$\lambda_2 = 2.18$ $\eta_2 = \frac{1}{3}$

After some trial we find that we must assume:

$h_2 = 2.7$ m $h_1 = q = 4.5 + 2.7 = 7.2$ m $h_6 = 7.2 - 1.5 = 5.7$ m $y_1 = 0.895 \times 7.2 = 6.45$ m

We can now calculate the unit pressures on the active side, using for the upper 2.0 m the constants indicated in the table in Section 523 for $\varphi = 30^\circ$ and a rough wall:

At level + 3.5 m: $0.273 \times 1 = 0.27$ t/m^2
Above level + 1.5 m: $0.27 + 0.266 \times 1.7 \times 2.0 = 1.17$ t/m^2
Below level + 1.5 m: $1.60 \times 4.4 = 7.03$ t/m^2
Above level + 0.75 m: $7.03 + 5.66 \times 1.7 \times 0.75 = 14.25$ t/m^2
Below level + 0.75 m: $0.17 \times 4.4 + 0.225 \times 1.7 \times 0.75 = 1.04$ t/m^2
At level 0.0 m: $1.04 + 0.225 \times 1.7 \times 0.75 = 1.33$ t/m^2
At level - 5.7 m: $1.33 + 0.225 \times 1.0 \times 5.7 = 2.61$ t/m^2

On the passive side we find:

At level - 5.7 m: $2.18 \times 1.0 \times 2.7 = 5.88$ t/m^2

The pressure diagrams are shown to scale in Fig.75B. With the aid of these we can now calculate:

$$E_1 = \tfrac{1}{2} \times 0.75 \times 7.03 + \tfrac{1}{2} \times 0.75 \times 14.25 + \tfrac{1}{2} \times 0.75 \times 1.04 + \tfrac{1}{2} \times 0.75 \times 1.33 + \tfrac{1}{2} \times 5.7 \times 1.33 + \tfrac{1}{2} \times 5.7 \times 2.61 = 2.64 + 5.34 + 0.39 + 0.50 + 3.80 + 7.43 = 20.1 \text{ t/m}$$

$$E_1 z_1 = 2.64 \times 6.95 + 5.34 \times 6.70 + 0.39 \times 6.20 + 0.50 \times 5.95 + 3.80 \times 3.80 + 7.43 \times 1.90 = 88.0 \text{ tm/m}$$

$$E_2 = \tfrac{1}{2} \times 2.7 \times 5.88 = 8.0 \text{ t/m} \qquad E_2 z_2 = 8.0 \times 0.9 = 7.2 \text{ tm/m}$$

The height h_4, at which the transversal force is zero, is determined by 7506:

$$e_4 h_4 - \tfrac{1}{2}\gamma_6 \lambda_1^y h_4^2 - E_2 = 2.61\, h_4 - \tfrac{1}{2} \times 1.0 \times 0.225\, h_4^2 - 8.0 = 0 \qquad \underline{h_4 \simeq 3.6\ \text{m}} \qquad h_3 = 3.6\ \text{m}$$

The moments M_1 and M_2 can now be found from 7505 and 7507:

$$-M_1 = 7.2\,(20.1 - 8.0) - 88.0 + 7.2 = 6.4\ \text{tm/m}$$

$$M_2 = \tfrac{1}{2} \times 2.61 \times 3.6^2 - \tfrac{1}{3} \times 1.0 \times 0.225 \times 3.6^3 - 7.2 = 6.2\ \text{tm/m}$$

As the agreement is fully satisfactory, we can finally calculate the anchor pull from 7504:

$$\underline{A} = 20.1 - 8.0 = \underline{12.1\ \text{t/m}}$$

If the sheet wall is to be made of reinforced concrete, it can be designed for the average moment 6.3 tm/m with "allowable" stresses as those indicated in Example 72a.

The anchor force and the fixing moment are transferred to the relieving platform. If this structure is designed in the conventional way with ordinary allowable stresses, the anchor force and the fixing moment calculated above must first be divided by about 1.3, as they already involve a safety factor of approximately this magnitude.

752. Design With Two Yield Hinges

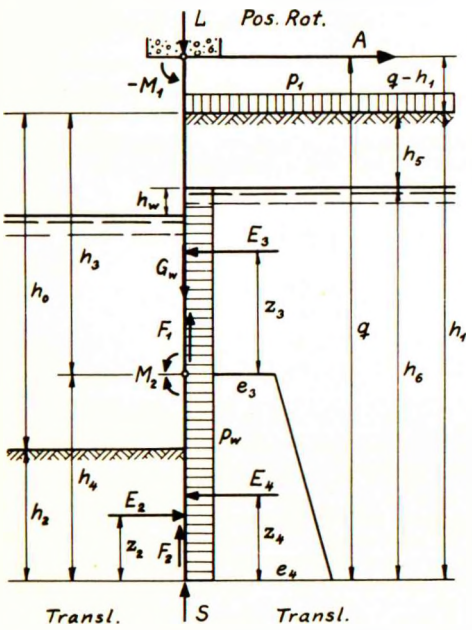

Fig.75C: Fixed sheet wall with two yield hinges

The design method described in Section 751 will yield the smallest possible driving depth, and also moderate moments, but a rather high anchor pull. A considerable reduction of the anchor pull can, however, be obtained by designing the wall on the assumption that two yield hinges develop in the wall. This method will usually give the most economical design, when the wall is driven into sand or firm clay with a horizontal surface.

Provided that the wall has a constant section modulus, the two yield moments M_1 and M_2 must be numerically equal. In the state of failure the upper part of the wall must rotate about the top yield hinge, whereas the lower part will undertake a translation as explained in Section 742. We have, consequently (see Fig.75C):

$$\xi_3 = 1 + \frac{q - h_1}{h_3} \qquad \xi_4 = \xi_2 = \infty \qquad 7508\text{-}09$$

The rupture-figures in the earth will be the same as those mentioned in Section 742. The earth pressure distribution is also, in principle, the same.

The conditions of equilibrium for the two separate parts of the wall give, provided that $h_4 < h_6$ (or $p_w = 0$):

$$E_2 - E_4 - p_w h_4 = 0 \qquad M_2 = E_4 z_4 - E_2 z_2 + \tfrac{1}{2} p_w h_4^2 \qquad 7510\text{-}11$$

$$A = E_3 + p_w(h_6 - h_4) \qquad M_2 - M_1 = E_3(q - h_4) - E_3 z_3 + \tfrac{1}{2} p_w (h_6 - h_4)(2q - h_6 - h_4) \qquad 7512\text{-}13$$

E_3 and $E_3 z_3$ are determined by means of the pressure diagram, whereas E_2, $E_2 z_2$, E_4 and $E_4 z_4$ can be found from 7412-17.

The calculation proceeds now as follows. We estimate a value of h_3 and find the corresponding ξ_3 from 7508. Using also 7509 we can find all the necessary earth pressure constants from the graphs in the Appendix. Next, we calculate e_3 from 7416 and determine h_4 by means of 7418. When this has been done we determine all the earth pressures and investigate then whether $M_2 - M_1$ (from 7513) is equal to twice M_2 (from 7511). If the difference is small, the average value can be used, but if it is considerable, h_3 must be altered and the whole calculation repeated. Finally, 7512 gives the anchor pull A.

Example 75b

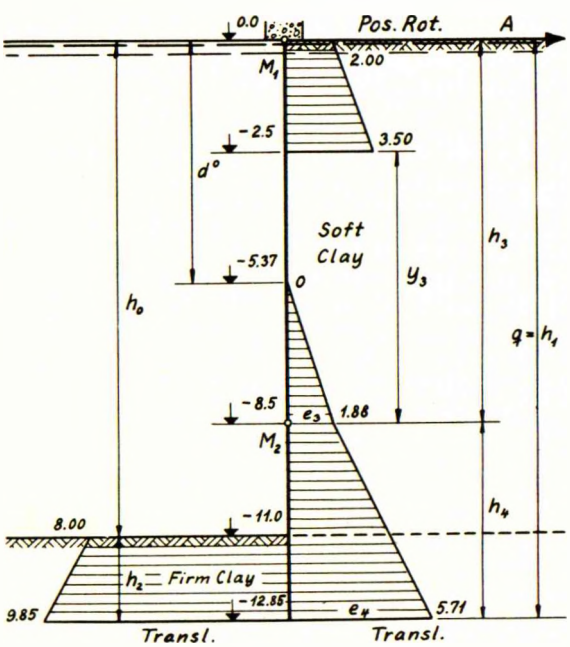

Fig.75D: Fixed sheet wall in stratified clay

As an example we shall consider a smooth sheet wall in stratified clay (Fig.75D). The upper layer, which has a thickness of 11 m, consists of soft clay, whereas the lower layer is a considerably firmer clay. For the sake of simplicity we assume the soft clay to exist over the entire height h_1 on the active side; this is, of course, on the safe side. The given quantities are:

$h_0 = 11$ m $\qquad q - h_1 = 0 \qquad h_5 = 0$

$\gamma_1 = 0.6$ t/m^3 $\qquad c_1 = 1.5 : 1.5 = 1$ t/m^2

$\gamma_2 = 1.0$ t/m^3 $\qquad c_2 = 6.0 : 1.5 = 4$ t/m^2

$p_1 = 0 \qquad p_w = 0 \qquad \varphi = 0$

where we have divided the actual cohesions by a safety factor 1.5.

Independently of the driving depth we have in this case $\xi_3 = 1$ and $\xi_4 = \xi_2 = \infty$. We find then from Graphs 1, 2, 5 and 6:

$\omega_3^0 = 0.705 \qquad \kappa_3^x = 2 \qquad \kappa_3^y = -3.22$

$\kappa_2 = 2 \qquad \zeta_2 = \tfrac{1}{2} \qquad \kappa_4^y = -2$

After some preliminary calculations we find that we must assume $h_3 = 8.5$ m. 7416 yields then, as $h_5 = 0$ and $h_6 = h_1$:

$$e_3 = 0.6 \times 8.5 - 1 \times 3.22 = 1.88 \text{ t/m}^2$$

The corresponding value of h_4 is determined by 7418:

$$h_4^2 (1.0 \times 1 - 0.6 \times 1) + 2.5 (1.0 \times 1 \times 2.5 - 2 \times 4 \times 2)$$
$$- h_4 (2 \times 1.0 \times 1 \times 2.5 - 2 \times 4 \times 2 + 0.6 \times 8.5 \times 1 - 1 \times 2 + 1.88) =$$
$$0.40\, h_4^2 + 6.02\, h_4 - 33.7 = 0 \qquad \underline{h_4 = 4.35 \text{ m}}$$

The remaining heights can now be calculated:

$h_1 = q = 8.5 + 4.35 = 12.85$ m $\quad \underline{h_2} = 12.85 - 11 = \underline{1.85 \text{ m}} \quad y_3 = 0.705 \times 8.5 = 6.00$ m

The depth d^o, at which the active pressure will be zero, is determined by the equation:

$$\gamma_1 d^o + c_1 \kappa_3^y = 0.6\, d^o - 1 \times 3.22 = 0 \qquad d^o = 5.37 \text{ m}$$

We can now calculate the unit pressures on the <u>active</u> side, disregarding negative pressures:

At level 0.0 m: $1 \times 2 = 2.00$ t/m^2
Above level - 2.5 m: $2.00 + 0.6 \times 2.5 = 3.50$ t/m^2
At level - 5.37 m: $0.6 \times 5.37 - 1 \times 3.22 = 0$ t/m^2
At level - 8.5 m: $0.6 \times 3.13 = 1.88$ t/m^2
At level -12.85 m: $0.6 \times 12.85 - 1 \times 2 = 5.71$ t/m^2

On the <u>passive</u> side we get:

At level -11.0 m: $4 \times 2 = 8.00$ t/m^2
At level -12.85 m: $8.00 + 1.0 \times 1.85 = 9.85$ t/m^2

The pressure diagrams are shown to scale in Fig.75D. Disregarding the negative pressures we find:

$$E_2 = \tfrac{1}{2} \times 1.85 \times 8.00 + \tfrac{1}{2} \times 1.85 \times 9.85 = 7.40 + 9.11 = 16.5 \text{ t/m}$$

$$E_2 z_2 = 7.40 \times 1.23 + 9.11 \times 0.62 = 14.7 \text{ tm/m}$$

$$E_3 = \tfrac{1}{2} \times 2.5 \times 2.00 + \tfrac{1}{2} \times 2.5 \times 3.50 + \tfrac{1}{2} \times 3.13 \times 1.88 = 2.50 + 4.37 + 2.94 = 9.8 \text{ t/m}$$

$$E_3 z_3 = 2.50 \times 7.67 + 4.37 \times 6.83 + 2.94 \times 1.04 = 52.1 \text{ tm/m}$$

$$E_4 = \tfrac{1}{2} \times 4.35 \times 1.88 + \tfrac{1}{2} \times 4.35 \times 5.71 = 4.09 + 12.45 = 16.5 \text{ t/m}$$

$$E_4 z_4 = 4.09 \times 2.90 + 12.45 \times 1.45 = 29.9 \text{ tm/m}$$

We can now calculate M_2 and $M_2 - M_1$ from 7511 and 7513:

$M_2 = 29.9 - 14.7 = 15.2$ tm/m $\quad M_2 - M_1 = 9.8\,(12.85 - 4.35) - 52.1 = 31.2$ tm/m $\quad -M_1 = 16.0$ tm/m

The agreement is satisfactory and the design should be based on the <u>average moment 15.6 tm/m</u>. The <u>anchor pull</u> is finally found from 7512, which gives <u>A = 9.8 t/m.</u>

For a sheet wall and anchors of steel 37, the necessary wall section modulus and anchor section are, respectively:

$$\underline{W} = 1560000 : 2000 = \underline{780 \text{ cm}^3/\text{m}} \qquad \underline{T} = 9800 : 2000 = \underline{4.9 \text{ cm}^2/\text{m}}$$

With <u>increasing driving depth</u> (and unyielding anchors) the possible state of failure changes as indicated in Fig.36M.

When the driving depth is made somewhat greater than necessary according to the calculation in Section 752, a certain reduction of the moments and the anchor pull can be obtained by making a new calculation, based on the state of failure shown in the centre of Fig. 36M. The corresponding pressure diagrams are shown in Fig. 74F.

Such a calculation can be made exactly as described at the end of Section 742, except that the criterion for a correct solution now is that $M_2 - M_1$ (from 7513) should be equal to twice M_2 (from 7511).

753. Design with Three Yield Hinges

When the driving depth is sufficiently great, a third yield hinge will develop, viz. in the buried part of the wall. The state of failure will then be as indicated in Fig. 36M, centre right or extreme right. The corresponding pressure diagrams are shown in Fig. 74G.

A calculation of this kind can be made exactly as described in Section 743, except that the criterion for a correct solution now is that $M_2 - M_3$ (from 7424) should be equal to $M_2 - M_1$ (from 7513). The necessary increase of the calculated driving depth is determined as described in Section 735.

Example 75c

We shall here consider a sheet wall (Fig. 75E), the top of which is fixed at the front of a relieving platform supported on piles (not shown).

We might, as in Example 75a, simplify the problem by assuming behind the platform, a horizontal ground surface at anchor level, loaded by a "surcharge" equal to the actual surcharge plus the weight of the earth above anchor level.

However, we would then still be faced with another problem, viz. that of a non-uniform surcharge, which has not been dealt with in the present work. The reason is, that although this problem can, in principle, be solved by means of the author's general method, it does not seem possible to indicate a simple, general rule expressing the actual effect of a non-uniform surcharge on the earth pressure diagram.

The conventional way to deal with this problem is the following. From the lower rear edge of the platform two straight lines are drawn, making angles of φ and $45^\circ + \frac{1}{2}\varphi$ respectively with the horizon. Above the point, where the upper line intersects the wall, the "surcharge" (actual surcharge + weight of earth) is assumed to have no effect at all. Below the point, where the lower line intersects the wall, this "surcharge" is assumed to have full effect. Between the two mentioned points a linear pressure variation is assumed.

Until a more accurate solution has been found, the author proposes to adopt, as an approximation, the method described above, but with the modification that he will use, instead of the two lines mentioned, a single line making an angle of 45° with the horizon.

The proposed procedure may be summarized as follows. From the lower rear edge of the platform a straight line is drawn, making an angle of 45° with the horizon. Above its point of intersection (P) with the wall, the usual pressure diagram, corresponding to no surcharge, is valid. Below this point a diagram, corresponding to the full "surcharge", is valid (see Fig. 75E).

Moreover, when we have a yield hinge in the central part of the wall, above point P, we shall simplify matters further by using above P, the constants corresponding to ξ_3, and below P, the constants corresponding to ξ_4.

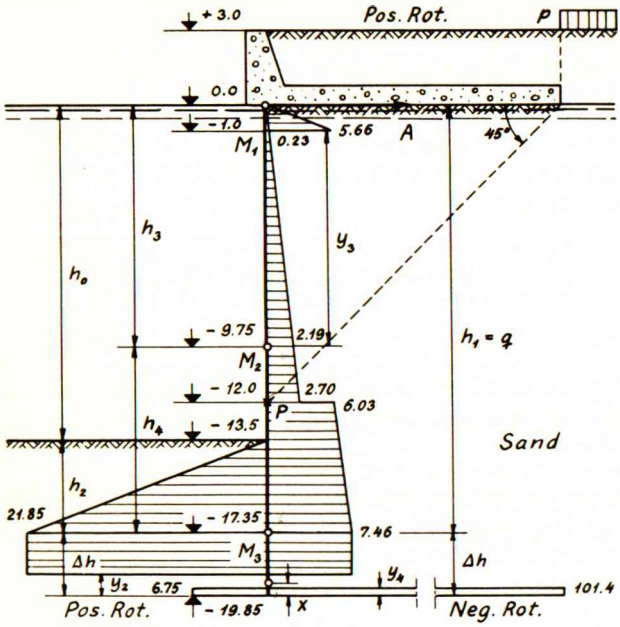

Fig.75E: Fixed sheet wall at front of relieving platform

In the example considered, the wall is assumed to be rough, and the earth on both sides to consist of coarse sand with an actual friction angle of 36°. Applying a safety factor 1.25 to μ, we find that the calculation should be made with $\varphi = 30^\circ$. The given quantities are then (see Fig.75E):

$h_o = 13.5$ m $q - h_1 = 0$ $h_5 = 0$

$\gamma_5 = 1.8$ t/m³ $\gamma_6 = \gamma_2 = 1.0$ t/m³

$p = 5$ t/m² $p_w = c = 0$ $\varphi = 30^\circ$

The effective "surcharge" at anchor level is, including the weight of the earth above this level:

$$p_1 = 5 + 1.8 \times 3.0 = 10.4 \text{ t/m}^2$$

As the load is considerable, and the water depth very great, it will be necessary to reduce the moments as much as possible. Consequently, we shall calculate the wall as fixed in the ground, as well as in the superstructure, i.e. we shall assume 3 yield hinges to develop.

Independently of the heights, we have in this case $\xi_3 = 1$ and $\xi_4 = \xi_2 = 0$. We find then from Graphs 15-18:

$\lambda_2^x = 5.66$ $\lambda_3^x = 5.66$ $\omega_3 = 0.895$ $\lambda_4^x = 0.266$ $\rho_4^x = 0.273$

$\lambda_2^y = 1.75$ $\lambda_3^y = 0.225$ $\rho_3^y = 0.17$ $\lambda_4^y = 4.4$ $\rho_4^y = 2.4$

After some preliminary calculations, we find that we must assume:

$$\underline{h_3 = 9.75 \text{ m}} \qquad y_3 = 0.895 \times 9.75 = 8.75 \text{ m}$$

We can then calculate the following active pressures:

Above level - 1.0 m: $1.0 \times 1.0 \times 5.66 = 5.66$ t/m²
Below level - 1.0 m: $1.0 \times 1.0 \times 0.225 = 0.23$ t/m²
At level - 9.75 m: $1.0 \times 9.75 \times 0.225 = 2.19$ t/m²
Above level -12.0 m: $1.0 \times 12.0 \times 0.225 = 2.70$ t/m²
Below level -12.0 m: $1.0 \times 12.0 \times 0.266 + 10.4 \times 0.273 = 6.03$ t/m²

The corresponding h_4 is found by means of 7510:

$$\tfrac{1}{2} \times 2.25(2.19 + 2.70) + 6.03(h_4 - 2.25) + \tfrac{1}{2} \times 1.0 \times 0.266(h_4 - 2.25)^2 - \tfrac{1}{2} \times 1.0 \times 5.66(h_4 - 3.75)^2$$

$$= -2.70\, h_4^2 + 26.7\, h_4 - 47.2 = 0 \qquad \underline{h_4 = 7.6 \text{ m}}$$

$$h_1 = q = 7.6 + 9.75 = 17.35 \text{ m} \qquad \underline{h_2} = 17.35 - 13.5 = \underline{3.85 \text{ m}}$$

At level - 17.35 m we have the following unit pressures:

$$e_4^x = 1.0 \times 17.35 \times 0.266 + 10.4 \times 0.273 = 7.46 \text{ t/m}^2$$

$$e_4^y = 1.0 \times 17.35 \times 4.4 + 10.4 \times 2.4 = 101.4 \text{ t/m}^2$$

$$e_2^x = 1.0 \times 3.85 \times 5.66 = 21.85 \text{ t/m}^2$$

$$e_2^y = 1.0 \times 3.85 \times 1.75 = 6.75 \text{ t/m}^2$$

By means of the pressure diagrams we can now calculate:

$$E_2 = \tfrac{1}{2} \times 3.85 \times 21.85 = 42.1 \text{ t/m} \qquad E_2 z_2 = 42.1 \times 1.28 = 54.0 \text{ tm/m}$$

$$E_3 = \tfrac{1}{2} \times 9.75 \times 2.19 + \tfrac{1}{2} \times 1.0 \,(5.66 - 0.23) = 10.68 + 2.72 = 13.4 \text{ t/m}$$

$$E_3 z_3 = 10.68 \times 3.25 + 2.72 \times 9.08 = 59.4 \text{ tm/m}$$

$$E_4 = \tfrac{1}{2} \times 2.25 \times 2.19 + \tfrac{1}{2} \times 2.25 \times 2.70 + \tfrac{1}{2} \times 5.35 \times 6.03 + \tfrac{1}{2} \times 5.35 \times 7.46 =$$
$$2.46 + 3.04 + 16.14 + 19.97 = 41.6 \text{ t/m}$$

$$E_4 z_4 = 2.46 \times 6.85 + 3.04 \times 6.10 + 16.14 \times 3.57 + 19.97 \times 1.78 = 128.6 \text{ tm/m}$$

The moments are found by means of 7513 and 7424:

$$M_2 - M_1 = 13.4 \,(17.35 - 7.6) - 59.4 = 71.4 \text{ tm/m} \qquad M_2 - M_3 = 128.6 - 54.0 = 74.6 \text{ tm/m}$$

The agreement is satisfactory, and the sheet wall should be designed for the average moment 36.5 tm/m. If it is to be made of reinforced concrete, we can use "allowable" stresses as those indicated in Example 72a.

The anchor pull is found from 7512, which gives A = 13.4 t/m. This force, and also the fixing moment M_1, is transferred to the relieving platform. If this structure is designed in the conventional way with ordinary allowable stresses, the anchor pull and the fixing moment must first be divided by about 1.3, as they already involve a safety factor of approximately this magnitude.

We shall, finally, determine the increase Δh of the calculated depth h_2, necessary for resisting the fixing moment M_3. First, we find from 7323-24 (with e_4 instead of e_1):

$$\Delta e^x = 21.85 - 7.46 = 14.4 \text{ t/m}^2 \qquad \Delta e^y = 101.4 - 6.75 = 94.7 \text{ t/m}^2$$

For a rough wall and $\varphi = 30^\circ$ we get, from the table in Section 735, the constants $K_1 = 0.5$ and $K_2 = 1.8$, with which we find from 7329-30 (for M = - 36.5 tm/m):

$$\frac{1}{x^2} = \frac{0.5 \times 94.7}{2 \times 36.5}\left[2 \times 1.8 + 0.5\left(\frac{94.7}{14.4} - 1\right)\right] = 4.14 \qquad x = 0.49 \text{ m}$$

$$\Delta h = 0.49\left(1.8 + 0.5\,\frac{94.7}{14.4}\right) = 2.5 \text{ m}$$

Thus, the actual driving depth should be 3.85 + 2.5 = 6.35 m. The complete pressure diagrams are shown to scale in Fig. 75E.

76. OTHER EARTH RETAINING STRUCTURES

761. Braced Walls

We shall consider here the bracing of vertical walls lining the sides of a cut. The bottom of the cut, as well as the original ground surface, is assumed horizontal. Water pressures, if any, are calculated separately, as usual.

Theoretically, a wall can be kept in place by a single row of struts, even if it is not driven into the bottom of the cut. This will be apparent from Graph 13 for example, but this graph shows also that (for $\varphi = 30^\circ$ and a rough wall) equilibrium is not possible outside the interval $0.10 < \eta < 0.61$. Moreover, as the wall must rotate about the bracing, if it rotates at all, we have in the limiting case $\eta = \xi$, and Graph 12 shows then that equilibrium is actually only possible within the interval $0.12 < \eta < 0.56$.

When the wall is driven somewhat into the bottom of the cut, the single row of struts can be placed higher than indicated above. In this case the necessary driving depth, the thrust in the struts and the moments in the wall can be calculated exactly as for an anchored sheet wall (Section 74).

If the cut is to be so deep that more than one row of struts must be used, we get a complicated system which can theoretically fail in several different ways. However, experience shows that we can always reckon with a certain state of failure in the earth behind the wall, due to the method of execution, which is as follows:

When the walls have been driven, a shallow cut is made, and the uppermost row of struts is put into position. The cut is then deepened sufficiently to allow the next row of struts to be placed, and so on, until the cut has attained its full depth and all bracings have been placed.

The first row of struts will be in position before any appreciable movement of the earth takes place, but, as the excavation proceeds, the exposed part of the wall will be pressed a little inwards. As the struts already placed are practically unyielding, the movement of this part of the wall will approximately be a rotation about the upper bracing, and this takes place before the next bracing is inserted. The movement which precedes the insertion of lower bracings, increases with the depth of the excavation.

Thus, when the excavation is completed, the wall will have undertaken a movement which is approximately a rotation about the uppermost row of struts. Measurements on struts in deep cuts (e.g. Spilker 1937, Peck 1943) have shown that this movement is usually sufficient to develop a state of rupture in the earth behind the wall. Consequently, we may calculate the earth pressure on the wall, corresponding to $\xi = q_1 : h$ and positive rotation. We have then for homogeneous earth:

$$\Sigma A = E = \tfrac{1}{2}\gamma h^2 \lambda + ph\rho + ch\kappa \qquad 7601$$

$$\Sigma Aq = Ez = \tfrac{1}{2}\gamma h^3 \lambda\eta + ph^2\rho\theta + ch^2\kappa\zeta \qquad 7602$$

In the case of partly submerged or stratified earth, the principles indicated in Sections 62-63 must be employed for determining the total earth pressure.

However, it is doubtful whether the distribution of the earth pressure will be as indicated by our usual pressure diagram (Section 473). So far, we have only used this diagram for walls which are either completely rigid, or which undergo elastic deformations in such a manner as to become concave on the side in contact with the earth on the "active" side.

Such a deformation will evidently tend to produce the pressure reduction on the central part of the wall, which is assumed in our diagrams for active line-ruptures. Even so, the diagrams are probably slightly "exaggerated" in this respect, which may be seen from the fact that a design of an anchored sheet wall with no yield hinge may give a smaller positive moment than a design with a yield hinge (see table at end of Example 74c), whereas actually the opposite should have been the case.

From the description of the way in which a braced wall is constructed, it will be seen that its deformations will make it convex on the side in contact with the earth. This will evidently tend to produce a pressure increase on the central part of the wall, and careful measurements (see above) have shown that the actual pressure distribution is roughly parabolic or trapezoidal.

Consequently, we shall use our usual pressure diagrams (indicated by dotted lines in Fig.76A) for determining the total earth pressure and its pressure centre, but we shall assume this pressure to have, actually, a trapezoidal distribution over the height of the wall (indicated by the unbroken line in Fig.76A). The corresponding unit pressures at the top and at the foot of the wall are, respectively:

$$e_t = \frac{6Ez}{h^2} - \frac{2E}{h} \qquad e_f = \frac{4E}{h} - \frac{6Ez}{h^2} \qquad 7603\text{-}04$$

As regards the distribution of the earth pressure over the different rows of struts, this may be found approximately by dividing the trapezoidal pressure diagram by horizontal lines bisecting the vertical distances between the individual rows of struts (see Fig.76A).

Example 76a

As an example, we shall consider a braced wall in stratified earth (Fig.76A). The upper layer consists of loose sand with an actual friction angle of 30°, whereas the lower layer is clay with an undrained shear strength of 4 t/m^2. In order to be able to design the wall and the bracing in the conventional way with ordinary allowable stresses, we shall not apply any safety factors to the above-mentioned constants. The given quantities are then:

$h = 12$ m $\quad x = 11$ m $\quad q_1 = 11$ m $\quad q_2 = 8$ m $\quad q_3 = 5$ m $\quad q_4 = 2$ m

$h_7 = 9$ m $\quad \gamma_7 = 1.7$ t/m^3 $\quad \varphi_7 = 30^\circ$ $\quad c_7 = 0$

$h_8 = 3$ m $\quad \gamma_8 = 1.5$ t/m^3 $\quad \varphi_8 = 0$ $\quad c_8 = 4$ t/m^2

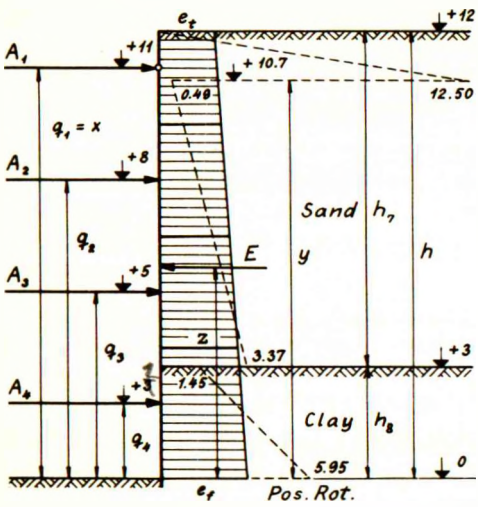

Fig.76A: Braced wall in stratified earth

We find first $\xi = 11 : 12 = 0.92$, and get then from Graphs 15-16 and 5-6 for positive rotation and a rough wall:

$$\omega_7 = 0.89 \qquad \lambda_7^x = 5.66 \qquad \lambda_7^y = 0.22$$

$$\omega_8^o = 0.765 \qquad \kappa_8^x = 2.57 \qquad \kappa_8^y = -3.46$$

As ω_7 and ω_8^o both correspond to a pressure jump within h_7, ω_7 is valid:

$$y = \omega_7 h = 0.89 \times 12 = 10.7 \text{ m}$$

We can now calculate the following unit pressures in the usual pressure diagram:

Above level +10.7 m: $1.7 \times 1.3 \times 5.66 = 12.50$ t/m²
Below level +10.7 m: $1.7 \times 1.3 \times 0.22 = 0.49$ t/m²
Above level + 3.0 m: $1.7 \times 9 \times 0.22 = 3.37$ t/m²
Below level + 3.0 m: $1.7 \times 9 - 4 \times 3.46 = 1.45$ t/m²
At level 0.0 m: $1.45 + 1.5 \times 3 = 5.95$ t/m²

By means of this diagram (dotted lines in Fig.76A) we can calculate:

$$E = \tfrac{1}{2} \times 9 \times 3.37 + \tfrac{1}{2} \times 1.3\ (12.50 - 0.49) + \tfrac{1}{2} \times 3 \times 1.45 + \tfrac{1}{2} \times 3 \times 5.95 =$$

$$15.2 + 7.8 + 2.2 + 8.9 = 34.1 \text{ t/m}$$

$$Ez = 15.2 \times 6.00 + 7.8 \times 11.13 + 2.2 \times 2.00 + 8.9 \times 1.00 = 191 \text{ tm/m}$$

When the total pressure is distributed trapezoidally (unbroken line in Fig.76A), the unit pressures at the top and the foot of the wall will be, respectively (7603-04):

$$e_t = \frac{6 \times 191}{12^2} - \frac{2 \times 34.1}{12} = 2.27 \text{ t/m}^2 \qquad e_f = \frac{4 \times 34.1}{12} - \frac{6 \times 191}{12^2} = 3.41 \text{ t/m}^2$$

Dividing this diagram in four parts as shown, the following brace thrusts are found:

$A_1 = 6.0$ t/m $\qquad A_2 = 7.95$ t/m $\qquad A_3 = 8.8$ t/m $\qquad A_4 = 11.35$ t/m

762. Unyielding Walls

In some cases a rigid wall may not even be able to make the small movement necessary to produce an active state of rupture in the earth. As examples may be mentioned a retaining wall founded on rock, and the side walls of a gravity dock.

In such cases we must reckon with the so-called earth pressure at rest. According to Tschebotarioff (1948, 1949) this pressure can, at least for gravel, sand and normally consolidated clay, be assumed equal to one half of the effective overburden pressure. This means that for i = j = 0 we must assume:

$$\lambda_o = \rho_o = \tfrac{1}{2} \qquad \kappa_o = 0 \qquad \eta_o = \tfrac{1}{3} \qquad \theta_o = \tfrac{1}{2} \qquad 7605\text{-}08$$

Possible water pressures must be considered separately. For the earth pressures the submerged unit weight should be used below the water table.

8. STABILITY AND FOUNDATION PROBLEMS

81. CELLULAR COFFERDAMS ON ROCK

811. General

We shall here investigate the stability of a double sheet wall (two parallel sheet walls connected by means of two or more rows of anchors) or a cellular cofferdam. The walls are placed on the rock surface, which is assumed horizontal. Between the walls an earth fill is provided.

For a cellular cofferdam, the effective width w may be assumed equal to the width of a strip with the same area as the actual horizontal cross section of the cofferdam.

Such a structure was formerly designed simply with a suitable safety against sliding and overturning (e.g. Verdeyen 1948). However, in 1944 Terzaghi introduced a new method of investigation, viz. regarding the safety against shear along the vertical central plane. He found that reasonable agreement with experience could be obtained when the earth pressure factor in this plane was assumed to be 0.4 - 0.5 (for sand).

However, two objections can be raised against this. First, it seems impossible to construct a kinematically possible rupture-figure involving one or more vertical rupture-lines. Second, according to 3339 (with $\beta = 90^\circ$) the earth pressure factor in a vertical rupture-line must be $\cos^2\varphi$ (0.75 for $\varphi = 30^\circ$ and 0.67 for $\varphi = 35^\circ$) and as Terzaghi found that lower values are sufficient, this means that a vertical rupture-line cannot be the critical one.

In a very wide cofferdam plastic zones may develop, corresponding to ordinary active and passive pressures, but for the usual dimensions this is not possible. We can, however, indicate one figure of rupture which is statically and kinematically possible, viz. the simple line-rupture shown in Fig.81A.

This rupture is of the type X, as the rupture-line consists of a single convex circle. The earth below this circle remains at rest, whereas the whole earth mass above the circle rotates as one rigid body about the centre of the circle. The walls will follow the horizontal movements of the rotating earth mass, but will probably not move vertically, although the left wall in Fig.81A may have a tendency to rise.

Incidentally, this concept of a single, curved rupture-line enables a very simple stability investigation to be carried out by means of the extreme-method.

For this purpose it is only necessary to approximate the rupture-line by a logarithmic spiral, take the moments about its pole, and find by trial the spiral involving the smallest safety factor. However, we shall here carry out an equilibrium calculation.

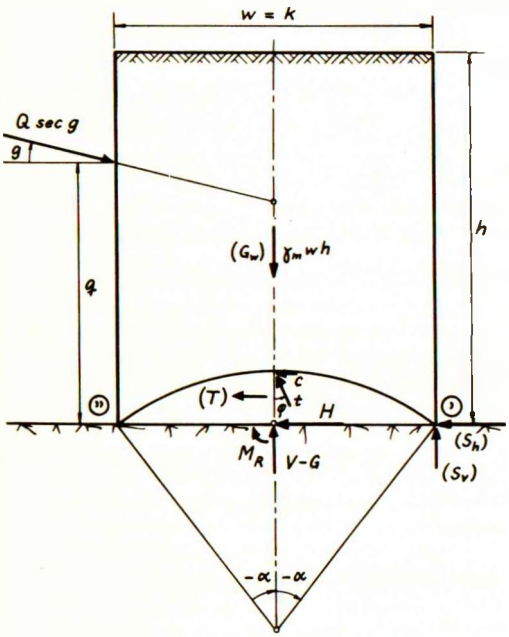

Fig.81A: Cellular cofferdam on rock

We consider the equilibrium of the walls plus the earth above the rupture-line. For the sake of simplicity we disregard the weight G_w of the walls, and also the tangential forces T acting on the transverse walls below the rupture-line. Further, we disregard the reactions S_v and S_h from the rock, acting upon the foot of the right wall in Fig.81A. All this is evidently on the safe side.

By horizontal projection, by vertical projection, and by taking the moments about the middle point of the chord of the rupture-circle, we get:

$$Q = H \qquad 8101$$

$$\gamma_m w h + G - V + Q \tan g = 0 \qquad 8102$$

$$M_R + Q(q - \tfrac{1}{2} w \tan g) = 0 \qquad 8103$$

G is here the (negative) weight of the earth between rock surface and rupture-line. γ_m is an average unit weight for the whole earth mass within the cofferdam, whereas γ (without subscript) is the unit weight of the earth in the vicinity of the rupture-line.

In the equations 8101-03 we can insert 3223, 3325-26 and 3335 with k = w and $\beta = 0$. We have then 3 equations with 3 unknown quantities, viz. α, t' and w, assuming Q, q, g and h to be given. These equations are solved by eliminating t' from 8101 and 8102, which gives a relation between α and w. With an arbitrary value of α, the corresponding w is found, and it is then investigated whether 8103 is satisfied. If not, α must be changed and the calculation repeated until satisfactory agreement is obtained. As the rupture-circle is convex, negative values of α must be used, whereas φ and c should be assumed positive according to Fig.81A.

In principle, a similar calculation can be made when the rock surface makes an angle β with the horizon, but the formulae for such a case will not be indicated here.

If we know the magnitude and sign of the wall friction angle δ, we can find the unit earth pressures at the foot of the walls by means of 3425 (and 3318), but apart from this the present theory does not enable the determination of the earth pressures on the two walls separately.

812. Frictionless Fill

Inserting 3223, 3353-54 and 3359 (with $\beta = 0$) in 8101-03, and using also 3355, we find the following equations:

$$w = \frac{Q}{c\,H^{cy}} \qquad \sigma' = \gamma_m h - cV^{cy} + \frac{Q}{w}\tan g \qquad 8104\text{-}05$$

$$cw^2 M_R^c + Q(q - \tfrac{1}{2}w \tan g) = 0 \qquad 8106$$

With an estimated value of α we find w from 8104, and investigate then whether 8106 is satisfied.

Example 81a

As an example, we consider a cellular cofferdam with firm clay fill, subjected to unilateral water pressure. The given quantities are (see Fig. 81A which, however, is not to scale):

$h = 9$ m $\qquad q = \frac{1}{3}h = 3$ m $\qquad Q = \frac{1}{2}\gamma_w h^2 = 40.5$ t/m

$g = 0 \qquad \gamma = \gamma_m = 1.7$ t/m^3 $\qquad c = 6.3 : 1.5 = 4.2$ t/m^2

We have here divided the actual cohesion by a safety factor 1.5. For a provisory structure this may be considered sufficient, so that no safety factor need be applied to the water pressure.

By means of Table 1 in the Appendix we find, after some trial:

$\alpha = -22^\circ \qquad H^{cy} = 0.901 \qquad V^{cy} = -0.768 \qquad M_R^c = -0.253$

$$w = \frac{40.5}{4.2 \times 0.901} = 10.7 \text{ m} \qquad \sigma' = 1.7 \times 9 + 4.2 \times 0.768 = 18.5 \text{ t/m}^2$$

We can then show that 8106 is satisfied, which means that α has been correctly chosen:

$$-4.2 \times 10.7^2 \times 0.253 + 40.5 \times 3 = 0$$

813. Cohesionless Fill

By insertion of 3223, 3325-26 and 3335 (with $c = 0$ and $\beta = 0$) in 8101-03, we find the following equations:

$$\gamma(G^{\gamma z} - V^\gamma + H^\gamma V^{ty} : H^{ty})w^2 + \gamma_m h w + Q(\tan g - V^{ty} : H^{ty}) = 0 \qquad 8107$$

$$t' = (\gamma_m h + \gamma_w G^{\gamma z} - \gamma_w V^\gamma + \frac{Q}{w}\tan g) : V^{ty} \qquad 8108$$

$$\gamma w^3 M_R^{\gamma y} + t' w^2 M_R^t + Q(q - \tfrac{1}{2}w \tan g) = 0 \qquad 8109$$

where: $V^\gamma = V^{\gamma z} + V^{\gamma x}\sin 2\varphi \qquad H^\gamma = H^{\gamma z} + H^{\gamma y}\cos 2\varphi \qquad 8110\text{-}11$

With an estimated value of α we find w from 8107, t' from 8108, and investigate then whether 8109 is satisfied.

Example 81b

We consider here a cellular cofferdam with the same height and exterior load as the one in Example 81a, but the fill is now assumed to be well-compacted sand with an actual friction angle of 36°. It is also assumed to be well-drained, so that we have an average unit weight of $\gamma_m = 1.6$ t/m^3. However, the ground water table probably cannot be lowered below the rupture-line, so that we must here assume $\gamma = 1.0$ t/m^3.

We apply, as usual, a safety factor of 1.25 to μ, but in addition we shall multiply the water pressure by 1.2, obtaining in this way a total safety of about 1.5. We have thus (see Fig.81A, which is to scale):

$$h = 9 \text{ m} \qquad q = \tfrac{1}{3}h = 3 \text{ m} \qquad Q = 1.2 \times \tfrac{1}{2}\gamma_w h^2 = 48.5 \text{ t/m}$$

$$g = 0 \qquad \gamma = 1.0 \text{ t/m}^3 \qquad \gamma_m = 1.6 \text{ t/m}^3 \qquad \varphi = 30^\circ$$

By means of Tables 1 and 3 in the Appendix we find, after some trial:

$$\alpha = -32^\circ \qquad G^{Yz} = -0.097 \qquad M_R^{Yy} = 0.011 \qquad M_R^{t} = -0.102$$

$$V^{Yz} = -0.054 \qquad V^{Yx} = -H^{Yy} = 0.167 \qquad H^{Yz} = 0.175 \qquad H^{ty} = 0.222 \qquad V^{ty} = 0.519$$

$$V^{Y} = -0.054 + 0.167 \times 0.866 = 0.091 \qquad H^{Y} = 0.175 - 0.167 \times 0.5 = 0.092$$

Equations 8107-08 give now:

$$1.0(-0.097 - 0.091 + 0.092 \times 0.519 : 0.222)w^2 + 1.6 \times 9\, w - 48.5 \times 0.519 : 0.222$$

$$= 0.027\, w^2 + 14.4\, w - 113.4 = 0 \qquad \underline{w = 7.75 \text{ m}}$$

$$t' = (1.6 \times 9 - 1.0 \times 7.75 \times 0.097 - 1.0 \times 7.75 \times 0.091) : 0.519 = 24.9 \text{ t/m}^2$$

We can then show that 8109 is satisfied:

$$1.0 \times 7.75^3 \times 0.011 - 24.9 \times 7.75^2 \times 0.102 + 48.5 \times 3 = 0$$

It should be noted that we have found $w : h = 0.86$, which is very nearly the same as the value most commonly used in practice (0.85).

82. CELLULAR COFFERDAMS IN EARTH

821. General

We shall now investigate the stability of a cellular cofferdam (or a double sheet wall), the piles of which are driven into the ground. The ground surfaces, which are assumed horizontal, may be located at different levels at the two sides of the cofferdam.

When the driving depth is shallow, the whole cofferdam will, in the state of failure, rotate about a point below itself (Fig.82A). Correspondingly, we get a rupture X between the walls, but in addition a rupture P (rough wall) or R (smooth wall) occurs at each exterior side, passive on the right side, and active on the left. The corresponding exterior earth pressures are, in this case, independent of the actual location of the rotation centre.

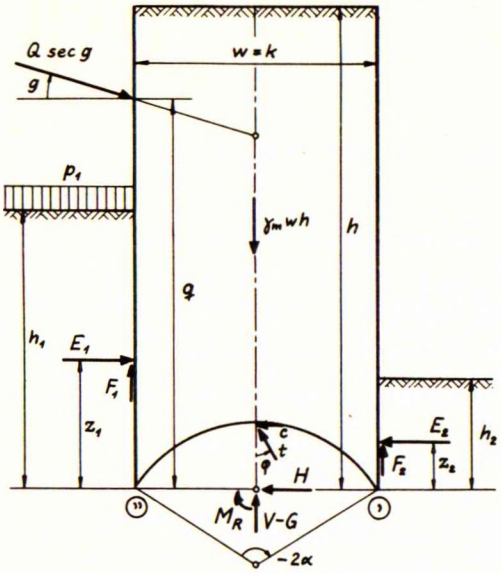

Fig.82A: Rupture X in cellular cofferdam

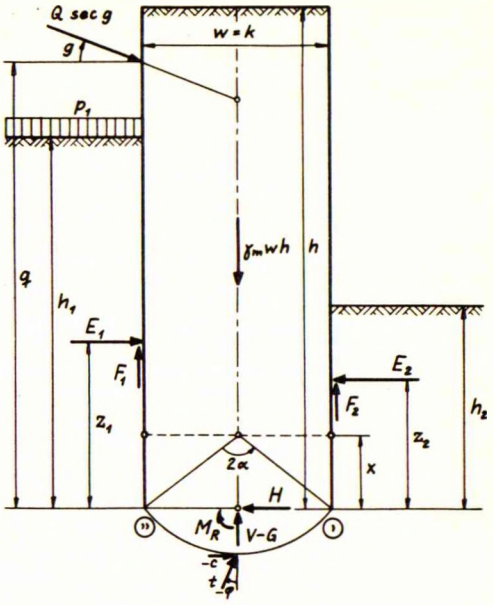

Fig.82B: Rupture A in cellular cofferdam

When the driving depth is greater, the rotation centre will be located above the foot of the walls. Between the walls we will get a rupture A (Fig.82B) or a rupture AwXwA (Fig.82C). Outside the walls the ruptures will probably be of the type AaR (smooth wall) or AaP (rough wall). In these cases the exterior earth pressures depend on the location of the rotation centre, and (in the case of rough walls) also on the vertical movements of the walls. We may, however, as an approximation, use the constants found from the graphs in the Appendix, although the values indicated for rough walls correspond to "normal" rotations only.

In principle, the rupture AwXwA can be treated by means of the present theory, but the formulae and the calculation become rather complicated. For this reason we shall investigate in the following the ruptures X and A only.

We consider the equilibrium of the cofferdam proper, including the inside earth above the rupture-line. By horizontal projection, by vertical projection, and by taking

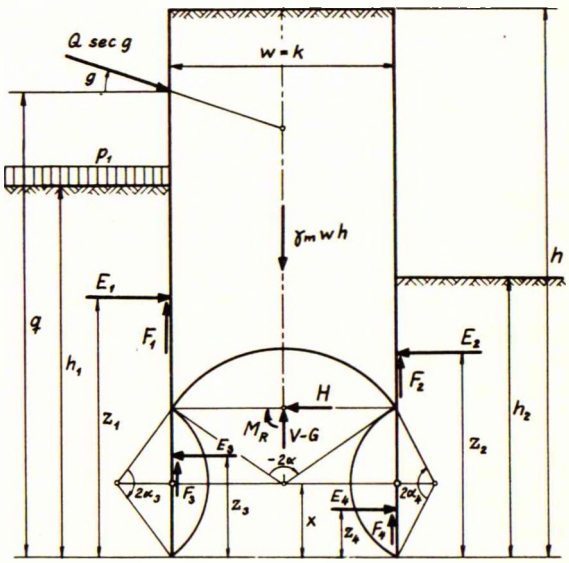

Fig.82C: Rupture AwXwA in cellular cofferdam

the moments about the middle point of the chord of the rupture-circle, we get (see Figs. 82A-B):

$$Q = H - E_1 + E_2 \qquad \gamma_m wh + G - V - F_1 - F_2 + Q \tan g = 0 \qquad 8201\text{-}02$$

$$M_R + Q(q - \tfrac{1}{2}w \tan g) + \tfrac{1}{2}w(F_1 - F_2) + E_1 z_1 - E_2 z_2 = 0 \qquad 8203$$

When we consider h, h_1, h_2, Q, q and g as given quantities, the only unknown quantities are α, t' and w as in Section 81. For E, F and z we have the usual expressions 6118-20, and the constants in these equations can be found by means of the graphs in the Appendix when ξ is known.

In order to solve the equations 8201-03 we insert 3223, 3325-26 and 3335 with $k = w$ and $\beta = 0$. Further, we eliminate t' from 8201 and 8202, obtaining thereby a relation between α and w.

In the case of a rupture X (Fig. 82A) we know the external earth pressures in advance. Therefore, we need only estimate a value of α, find successively the corresponding w and t', and change α, if necessary, until 8203 is satisfied.

In the case of a rupture A (Fig. 82B) we can use the same procedure in principle, but we must start by estimating not only α but also w in order to be able to calculate the external earth pressures. We have namely:

$$\xi_1 = \frac{x}{h_1} = \frac{w \cot \alpha}{2h_1} \qquad \xi_2 = \frac{x}{h_2} = \frac{w \cot \alpha}{2h_2} \qquad 8204\text{-}05$$

When w has been found from the above-mentioned relation between α and w, we must adjust the values of ξ_1 and ξ_2 and recalculate w before proceeding to find t' and investigate whether 8203 is satisfied.

Whereas we must assume φ and c positive and α negative for the rupture X, the reverse should be done for the rupture A.

Apart from the unit earth pressures at the foot of the walls, the inside pressures on the two walls cannot be determined separately by means of the present theory. However, in the case of a double sheet wall with only one row of anchors, the right wall in Figs. 82A-C may be calculated approximately by assuming a state of failure as shown in Fig. 74F.

For shallow driving depths the rupture X will always be the most critical one. For greater driving depths the most critical rupture cannot be indicated in advance, and in such cases it may therefore be necessary to investigate both rupture X and A, and possibly also AwXwA.

Moreover, when the driving depth is considerable, it will be necessary to investigate whether the walls of the structure are strong enough to prevent a failure as the one shown in Fig. 82D. It is here assumed that a yield hinge will develop in each wall and that the upper parts of the walls and the fill will rotate about the centre of a convex rupture-circle, whereas the lower parts remain stationary.

For kinematical reasons the rupture-circle must meet the walls tangentially, which means that we have $\alpha = -90^\circ$. In each yield hinge we have a yield moment M and no transversal force, whereas an axial force may occur, unless the walls are perfectly smooth. However, as we cannot calculate the individual earth pressures on the two walls, we cannot find these axial forces either, and we shall therefore disregard them, this being on the safe side.

If we measure the different heights from yield hinge level (Fig.82D), the equations of equilibrium for the moving parts of the walls and the fill will be identical with 8201-03, with the exception that the left side of 8203 should equal 2M instead of zero.

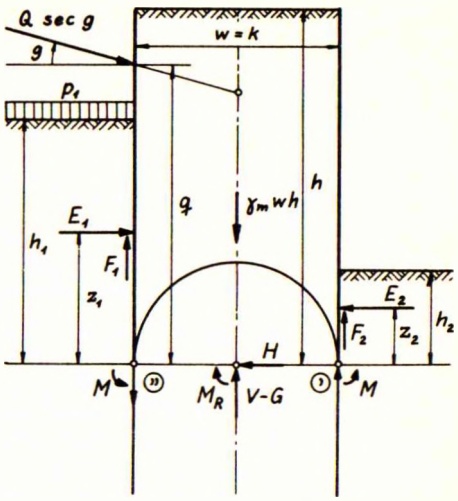

Fig.82D: Cellular cofferdam with yield hinges

The procedure is now the following. After having found the necessary width w by means of the stability calculation as previously described, we estimate a smaller h than the actual height of the cofferdam, and investigate whether the corresponding relation between α and w is satisfied with $\alpha = -90^\circ$ and the actual value of w. If not, we must change h, until satisfactory agreement is obtained. The left side of equation 8203 indicates then the corresponding yield moments 2M.

If M is found to be negative, or h to exceed the actual height of the cofferdam, this means that the considered rupture-figure with two yield hinges (Fig. 82D) is less critical than the rupture-figure used in the stability calculation.

If, on the other hand, we find a positive M, and a smaller h than the actual height of the cofferdam, we must either make the walls of the cofferdam strong enough to resist the calculated moments with our usual "allowable" stresses, or we must increase the width w in order to reduce the moments.

The above applies to double sheet walls. In a cellular cofferdam the flat sheet piles have only a negligible section modulus, and, although the transverse walls will probably provide a certain resistance, this is difficult to calculate. Therefore, in order to be on the safe side it is recommended to construct cellular cofferdams of such a width that no critical failure of the type shown in Fig. 82D can occur with positive yield moments M.

It should be noted that, even if the width is so great that positive yield hinge moments are not found, or even if the walls are designed to resist the calculated yield hinge moments, this does not necessarily mean that the walls will be strong enough to resist any type of failure. On the contrary, it is probable that other, considerably more complicated types of failure may occur, which have not been investigated here.

822. Frictionless Earth

By insertion of 3223, 3353-54 and 3359 (with $\beta = 0$) in 8201-03 (8203 with 2M instead of 0 on the right side), we find the following equations:

$$w = \frac{Q + E_1 - E_2}{c\, H^{cy}} \qquad \sigma' = \gamma_m h - cV^{cy} + \frac{Q}{w}\tan g - \frac{F_1 + F_2}{w} \qquad 8206\text{-}07$$

$$cw^2 M_R^c + Q(q - \tfrac{1}{2}w \tan g) + \tfrac{1}{2}w(F_1 - F_2) + E_1 z_1 - E_2 z_2 = 2M \qquad 8208$$

In a stability calculation we find w from 8206 with an estimated value of α, and investigate then whether 8208 is satisfied, with $M = 0$.

In a yield moment calculation we estimate h and investigate whether 8206 is satisfied, with $\alpha = -90^\circ$ and the actual w. 8208 gives then the yield hinge moment M.

823. Cohesionless Earth

By insertion of 3223, 3325-26 and 3335 (with $c = 0$ and $\beta = 0$) in 8201-03 (8203 with 2M instead of 0 on the right side), we find the following equations:

$$\gamma(G^{\gamma z} - V^{\gamma} + H^{\gamma} V^{ty} : H^{ty}) w^2 + \gamma_m h w + Q \tan g - (Q + E_1 - E_2) V^{ty} : H^{ty} - F_1 - F_2 = 0 \qquad 8209$$

$$t' = (\gamma_m h + \gamma w G^{\gamma z} - \gamma w V^{\gamma} + \frac{Q}{w}\tan g - \frac{F_1 + F_2}{w}) : V^{ty} \qquad 8210$$

$$\gamma w^3 M_R^{\gamma y} + t' w^2 M_R^t + Q(q - \tfrac{1}{2}w \tan g) + \tfrac{1}{2}w(F_1 - F_2) + E_1 z_1 - E_2 z_2 = 2M \qquad 8211$$

where V^{γ} and H^{γ} are defined by 8110-11.

In a stability calculation we find w from 8209 with an estimated value of α, then t' from 8210, and finally we investigate whether 8211 is satisfied, with $M = 0$.

In a yield moment calculation we estimate h and investigate whether 8209 is satisfied, with $\alpha = -90^\circ$ and the actual w. 8211 gives then the yield hinge moment M.

In the case of hydrodynamic water pressures the design is, as pointed out by Terzaghi (1944), more often governed by the necessity of obtaining safety against piping and boiling than by stability considerations.

Example 82a

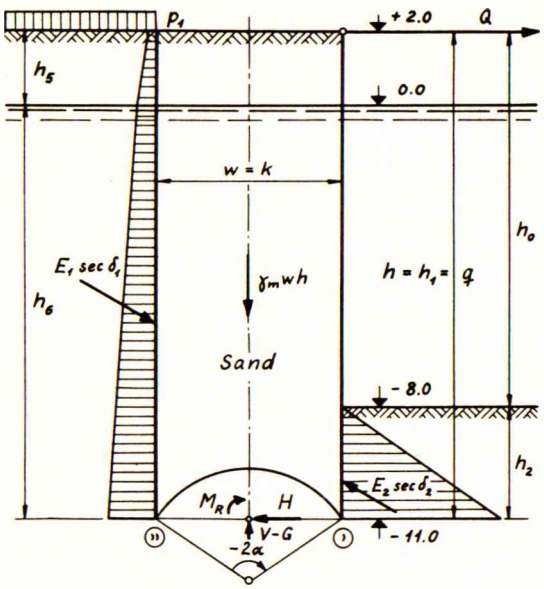

Fig.82E: Cellular cofferdam as quay wall in sand

As an example we shall consider a quay wall built of cellular cofferdams (Fig.82E). The natural ground as well as the fill consists of sand with an actual friction angle 36°. Applying a safety factor 1.25 to μ we find that the calculation should be carried out with $\varphi = 30^\circ$. The exterior force Q is a bollard pull. The given quantities are:

$h_0 = 10$ m $h = h_1 = q = 13$ m

$h_2 = 3$ m $h_5 = 2$ m $h_6 = 11$ m

$p_1 = 3$ t/m^2 $Q = 2$ t/m $g = 0$

$\gamma_5 = 1.8$ t/m^3 $\gamma_6 = \gamma_2 = \gamma = 1.0$ t/m^3

$\varphi = \delta_2 = -\delta_1 = 30^\circ$ $c = a = 0$

We find first the average unit weight of the fill inside the cofferdam:

$$\gamma_m = (2 \times 1.8 + 11 \times 1.0) : 13 = 1.12 \text{ t/m}^3$$

and then the exterior earth pressures, using the constants indicated in the table in Section 523 for $\varphi = 30^\circ$ and a rough wall:

$$E_1 = 3 \times 13 \times 0.273 + \tfrac{1}{2} \times 1.8 \times 13^2 \times 0.266 - \tfrac{1}{2} \times 0.8 \times 11^2 \times 0.266 = 10.6 + 40.5 - 12.9 = 38.2 \text{ t/m}$$

$$E_1 z_1 = 10.6 \times \tfrac{1}{2} \times 13 + 40.5 \times \tfrac{1}{3} \times 13 - 12.9 \times \tfrac{1}{3} \times 11 = 197 \text{ tm/m}$$

$$E_2 = \tfrac{1}{2} \times 1.0 \times 3^2 \times 5.66 = 25.5 \text{ t/m} \qquad E_2 z_2 = 25.5 \times \tfrac{1}{3} \times 3 = 25.5 \text{ tm/m}$$

$$F_1 = -38.2 \times 0.577 = -22.0 \text{ t/m} \qquad F_2 = 25.5 \times 0.577 = 14.7 \text{ t/m}$$

By means of Tables 1 and 3 in the Appendix we find, after some trial, for the rupture X:

$\alpha = -56^\circ$ $G^{YZ} = -0.187$ $M_R^{Yy} = 0.004$ $M_R^{t} = -0.118$

$V^{YZ} = -0.073$ $V^{YX} = -H^{Yy} = 0.121$ $H^{YZ} = 0.157$ $H^{ty} = 0.068$ $V^{ty} = 0.406$

$$V^{Y} = -0.073 + 0.121 \times 0.866 = 0.032 \qquad H^{Y} = 0.157 - 0.121 \times 0.5 = 0.096$$

Equations 8209-10 give now:

$$1.0(-0.187 - 0.032 + 0.096 \times 0.406 : 0.068)w^2 + 1.12 \times 13\, w - (2 + 38.2 - 25.5) \times 0.406 : 0.068 + 22.0 - 14.7 =$$

$$0.354\, w^2 + 14.5\, w - 80.5 = 0 \qquad w = 4.95 \text{ m}$$

$$t' = (1.12 \times 13 - 1.0 \times 4.95 \times 0.187 - 1.0 \times 4.95 \times 0.032 + 7.3 : 4.95) : 0.406 = 36.8 \text{ t/m}^2$$

We can then show that 8211 is satisfied (with M = 0):

$$1.0 \times 4.95^3 \times 0.004 - 36.8 \times 4.95^2 \times 0.118 + 2 \times 13 - \tfrac{1}{2} \times 4.95 \times 36.7 + 197 - 25.5 = 0$$

By a yield moment calculation with w = 4.95 m and $\alpha = -90^\circ$ we would find h = 14.9 m and M = - 37 tm/m. This shows that the yield hinge failure is less critical than the stability failure.

By a stability calculation with a rupture A, we would find $\alpha = 85.5^\circ$, x = 0.17 m and w = 4.35 m. This shows that the rupture A is less critical than the rupture X. A rupture AwXwA has not been investigated.

83. FURTHER POSSIBLE APPLICATIONS

831. Determination of Anchor Lengths

In Section 364 (Example 36m) it has been explained that, in order to determine the necessary anchor length, i.e. the safe distance between an anchored sheet wall and its anchor slab, we must investigate a stability failure of the composite X-type (Fig.36L, right).

Such an investigation can, in principle, be made by means of the equilibrium method in a similar way as for a double sheet wall (Section 82), the only difference being that we must reckon with $\beta \neq 0$.

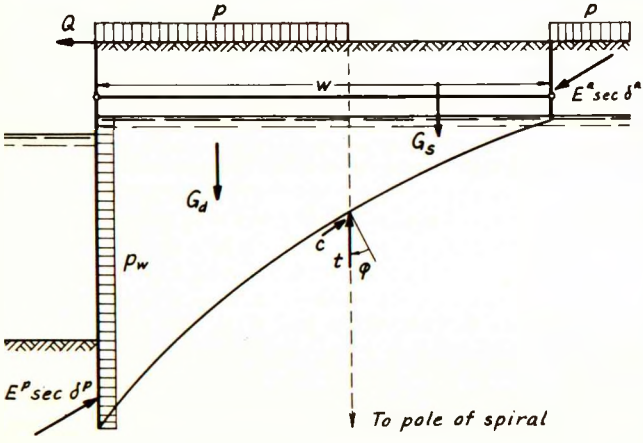

Fig.83A: Determination of anchor length

However, in this case it is actually much simpler to employ the extreme-method, using a logarithmic spiral as the main rupture-line (Fig. 83A). The spiral should not correspond to the actual friction angle but to a smaller angle obtained by applying a safety factor to μ. The actual cohesion, if any, should also be divided by a safety factor.

For an arbitrary spiral we consider now the equilibrium of the two walls plus the earth mass above the spiral (Fig. 83A). A vertical line through the pole of the spiral divides the weight of this mass in a driving part G_d and a stabilizing part G_s (submerged unit weights should be used below the water table). Further driving forces may be a surcharge to the left of the pole, a differential water pressure on the sheet wall, and a bollard pull. Finally, the active earth pressure on the back of the anchor slab is also a driving force, whereas the passive earth pressure on the front of the sheet wall is a stabilizing force. Both these forces are known, as they correspond to ruptures R (smooth wall) or P (rough wall). A possible cohesion in the rupture-line is, of course, also a stabilizing force.

Taking the moments of all these forces about the pole of the spiral, we can define a ratio f by the equation:

$$f = \frac{M_s}{M_d} = \frac{M_{G_s} + M_E{}^p + M_c}{M_{G_d} + M_E{}^a + M_p + M_{p_w} + M_Q} \qquad 8301$$

By trial we find now the critical spiral, i.e. the one for which f is a minimum, and if min. f > 1, the structure is sufficiently stable. If we wish to determine the smallest possible anchor length, we must find min.f for two or three different lengths w, and min.w will then be the value, for which we get min.f = 1, (provided that safety factors have already been applied to φ and c).

Example 83a

We shall determine the necessary length of the anchors connecting the sheet wall in Example 74c (Fig.74E) with the anchor slab in Example 72b (Fig.72C). We have from these examples:

$\varphi = \delta^p = -\delta^a = 30^\circ$ $\quad c = a = 0$ $\quad Q = 0$ $\quad h_2 = 2.2$ m $\quad h_5 = 2$ m

$\gamma_5 = 1.8$ t/m^3 $\quad \gamma_6 = \gamma_2 = 1.0$ t/m^3 $\quad p = 1$ t/m^2 $\quad p_w = 0.5$ t/m^2

$E^a = 1.70$ t/m $\quad z^a = 0.84$ m $\quad F^a = -0.98$ t/m

In Example 74c we have calculated E_2 as for a rupture SfP, but here we must assume a rupture P, for which we find:

$E^p = \frac{1}{2} \times 1.0 \times 2.2^2 \times 5.66 = 13.7$ t/m $\quad z^p = \frac{1}{3} \times 2.2 = 0.73$ m $\quad F^p = 13.7 \times 0.577 = 7.9$ t/m

After some trial we find with w = 12.3 m the critical spiral shown in Fig.83A. Its pole is situated 6.8 m behind the sheet wall and 27.7 m below ground surface. For this spiral we get (see indicated levels on Fig.74E):

$M_{G_s} = (1.8 \times 2 + 1.0 \times 0.15) \times \frac{1}{2} \times 5.5^2 + 1.0 \times 2.4 \times \frac{1}{6} \times 5.5^2 - 1.0 \times 0.2 \times \frac{1}{3} \times 5.5^2 = 67$ tm/m

$M_{G_d} = (1.8 \times 2 + 1.0 \times 2.55) \times \frac{1}{2} \times 6.8^2 + 1.0 \times 5.65 \times \frac{1}{3} \times 6.8^2 - 1.0 \times 0.55 \times \frac{1}{3} \times 6.8^2 = 220$ tm/m

$M_{E^a} = 1.70 \times 26.39 - 0.98 \times 5.5 = 39$ tm/m $\quad M_p = 1 \times \frac{1}{2} \times 6.8^2 = 23$ tm/m $\quad M_c = 0$

$M_{E^p} = 13.7 \times 18.23 + 7.9 \times 6.8 = 304$ tm/m $\quad M_{p_w} = 0.5 \times 8.2 \times 21.6 = 89$ tm/m $\quad M_Q = 0$

$$\underline{\text{min. f}} = \frac{67 + 304}{220 + 39 + 23 + 89} = \underline{1.00}$$

Any other position of the spiral gives a greater f. Consequently, the minimum anchor length is 12.3 m.

832. Stability of Slopes

In the usual investigation of stability problems, curved rupture-lines are used in combination with the extreme-method. For $\varphi = 0$ circles are used, and for $\varphi \neq 0$ logarithmic spirals. An example of such an investigation is given in Section 831.

However, as explained in Section 364, stability investigations can also be made by means of the equilibrium method, viz. by means of Kötter's equation and the boundary conditions developed in Section 34. This implies the advantage that circular rupture-lines can be used, even for $\varphi \neq 0$.

In the general case of an A-failure (see Fig. 36K, left) the rupture-circle involves 3 unknown geometrical parameters (e.g. the coordinates of its centre and the length of its radius). A fourth unknown quantity is the actual factor of safety. However, we also have 4 equations, viz. 3 equations of equilibrium for the earth mass above the rupture-line, and a relation (3318) between the boundary stresses at the two ends of the rupture-line.

The latter condition does not apply when the rupture-line ends at a singular point such as the corner at the foot of a slope, as at such a point the boundary condition becomes indefinite. As, however, in this case the rupture-circle involves 2 unknown geometrical parameters only, the problem is still soluble.

The same applies when the rupture-circle touches firm bottom or a structure. In such cases it involves 2 unknown geometrical parameters only and these, together with the safety factor, are determined by means of the 3 equilibrium conditions. In order to find the forces in the rupture-line the two parts must be considered separately, using for each part the boundary condition at the point where it meets the surface. No definite relation exists between the stresses at the sides of the point where the rupture-line touches firm bottom or a structure.

In the special case of the rupture-circle ending at a singular point and touching firm bottom or a structure, it involves only one unknown geometrical parameter. However, in this case the boundary stress at the singular point is another unknown quantity. These two, together with the safety factor, are determined by means of the 3 equilibrium conditions.

It will be seen that stability problems can, in principle, always be solved by means of the equilibrium method. However, in view of the simplicity of the usual extreme-method, it is doubtful whether anything would be gained by substituting it with the equilibrium method, except perhaps in special cases.

833. Strip Foundations

The case of a strip foundation can, in principle, be treated in the same way as that of an inclined wall exerting passive pressure on the ground.

Usually, the underside of the foundation will be located somewhat below ground level, but it will be simpler to consider the soil above foundation level merely as a surcharge and thus reduce the case to that of a foundation with its underside at ground level.

Moreover, although the law of superposition is, strictly speaking, not valid, it will probably be preferable to consider the effect of a surcharge and that of the weight of the soil separately. Later, the results may be added, giving a very good approximation. The effect of a possible cohesion can be found on

the basis of the calculation for the surcharge in a similar way as that indicated in Section 612 for a vertical wall. For $\varphi = 0$, the effect of the cohesion must, of course, be calculated separately.

With regard to the relative roughness of the underside, both the extreme cases may be considered, viz. a perfectly smooth base and a perfectly rough one. The investigation might comprise centrally, as well as eccentrically loaded foundations, and also foundations with horizontal as well as vertical loads.

All this can in principle be done by means of the equilibrium method in very nearly the same way as employed in Section 5 for the investigation of earth pressures on a vertical wall, but other rupture-figures must, of course, be considered. However, a complete investigation of this kind lies beyond the scope of the present work.

Moreover, it is possible that such an investigation would be of rather limited value in practice, as foundations designed with a reasonable safety against ultimate failure would probably, even under normal loads, undergo settlements which would be unallowable for most superstructures.

9. CONCLUSION

91. Review of Method and Applications

The proposed new method is an equilibrium method, i.e., the unknown quantities are determined by means of the statical equilibrium conditions for finite parts of the structures and the earth masses. The latter are bounded by rupture-lines, which are approximated by one or more circles and straight lines.

The necessary knowledge of the stresses in an arbitrary rupture-circle is obtained from two sources. First, the stress variation is determined by means of Kötter's equation. Second, the stress at the surface or at any other boundary is determined by means of a certain boundary condition in such a way that the equilibrium-method will give the same results as a corresponding extreme-method.

In order to calculate or design an earth-retaining structure it is necessary to choose first an arbitrary but plausible state of failure as the basis of the calculation. The next step is to investigate one or more figures of rupture in the earth, involving plastic deformations which are compatible with the movements of the structure in the chosen state of failure.

The corresponding earth pressures on the structure are found by means of the equilibrium conditions for the earth masses bounded by the critical rupture-lines. Finally, the dimensions of the structure are determined in such a way that the equilibrium conditions for the structure proper are satisfied.

This method has been applied to the majority of plane earth pressure problems encountered in practical engineering, viz. retaining walls, anchor slabs, free sheet walls, anchored sheet walls, fixed sheet walls, braced walls, double sheet walls and cellular cofferdams. The method is also applicable to stability and foundation problems, but these lie beyond the scope of the present work.

The proposed method is applicable to earth with internal friction or cohesion or both, to walls with any inclination and roughness, and to ground surfaces with any slope and surcharge. The effects of hydrostatic or hydrodynamic water pressures can be taken into account, at least approximately, and the same applies to the case of stratified earth.

92. Comparison of Theory with Experience

Like most other calculation methods, the author's is based on several simplifying assumptions and approximations, sometimes of a merely tentative character.

It is, therefore, most important and necessary to compare the results of the new theory with suitable tests and general practical experience. Considering the wide range of applications this is a tremendous task, and one which the author has felt himself unable to cope with. He has, therefore, confined his own work mainly to the development of the theoretical calculation methods, hoping that others will later attempt to prove or disprove his results and that, in the meantime, his methods may be used with suitable caution, until better methods are available.

However, the connection established by the author between the new method and the well-known and widely used extreme-methods should be a safe-guard against serious errors, because it has been demonstrated repeatedly that extreme-methods will produce very reliable results when used properly. Important examples are the "$\varphi = 0$"-analysis of slopes and the use of Coulomb's method for the design of retaining walls.

Further checking of the new method can be undertaken by comparison with suitable model tests, of which a considerable number has already been carried out.

In a small way the author's own model tests (see Section 5) have shown that most of the rupture-figures assumed in the calculations will actually occur in nature. They have also shown, however, that the actual rupture-figures are sometimes considerably more complicated than those assumed in the calculations. On the other hand, this does not necessarily mean that serious errors are introduced. As an example may be mentioned the fact that the straight rupture-lines assumed in Coulomb's calculation of active zone-ruptures give practically the same value of the active earth pressure as the actual, more complicated rupture-figure. This shows that small deviations between the theoretical and the actual rupture-figure are unimportant from a practical point of view.

Not all tests can be used for checking the results of the new method, but only those corresponding to the state of ultimate failure on which the method is based. This excludes, for example, most of the otherwise very valuable Princeton Tests (Tschebotarioff 1948, 1949), because these tests were intended for the investigation of anchored steel sheet walls under normal working conditions. Consequently, the tests were not carried to actual failure. That this is so may be seen from the fact that very different results were obtained with backfilled and with "sunk" walls. In the ultimate state of failure it would make no difference which of these construction methods had originally been employed. Similar remarks apply to the extremely interesting and very comprehensive series of tests made by Rowe (1952).

In addition to model tests also a number of full-scale tests are already available, some of which might be used for the purpose of checking the results of the new calculation method. This applies particularly to the problem of braced walls in cuts. For such walls the theory indicates that the pressure centre should usually be located near the middle of the wall. Actual measurements have given the same result (Spilker 1937, Peck 1943). Also the magnitudes of the calculated and the observed pressures agree rather well, being somewhat in excess of the normal active pressures.

Further, there exists a considerable amount of general practical experience, which may be used as an approximate check on the designs arrived at by means of the new method. An example of this is provided by a sand-filled cellular cofferdam on rock, subjected to unilateral water pressure. With a safety factor of 1.5 the new method leads to very nearly the same ratio between width and height as that which has proved satisfactory in practice.

Finally, in a few cases it is possible to compare the new method with empirical calculation methods, which have proved their suitability in practice. An outstanding example of this are the so-called Danish Rules for the design of anchored sheet walls. Although resulting in smaller dimensions than most other design methods, they have been used successfully for the design of a great number of structures (Brinch Hansen 1946).

It is, therefore, of interest to note that with suitable safety-factors the author's design methods may lead to virtually the same results as might have been obtained by means of the Danish Rules. A demonstration of this fact has been given at the end of Example 74c, where it is also shown that the empirical methods of Tschebotarioff and Rowe would lead to practically the same results, except for the driving depth.

However, in view of the still rather scanty corroboration the reader is warned not to go to extremes in the application of the new method, e.g. by designing structures which deviate very considerably from those which have proved safe in practice. This warning applies especially to cellular cofferdams (or double sheet walls) in earth, because the stresses in the walls cannot be calculated, and also to anchored or fixed sheet walls in not too soft clay. In the latter case the theory of rupture might lead to very small earth pressures, which, however, in time are almost certain to increase considerably, due to the viscosity of the clay.

Finally, as regards the question of whether to assume rough or smooth walls, it is evident that concrete walls in sand are perfectly rough, and the same is approximately true for steel and timber walls in sand. In clay, the layer in contact with the wall is likely to be softened (under water), and for this reason the author prefers, usually, to assume walls in clay to be perfectly smooth.

93. Original Contributions by the Author

As far as the author is aware, the main part of what is contained in Sections 3-8 is new. However, the most important of the author's original contributions to the subject of earth pressure calculation are, in his own opinion, the following:

1) A connection has been established between the extreme-method and the equilibrium-method, leading to a certain boundary condition by means of which a general application of the equilibrium-method has been made possible.

2) The principles have been developed for a general earth pressure theory, based mainly on the equilibrium-method, and making use of Kötter's equation as well as the above-mentioned boundary condition.

3) A set of tables has been prepared by means of which the internal forces in a rupture-circle can be calculated quickly and easily for $\varphi = 0^\circ$ or $\varphi = 30^\circ$.

4) A systematic analysis has been made of different rupture-figures, especially the so-called composite ruptures, which have hardly received any attention before. A convenient system of denominations for rupture-figures has also been proposed.

5) An analysis has been made of different states of failure which may occur in earth pressure and stability investigations.

6) General methods have been indicated for calculation of the earth pressures corresponding to the most important figures of rupture. They include a new approximate method for the calculation of zone-ruptures.

7) A set of graphs has been prepared, by means of which it is possible to calculate the earth pressure on a vertical wall (horizontal ground surface) rotating about any given point on the wall proper or its extensions. The graphs may be used for any friction angle, and for smooth as well as rough walls.

8) Although the earth pressure distribution is, in principle, indeterminable (except for zone-ruptures), a simple, tentative earth pressure diagram has been proposed. Moreover, this diagram has been used to take into account, in an approximate but simple way, the effects of water pressures and stratified earth.

9) For the design of retaining walls new formulae have been developed which are more accurate than Coulomb's and usually on the safe side.

10) For the design of anchor slabs a new method has been indicated which takes into account the fact that the inclination of the passive earth pressure is limited by the equilibrium conditions.

11) For free sheet walls, anchored sheet walls and fixed sheet walls, completely new design methods have been developed.

12) For the design of braced walls in cuts a simple approximate method has been proposed.

13) Completely new methods have been developed for the stability investigation of cellular cofferdams, on rock as well as in earth.

14) A simple extreme-method has been indicated for the determination of the necessary distance between an anchored sheet wall and its anchor slab.

15) A number of small-scale model tests have been carried out in order to study the different rupture-figures occuring in sand by the rotation of a rigid vertical wall about different points.

94. Unsolved Problems

Although the proposed new method has proved its ability to solve many different problems, it has, of course, its limitations. The most important of the problems which the author has not solved, or for which he has proposed tentative solutions only, concern the following:

1) Calculation methods for clay, considered as a material with internal friction and pore water pressures, possibly also as an inhomogeneous, anisotropic and viscous material.

2) Calculation methods for sand, considered as a dilating material.

3) Calculation methods for soils with intermediate permeabilities, e.g. silts and mixtures of sand and clay.

4) More complete investigations of rupture-figures for cohesive soils with partly unsupported earth fronts.

5) Establishment of the proper boundary condition for rupture-lines meeting at a rough wall, or at an internal boundary between layers with different friction angles.

6) A quantitative investigation of the plastic deformations which may take place in zone-ruptures and composite ruptures, and a corresponding calculation of the more complicated ruptures which actually occur by the rotation of a vertical wall.

7) Calculation of earth pressures corresponding to the rotation of a rough vertical wall about points which are not situated at the wall proper or its extensions.

8) Determination of the actual pressure distribution on rigid, hinged and flexible walls.

9) Construction of earth pressure graphs for inclined walls and sloping ground surfaces, and development of calculation methods for walls and surfaces of any shape.

10) Calculation methods for non-uniform surcharges.

11) More exact calculation methods for cases of hydrodynamic pressures.

12) Calculation methods for anchor slabs at considerable depths, and for non-continuous anchor slabs.

13) The effect of piles behind a sheet wall, e.g. in a C&N-wharf.

14) More exact calculation methods for braced walls in cuts.

15) Determination of earth pressures on the individual walls of cellular cofferdams or double sheet walls.

16) Methods for calculating the deformations and movements of earth retaining structures under normal working conditions.

17) Determination of earth pressures on unyielding walls and underground structures.

18) Application of the new method to slopes and other stability problems.

19) Application of the new method to strip foundations and similar problems.

20) Calculation methods for non-plane problems.

APPENDIX

NOTATIONS AND SIGN RULES

The following list contains all main symbols used in the present book. The special symbols used in Section 2 are not listed, however. In a few cases, where no misunderstandings could possibly be made, the same symbol has been used to represent two or more different quantities.

The symbol K has, with various subscripts, been used to represent a great number of different constants or abbreviations, and any such symbol K can therefore only be used in the Section, in which it is defined.

For many of the symbols various subscripts or superscripts are used. The most important of these are listed below, and for the others the meaning is given in that section, wherein they first occur.

Many of the symbols can have either positive or negative values. In such cases the definition of signs is indicated in a parenthesis. Compare also Fig.N, in which all the indicated quantities are shown positive.

In order to be able to state general sign rules it is necessary to define first the following concepts. A concave (resp. convex) rupture-circle is one which turns its concave (resp. convex) side towards the moving earth mass. One end point of the circle is chosen as the starting point (') and the other as the finishing point (''). A positive (resp. negative) rotation is one which corresponds to a movement through a concave (resp. convex) circle from the starting point towards the finishing point.

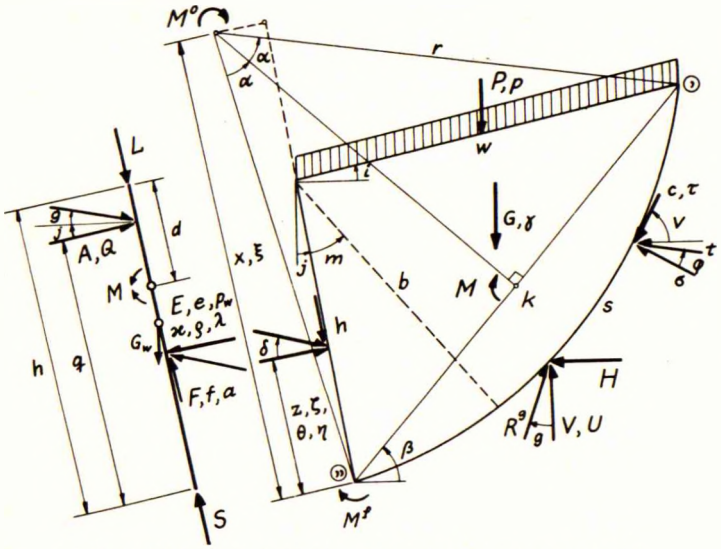

Fig.N: Symbols regarding wall and adjacent earth wedge

A = Component normal to wall of anchor pull or brace thrust.
E = Normal component of total earth pressure on wall (positive when producing compression).
F = Tangential Component of total earth pressure on wall (positive when acting upwards on wall, downwards on earth).
G = Weight of earth wedge or part thereof (positive downwards).
G_w = Weight of wall (positive downwards).
H = Horizontal component of internal forces in rupture-line (positive when, acting on moving earth mass, a positive rotation of 90^o would direct it upwards).
K = Various constants and abbreviations (defined where they occur).
L = Axial load on top of wall (positive downwards).
M = Moment in wall (positive when producing tension in exterior side of wall).
M = Moment about middle point of chord in rupture-circle (positive when, acting on moving earth mass, it corresponds to a positive rotation).
M^o = Moment about centre of rupture-circle (sign rule as above).
M^f = Moment about foot of wall (sign rule as above).
P = Total vertical surcharge on surface of earth wedge or part thereof (positive downwards).
Q = Normal component of exterior force on wall.
R^g = Component, in a direction making angle g with vertical, of internal forces in rupture-line (positive when, acting on moving earth mass, a negative rotation g would direct it upwards).
S = Axial point resistance on foot of wall (positive upwards).
T = Section area, especially of anchor bars.
U = Vertical resultant of V, G and P (positive upwards).
V = Vertical component of internal forces in rupture-line (positive upwards when acting on moving earth mass).
W = Section modulus, especially of sheet walls.

a = Unit adhesion between wall and earth (positive when acting upwards on wall, downwards on earth).
b = Distance from top of wall to meeting point of two rupture-lines.
c = Unit cohesion in rupture-line (positive when acting on moving earth mass in direction from starting point towards finishing point).
c = Apparent cohesion of the earth (always positive in equations such as 4119-25 and 6118-22).
d = Depth below ground surface, measured along wall (positive downwards).
d^o = Depth at which the unit normal earth pressure is zero.
e = Normal component of unit earth pressure on wall (positive when producing compression).
f = Tangential component of unit earth pressure on wall (positive when acting upwards on wall, downwards on earth).
f = Ratio between stabilizing and driving moments in stability investigations.
g = Angle between vertical and direction of R^g (positive when R^g must make a negative rotation g in order to be directed upwards).
g = Angle between horizon and direction of Q (positive when Q must make a negative rotation of 90^o+g in order to be directed upwards).
h = Height of wall or part thereof, measured along wall.
h^c = Critical height of unsupported earth front.
h_c = Height of capillary rise.
h_w = Difference between water levels on two sides of wall (positive when inside water level is higher than outside).
i = Angle between horizon and ground surface (positive when the surface must make a positive rotation i in order to become horizontal).
i = Hydraulic gradient (positive when directed downwards).
j = Angle between vertical and wall (positive when the wall must make a positive rotation j in order to become vertical).
k = Length of chord in rupture-circle.
m = Angle between wall and straight line with length b.
m = Critical ratio between two heights.
n = Factor of safety.
n = Porosity of soil.
p = Unit vertical surcharge, per unit area of sloping surface (positive downwards).

p_c = $\gamma_w h_c$ = Unit capillary pressure.
p_w = $\gamma_w h_w$ = Unit differential water pressure (positive when acting on interior side of wall).
q = Distance from foot of wall to pressure centre of A or Q (positive upwards).
r = Radius of rupture-circle (positive for a concave circle, negative for a convex one).
s = Actual height of anchor slab, measured along slab.
s = Length of arch along rupture-line.
t = $\sigma \sec \varphi$ = Resulting stress, exclusive of cohesion c, in rupture-line (positive when producing compression).
u = Displacement or velocity vector in rupture-line (positive when directed against shear stress from below).
u = Water pressure potential.
v = Angle between horizon and rupture-line (positive when the tangent, directed from starting point towards finishing point, must make a positive rotation of $90^\circ+v$ in order to be directed upwards).
w = Width of earth wedge or part thereof, measured along ground surface.
w = Width of cellular cofferdam or double sheet wall.
x = Distance from foot of wall to rotation centre for wall (positive upwards).
y = Distance from foot of wall to jump in pressure diagram.
z = Distance from foot of wall to earth pressure centre (positive upwards).
z_w = Distance from foot of wall to gravity centre of wall.

α = Half central angle in rupture-circle (positive for a concave circle, negative for a convex one).
β = Angle between horizon and chord in rupture-circle (positive when the chord, directed from starting point towards finishing point, must make a positive rotation of $90^\circ+\beta$ in order to be directed upwards).
γ = Effective unit weight of earth.
γ_m = Average unit weight of earth in cellular cofferdam or double sheet wall.
γ_s = Specific gravity of solid earth particles.
γ_w = Specific gravity of water.
δ = Angle of wall friction (positive when the pressure is directed upwards on wall, downwards on earth).
ε = Normal strain (single subscript, shortening positive) or shear strain (double subscript).
ζ = Height-factor for c-term in formula for Ez.
η = Height-factor for γ-term in formula for Ez.
θ = Height-factor for p-term in formula for Ez.
κ = Pressure-factor for c-term in formula for E or e.
λ = Pressure-factor for γ-term in formula for E or e.
μ = $\tan \varphi$ = Coefficient of internal friction (sign as φ).
ν = $e^{4\mu\alpha}$ = Abbreviation in stress formulae (e = basis of natural logarithms).
ξ = x : h = Height-factor for rotation centre of wall.
ρ = Pressure-factor for p-term in formula for E or e.
σ = Normal stress, especially in rupture-line (positive when producing compression).
σ = "Allowable" stress for structural material.
τ = Shear stress , especially in rupture-line (positive when acting on moving earth mass in direction from starting point towards finishing point).
φ = Apparent angle of internal friction (positive when corresponding to a positive τ).
ψ = arc tan 2μ = Abbreviation for constant angle in stress formulae (sign as φ).
ω = y : h = Height-factor for jump in pressure diagram.

Superscript ' indicates the starting point of a rupture-line.
Superscript " indicates the finishing point of a rupture-line.
Superscript ^{a} indicates active earth pressure.
Superscript ^{p} indicates passive earth pressure.
Superscript ^{x} indicates earth pressures above pressure jump.
Superscript ^{y} indicates earth pressures below pressure jump.
Subscript $_f$ indicates the foot of the wall.
Subscript $_t$ indicates the top of the wall.
Subscript $_r$ indicates a perfectly rough wall.
Subscript $_s$ indicates a perfectly smooth wall.

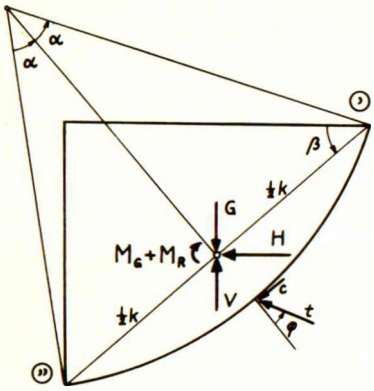

Fig.T: Internal forces in rupture-circle

We consider an earth wedge bounded by a circular rupture-line, a horizontal ground surface and a vertical wall (see Fig.T). For the weight of the earth wedge (unit weight γ) and its moment about the middle point of the chord we have:

$$G = \gamma k^2 (G^{\gamma z} + \tfrac{1}{4} \sin 2\beta) \qquad 3223$$

$$M_G = \gamma k^3 (M_G^{\gamma x} \sin \beta + \tfrac{1}{12} \sin^3 \beta) \qquad 3224$$

The dimensionless constants $G^{\gamma z}$ and $M_G^{\gamma x}$ are indicated in the following Table 1.

Denoting by σ' and σ'' the normal stresses at the ends of the rupture-circle, we have for the stresses in this circle and their resultants the following equations, valid for the special case of frictionless earth ($\varphi = 0$):

$$\sigma'' = \gamma k \sin \beta + c t^c + \sigma' \qquad M_R = \gamma k^3 M_R^{\gamma x} \sin \beta + c k^2 M_R^c \qquad 3350\text{-}59$$

$$V = \gamma k^2 (V^{\gamma z} + \tfrac{1}{4} \sin 2\beta) + c k (V^{cx} \sin \beta + V^{cy} \cos \beta) + k\sigma' \cos \beta \qquad 3353$$

$$H = \tfrac{1}{2} \gamma k^2 \sin^2 \beta + c k (H^{cx} \sin \beta + H^{cy} \cos \beta) + k\sigma' \sin \beta \qquad 3354$$

The dimensionless constants are indicated in the following Table 1.

Denoting by t' and t'' the oblique stresses (excl. c) at the ends of the rupture circle, we have for the stresses in this circle and their resultants the following equations, valid for the general case of earth with internal friction:

$$t'' = \gamma k \, (t^{\gamma x} \sin \beta + t^{\gamma y} \cos \beta) + (t' + \frac{c}{\sin \varphi}) \, t^t - \frac{c}{\sin \varphi} \qquad 3318$$

$$M_R = \gamma k^3 (M_R^{\gamma x} \sin \beta + M_R^{\gamma y} \cos \beta) + (t' + \frac{c}{\sin \varphi}) \, k^2 M_R^t \qquad 3335$$

$$V = \gamma k^2 \left[V^{\gamma z} + V^{\gamma x} \sin(2\beta + 2\varphi) \right] - c k \cot \varphi \cos \beta + (t' + \frac{c}{\sin \varphi}) \, k \left[V^{tx} \sin \beta + V^{ty} \cos \beta \right] \qquad 3325$$

$$H = \gamma k^2 \left[H^{\gamma z} + H^{\gamma y} \cos(2\beta + 2\varphi) \right] - c k \cot \varphi \sin \beta + (t' + \frac{c}{\sin \varphi}) \, k \left[H^{tx} \sin \beta + H^{ty} \cos \beta \right] \qquad 3326$$

The dimensionless constants are indicated in the following Tables 2-3.

The positive directions of the different stresses, forces and moments are indicated in Fig.T. φ and c should be assumed positive for passive pressure, negative for active pressure in the circle. α is positive for a concave circle, negative for a convex one. Table 2 is valid when α and φ have identical signs, whereas Table 3 is valid when they have different signs.

TABLE 1 : Functions of α for φ = 0°

(G^{Yz} and M_G^{Yx} are independent of φ)

+α	+t^c	+M_R^{Yx} / −M_G^{Yx}	+M_R^c	+V^{Yz} / +G^{Yz}	−V^{cx} / +H^{cy}	+V^{cy} / +H^{cx}
−α	−t^c	+M_R^{Yx} / −M_G^{Yx}	−M_R^c	−V^{Yz} / −G^{Yz}	−V^{cx} / +H^{cy}	−V^{cy} / −H^{cx}
0	.0000	.0833	.0000	.0000	1.000	.0000
1	.0698	.0833	.0117	.0029	.9998	.0349
2	.1396	.0833	.0233	.0059	.9992	.0698
3	.2094	.0833	.0349	.0088	.9982	.1047
4	.2793	.0833	.0465	.0117	.9968	.1396
5	.3491	.0833	.0581	.0146	.9949	.1745
6	.4189	.0832	.0697	.0175	.9927	.2094
7	.4887	.0832	.0813	.0204	.9901	.2443
8	.5585	.0831	.0929	.0233	.9870	.2793
9	.6283	.0830	.1045	.0263	.9835	.3142
10	.6981	.0829	.1161	.0292	.9797	.3491
11	.7679	.0828	.1277	.0322	.9754	.3840
12	.8378	.0827	.1392	.0351	.9707	.4189
13	.9076	.0826	.1508	.0381	.9656	.4538
14	.9774	.0824	.1623	.0410	.9601	.4887
15	1.047	.0823	.1738	.0440	.9542	.5236
16	1.117	.0821	.1852	.0470	.9478	.5585
17	1.187	.0819	.1966	.0500	.9410	.5934
18	1.257	.0817	.2080	.0531	.9338	.6283
19	1.327	.0815	.2194	.0561	.9262	.6632
20	1.396	.0813	.2308	.0591	.9181	.6981
21	1.466	.0810	.2421	.0622	.9096	.7330
22	1.536	.0808	.2534	.0653	.9007	.7680
23	1.606	.0805	.2646	.0684	.8914	.8029
24	1.676	.0803	.2759	.0715	.8816	.8378
25	1.746	.0800	.2871	.0747	.8714	.8727
26	1.815	.0797	.2983	.0778	.8608	.9076
27	1.885	.0794	.3094	.0810	.8497	.9425
28	1.955	.0791	.3204	.0841	.8382	.9774
29	2.025	.0787	.3314	.0873	.8262	1.012
30	2.094	.0784	.3424	.0906	.8138	1.047
31	2.164	.0780	.3533	.0939	.8009	1.082
32	2.234	.0777	.3642	.0971	.7876	1.117
33	2.304	.0773	.3750	.1004	.7738	1.152
34	2.374	.0769	.3858	.1038	.7595	1.187
35	2.444	.0765	.3965	.1072	.7448	1.222
36	2.513	.0761	.4072	.1106	.7296	1.257
37	2.583	.0757	.4178	.1140	.7139	1.292
38	2.653	.0752	.4283	.1175	.6978	1.326
39	2.723	.0747	.4388	.1210	.6811	1.361
40	2.793	.0742	.4492	.1245	.6640	1.396
41	2.863	.0737	.4595	.1281	.6463	1.431
42	2.932	.0731	.4697	.1317	.6282	1.466
43	3.002	.0725	.4799	.1353	.6096	1.501
44	3.072	.0719	.4900	.1390	.5905	1.536
45	3.142	.0713	.5000	.1427	.5708	1.571

+α	+t^c	+M_R^{Yx} / −M_G^{Yx}	+M_R^c	+V^{Yz} / +G^{Yz}	−V^{cx} / +H^{cy}	+V^{cy} / +H^{cx}
−α	−t^c	+M_R^{Yx} / −M_G^{Yx}	−M_R^c	−V^{Yz} / −G^{Yz}	−V^{cx} / +H^{cy}	−V^{cy} / −H^{cx}
45	3.142	.0713	.5000	.1427	.5708	1.571
46	3.211	.0707	.5099	.1465	.5506	1.606
47	3.281	.0700	.5197	.1503	.5299	1.641
48	3.351	.0694	.5295	.1541	.5086	1.676
49	3.421	.0687	.5392	.1580	.4868	1.711
50	3.491	.0680	.5487	.1620	.4645	1.745
51	3.561	.0672	.5581	.1660	.4416	1.780
52	3.630	.0665	.5674	.1701	.4182	1.815
53	3.700	.0657	.5766	.1742	.3941	1.850
54	3.770	.0648	.5858	.1784	.3695	1.885
55	3.840	.0639	.5948	.1826	.3443	1.920
56	3.910	.0630	.6037	.1869	.3185	1.955
57	3.980	.0621	.6124	.1913	.2921	1.990
58	4.049	.0611	.6210	.1957	.2651	2.025
59	4.119	.0601	.6294	.2002	.2375	2.060
60	4.189	.0591	.6377	.2047	.2092	2.094
61	4.259	.0580	.6459	.2094	.1803	2.129
62	4.328	.0569	.6539	.2141	.1507	2.164
63	4.398	.0557	.6618	.2189	.1205	2.199
64	4.468	.0545	.6695	.2238	.0896	2.234
65	4.538	.0533	.6770	.2288	.0580	2.269
66	4.608	.0520	.6844	.2338	.0257	2.304
67	4.678	.0507	.6916	.2389	-.0073	2.339
68	4.747	.0493	.6986	.2441	-.0410	2.374
69	4.817	.0479	.7053	.2494	-.0755	2.409
70	4.887	.0464	.7119	.2549	-.1107	2.443
71	4.957	.0448	.7183	.2604	-.1467	2.478
72	5.027	.0432	.7245	.2661	-.1834	2.513
73	5.097	.0415	.7304	.2719	-.2209	2.548
74	5.166	.0398	.7361	.2778	-.2593	2.583
75	5.236	.0380	.7415	.2838	-.2985	2.618
76	5.306	.0361	.7467	.2899	-.3386	2.653
77	5.376	.0342	.7516	.2962	-.3795	2.688
78	5.445	.0322	.7562	.3026	-.4213	2.723
79	5.515	.0301	.7606	.3091	-.4640	2.758
80	5.585	.0279	.7646	.3158	-.5076	2.793
81	5.655	.0256	.7683	.3227	-.5522	2.828
82	5.725	.0232	.7717	.3297	-.5977	2.862
83	5.795	.0207	.7748	.3369	-.6442	2.897
84	5.864	.0181	.7775	.3443	-.6918	2.932
85	5.934	.0154	.7798	.3519	-.7404	2.967
86	6.004	.0126	.7818	.3596	-.7901	3.002
87	6.074	.0097	.7834	.3675	-.8408	3.037
88	6.144	.0066	.7845	.3757	-.8927	3.072
89	6.214	.0034	.7852	.3841	-.9457	3.107
90	6.283	.0000	.7854	.3927	-1.000	3.142

TABLE 2a : Functions of α for φ = 30°

(Identical signs of α and φ)

(+φ) +α	$+t^{Yx}$	$+t^{Yy}$	$+t^{t}$	$+M_R^{Yx}$	$+M_R^{Yy}$	$+M_R^{t}$	$+V^{Yz}$	$+V^{Yx}$ / $-H^{Yy}$	$+H^{Yz}$	$-V^{tx}$ / $+H^{ty}$	$+V^{ty}$ / $+H^{tx}$	(+φ) +α
(-φ) -α	$+t^{Yx}$	$-t^{Yy}$	$+t^{t}$	$+M_R^{Yx}$	$-M_R^{Yy}$	$+M_R^{t}$	$-V^{Yz}$	$+V^{Yx}$ / $-H^{Yy}$	$+H^{Yz}$	$+V^{tx}$ / $-H^{ty}$	$+V^{ty}$ / $+H^{tx}$	(-φ) -α
0	.8660	.5000	1.000	.0625	.0361	.0000	.0000	.2500	.2500	.5000	.8660	0
1	.8836	.5102	1.041	.0651	.0376	.0059	.0030	.2535	.2535	.5101	.8837	1
2	.9015	.5210	1.084	.0677	.0392	.0121	.0062	.2571	.2570	.5203	.9021	2
3	.9198	.5324	1.129	.0704	.0408	.0186	.0095	.2607	.2606	.5305	.9211	3
4	.9385	.5443	1.175	.0731	.0425	.0253	.0129	.2644	.2642	.5408	.9408	4
5	.9576	.5568	1.224	.0758	.0443	.0323	.0165	.2681	.2679	.5511	.9611	5
6	.9771	.5698	1.274	.0786	.0461	.0395	.0202	.2719	.2716	.5615	.9822	6
7	.9970	.5834	1.326	.0814	.0480	.0470	.0240	.2757	.2754	.5719	1.004	7
8	1.018	.5977	1.381	.0842	.0500	.0549	.0280	.2796	.2792	.5824	1.026	8
9	1.039	.6126	1.438	.0870	.0521	.0630	.0321	.2835	.2831	.5929	1.050	9
10	1.060	.6283	1.497	.0899	.0543	.0715	.0364	.2876	.2870	.6033	1.074	10
11	1.081	.6447	1.558	.0928	.0566	.0803	.0408	.2918	.2910	.6138	1.099	11
12	1.103	.6618	1.622	.0958	.0590	.0894	.0454	.2961	.2951	.6242	1.125	12
13	1.125	.6797	1.689	.0989	.0615	.0989	.0502	.3005	.2993	.6346	1.152	13
14	1.148	.6985	1.758	.1020	.0642	.1088	.0551	.3050	.3035	.6450	1.179	14
15	1.171	.7181	1.830	.1052	.0669	.1191	.0602	.3096	.3078	.6554	1.208	15
16	1.195	.7386	1.906	.1084	.0698	.1298	.0656	.3144	.3121	.6657	1.237	16
17	1.219	.7601	1.984	.1117	.0728	.1409	.0712	.3193	.3165	.6759	1.268	17
18	1.244	.7825	2.066	.1150	.0759	.1525	.0771	.3243	.3210	.6861	1.300	18
19	1.269	.8060	2.151	.1183	.0791	.1645	.0832	.3295	.3255	.6961	1.333	19
20	1.295	.8306	2.239	.1217	.0825	.1770	.0896	.3348	.3300	.7060	1.367	20
21	1.321	.8563	2.331	.1251	.0860	.1899	.0963	.3402	.3346	.7158	1.402	21
22	1.347	.8831	2.427	.1286	.0897	.2034	.1032	.3458	.3392	.7254	1.439	22
23	1.374	.9112	2.527	.1321	.0935	.2173	.1104	.3515	.3439	.7348	1.477	23
24	1.402	.9405	2.631	.1357	.0975	.2318	.1180	.3574	.3486	.7440	1.516	24
25	1.430	.9710	2.739	.1393	.1017	.2468	.1258	.3635	.3533	.7529	1.556	25
26	1.459	1.003	2.852	.1430	.1060	.2624	.1340	.3697	.3580	.7616	1.598	26
27	1.488	1.037	2.969	.1467	.1105	.2786	.1425	.3762	.3627	.7700	1.642	27
28	1.517	1.072	3.091	.1504	.1152	.2954	.1513	.3828	.3675	.7781	1.687	28
29	1.547	1.109	3.218	.1542	.1201	.3129	.1605	.3896	.3723	.7858	1.734	29
30	1.578	1.147	3.350	.1580	.1252	.3310	.1700	.3966	.3770	.7932	1.782	30
31	1.609	1.187	3.488	.1619	.1305	.3498	.1799	.4038	.3818	.8001	1.832	31
32	1.641	1.229	3.631	.1658	.1361	.3693	.1902	.4113	.3865	.8065	1.884	32
33	1.673	1.273	3.781	.1697	.1419	.3896	.2009	.4190	.3912	.8124	1.938	33
34	1.705	1.318	3.937	.1737	.1479	.4106	.2121	.4269	.3958	.8178	1.994	34
35	1.738	1.365	4.099	.1777	.1541	.4324	.2237	.4351	.4004	.8225	2.052	35
36	1.771	1.415	4.268	.1817	.1606	.4550	.2358	.4435	.4049	.8266	2.111	36
37	1.805	1.467	4.443	.1857	.1674	.4784	.2484	.4522	.4093	.8300	2.173	37
38	1.840	1.521	4.626	.1898	.1744	.5027	.2614	.4612	.4137	.8326	2.237	38
39	1.875	1.578	4.816	.1938	.1817	.5279	.2750	.4705	.4180	.8343	2.304	39
40	1.910	1.637	5.014	.1979	.1894	.5540	.2891	.4801	.4222	.8352	2.373	40
41	1.945	1.699	5.220	.2020	.1973	.5811	.3038	.4901	.4263	.8351	2.444	41
42	1.981	1.764	5.435	.2061	.2056	.6092	.3190	.5004	.4302	.8340	2.518	42
43	2.017	1.831	5.658	.2102	.2142	.6383	.3348	.5111	.4339	.8318	2.595	43
44	2.054	1.902	5.891	.2143	.2231	.6685	.3512	.5221	.4375	.8283	2.674	44
45	2.091	1.976	6.134	.2184	.2324	.6997	.3683	.5335	.4409	.8236	2.756	45

TABLE 2b : Functions of α for φ = 30°

(Identical signs of α and φ)

(+φ) +α	$+t^{Yx}$	$+t^{Yy}$	$+t^{t}$	$+M_R^{Yx}$	$+M_R^{Yy}$	$+M_R^{t}$	$+V^{Yz}$	$+V^{Yx}$ / $-H^{Yy}$	$+H^{Yz}$	$-V^{tx}$ / $+H^{ty}$	$+V^{ty}$ / $+H^{tx}$	(+φ) +α
(-φ) -α	$+t^{Yx}$	$-t^{Yy}$	$+t^{t}$	$+M_R^{Yx}$	$-M_R^{Yy}$	$+M_R^{t}$	$-V^{Yz}$	$+V^{Yx}$ / $-H^{Yy}$	$+H^{Yz}$	$+V^{tx}$ / $-H^{ty}$	$+V^{ty}$ / $+H^{tx}$	(-φ) -α
45	2.091	1.976	6.134	.2184	.2324	.6997	.3683	.5335	.4409	.8236	2.756	45
46	2.129	2.053	6.386	.2225	.2420	.7321	.3860	.5453	.4440	.8174	2.842	46
47	2.166	2.133	6.649	.2266	.2521	.7656	.4043	.5575	.4468	.8098	2.930	47
48	2.204	2.217	6.922	.2306	.2625	.8004	.4234	.5702	.4494	.8005	3.022	48
49	2.242	2.305	7.207	.2345	.2733	.8364	.4432	.5833	.4517	.7895	3.117	49
50	2.280	2.396	7.503	.2385	.2846	.8737	.4637	.5970	.4536	.7767	3.215	50
51	2.318	2.491	7.812	.2424	.2963	.9124	.4850	.6112	.4552	.7619	3.317	51
52	2.356	2.591	8.133	.2462	.3085	.9525	.5072	.6259	.4564	.7451	3.422	52
53	2.394	2.695	8.468	.2500	.3211	.9940	.5302	.6412	.4572	.7260	3.531	53
54	2.432	2.804	8.816	.2538	.3342	1.037	.5540	.6570	.4575	.7046	3.644	54
55	2.470	2.918	9.178	.2573	.3478	1.081	.5787	.6735	.4573	.6806	3.761	55
56	2.508	3.036	9.556	.2607	.3619	1.127	.6043	.6906	.4566	.6540	3.883	56
57	2.545	3.160	9.950	.2641	.3766	1.175	.6309	.7084	.4553	.6245	4.009	57
58	2.582	3.289	10.36	.2673	.3918	1.224	.6584	.7269	.4533	.5918	4.140	58
59	2.618	3.424	10.79	.2704	.4076	1.275	.6869	.7461	.4506	.5558	4.275	59
60	2.654	3.565	11.23	.2734	.4239	1.327	.7164	.7662	.4472	.5163	4.415	60
61	2.689	3.712	11.69	.2761	.4409	1.382	.7470	.7871	.4430	.4731	4.560	61
62	2.724	3.866	12.17	.2787	.4585	1.438	.7786	.8089	.4378	.4259	4.710	62
63	2.757	4.026	12.67	.2811	.4768	1.496	.8114	.8316	.4319	.3745	4.865	63
64	2.789	4.194	13.19	.2832	.4957	1.556	.8453	.8553	.4248	.3186	5.026	64
65	2.820	4.369	13.73	.2851	.5153	1.618	.8804	.8800	.4167	.2580	5.193	65
66	2.850	4.551	14.30	.2867	.5357	1.682	.9167	.9058	.4075	.1922	5.366	66
67	2.878	4.742	14.89	.2881	.5568	1.748	.9542	.9326	.3970	.1210	5.545	67
68	2.904	4.941	15.50	.2891	.5786	1.817	.9931	.9607	.3851	.0441	5.731	68
69	2.928	5.149	16.14	.2898	.6012	1.888	1.033	.9901	.3719	-.0389	5.923	69
70	2.950	5.366	16.80	.2901	.6245	1.961	1.075	1.021	.3571	-.1285	6.122	70
71	2.969	5.592	17.49	.2900	.6487	2.036	1.118	1.053	.3407	-.2249	6.328	71
72	2.986	5.829	18.21	.2896	.6737	2.113	1.162	1.086	.3225	-.3287	6.541	72
73	3.000	6.076	18.96	.2887	.6996	2.193	1.207	1.121	.3025	-.4403	6.762	73
74	3.010	6.334	19.74	.2873	.7263	2.275	1.254	1.158	.2804	-.5602	6.990	74
75	3.017	6.604	20.55	.2853	.7540	2.360	1.303	1.197	.2562	-.6888	7.227	75
76	3.020	6.885	21.40	.2828	.7826	2.448	1.353	1.237	.2297	-.8268	7.472	76
77	3.019	7.179	22.28	.2797	.8122	2.539	1.405	1.279	.2008	-.9745	7.726	77
78	3.013	7.485	23.20	.2760	.8428	2.632	1.458	1.324	.1693	-1.133	7.988	78
79	3.003	7.805	24.15	.2716	.8743	2.728	1.512	1.370	.1350	-1.303	8.260	79
80	2.986	8.139	25.14	.2665	.9068	2.826	1.568	1.419	.0977	-1.484	8.541	80
81	2.963	8.488	26.17	.2607	.9403	2.927	1.626	1.470	.0572	-1.678	8.832	81
82	2.934	8.853	27.25	.2540	.9747	3.031	1.685	1.524	.0134	-1.886	9.133	82
83	2.897	9.233	28.37	.2464	1.010	3.138	1.746	1.581	-.0341	-2.107	9.445	83
84	2.853	9.631	29.54	.2380	1.047	3.247	1.809	1.640	-.0854	-2.344	9.767	84
85	2.800	10.05	30.75	.2286	1.085	3.360	1.873	1.702	-.1411	-2.597	10.10	85
86	2.739	10.48	32.02	.2181	1.124	3.475	1.939	1.768	-.2007	-2.867	10.44	86
87	2.668	10.93	33.34	.2066	1.164	3.593	2.006	1.837	-.2652	-3.155	10.80	87
88	2.586	11.40	34.71	.1939	1.205	3.714	2.074	1.910	-.3347	-3.462	11.17	88
89	2.493	11.89	36.14	.1800	1.247	3.838	2.144	1.988	-.4097	-3.789	11.55	89
90	2.389	12.40	37.62	.1649	1.290	3.964	2.216	2.069	-.4899	-4.138	11.95	90

TABLE 3a : Functions of α for φ = 30°

(Different signs of α and φ)

$(-\varphi)$ $+\alpha$	$+t^{Yx}$	$-t^{Yy}$	$+t^{t}$	$+M_R^{Yx}$	$-M_R^{Yy}$	$-M_R^{t}$	$+V^{Yz}$	$+V^{Yx}$ / $-H^{Yy}$	$+H^{Yz}$	$+V^{tx}$ / $-H^{ty}$	$+V^{ty}$ / $+H^{tx}$	$(-\varphi)$ $+\alpha$
$(+\varphi)$ $-\alpha$	$+t^{Yx}$	$+t^{Yy}$	$+t^{t}$	$+M_R^{Yx}$	$+M_R^{Yy}$	$-M_R^{t}$	$-V^{Yz}$	$+V^{Yx}$ / $-H^{Yy}$	$+H^{Yz}$	$-V^{tx}$ / $+H^{ty}$	$+V^{ty}$ / $+H^{tx}$	$(+\varphi)$ $-\alpha$
0	.8660	.5000	1.000	.0625	.0361	.0000	.0000	.2500	.2500	.5000	.8660	0
1	.8488	.4902	.9605	.0599	.0347	.0057	.0029	.2466	.2466	.4899	.8488	1
2	.8319	.4808	.9225	.0574	.0333	.0112	.0057	.2432	.2432	.4799	.8322	2
3	.8153	.4719	.8861	.0549	.0320	.0164	.0084	.2399	.2400	.4700	.8162	3
4	.7991	.4634	.8511	.0525	.0307	.0214	.0109	.2367	.2368	.4602	.8007	4
5	.7831	.4553	.8175	.0502	.0295	.0262	.0133	.2336	.2337	.4505	.7857	5
6	.7675	.4475	.7852	.0479	.0284	.0309	.0156	.2306	.2308	.4408	.7712	6
7	.7522	.4401	.7542	.0457	.0273	.0354	.0178	.2277	.2280	.4313	.7571	7
8	.7371	.4330	.7244	.0435	.0263	.0397	.0199	.2248	.2252	.4218	.7435	8
9	.7223	.4263	.6958	.0413	.0253	.0438	.0219	.2220	.2225	.4124	.7303	9
10	.7079	.4199	.6683	.0392	.0243	.0478	.0239	.2192	.2198	.4031	.7176	10
11	.6938	.4138	.6419	.0371	.0234	.0516	.0258	.2165	.2171	.3939	.7053	11
12	.6799	.4080	.6165	.0350	.0225	.0552	.0276	.2138	.2145	.3848	.6933	12
13	.6663	.4025	.5921	.0329	.0217	.0586	.0294	.2112	.2120	.3758	.6817	13
14	.6530	.3973	.5687	.0309	.0209	.0619	.0311	.2086	.2095	.3669	.6705	14
15	.6399	.3923	.5463	.0289	.0202	.0651	.0328	.2060	.2071	.3581	.6597	15
16	.6271	.3876	.5247	.0269	.0195	.0681	.0344	.2035	.2048	.3493	.6492	16
17	.6145	.3831	.5040	.0250	.0188	.0710	.0360	.2010	.2025	.3407	.6390	17
18	.6022	.3788	.4841	.0231	.0182	.0738	.0375	.1985	.2003	.3321	.6291	18
19	.5901	.3747	.4650	.0212	.0175	.0765	.0389	.1960	.1981	.3236	.6195	19
20	.5782	.3709	.4466	.0194	.0169	.0790	.0403	.1936	.1960	.3153	.6103	20
21	.5665	.3673	.4289	.0175	.0163	.0815	.0416	.1912	.1940	.3071	.6013	21
22	.5551	.3638	.4120	.0157	.0157	.0838	.0429	.1889	.1920	.2989	.5926	22
23	.5439	.3606	.3957	.0139	.0152	.0860	.0442	.1866	.1901	.2908	.5842	23
24	.5329	.3575	.3801	.0122	.0147	.0881	.0454	.1843	.1882	.2828	.5760	24
25	.5221	.3546	.3651	.0105	.0142	.0901	.0466	.1820	.1864	.2749	.5681	25
26	.5115	.3518	.3507	.0088	.0137	.0920	.0477	.1798	.1847	.2671	.5604	26
27	.5011	.3492	.3368	.0071	.0132	.0938	.0488	.1776	.1830	.2594	.5529	27
28	.4908	.3467	.3235	.0055	.0128	.0956	.0498	.1754	.1814	.2517	.5457	28
29	.4808	.3444	.3107	.0038	.0124	.0972	.0509	.1732	.1798	.2442	.5387	29
30	.4709	.3422	.2984	.0022	.0120	.0988	.0519	.1711	.1783	.2367	.5318	30
31	.4612	.3401	.2866	.0006	.0116	.1003	.0529	.1690	.1768	.2293	.5252	31
32	.4517	.3382	.2753	-.0010	.0112	.1017	.0539	.1669	.1754	.2220	.5187	32
33	.4423	.3364	.2644	-.0026	.0108	.1030	.0548	.1648	.1740	.2148	.5124	33
34	.4331	.3347	.2540	-.0041	.0105	.1043	.0557	.1628	.1727	.2077	.5064	34
35	.4240	.3331	.2439	-.0057	.0101	.1055	.0566	.1607	.1714	.2007	.5005	35
36	.4151	.3316	.2343	-.0072	.0098	.1066	.0574	.1587	.1702	.1937	.4948	36
37	.4063	.3302	.2251	-.0087	.0094	.1077	.0583	.1567	.1691	.1868	.4892	37
38	.3977	.3289	.2162	-.0102	.0091	.1087	.0591	.1547	.1680	.1800	.4837	38
39	.3892	.3277	.2076	-.0117	.0088	.1096	.0600	.1527	.1670	.1733	.4784	39
40	.3809	.3265	.1994	-.0131	.0085	.1105	.0608	.1508	.1660	.1666	.4732	40
41	.3727	.3255	.1915	-.0146	.0082	.1113	.0616	.1488	.1650	.1600	.4682	41
42	.3646	.3245	.1839	-.0160	.0079	.1121	.0624	.1469	.1641	.1535	.4633	42
43	.3566	.3236	.1766	-.0174	.0076	.1128	.0632	.1450	.1633	.1470	.4585	43
44	.3487	.3228	.1697	-.0188	.0073	.1135	.0640	.1431	.1625	.1406	.4539	44
45	.3409	.3221	.1630	-.0202	.0070	.1141	.0648	.1412	.1618	.1343	.4494	45

TABLE 3b : Functions of α for φ = 30°

(Different signs of α and φ)

(-φ) / +α	$+t^{Yx}$	$-t^{Yy}$	$+t^{t}$	$+M_R^{Yx}$	$-M_R^{Yy}$	$-M_R^{t}$	$+V^{Yz}$	$+V^{Yx}$ / $-H^{Yy}$	$+H^{Yz}$	$+V^{tx}$ / $-H^{ty}$	$+V^{ty}$ / $+H^{tx}$	(-φ) / +α
(+φ) / -α	$+t^{Yx}$	$+t^{Yy}$	$+t^{t}$	$+M_R^{Yx}$	$+M_R^{Yy}$	$-M_R^{t}$	$-V^{Yz}$	$+V^{Yx}$ / $-H^{Yy}$	$+H^{Yz}$	$-V^{tx}$ / $+H^{ty}$	$+V^{ty}$ / $+H^{tx}$	(+φ) / -α
45	.3409	.3221	.1630	-.0202	.0070	.1141	.0648	.1412	.1618	.1343	.4494	45
46	.3333	.3214	.1566	-.0216	.0068	.1146	.0655	.1393	.1611	.1280	.4450	46
47	.3258	.3208	.1504	-.0230	.0065	.1151	.0663	.1374	.1604	.1218	.4407	47
48	.3184	.3202	.1445	-.0243	.0062	.1156	.0671	.1356	.1598	.1156	.4365	48
49	.3111	.3197	.1388	-.0257	.0059	.1160	.0679	.1337	.1593	.1095	.4324	49
50	.3039	.3193	.1333	-.0270	.0056	.1164	.0686	.1318	.1588	.1035	.4284	50
51	.2968	.3189	.1280	-.0284	.0053	.1168	.0694	.1299	.1583	.0975	.4245	51
52	.2897	.3186	.1229	-.0297	.0050	.1171	.0701	.1281	.1579	.0916	.4207	52
53	.2828	.3183	.1180	-.0311	.0047	.1174	.0709	.1262	.1576	.0857	.4170	53
54	.2759	.3181	.1134	-.0324	.0044	.1176	.0717	.1244	.1573	.0799	.4134	54
55	.2692	.3179	.1090	-.0338	.0041	.1178	.0725	.1226	.1571	.0741	.4099	55
56	.2625	.3177	.1047	-.0351	.0038	.1180	.0733	.1208	.1569	.0684	.4064	56
57	.2559	.3176	.1006	-.0364	.0035	.1181	.0741	.1190	.1568	.0627	.4030	57
58	.2493	.3175	.0966	-.0377	.0032	.1181	.0749	.1172	.1567	.0571	.3997	58
59	.2428	.3175	.0928	-.0390	.0029	.1182	.0757	.1154	.1566	.0515	.3964	59
60	.2364	.3175	.0891	-.0404	.0025	.1182	.0765	.1135	.1566	.0460	.3932	60
61	.2301	.3175	.0856	-.0417	.0022	.1182	.0773	.1117	.1567	.0405	.3901	61
62	.2238	.3176	.0822	-.0431	.0018	.1181	.0782	.1099	.1568	.0350	.3870	62
63	.2176	.3177	.0789	-.0444	.0014	.1181	.0791	.1081	.1570	.0296	.3840	63
64	.2114	.3179	.0758	-.0458	.0010	.1180	.0800	.1062	.1572	.0242	.3811	64
65	.2053	.3181	.0728	-.0471	.0006	.1178	.0809	.1044	.1575	.0188	.3782	65
66	.1992	.3183	.0699	-.0485	.0002	.1176	.0819	.1025	.1578	.0135	.3753	66
67	.1932	.3185	.0671	-.0499	-.0002	.1174	.0828	.1007	.1582	.0082	.3725	67
68	.1873	.3188	.0645	-.0513	-.0007	.1172	.0838	.0988	.1587	.0029	.3697	68
69	.1814	.3191	.0620	-.0527	-.0012	.1170	.0848	.0970	.1592	-.0024	.3670	69
70	.1756	.3194	.0595	-.0541	-.0017	.1167	.0858	.0951	.1598	-.0077	.3644	70
71	.1698	.3197	.0572	-.0555	-.0022	.1164	.0868	.0933	.1605	-.0129	.3618	71
72	.1640	.3201	.0549	-.0569	-.0028	.1160	.0879	.0914	.1612	-.0181	.3592	72
73	.1582	.3205	.0527	-.0583	-.0033	.1157	.0890	.0895	.1620	-.0233	.3566	73
74	.1525	.3209	.0506	-.0598	-.0039	.1153	.0901	.0876	.1628	-.0284	.3541	74
75	.1468	.3213	.0486	-.0613	-.0045	.1149	.0913	.0857	.1637	-.0335	.3516	75
76	.1411	.3218	.0467	-.0628	-.0052	.1144	.0925	.0838	.1646	-.0386	.3492	76
77	.1354	.3222	.0449	-.0643	-.0059	.1140	.0937	.0819	.1656	-.0437	.3468	77
78	.1298	.3227	.0431	-.0658	-.0066	.1135	.0950	.0799	.1667	-.0489	.3444	78
79	.1242	.3232	.0414	-.0674	-.0073	.1130	.0963	.0779	.1679	-.0540	.3420	79
80	.1187	.3237	.0398	-.0690	-.0081	.1124	.0977	.0759	.1691	-.0590	.3397	80
81	.1132	.3242	.0382	-.0706	-.0089	.1118	.0991	.0739	.1705	-.0641	.3374	81
82	.1077	.3248	.0367	-.0723	-.0098	.1112	.1005	.0719	.1719	-.0692	.3352	82
83	.1022	.3254	.0352	-.0740	-.0107	.1106	.1020	.0699	.1734	-.0743	.3329	83
84	.0967	.3260	.0338	-.0757	-.0116	.1099	.1035	.0678	.1750	-.0794	.3307	84
85	.0912	.3266	.0325	-.0775	-.0126	.1092	.1051	.0657	.1767	-.0845	.3285	85
86	.0856	.3273	.0312	-.0793	-.0136	.1085	.1067	.0636	.1785	-.0895	.3263	86
87	.0801	.3279	.0300	-.0811	-.0147	.1078	.1084	.0615	.1804	-.0946	.3241	87
88	.0745	.3286	.0288	-.0830	-.0159	.1070	.1102	.0594	.1823	-.0997	.3219	88
89	.0690	.3293	.0277	-.0849	-.0171	.1062	.1120	.0572	.1844	-.1048	.3197	89
90	.0635	.3300	.0266	-.0869	-.0184	.1054	.1139	.0550	.1865	-.1100	.3175	90

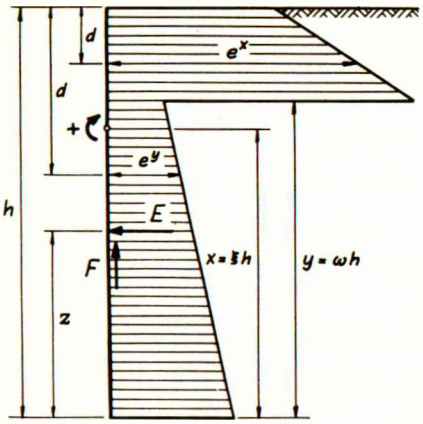

Fig.G: Earth pressure diagram

We consider the case of a horizontal ground surface and a vertical wall rotating about a point located at a height $x = \xi h$ above the foot of the wall (see Fig.G). The rotation is called positive, when it increases the angle between wall and surface, and negative when it decreases this angle. The following general formulae are valid, and in these c should always be assumed positive:

$$E = \tfrac{1}{2}\gamma h^2\lambda + ph\rho + ch\kappa \qquad 6118$$

$$Ez = \tfrac{1}{2}\gamma h^3\lambda\eta + ph^2\rho\theta + ch^2\kappa\zeta \qquad 6119$$

$$F = \tfrac{1}{2}\gamma h^2\lambda \tan\delta^\gamma + (ph\rho + ch\kappa)\tan\delta^p + ah \qquad 6120$$

$$e_d^x = \gamma d\lambda^x + p\rho^x + c\kappa^x \qquad e_d^y = \gamma d\lambda^y + p\rho^y + c\kappa^y \qquad y = \omega h \qquad 6121\text{-}23$$

In the special case of frictionless earth ($\varphi = 0$) the dimensionless constants κ, ζ, a : c, ω^o, κ^x and κ^y can be taken from the following Graphs 1-6, corresponding to a given $\xi = x : h$. Further, we have in this case:

$$\lambda = \lambda^x = \lambda^y = \rho = \rho^x = \rho^y = 1 \qquad \eta = \tfrac{1}{3} \qquad \theta = \tfrac{1}{2}$$

In the other special case of a friction angle of 30° ($\varphi = 30^\circ$) the dimensionless constants ρ, θ, $\tan\delta^p$, λ, η, $\tan\delta^\gamma$, ω, λ^x, λ^y, ρ^x and ρ^y can be taken direct from the following Graphs 7-18. The constants κ, ζ, a : c, κ^x and κ^y cannot be taken from Graphs 1-6 (which are valid for $\varphi = 0$ only) but must be calculated by means of the following formulae, the first of which is also valid with superscripts x or y:

$$\kappa = (\rho - 1)\cot|\varphi| \qquad \zeta = (\rho\theta - \tfrac{1}{2}) : (\rho - 1) \qquad a : c = \cot|\varphi|\tan\delta^p \qquad 6112\text{-}15$$

In the case of friction angles other than 0° or 30° we find first ρ_{30}, $\tan\delta_{30}^p$, λ_{30}, $\tan\delta_{30}^\gamma$, λ_{30}^x, λ_{30}^y, ρ_{30}^x and ρ_{30}^y for $\varphi = 30^\circ$ from Graphs 7, 10-11, 14 and 16-18. Next, we find the values ρ, λ, λ^x, λ^y, ρ^x and ρ^y by means of Graph 19 (smooth wall) or 20 (rough wall). Further, the constants ω, η, θ, $\tan\delta^p$ and $\tan\delta^\gamma$ are found from the following equations:

$$\omega = 1 - \sqrt{\frac{\lambda - \lambda^y}{\lambda^x - \lambda^y}} \qquad \eta = \tfrac{1}{3} + \tfrac{2}{3}\omega\,\frac{\lambda - \lambda^y}{\lambda} \qquad 5904\text{-}05$$

$$\theta = \tfrac{1}{2} + \tfrac{1}{2}\omega\,\frac{\rho - \rho^y}{\rho} \qquad \tan\delta = \sqrt{3}\,\tan|\varphi|\tan\delta_{30} \qquad 5906\text{-}07$$

Finally, the remaining constants κ, ζ, a : c, κ^x and κ^y are calculated by means of the above formulae 6112-15.

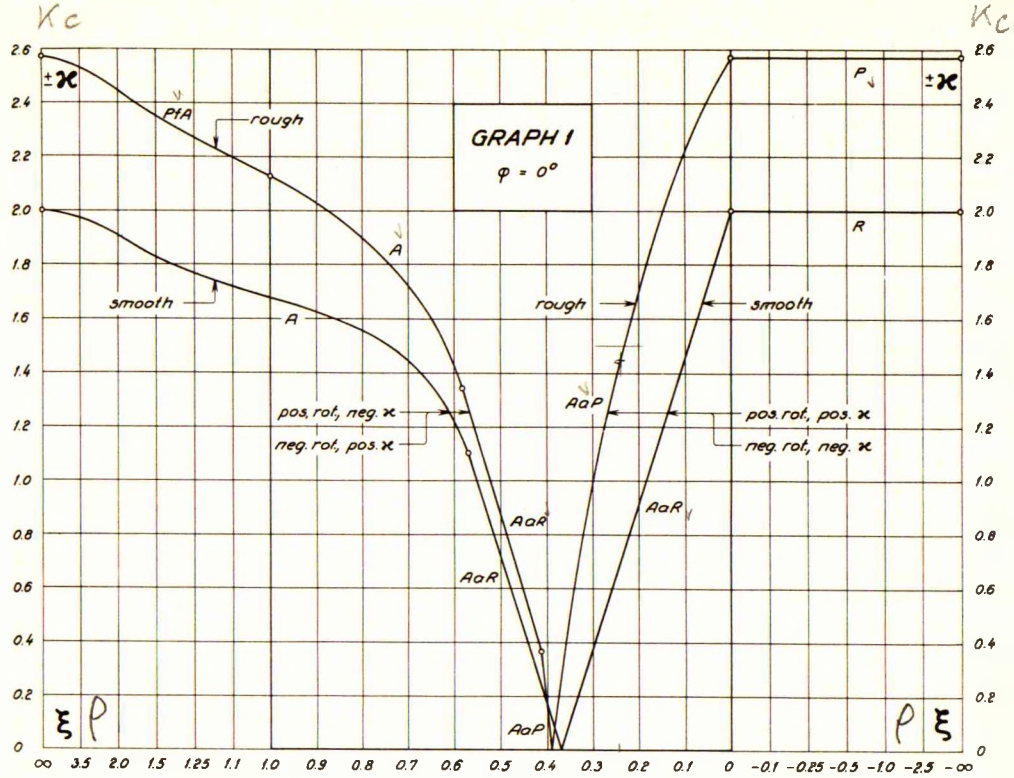
Kc
±κ
PfA
rough
A
smooth
A
GRAPH 1
φ = 0°
P
±κ
R
rough
smooth
AaP
pos. rot., neg. κ
neg. rot., pos. κ
pos. rot., pos. κ
neg. rot., neg. κ
AaR
AaR
AaR
AaP
ξ P
P ξ
2.6 2.4 2.2 2.0 1.8 1.6 1.4 1.2 1.0 0.8 0.6 0.4 0.2 0
∞ 3.5 2.0 1.5 1.25 1.1 1.0 0.9 0.8 0.7 0.6 0.5 0.4 0.3 0.2 0.1 0 -0.1 -0.25 -0.5 -1.0 -2.5 -∞

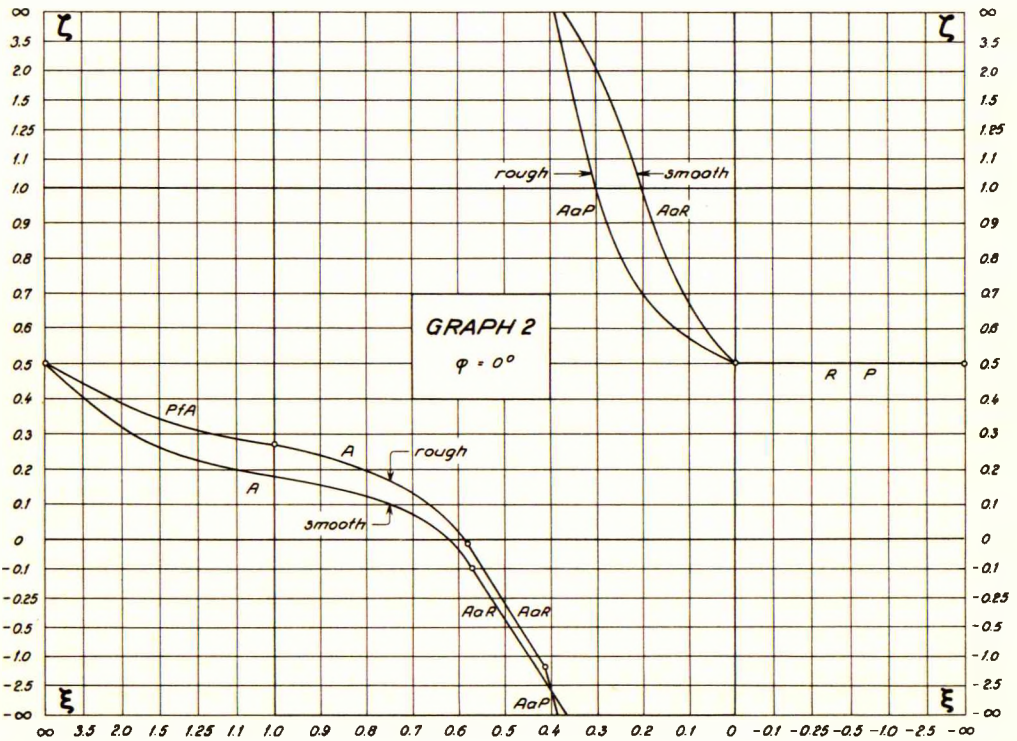
ζ
ζ
rough
smooth
AaP
AaR
GRAPH 2
φ = 0°
R P
PfA
A
rough
A
smooth
AaR
AaR
AaP
ξ
ξ
∞ 3.5 2.0 1.5 1.25 1.1 1.0 0.9 0.8 0.7 0.6 0.5 0.4 0.3 0.2 0.1 0 -0.1 -0.25 -0.5 -1.0 -2.5 -∞

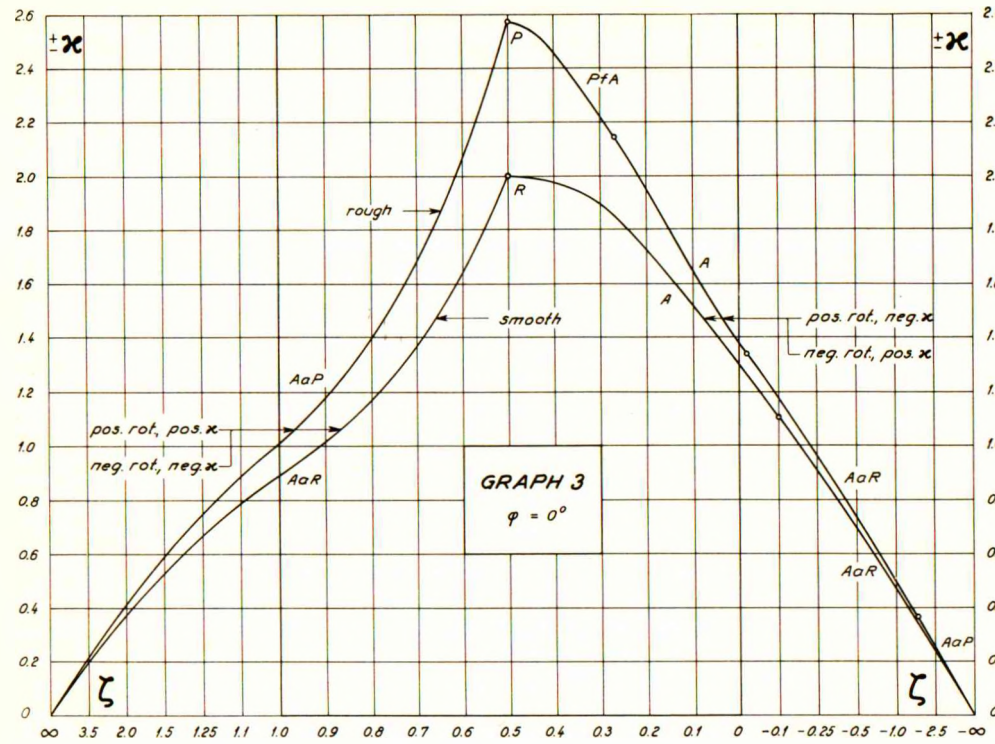
±κ
P
PfA
R
rough
A
A
smooth
pos. rot., neg. κ
neg. rot., pos. κ
AaP
pos. rot., pos. κ
neg. rot., neg. κ
AaR
GRAPH 3
φ = 0°
AaR
AaR
AaP
ζ
ζ
2.6 2.4 2.2 2.0 1.8 1.6 1.4 1.2 1.0 0.8 0.6 0.4 0.2 0
∞ 3.5 2.0 1.5 1.25 1.1 1.0 0.9 0.8 0.7 0.6 0.5 0.4 0.3 0.2 0.1 0 -0.1 -0.25 -0.5 -1.0 -2.5 -∞

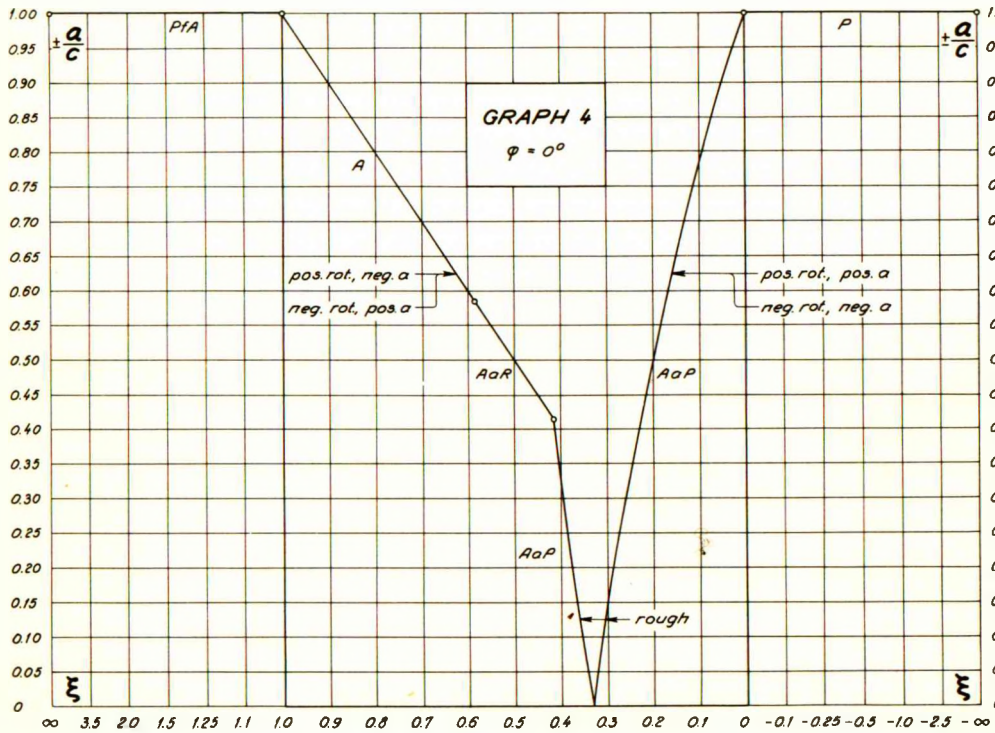
±a/c
PfA
A
GRAPH 4
φ = 0°
P
pos. rot., neg. a
neg. rot., pos. a
pos. rot., pos. a
neg. rot., neg. a
AaR
AaP
AaP
rough
ξ
ξ
1.00 0.95 0.90 0.85 0.80 0.75 0.70 0.65 0.60 0.55 0.50 0.45 0.40 0.35 0.30 0.25 0.20 0.15 0.10 0.05 0
∞ 3.5 2.0 1.5 1.25 1.1 1.0 0.9 0.8 0.7 0.6 0.5 0.4 0.3 0.2 0.1 0 -0.1 -0.25 -0.5 -1.0 -2.5 -∞

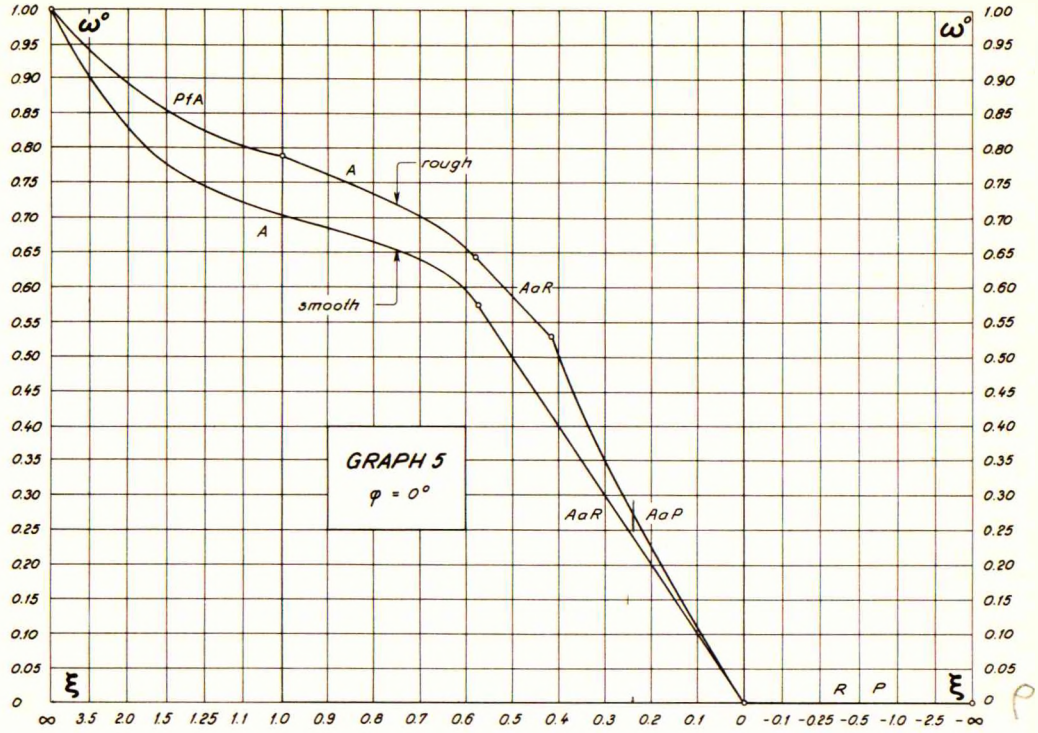
ω°
PfA
A
rough
A
smooth
AaR
AaR
AaP
GRAPH 5
φ = 0°
ξ
R P
1.00 0.95 0.90 0.85 0.80 0.75 0.70 0.65 0.60 0.55 0.50 0.45 0.40 0.35 0.30 0.25 0.20 0.15 0.10 0.05 0
∞ 3.5 2.0 1.5 1.25 1.1 1.0 0.9 0.8 0.7 0.6 0.5 0.4 0.3 0.2 0.1 0 -0.1 -0.25 -0.5 -1.0 -2.5 -∞

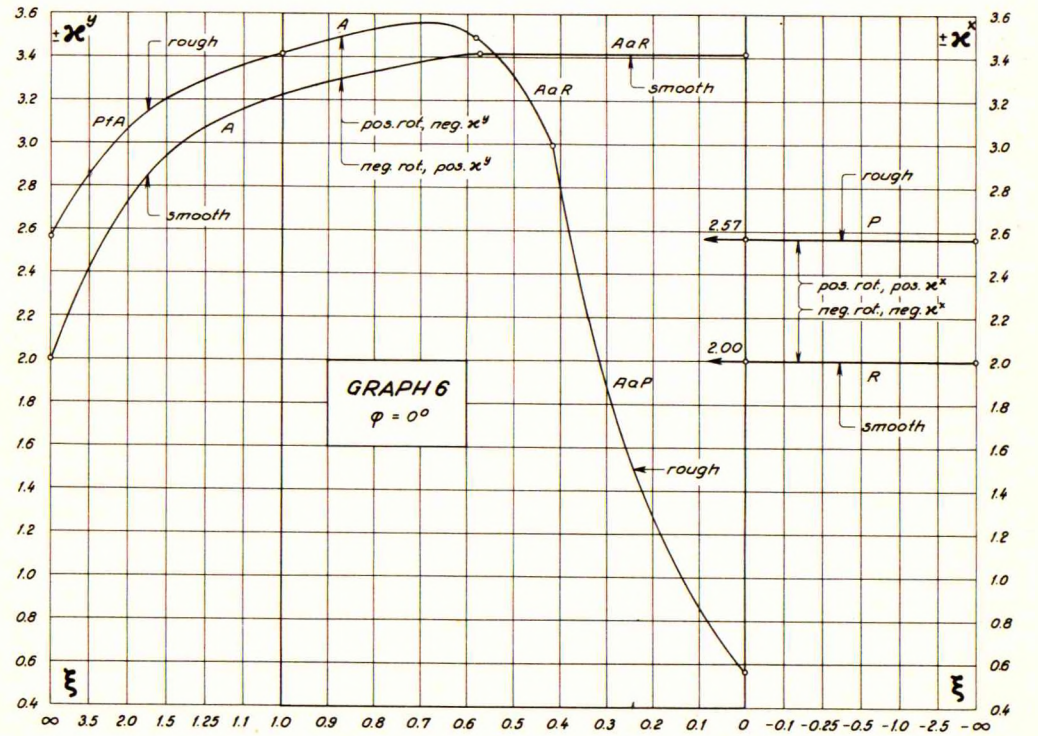
±x^y
rough
A
AaR
smooth
AaR
PfA
A
pos. rot., neg. x^y
neg. rot., pos. x^y
smooth
rough
2.57
P
pos. rot., pos. x^x
neg. rot., neg. x^x
2.00
R
smooth
AaP
rough
GRAPH 6
φ = 0°
±x^x
ξ
3.6 3.4 3.2 3.0 2.8 2.6 2.4 2.2 2.0 1.8 1.6 1.4 1.2 1.0 0.8 0.6 0.4
∞ 3.5 2.0 1.5 1.25 1.1 1.0 0.9 0.8 0.7 0.6 0.5 0.4 0.3 0.2 0.1 0 -0.1 -0.25 -0.5 -1.0 -2.5 -∞

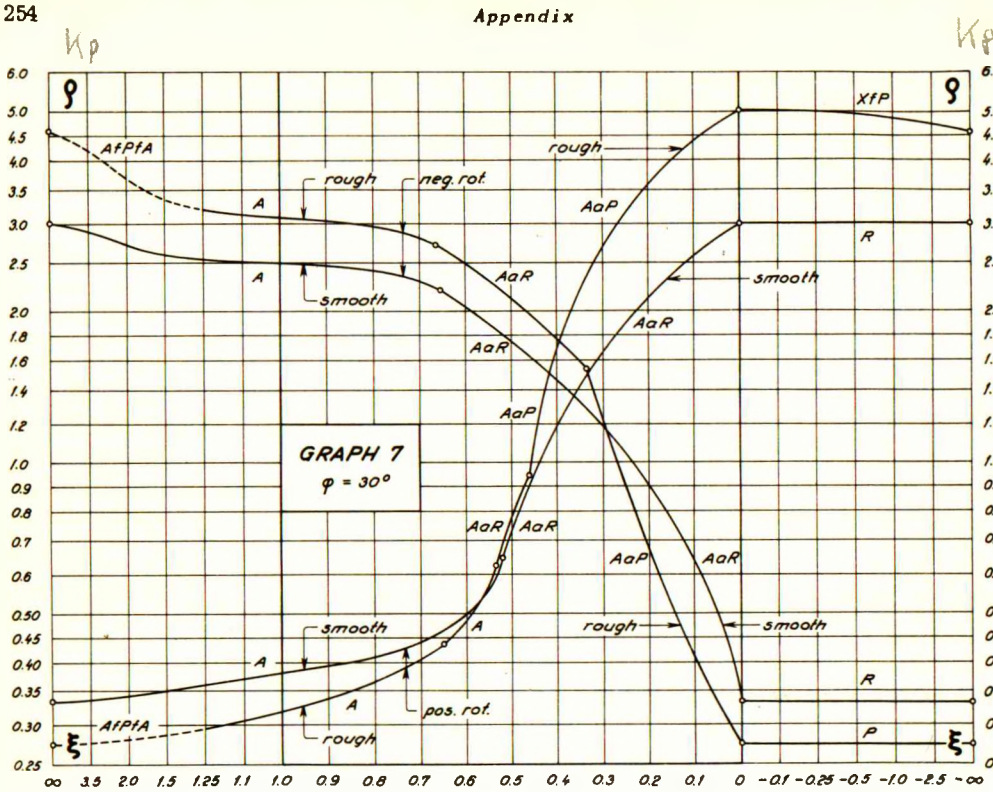
Kρ
ρ
AfPfA
A
rough
neg. rot.
smooth
AaR
AaP
XfP
R
P
pos. rot.
GRAPH 7
φ = 30°
ξ
∞ 3.5 2.0 1.5 1.25 1.1 1.0 0.9 0.8 0.7 0.6 0.5 0.4 0.3 0.2 0.1 0 -0.1 -0.25 -0.5 -1.0 -2.5 -∞

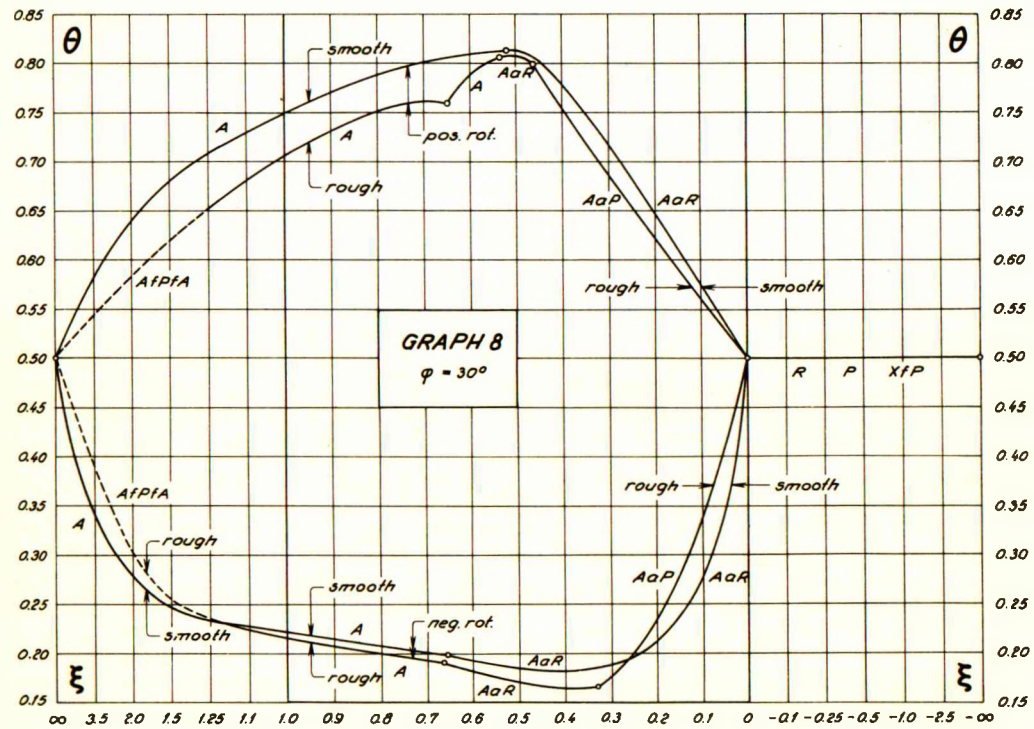
θ
ξ
AfPfA
A
smooth
rough
pos. rot.
neg. rot.
AaR
AaP
R
P
XfP
GRAPH 8
φ = 30°
∞ 3.5 2.0 1.5 1.25 1.1 1.0 0.9 0.8 0.7 0.6 0.5 0.4 0.3 0.2 0.1 0 -0.1 -0.25 -0.5 -1.0 -2.5 -∞

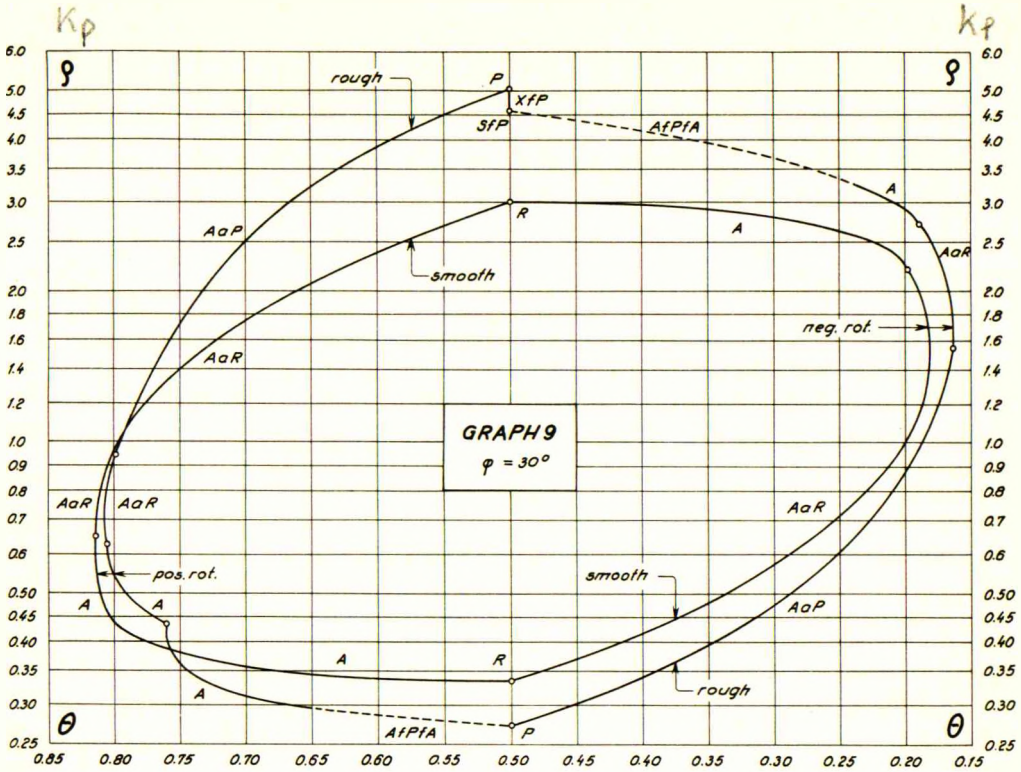
Kp
Kp
rough
P
XfP
SfP
AfPfA
A
AaP
R
A
AaR
smooth
neg. rot.
AaR
GRAPH 9
φ = 30°
AaR
AaR
AaR
pos. rot.
smooth
A
A
AaP
A
R
A
rough
AfPfA
P
θ
θ
6.0 5.0 4.5 4.0 3.5 3.0 2.5 2.0 1.8 1.6 1.4 1.2 1.0 0.9 0.8 0.7 0.6 0.50 0.45 0.40 0.35 0.30 0.25
0.85 0.80 0.75 0.70 0.65 0.60 0.55 0.50 0.45 0.40 0.35 0.30 0.25 0.20 0.15

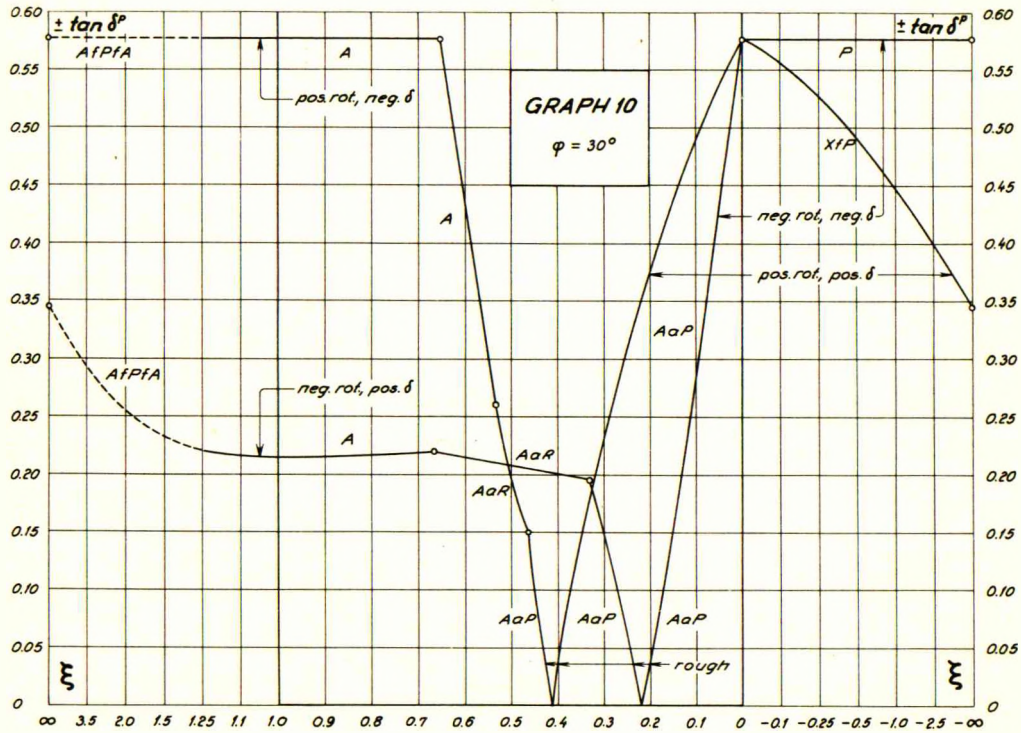
± tan δP
± tan δP
AfPfA
A
pos. rot., neg. δ
GRAPH 10
φ = 30°
P
XfP
A
neg. rot, neg. δ
pos. rot., pos. δ
AaP
AfPfA
neg. rot., pos. δ
A
AaR
AaR
AaP
AaP
AaP
rough
ξ
ξ
0.60 0.55 0.50 0.45 0.40 0.35 0.30 0.25 0.20 0.15 0.10 0.05 0
∞ 3.5 2.0 1.5 1.25 1.1 1.0 0.9 0.8 0.7 0.6 0.5 0.4 0.3 0.2 0.1 0 -0.1 -0.25 -0.5 -1.0 -2.5 -∞

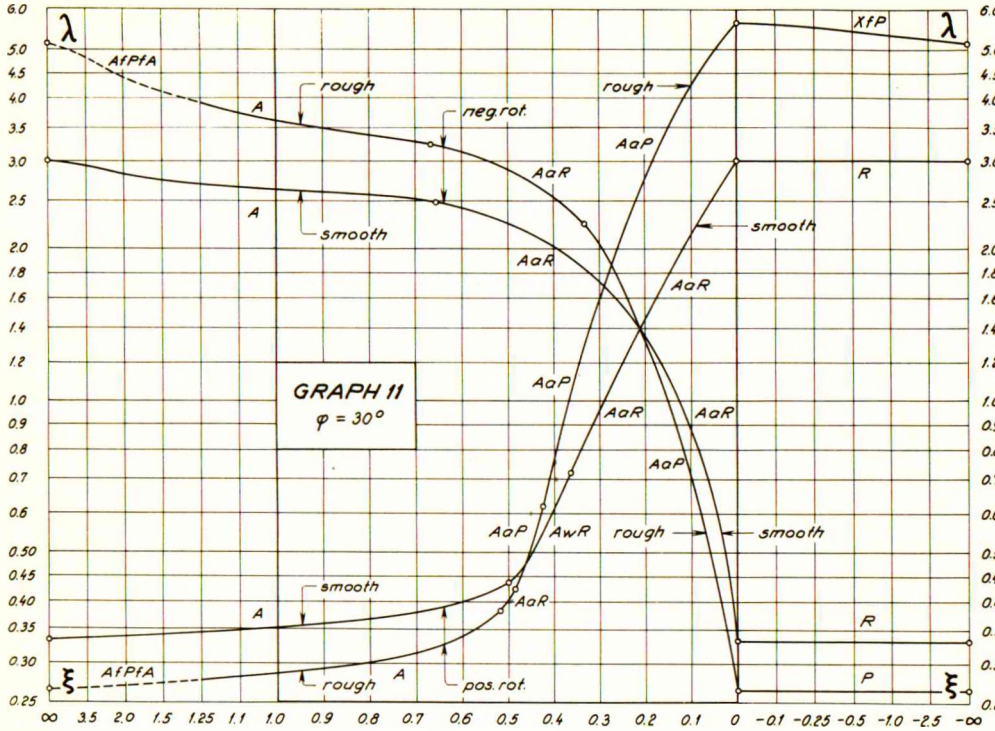
λ
ξ
AfPfA
A
rough
neg.rot.
smooth
AaR
AaP
AwR
XfP
R
P
pos.rot.
GRAPH 11
φ = 30°

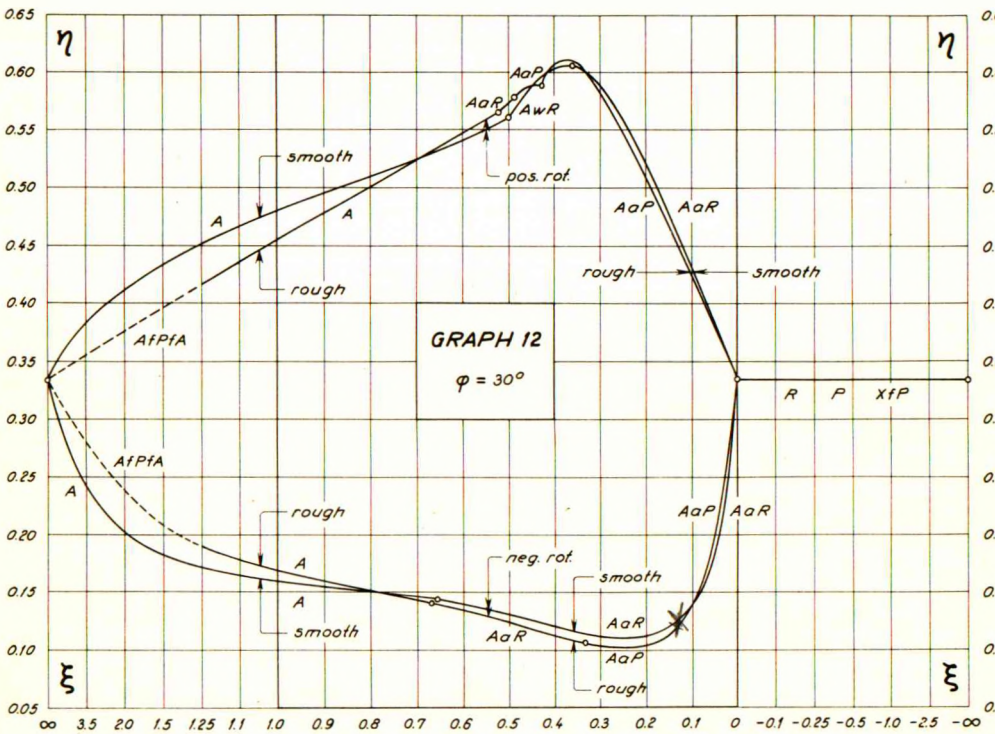
η
ξ
AfPfA
A
smooth
rough
AaP
AaR
AwR
pos.rot.
neg.rot.
R
P
XfP
GRAPH 12
φ = 30°

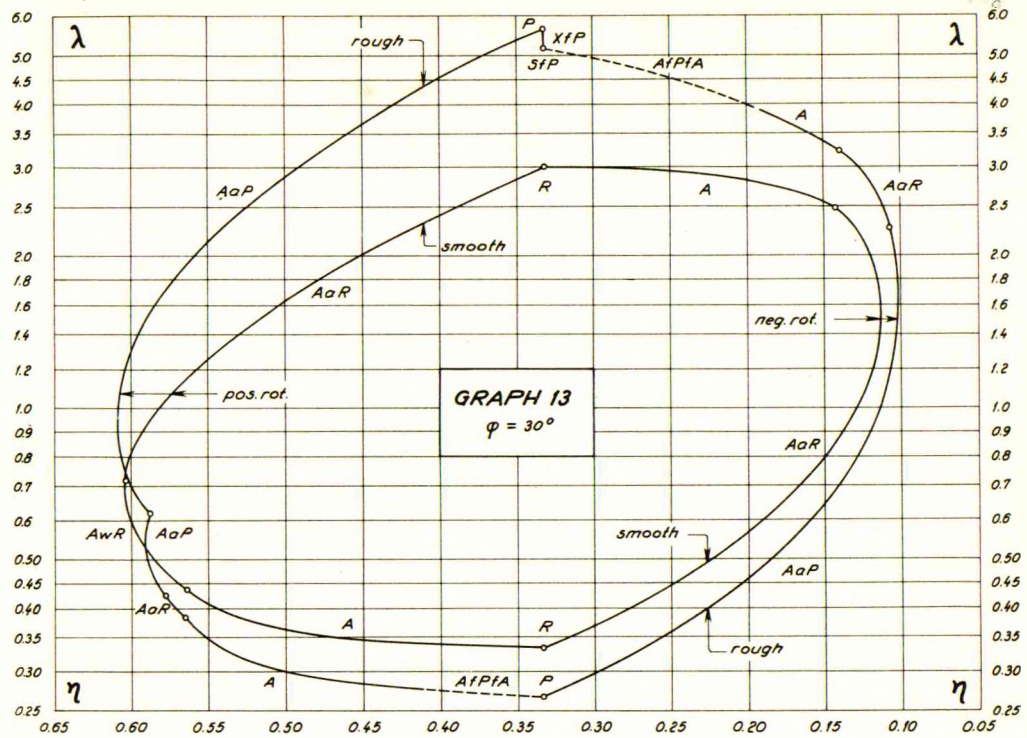
λ
η
rough
P
XfP
SfP
AfPfA
A
AaP
R
AaR
smooth
neg. rot.
pos. rot.
GRAPH 13
φ = 30°
AwR
smooth
rough

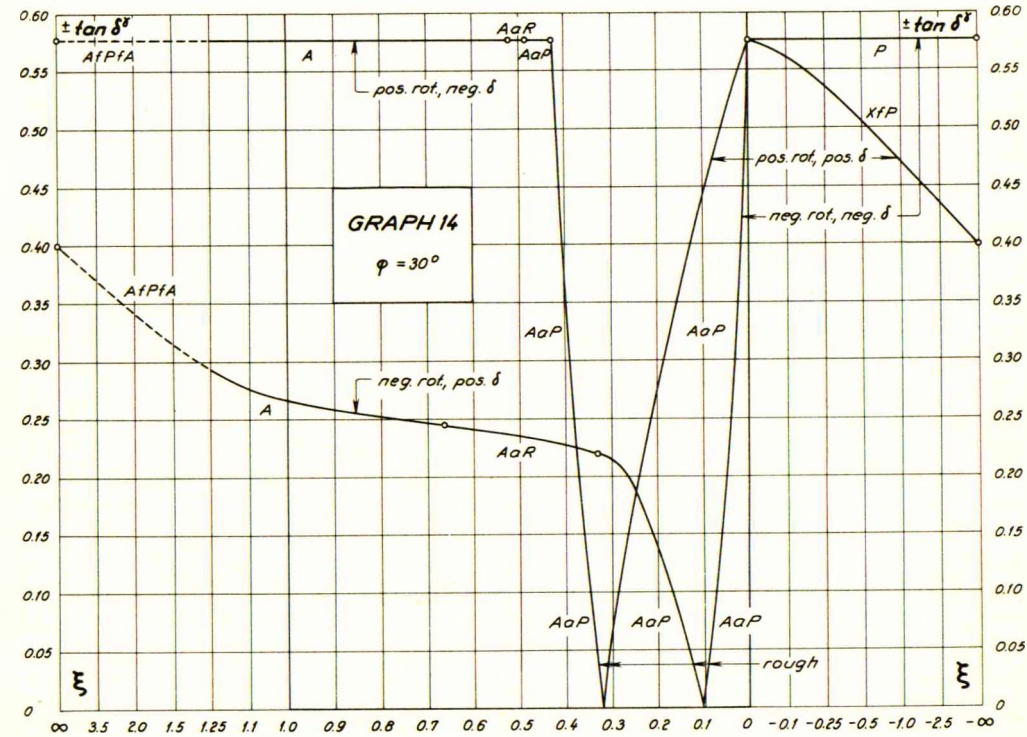
± tan δ'
ξ
AfPfA
A
AaR
AaP
P
pos. rot, neg. δ
XfP
pos. rot, pos. δ
neg. rot, neg. δ
GRAPH 14
φ = 30°
neg. rot, pos. δ
rough

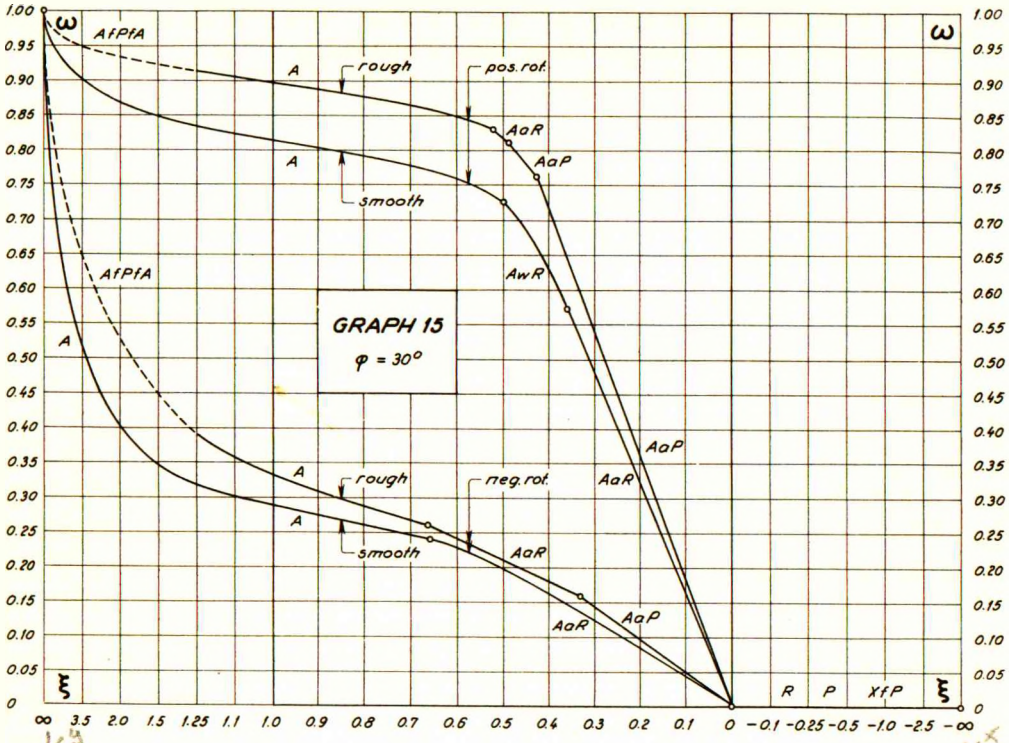
ω
AfPfA
A
rough
pos. rot.
AaR
AaP
smooth
AwR
GRAPH 15
φ = 30°
neg. rot.
R
P
XfP
ξ
∞ 3.5 2.0 1.5 1.25 1.1 1.0 0.9 0.8 0.7 0.6 0.5 0.4 0.3 0.2 0.1 0 −0.1 −0.25 −0.5 −1.0 −2.5 −∞

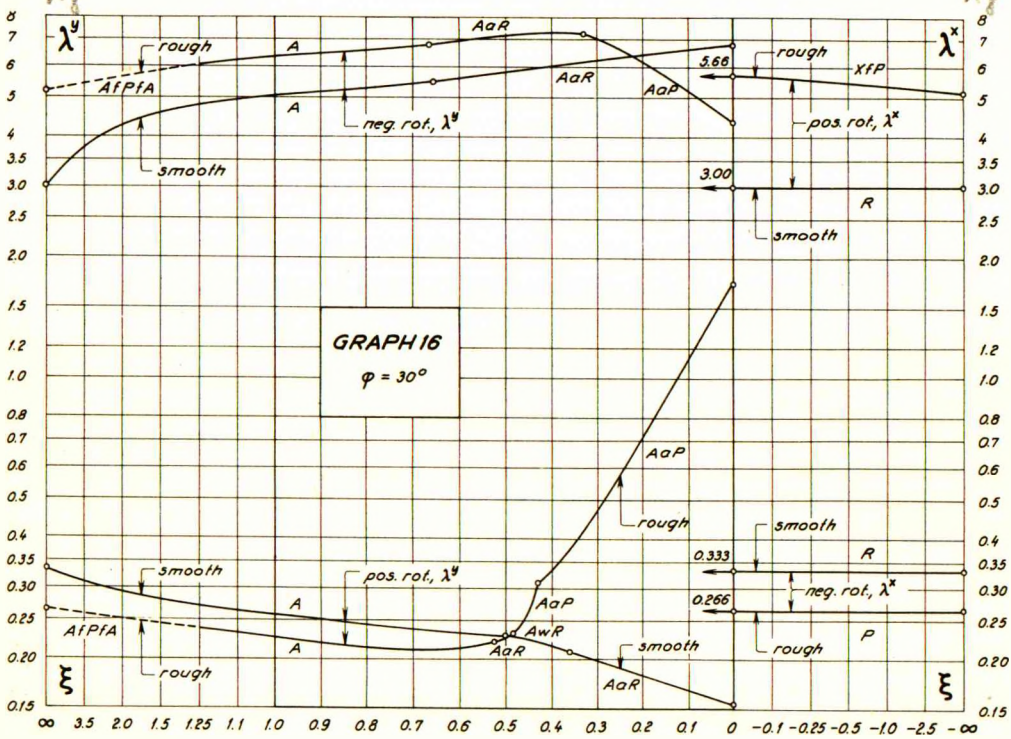
λ^y
λ^x
AaR
rough
A
AfPfA
AaP
neg. rot., λ^y
smooth
5.66
XfP
pos. rot, λ^x
3.00
R
GRAPH 16
φ = 30°
0.333
0.266
P
AwR
ξ
∞ 3.5 2.0 1.5 1.25 1.1 1.0 0.9 0.8 0.7 0.6 0.5 0.4 0.3 0.2 0.1 0 −0.1 −0.25 −0.5 −1.0 −2.5 −∞

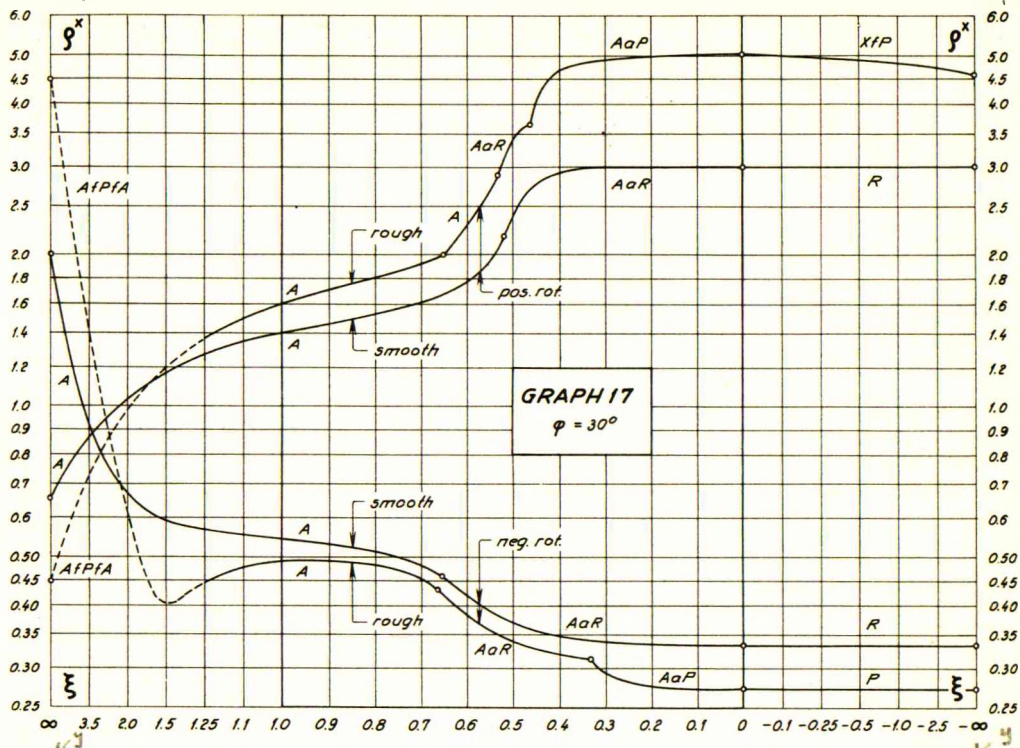
K_p^x
ρ^x
AaP
XfP
AaR
AfPfA
R
rough
A
pos. rot.
smooth
GRAPH 17
$\varphi = 30^\circ$
neg. rot.
P
ξ
∞ 3.5 2.0 1.5 1.25 1.1 1.0 0.9 0.8 0.7 0.6 0.5 0.4 0.3 0.2 0.1 0 -0.1 -0.25 -0.5 -1.0 -2.5 -∞

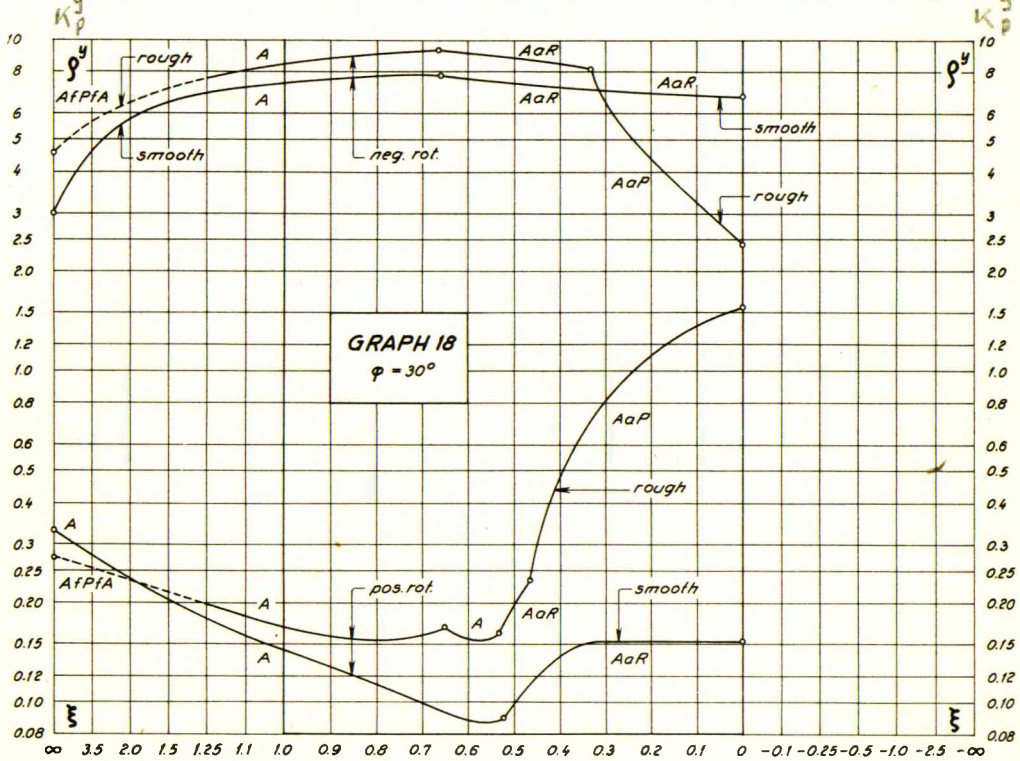
K_p^y
ρ^y
rough
AfPfA
A
AaR
smooth
neg. rot.
AaP
GRAPH 18
$\varphi = 30^\circ$
pos. rot.
ξ
∞ 3.5 2.0 1.5 1.25 1.1 1.0 0.9 0.8 0.7 0.6 0.5 0.4 0.3 0.2 0.1 0 -0.1 -0.25 -0.5 -1.0 -2.5 -∞

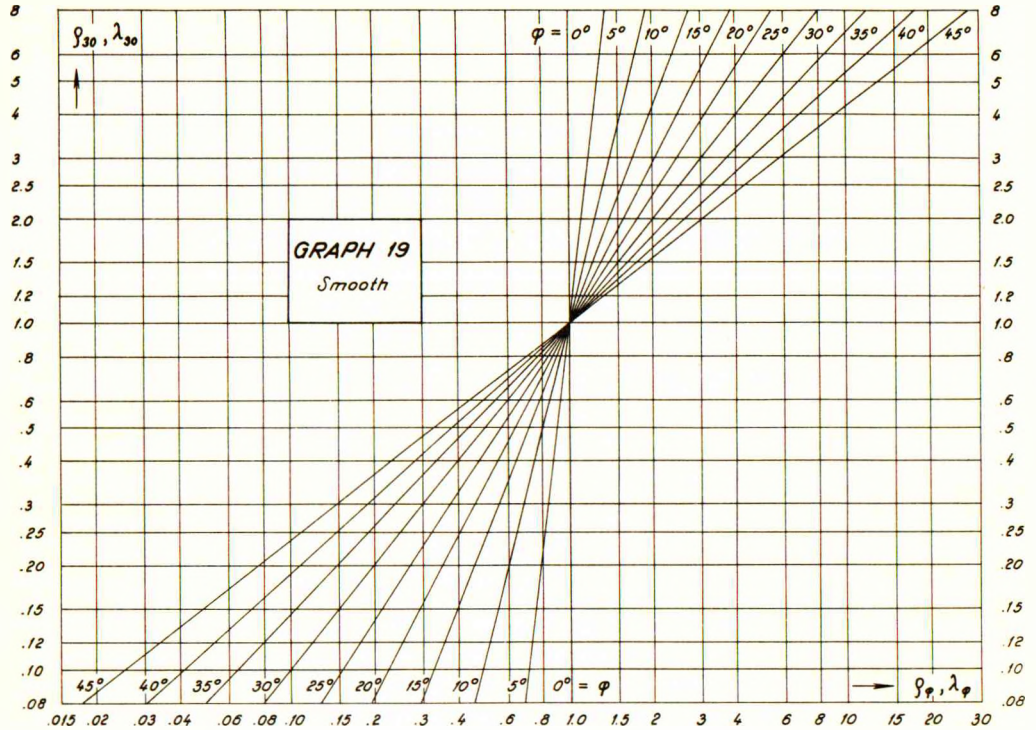
GRAPH 19
Smooth
φ = 0° 5° 10° 15° 20° 25° 30° 35° 40° 45°
ϱ_{30}, λ_{30}
45° 40° 35° 30° 25° 20° 15° 10° 5° 0° = φ
ϱ_φ, λ_φ

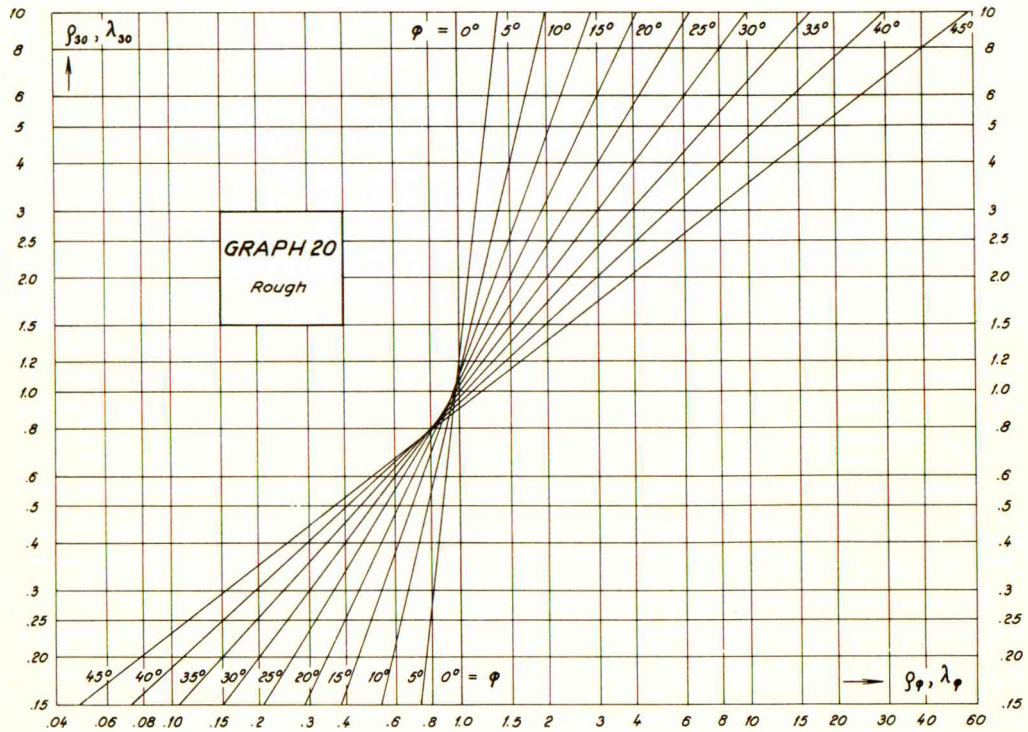
GRAPH 20
Rough
φ = 0° 5° 10° 15° 20° 25° 30° 35° 40° 45°
ϱ_{30}, λ_{30}
45° 40° 35° 30° 25° 20° 15° 10° 5° 0° = φ
ϱ_φ, λ_φ

ENGLISH SUMMARY

The present work contains, in addition to a short description of the known methods for earth pressure calculation, the principles of a new general calculation method, as well as a number of applications to practical earth pressure and stability problems (with numerical examples).

The fundamental basis of the new method is a connection, established by the author, between two known methods, which may be termed the extreme-method and the equilibrium-method respectively. In both these methods a state of rupture in the earth is considered, and an earth wedge is investigated, which is bounded by the ground surface, the wall and a rupture-line through the lowest point of the wall.

In the extreme-method a statical condition of equilibrium for the said earth wedge is set up in such a way, that it does not contain the unknown internal forces in the rupture-line. The earth pressure on the wall is then determined by an extreme-condition which states that the active earth pressure should be a maximum, or the passive a minimum. This method necessitates the assumption that the rupture-line is a logarithmic spiral (Rendulic), in special cases a circle (Fellenius) or a straight line (Coulomb).

In the equilibrium-method no extreme-condition is employed, but the earth pressure is determined by means of all three statical conditions of equilibrium for the above-mentioned earth wedge. This presumes, of course, that the internal forces in the rupture-line are known, which is effected by means of the so-called Kötter's Equation in connection with a boundary condition at the ground surface. However, so far, it has only been possible to indicate this boundary condition in special cases, viz., when the rupture-line meets the ground surface at a certain angle, or when the ground surface is unloaded and the earth cohesionless (Ohde).

In order to judge the applicability and limitations of these methods it is necessary to first consider the figures of rupture which may develop in the earth. The author distinguishes here between the following three different types:

1) Zone-ruptures, in which the stresses at any point within a certain area satisfy the condition of failure.

2) Line-ruptures, in which only the stresses at the points on a certain curve satisfy the condition of failure.

3) Composite ruptures, which consist of more than one rupture-zone or rupture-line.

Many rupture-figures consist thus exclusively or partly of a single rupture-line separating two zones, in which the state of rupture is not attained. Disregarding the elastic deformations, and assuming incompressibility, such a single rupture-line must, for kinematical reasons, be a circle, the centre of which is located on a normal to the wall through its rotation centre. Consequently, this rupture-figure cannot usually be dealt with by means of the extreme-method, which requires the use of logarithmic spirals, and the indefinite boundary condition excludes normally the employment of the equilibrium-method.

The author has succeeded in overcoming these difficulties by proving that the two methods will give identical results, when a logarithmic spiral is used as a rupture-line in both, and when a certain boundary condition is used in the equilibrium-method. This boundary condition is namely also, as a very good approximation, applicable to the circular rupture-line which must be used in the case of a given rotation centre. In this way the author has made possible a general application of the equilibrium-method.

For the design or calculation of a certain earth retaining structure it is necessary to determine first the type of movement to be performed by the structure in the state of failure. Disregarding the elastic deformations, the structure must either move as one rigid body, or as a finite number of rigid parts connected by yield hinges. A further investigation seems to show

that, to a certain degree, it is possible to choose freely the type of movement on which to base the calculation.

Corresponding to the chosen type of movement for the structure such figures of rupture in the adjacent earth masses are then investigated, which imply movements and deformations of the earth compatible with those of the structure. The corresponding earth pressures on the structure are determined by means of the equilibrium-method in its general form. If more than one figure of rupture satisfies the kinematical conditions, the design of the structure must be based on the rupture-figure, for which the work done by the earth pressure (acting upon the earth) is a minimum.

Finally, the dimensions of the structure are so determined that the statical equilibrium conditions for the structure proper are satisfied and the allowable stresses not exceeded. As in the whole calculation the state of failure is considered, it is necessary to divide the actual shear strengths of the soils by suitable safety factors before carrying out the calculation. As corresponding "allowable" stresses are used the ultimate strengths of the structural materials after division by other safety factors.

The author has applied the outlined method to the majority of plane earth pressure problems encountered in practice, viz., retaining walls, anchor slabs, free sheet walls, fixed sheet walls, braced walls, double sheet walls and cellular cofferdams. Incidentally, the method is also applicable to stability and foundation problems.

The proposed method is applicable to earth with internal friction or cohesion or both, to walls with any inclination and roughness, and to ground surfaces with any slope and surcharge. The effects of hydrostatic or hydrodynamic water pressures can be taken into account, at least approximately, and the same applies also in the case of stratified earth.

The practical calculations are facilitated considerably by the use of the tables and graphs in the Appendix. The tables enable an easy and quick calculation of the internal forces in a rupture-circle, but only for a friction angle of either 0° or 30°. By means of the graphs it is possible to easily determine the earth pressure on a vertical wall (horizontal ground surface) for any friction angle, and for any given location of the rotation centre for the wall.

Due to the wide range of application of the new method the author has only been able to check its results against practical experience in a few instances. However, the connection established between the new method and the extreme-method should be a safeguard against serious errors, as it is a well-known fact that extreme-methods (e.g. the so-called "φ=0"-analysis) will produce very reliable results when used properly.

Further, it may be mentioned that a stability calculation of a cellular cofferdam on rock, by means of the new method, leads to very nearly the same dimensions as those most commonly used in practice. It is also of interest to note that, with suitable safety factors, the author's design methods for anchored sheet walls in sand may lead to virtually the same results as the so-called Danish Rules, which have proved their suitability in practice for a considerable number of years.

Consequently, provided that the author's methods are used with appropriate caution, it is to be expected that they will result in sufficiently safe and rather economical structures.

DANSK RESUMÉ

Den foreliggende afhandling indeholder, foruden en kort gennemgang af de allerede kendte metoder til jordtryks-beregning, principperne for en ny generel beregningsmetode, samt en række anvendelser paa praktiske jordtryks- og stabilitetsproblemer (med taleksempler).

Grundlaget for den ny metode er en af forfatteren opdaget sammenhäng mellem to kendte metoder, der kan betegnes som henholdsvis extrem-metoden og ligevägts-metoden. Ved begge disse metoder betragter man en brudtilstand i jorden og undersøger et jordlegeme, der er begränset af jordoverfladen, väggen og en brudlinie gennem väggens nederste punkt.

Ved extrem-metoden opstiller man for det nävnte jordlegeme en statisk ligevägtsbetingelse af en saadan art, at den ikke indeholder de ubekendte indre kräfter i brudlinien. Derefter bestemmes jordtrykket paa väggen ved en extrem-betingelse, som udtrykker, at det aktive jordtryk skal väre et maximum, eller det passive et minimum. Denne metode kräver, at brudlinien antages at väre en logaritmisk spiral (Rendulic), i specielle tilfälde en cirkel (Fellenius) eller en ret linie (Coulomb).

Ved ligevägts-metoden anvendes ikke nogen extrem-betingelse, men jordtrykket bestemmes ved hjälp af alle tre statiske ligevägtsbetingelser for det ovenfor nävnte jordlegeme. Dette forudsätter naturligvis, at de indre kräfter i brudlinien kendes, hvilket opnaas ved hjälp af den saakaldte Kötters Ligning i forbindelse med en gränsebetingelse ved jordoverfladen. Imidlertid har denne gränsebetingelse hidtil kun kunnet angives i specielle tilfälde, nemlig naar brudlinien skärer jordoverfladen under en bestemt vinkel, eller naar jordoverfladen er ubelastet og jorden kohäsionsløs (Ohde).

For at kunne bedømme disse metoders anvendelighed og begränsning maa man først betragte de brudfigurer, der kan opstaa i jorden. Forfatteren skelner her mellem følgende tre forskellige typer:

1) Zone-brud, ved hvilke spändingerne i ethvert punkt inden for et bestemt omraade tilfredsstiller brudbetingelsen.

2) Linie-brud, ved hvilke kun spändingerne i punkterne paa en bestemt kurve tilfredsstiller brudbetingelsen.

3) Kombinerede brud, der bestaar af mere end een brudzone eller brudlinie.

Mange brudfigurer bestaar saaledes helt eller delvis af en enkelt brudlinie, som adskiller to omraader, der ikke befinder sig i brudtilstanden. Naar man ser bort fra elastiske deformationer, og desuden antager volumenkonstans, maa en saadan enkelt brudlinie af kinematiske grunde väre en cirkel, hvis centrum ligger paa en normal til väggen gennem dennes rotationscentrum. Denne brudfigur kan derfor i almindelighed ikke behandles ved hjälp af extrem-metoden, der forudsätter anvendelse af logaritmiske spiraler, ligesom den ubestemte gränsebetingelse normalt udelukker anvendelsen af ligevägts-metoden.

Disse vanskeligheder er det lykkedes forfatteren at overvinde ved at bevise, at de to metoder vil give identiske resultater, naar der i dem begge anvendes en logaritmisk spiral som brudlinie, og naar der anvendes en särlig gränsebetingelse i ligevägts-metoden. Denne gränsebetingelse kan nemlig med god tilnärmelse ogsaa anvendes paa den cirkuläre brudlinie, der maa anvendes i tilfälde af et givet rotationscentrum. Paa denne maade har forfatteren muliggjort en generel anvendelse af ligevägtsmetoden.

Ved dimensionering eller beregning af en bestemt konstruktion, paavirket af jordtryk, maa man først fastslaa arten af den bevägelse, som konstruktionen foretager i brudstadiet. Idet man ser bort fra de elastiske deformationer, maa konstruktionen enten bevåge sig som eet stift legeme, eller som et endeligt antal stive dele, forbundet ved flyde-charnierer. En närmere undersøgelse synes at vise, at man til en vis grad frit kan välge, hvilken art bevägelse man vil basere sin beregning paa.

Svarende til den valgte art bevägelse af konstruktionen maa man dernäst undersøge saadanne brudfigurer i de tilstødende jordmasser, som medfører bevägelser og deformationer, der passer sammen med konstruktionens. De hertil svarende jordtryk paa konstruktionen bestemmes ved hjälp af ligevägts-metoden i dens generelle form. Hvis mere end een brudfigur tilfredsstiller de kinematiske betingelser, skal dimensioneringen af konstruktionen baseres paa den brudfigur, for hvilken det af jordtrykket (virkende paa jorden) udførte arbejde er et minimum.

Til sidst bestemmes konstruktionens dimensioner paa en saadan maade, at de statiske ligevägtsbetingelser for selve konstruktionen er opfyldt og de tilladelige spändinger ikke er overskredet. Da man i hele beregningen betragter brudstadiet, er det nødvendigt at dividere jordarternes forskydningsstyrker med passende sikkerhedsfaktorer, inden beregningen udføres. Som tilsvarende "tilladelige" spändinger anvendes brudstyrkerne for byggematerialerne efter division med andre sikkerhedsfaktorer.

Den skitserede metode er af forfatteren blevet anvendt paa hovedparten af de plane jordtryksproblemer, der forekommer i praksis, nemlig støttemure, ankerplader, frie spunsvägge, forankrede spunsvägge, indspändte spunsvägge, afstivede byggegrube-vägge, dobbelte spunsvägge og cellefangedämninger. Metoden kan iøvrigt ogsaa anvendes paa problemer vedrørende stabilitet og fundamentstryk.

Den foreslaaede metode kan anvendes paa jord med indre friktion eller kohäsion eller begge dele. Den kan anvendes paa vägge af enhver häldning og ruhed, og paa jordoverflader med enhver häldning og belastning. Virkningerne af hydrostatiske eller hydrodynamiske vandtryk kan tages i betragtning, i hvert fald med tilnärmelse, og det samme gälder tilfældet lagdelt jord.

De praktiske beregninger lettes i betydelig grad ved anvendelse af tabellerne og diagrammerne i bogens appendix. Tabellerne muliggør en let og hurtig beregning af de indre kräfter i en brudcirkel, men kun for en friktionsvinkel paa enten 0° eller 30°. Ved hjälp af diagrammerne kan man paa en meget simpel maade bestemme jordtrykket paa en lodret väg (vandret jordoverflade) for enhver friktionsvinkel, og for enhver given beliggenhed af väggens rotationscentrum.

Paa grund af den ny metodes omfattende anvendelsesomraade har forfatteren kun været i stand til at sammenligne dens resultater med praktiske erfaringer i nogle faa tilfälde. Imidlertid skulde den forbindelse, der er etableret mellem den ny metode og extrem-metoden være en garanti mod väsentlige fejl, idet det er et velkendt faktum, at extrem-metoder (f.eks. den saakaldte "φ=0"-analyse) vil føre til meget paalidelige resultater, naar de anvendes rigtigt.

Endvidere kan det nævnes, at en stabilitetsberegning for en cellefangedämning paa klippe ved hjälp af den ny metode fører til meget när samme dimensioner som de, der almindeligvis anvendes i praksis. Det er ogsaa af interesse at bemärke, at forfatterens dimensioneringsmetoder for forankrede spunsvägge i sand med passende sikkerhedsfaktorer kan føre til nästen samme resultater som de danske Vandbygnings-Normer, der har vist deres velegnethed i praksis i en lang aarräkke.

Forudsat, at forfatterens metoder anvendes med en passende forsigtighed, kan man derfor forvente, at de vil føre til tilsträkkeligt solide og ganske økonomiske konstruktioner.

REFERENCES

The following list of references does not pretend to be a complete bibliography of earth pressure literature; in fact, the indicated references constitute only a small fraction of this literature. They have, however, been selected as being the most important and interesting from the point of view of the present work.

AGATZ, A. (1943), Grundbau, in F. Schleicher: Taschenbuch für Bauingenieure, Springer, Berlin 1943.

AGATZ, A. & SCHULTZE, E. (1936), Der Kampf des Ingenieurs gegen Erde und Wasser im Grundbau, Springer, Berlin 1936.

BELL, A.L. (1915), The Lateral Pressure and Resistance of Clay, and the Supporting Power of Clay Foundations, Min. Proc. Inst. Civ. Eng., London 1915.

BISHOP, A.W. (1948), A New Sampling Tool for Use in Cohesionless Sands below Ground Water Level, Géotechnique, Vol. I, No. 2, Dec. 1948.

BLUM, H. (1931), Einspannungsverhältnisse bei Bohlwerken, Ernst, Berlin 1931.

BLUM, H. (1951), Beitrag zur Berechnung von Bohlwerken, Ernst, Berlin 1951.

BOUSSINESQ, J. (1885), Application des Potentiels à l'Étude de l'Équilibre et du Mouvement des Solides Élastiques, Gauthier-Villars, Paris 1885.

BRENNECKE, L. & LOHMEYER, E. (1930), Der Grundbau, Ernst, Berlin 1930.

BRETTING, A.E. (1948), General Report, Section V: Earth Pressure, Proc. Sec. Int. Conf., Soil Mech., Vol. VI, Rotterdam 1948.

BROWN, P.P. (1948), A Critical Study of Existing Lateral Earth Pressure Theories, Including the Design of a Model Flexible Anchored Bulkhead for the Investigation of these Theories, Master's Thesis, Princeton 1948.

BROWZIN, B.S. (1948), Upon the Deflection and Strength of Anchored Bulkheads, Proc. Sec. Int. Conf., Soil Mechn., Vol. III, Rotterdam 1948.

BUCHHOLZ, W. (1930), Erdwiderstand auf Ankerplatten, Jahrbuch der Hafenbautechnischen Gesellschaft, Berlin 1930-31.

BUISMAN, A.K. (1943), Grondmechanica, Waltman, Delft 1943.

CADLING, L. & ODENSTAD, S. (1950), The Vane Borer, Royal Swedish Geotechnical Institute, Proceedings No. 2, Stockholm 1950.

CAQUOT, A. (1934), Équilibre des Massifs à Frottement Interne, Gauthier-Villars, Paris 1934.

CAQUOT, A. & KERISEL, J. (1949), Tables de Butée, de Poussée et de Force Portante des Fondations, Gauthier-Villars, Paris 1949.

CARILLO, N. (1942), Differential Equation of a Sliding Surface in an Ideal Saturated Plastic Soil, Journ. Math. Physics, Vol. 21, 1942.

COOK, G. (1951), Rankine and the Theory of Earth Pressure, Géotechnique, Vol. II, No. 4, Dec. 1951.

COULOMB, C.A. (1776), Essai sur une Application des Règles des Maximis et Minimis à quelques Problèmes de Statique, Mémoires Academie Royale des Sciences, Vol. 7, Paris 1776.

DANSK INGENIØRFORENING (1937), Normer for Vandbygnings-Konstruktioner, Copenhagen 1937.

DANSK INGENIØRFORENING (1952), Normer for Bygningskonstruktioner, Fundering og Jordtryk, Teknisk Forlag, Copenhagen 1952.

DRUCKER, D.C. & PRAGER, W. (1951), Soil Mechanics and Plastic Analysis or Limit Design, Office of Naval Research, Technical Report No. 64, Providence, November 1951.

DUKE, C.M. (1952), Field Study of a Sheet-Pile Bulkhead, Proc. ASCE, Oct. 1952, Vol. 78, Sep. No. 155.

EHLERS, H. (1910), Beitrag zur statischen Berechnung von Spundwänden, Hamburg 1910.

FELD, J. (1928), History of Development of Lateral Earth Pressure Theories, Proc. Brooklyn Engineers Club, 1928.

FELD, J. (1940), Review of Pioneer Work in Earth Pressure Determination, Proc. Highway Research Board, U.S.A. 1940.

FELLENIUS, W. (1927), Erdstatische Berechnungen mit Reibung und Kohäsion und unter Annahme kreiszylindrischer Gleitflächen, Ernst, Berlin 1927.

FRANZIUS, O. (1924), Versuche mit passivem Erddruck, Der Bauingenieur 1924, Heft 10.

FREUDENTHAL, A.M. (1950), The Inelastic Behaviour of Engineering Materials and Structures, Wiley, New York 1950.

FRONTARD, J. (1922), Cycloides de Glissement des Terres, Comptes Rendus, Paris 1922.

FRONTARD, J. (1948), Série d'Expériences sur la Stabilité des Talus d'un Massif Constitué au moyen d'une Matière Cohérente ayant un Angle de Frottement voisin de Zéro, Travaux, October 1948.

GOLDER, H.Q. (1948), Coulomb and Earth Pressure, Géotechnique, Vol.I, No.1, June 1948.

GOLDER, H.Q. (1948), Measurement of Pressure in Timbering of a Trench in Clay, Proc. Sec. Int. Conf., Soil Mech., Vol.II, Rotterdam 1948.

HANSEN, J. BRINCH (1946), Development of the C&N Wharf Type, Christiani & Nielsen Bulletin No. 56, Copenhagen 1946.

HANSEN, J. BRINCH (1948), Reinforced Concrete Wharf at Bangkok, Indian Concrete Journal, April 15, 1948.

HANSEN, J. BRINCH (1948), The Stabilizing Effect of Piles in Clay, CN-Post No.3, Nov. 1948.

HANSEN, J. BRINCH & GIBSON, R.E. (1949), Undrained Shear Strengths of Anisotropically Consolidated Clays, Géotechnique, Vol.I, No.3, June 1949.

HANSEN, J. BRINCH (1951), Simple Statical Computation of Permissible Pileloads, CN-Post No.13, May 1951.

HANSEN, J. BRINCH (1952), Simple Stability Investigations, CN-Post No.19, Nov. 1952. The Dock and Harbour Authority, March 1953.

HANSEN, J. BRINCH (1952), A General Plasticity Theory for Clay, Géotechnique, Vol.III, No.4, Dec. 1952.

HANSEN, J. BRINCH (1953), A General Earth Pressure Theory, Proc. Third Int. Conf., Soil Mech., Vol.II, Zürich 1953.

HAYASHI, K. (1921), Theorie des Trägers auf elastischer Unterlage, Springer, Berlin 1921.

HENCKY, H. (1923), Über einige statisch bestimmte Fälle des Gleichgewichts in plastischen Körpern. Zeitschr.f. angew. Math. und Mech. 1923.

HENCKY, H. (1924), Zur Theorie plastischer Deformationen und der hierdurch im Material hervorgerufenen Nebenspannungen, Proc. First Int. Congr. Appl. Mech., Delft 1924.

HERTWIG, A. (1939), Bemerkungen über neuere Erddruckuntersuchungen, Veröffentlichungen der Degebo 1939, Heft 7, Berlin.

HILL, R. (1950), The Mathematical Theory of Plasticity, Oxford 1950.

ITERSON, F.K.Th.v. (1947), Plasticity in Engineering, London 1947.

JAKOBSSON, B. (1947), Semi-Invert-Diagram, Teknisk Tidskrift (Swedish), Aug. 2, 1947.

JÁKY, J. (1936), Stability of Earth Slopes, Proc. First Int. Conf., Soil Mech., Vol.II, Harvard 1936.

JÁKY, J. (1938), Die klassische Erddrucktheorie mit besonderer Rücksicht auf die Stützwandbewegung, Abh. der Int. Ver. für Brückenbau und Hochbau, Vol.5, 1938.

JENSEN, C. (1923), Beregning af forankrede Kajindfatninger, Ingeniøren 1923, No.46, Copenhagen.

JENSEN, C. (1931), Metode til Løsning af det teoretiske Jordtryksproblem for plan Jordoverflade og plan Forflade, Bygningsstatiske Meddelelser 1931, Copenhagen.

JOHANSEN, K.W. (1943), Brudlinieteorier, Doctor's Thesis, Gjellerup, Copenhagen 1943.

JÜRGENSON, L. (1934), The Application of Theories of Elasticity and Plasticity to Foundation Problems, J. Boston Soc. Civil Eng., July 1934.

KÁRMAN, Th.v. (1926), Über elastische Grenzzustände, Proc. Sec. Int. Congr., Appl. Mech., Zürich 1926.

KERISEL, M.J.L. (1939), La force portante des pieux, Annales des Ponts et Chaussées, Paris 1939, Vol.V, No.21.

KREY, H. (1936), Erddruck, Erdwiderstand und Tragfähigkeit des Baugrundes, Ernst, Berlin 1936.

KÖGLER, F. & SCHEIDIG, A. (1948), Baugrund und Bauwerk, Ernst, Berlin 1948.

KÖTTER, F. (1888), Über das Problem der Erddruckbestimmung, Verhandl. Phys. Ges. Berlin, Vol.7, 1888.

KÖTTER, F. (1892), Die Entwicklungen der Lehre vom Erddruck, Jahresber. deutsch. Math. Ver., Vol. 2, 1892.

KÖTTER, F. (1903), Die Bestimmung des Druckes an gekrümmten Gleitflächen, Sitzungsber. Kgl. Preuss. Akad. der Wiss., Berlin 1903.

LEHMANN, H. (1942), Die Verteilung des Erdangriffs an einer oben drehbar gelagerten Wand, Die Bautechnik 1942, Heft 31/32.

LUNDGREN, H. (1949), Cylindrical Shells, Vol. I: Cylindrical Roofs, Doctor's Thesis, Teknisk Forlag, Copenhagen 1949.

MANDEL, J. (1948), Le Problème de l'Équilibre Limite des Terres et les Travaux de l'École Française, Travaux, Oct. 1948.

MANDEL, J. (1951), Ecoulement de l'Eau sous une Ligne de Palplanches, Travaux, Mars 1951.

MISES, R. v. (1913), Mechanik der festen Körper im plastisch-deformablen Zustand, Nachr. Ges. d. Wiss. zu Göttingen, 1913.

MOHR, O. (1871), Beiträge zur Theorie des Erddruckes, Z. Arch. und Ing. Ver. Hannover, Vol. 17, 1871, Vol. 18, 1872.

MÜLLER-BRESLAU (1906), Erddruck auf Stützmauern, Kröner, Stuttgart, 1906.

NADAI, A. (1928), Plasticität und Erddruck, in Handbuch der Physik, Vol. VI, Chapter 6, 1928.

NADAI, A. (1950), Theory of Flow and Fracture of Solids, McGraw-Hill, New York 1950.

ODQVIST, F. (1934), Plasticitetsteori med Tillämpningar, Ingeniørvetenskapsakademien, Stockholm 1934.

OHDE, J. (1938), Zur Theorie des Erddruckes unter besonderer Berücksichtigung der Erddruckverteilung, Die Bautechnik 1938, Heft 10/11, 13, 19, 25, 37, 42, 53/54.

OHDE, J. (1948-52), Zur Erddruck-Lehre, Die Bautechnik 1948, Heft 6, 1949 Heft 12, 1950 Heft 4, 1951 Heft 12, 1952 Heft 2, 1952 Heft 8, 1952 Heft 11 (unfinished).

OLSEN, H. O. C. (1926), Om Jordtrykket paa en forankret Väg , Ingeniøren 1926, No. 27, Copenhagen.

OLSEN, H. O. C. (1926), Jordtrykkets rationelle Teori, Ingeniøren 1926, No. 33, Copenhagen.

OSTENFELD, A. (1923), Om Beregning af forankrede Kajindfatninger, Ingeniøren 1923, No. 48, Copenhagen.

PECK, R. B. (1943), Earth Pressure Measurements in Open Cuts, Chicago Subway, Trans. ASCE, Vol. 108, 1943.

PONCELET, V. (1840), Mém. sur la Stabilité des Revêtements et de leur Fondations, Mém. de l'Officier du Génie, Vol. 13, 1840.

PRAGER, W. & HODGE, P. G. (1951), Theory of Perfectly Plastic Solids, Wiley, New York 1951.

PRANDTL, L. (1920), Über die Härte plastischer Körper, Nachr. d. Ges. d. Wiss., Göttingen 1920.

PRANDTL, L. (1927), Über die Eindringungsfestigkeit plastischer Baustoffe und die Festigkeit der Schneiden, Zeitschr. f. angew. Math. und Mech., Febr. 1927.

PRESS, H. (1948), Über die Druckverteilung im Boden hinter Wänden verschiedener Art, Bautechnik-Archiv 1948, Heft 2.

RANKINE, W. J. M. (1857), On the Stability of Loose Earth, Trans. Royal Soc., London, Vol. 147, 1857.

RASMUSSEN, Th. (1948), Ankerpladers Stabilitet, Ingeniøren 1948, No. 4, Copenhagen.

REBHANN, G. (1871), Theorie des Erddruckes und der Futtermauern, Wien, Gerold, 1871.

REISSNER, H. (1909), Theorie des Erddruckes, Enzyklopädie der math. Wiss., Vol. 4, Teubner, Leipzig 1909.

RENDULIC, L. (1935), Ein Beitrag zur Bestimmung der Gleitsicherheit, Der Bauingenieur 1935, Heft 19/20.

RENDULIC, L. (1938), Der Erddruck im Strassenbau und Brückenbau, Forschungsarb. Strassenwesen, Bd. 10, Volk und Reich, Berlin 1938.

RENDULIC, L. (1940), Gleitflächen, Prüfflächen und Erddruck, Die Bautechnik 1940, Heft 13/14.

RESAL, J. (1910), La Poussée des Terres, Béranger, Paris 1910.

RIFAAT, T. (1935), Die Spundwand als Erddruckproblem, Mitt. Inst. Baustatik, Zürich 1935.

RIMSTAD, I. A. (1940), Zur Bemessung des dobbelten Spundwandbauwerkes, Ingeniørvidenskabelige Skrifter, Copenhagen 1940.

ROWE, P. W. (1952), Anchored Sheet-Pile Walls, Proc. Inst. Civil Eng., Vol. I, Jan. and Sept. 1952.

SCHULTZE, E. (1948), Zusammensetzung und Zerlegung von Gleitlinien, Abhandlungen über Bodenmechanik und Grundbau, Berlin 1948.

SCHÜTTE, H.G. (1940), Anwendungen der Erddrucktheorie bei der Berechnung von Spundwänden und Kaimauern, Der Bauingenieur 1940, Heft 14/16.

SCHØNWELLER, G. (1945), Fundering, Danmarks Tekniske Højskole, Copenhagen 1945.

SKEMPTON, A.W. (1946), Earth Pressure and the Stability of Slopes, The Principles and Applications of Soil Mechanics, Inst. Civil Eng., London 1946.

SKEMPTON, A.W. (1948), The φ=0-Analysis of Stability and its Theoretical Basis, Proc. Sec. Int. Conf., Soil Mech., Vol.I, Rotterdam 1948.

SKEMPTON, A.W. (1948), Practical Examples of the φ=0-Analysis of Stability of Clays, Proc. Sec. Int . Conf., Soil Mech., Vol.II, Rotterdam 1948.

SKEMPTON, A.W. & BISHOP, A.W. (1950), The Measurement of the Shear Strength of Soils, Géotechnique, Vol.II, No.2, Dec. 1950.

SKEMPTON, A.W. & WARD, W.H. (1952), Investigations Concerning a Deep Cofferdam in the Thames Estuary Clay at Shellhaven, Géotechnique, Vol.III, No.3, Sept. 1952.

SOKOLOVSKI, V.V. (1942), Statics of Earthy Mediums, Moscow 1942 (in Russian with summaries in English).

SPILKER, A. (1937), Mitteilung über die Messung der Kräfte in einer Baugrubenaussteifung, Die Bautechnik 1937, Heft 1.

STRECK, A. (1926), Beitrag zur Frage des Erdwiderstandes, Diss. T.H. Hannover, 1926.

STROYER, J.R. (1935), Earth Pressure on Flexible Walls, J. Inst. Civil Eng., London, Nov. 1935.

TAYLOR, D.W. (1948), Fundamentals of Soil Mechanics, Wiley, New York, 1948.

TERZAGHI, K. (1920), Old Earth Pressure Theories and New Test Results, Eng. News Record, September 20, 1920.

TERZAGHI, K. (1925), Erdbaumechanik, Leipzig 1925.

TERZAGHI, K. (1929), The Mechanics of Shear Failure on Clay Slopes and the Creep of Retaining Walls, Public Roads, Vol.10, 1929.

TERZAGHI, K. (1934), Large Retaining-Wall Tests, Eng. News Record, 1934.

TERZAGHI, K. (1936), A Fundamental Fallacy in Earth Pressure Computations, J. Boston Soc. Civil Eng., Vol.23, 1936.

TERZAGHI, K. (1936), Distribution of the Lateral Pressure of Sand on the Timbering of Cuts, Proc. First Int. Conf., Soil Mech., Vol.I, Harvard 1936.

TERZAGHI, K. (1940), Anchored Bulkheads, Proc. Purdue Conf., Soil Mech., 1940.

TERZAGHI, K. (1941), General Wedge Theory of Earth Pressure, Trans. ASCE, Vol.106, 1941.

TERZAGHI, K. (1944), Stability and Stiffness of Cellular Cofferdams, Proc. ASCE, Sept. 1944.

TERZAGHI, K. (1947), Theoretical Soil Mechanics, Wiley, New York 1947.

TERZAGHI, K. & PECK, R.B. (1948), Soil Mechanics in Engineering Practice, Wiley, New York 1948.

THE INSTITUTION OF STRUCTURAL ENGINEERS, (1949), Earth Retaining Structures, Civil Engineering Code of Practice , No.2, London 1949.

TSCHEBOTARIOFF, G.P. (1948), Large-Scale Model Earth Pressure Tests on Flexible Bulkheads, Proc. ASCE, Jan. 1948.

TSCHEBOTARIOFF, G.P. & BROWN, P.P. (1948), Lateral Earth Pressure as a Problem of Deformation or of Rupture, Proc. Sec. Int. Conf., Soil Mech., Vol.II, Rotterdam 1948.

TSCHEBOTARIOFF, G.P. (1949), Final Report on Large-Scale Earth Pressure Tests with Model Flexible Bulkheads, Princeton 1949.

TSCHEBOTARIOFF, G.P. (1951), Soil Mechanics, Foundations and Earth Structures, McGraw-Hill, New York 1951.

TSCHEBOTARIOFF, G.P. (1952), Einfluss der "Gewölbebildung" auf die Erddruckverteilung, Bautechnik-Archiv, Heft 8, 1952.

VENANT, B. de Saint (1870), Comptes Rendus , Vol.70, Vol.73, Vol.74, Gauthier-Villars, Paris 1870-72.

VERDEYEN, J. (1948), The Use of Flat Sheet-Piling in Cellular Construction, Proc. Sec. Int. Conf., Soil Mech., Vol.VII, Rotterdam 1948.

VERMEIDEN, J. (1948), Improved Sounding Apparatus, as developed in Holland since 1936, Proc. Sec. Int. Conf., Soil Mech., Vol.I, Rotterdam 1948.

WEISKOPF, W.H. (1945), Stresses in Soils under a Foundation, J. Franklin Institute, Vol.239, June 1945.

INDEX

In the following Index, most of the subjects dealt with in this book are listed. However, such subjects which occur repeatedly on a very large number of pages are not listed here. This applies, for example, to subjects such as "active earth pressures", "friction angles", "smooth walls", "zone-ruptures", "equilibrium-calculations", "boundary conditions", "earth pressure distribution", etc. Such subjects of a general nature are best located from the Table of Contents (pgs. 5-9).